

PLEASE TYPE**THE UNIVERSITY OF NEW SOUTH WALES**
Thesis/Dissertation SheetSurname or Family name: **Yau**First name: **Sheree**

Other name/s:

Abbreviation for degree as given in the University calendar: **PhD**School: **Biotechnology and Biomolecular Sciences**Faculty: **Faculty of Science**Title: **Molecular microbial ecology of Antarctic lakes****Abstract 350 words maximum: (PLEASE TYPE)**

The Vestfold Hills is a coastal Antarctic oasis, a rare ice-free region on the continent containing hundreds of marine-derived lakes. These lakes are microbially-dominated systems constrained by extremes of cold, salinity and light availability. Most Antarctic lakes are ice-covered for the majority of the year and are thus largely closed systems that often become meromictic (permanently stratified). The physical and chemical gradients that exist within an isolated system makes it possible to relate microbial taxa to abiotic variables. These factors make Antarctic lakes ideal model ecosystems to study microbial diversity, evolution and influence on geochemistry.

Sequencing of ribosomal genes from the environment has revolutionised microbial ecology by revealing the immense diversity of microbial life. However, this approach does not directly describe the physiology and ecological roles of members in a community. Random sequencing of genetic material from the environment (metagenomics) allows the determination not only of the microbial composition, but also its metabolic potential. Historic, physical, chemical and biological data available for two meromictic lakes in the Vestfold Hills, Ace Lake and Organic Lake, indicate each has unique microbial populations and biogeochemical properties. Metagenomic sequencing was applied to these two lakes to gain insight into their microbial ecology. Analytical methods to support metagenomic inferences were also developed and applied. These included identification and quantification of proteins from environmental samples (metaproteomics), which indicates active community members and biochemical processes; as well as microscopy, for determination microbial/viral abundances and morphology.

Analysis of these lake ecosystems yielded extensive genetic information from taxa previously unknown in the lakes, in particular, phycodnaviruses and a member of the newly described virophage viral family. The combination of metagenomics, metaproteomics and physico-chemical data enabled the ecological roles of taxa in the lakes and potential mechanisms of adaptation to the Antarctic environment to be determined. These analyses revealed viral predation, higher propensity of nutrient recycling and strategies of carbon conservation in Antarctic lake ecosystems. These molecular-based discoveries allowed the role of previously unrecognised taxa and metabolic processes to be modelled enabling implication to be drawn about Antarctic and other aquatic environments.

Declaration relating to disposition of project thesis/dissertation

I hereby grant to the University of New South Wales or its agents the right to archive and to make available my thesis or dissertation in whole or in part in the University libraries in all forms of media, now or here after known, subject to the provisions of the Copyright Act 1968. I retain all property rights, such as patent rights. I also retain the right to use in future works (such as articles or books) all or part of this thesis or dissertation.

I also authorise University Microfilms to use the 350 word abstract of my thesis in Dissertation Abstracts International (this is applicable to doctoral theses only).

.....
Signature.....
Witness.....
Date

The University recognises that there may be exceptional circumstances requiring restrictions on copying or conditions on use. Requests for restriction for a period of up to 2 years must be made in writing. Requests for a longer period of restriction may be considered in exceptional circumstances and require the approval of the Dean of Graduate Research.

FOR OFFICE USE ONLY

Date of completion of requirements for Award:

THIS SHEET IS TO BE GLUED TO THE INSIDE FRONT COVER OF THE THESIS

Molecular microbial ecology of Antarctic lakes

Sheree Yau

A thesis in fulfilment of the requirements for the degree of Doctor of Philosophy

School of Biotechnology and Biomolecular Sciences
Faculty of Science
University of New South Wales, Australia

February, 2013

Originality Statement

'I hereby declare that this submission is my own work and to the best of my knowledge it contains no materials previously published or written by another person, or substantial proportions of material which have been accepted for the award of any other degree or diploma at UNSW or any other educational institution, except where due acknowledgement is made in the thesis. Any contribution made to the research by others, with whom I have worked at UNSW or elsewhere, is explicitly acknowledged in the thesis. I also declare that the intellectual content of this thesis is the product of my own work, except to the extent that assistance from others in the project's design and conception or in style, presentation and linguistic expression is acknowledged.'

Signed

Date

Abstract

The Vestfold Hills is a coastal Antarctic oasis, a rare ice-free region on the continent containing hundreds of marine-derived lakes. These lakes are microbially-dominated systems constrained by extremes of cold, salinity and light availability. Most Antarctic lakes are ice-covered for the majority of the year and are thus largely closed systems that often become meromictic (permanently stratified). The physical and chemical gradients that exist within an isolated system makes it possible to relate microbial taxa to abiotic variables. These factors make Antarctic lakes ideal model ecosystems to study microbial diversity, evolution and influence on geochemistry.

Sequencing of ribosomal genes from the environment has revolutionised microbial ecology by revealing the immense diversity of microbial life. However, this approach does not directly describe the physiology and ecological roles of members in a community. Random sequencing of genetic material from the environment (metagenomics) allows the determination not only of the microbial composition, but also its metabolic potential. Historic, physical, chemical and biological data available for two meromictic lakes in the Vestfold Hills, Ace Lake and Organic Lake, indicate each has unique microbial populations and biogeochemical properties. Metagenomic sequencing was applied to these two lakes to gain insight into their microbial ecology. Analytical methods to support metagenomic inferences were also developed and applied. These included identification and quantification of proteins from environmental samples (metaproteomics), which indicates active community members and biochemical processes; as well as microscopy, for determination microbial/viral abundances and morphology.

Analysis of these lake ecosystems yielded extensive genetic information from taxa previously unknown in the lakes, in particular, phycodnaviruses and a member of the newly described virophage viral family. The combination of metagenomics, metaproteomics and physico-chemical data enabled the ecological roles of taxa in the lakes and potential mechanisms of adaptation to the Antarctic environment to be determined. These analyses revealed viral predation, higher propensity of nutrient recycling and strategies of carbon conservation in Antarctic lake ecosystems. These molecular-based discoveries allowed the role of previously unrecognised taxa and metabolic processes to be modelled enabling implication to be drawn about Antarctic and other aquatic environments.

Acknowledgements

List of Publications

In publications arising from my PhD work, my supervisor Prof Ricardo Cavicchioli and my co-supervisor Dr Federico Lauro were involved in the research design and editing of the manuscripts. Where versions of published material, or material submitted for publication appears in this thesis, details of the contributions made by myself and others precede it.

- **Sheree Yau**, Federico M. Lauro, Timothy J. Williams, Matthew Z. DeMaere, Mark V. Brown, John Rich, John A.E. Gibson, Ricardo Cavicchioli. Strategies of carbon conservation and unusual sulfur biogeochemistry in a hypersaline lake. *The ISME Journal* (submitted), 2013.
- Khawar S. Siddiqui, Timothy J. Williams, David Wilkins, **Sheree Yau**, Michelle A. Allen, Mark V. Brown, Federico M. Lauro, Ricardo Cavicchioli. Psychrophiles. *Annual Review of Earth and Planetary Sciences* (doi: 10.1146/annurev-earth-040610-133514), 2013.
- David Wilkins, **Sheree Yau**, Timothy J. Williams, Michelle Allen, Mark V. Brown, Matthew Z. DeMaere, Federico M. Lauro and Ricardo Cavicchioli. Key Microbial Drivers in Antarctic Aquatic Environments. *FEMS Microbiology Reviews* (doi:10.1111/1574-6976.12007), 2012.
- **Sheree Yau** and Ricardo Cavicchioli. Microbial communities in Antarctic lakes: Entirely new perspectives from metagenomics and metaproteomics. *Microbiology Australia* 32:157–159, 2011.
- **Sheree Yau**, Federico M. Lauro, Matthew Z. DeMaere, Mark V. Brown, Torsten Thomas, Mark J. Raftery, Cynthia Andrews-Pfannkoch, Matthew Lewis, Jeffrey M. Hoffman, John A. Gibson and Ricardo Cavicchioli. Virophage control of antarctic algal host–virus dynamics. *Proceedings of the National Academy of Sciences USA* 108:6163–6168, 2011.
- Federico M. Lauro, Matthew Z. DeMaere, **Sheree Yau**, Mark V. Brown, Charmaine Ng, David Wilkins, Mark J. Raftery, John A.E. Gibson, Cynthia Andrews-Pfannkoch, Matthew Lewis, Jeffrey M. Hoffman, Torsten Thomas and Ricardo Cavicchioli. An integrative study of a meromictic lake ecosystem in Antarctica. *The ISME Journal* 5:879–895, 2011.

Contents

1 General introduction	1
Co-authorship statement	1
1.1 Antarctic lakes	2
1.2 The Vestfold Hills	3
1.3 Insights from molecular studies of Antarctic lakes	3
1.3.1 Bacterial diversity: adaptation to unique physical and chemical conditions	5
1.3.2 <i>Archaea</i> : methanogens and haloarchaea	7
1.3.3 <i>Eucarya</i> perform multiple ecosystem roles	8
1.4 Integrative studies to derive whole ecosystem function	9
1.4.1 A single gene approach	9
1.4.2 ‘-omics’ approaches	10
1.5 Objectives	12
2 Development of methods to complement metagenomic sequencing for an integrative study of Ace Lake	13
Co-authorship statement	13
2.1 Abstract	14
2.2 Introduction	14
2.3 Materials and methods	16
2.3.1 Ace Lake samples	16
2.3.2 DNA extraction, sequencing and data cleanup	17
2.3.3 Metagenomic DNA assembly and annotation	18
2.3.4 Epifluorescence microscopy	18
2.3.5 Protein extraction	18
2.3.6 1D-SDS PAGE and LC-MS-MS	19
2.3.7 Metaproteomic mass spectra analysis	19
2.4 Results and discussion	20
2.4.1 Development of an epifluorescence microscopy method	20
2.4.2 Community stratification supported by cell and VLP densities . .	22
2.4.3 Development of a metaproteomic mass spectra analysis workflow	24
2.4.4 Insights from the metaproteomic analysis of Ace Lake	29
2.5 Conclusions	32

3 Virophage control of Antarctic algal host–virus dynamics	33
Co-authorship statement	33
3.1 Abstract	34
3.2 Introduction	35
3.3 Materials and methods	36
3.3.1 Samples and DNA sequencing	36
3.3.2 Transmission electron microscopy	36
3.3.3 Metagenomic assembly and annotation	36
3.3.4 Genome completion and annotation	37
3.3.5 Phylogenetic analysis	38
3.3.6 Metaproteomic analysis	38
3.3.7 Model of algal host–virus and virophage dynamics	38
3.4 Results and discussion	39
3.4.1 Dominance of phycodnaviruses in Organic Lake	39
3.4.2 Complete genome of an Organic Lake virophage	44
3.4.3 Gene exchange between virophage and phycodnaviruses	51
3.4.4 Virophage in algal host–phycodnavirus dynamics	52
3.4.5 Ecological relevance of virophages in aquatic systems	54
3.5 Acknowledgements	57
4 Strategies of carbon conservation and unusual sulphur biogeochemistry in Organic Lake	59
Co-authorship statement	59
4.1 Abstract	60
4.2 Introduction	61
4.3 Materials and methods	62
4.3.1 Characteristics of the lake and sample collection	62
4.3.2 Physical and chemical analyses	63
4.3.3 Epifluorescence microscopy	63
4.3.4 Cellular diversity analyses	64
4.3.5 Analysis of functional potential	64
4.4 Results and discussion	68
4.4.1 Abiotic properties and water column structure	68
4.4.2 Overall microbial diversity	70
4.4.3 Variation of microbial composition according to size and depth .	72
4.4.4 Organic Lake functional potential	78
4.4.5 Carbon resourcefulness in dominant heterotrophic bacteria . . .	79
4.4.6 Regenerated nitrogen is predominant in the nitrogen cycle . . .	86
4.4.7 Molecular basis for unusual sulphur chemistry	89
4.5 Conclusions	97

5 General discussion, future work and conclusions	99
5.1 Possibile future work on Organic Lake	99
5.1.1 Organic Lake community dynamics	100
5.1.2 OLV physiology and ecology	102
5.1.3 Organic lake biogeochemistry	104
5.2 Perspectives on ‘-omics’ approaches	106
5.2.1 Next generation sequencing technologies	107
5.2.2 Emerging bioinformatic bottlenecks	107
5.2.3 Prospects for closing the bioinformatic gap	108
5.2.4 ‘omes are only as good as our databases	112
5.2.5 Metagenomes and metaproteomes are time capsules	112
5.3 Concluding remarks	113
References	135
Appendix A PCR-based studies of Antarctic Lakes	137
Appendix B Proteins identified in Ace Lake metaproteomic analysis	147
Appendix C Peptide sequences of OLV and OLPV proteins identified in the metaproteome	213
Appendix D Microbial taxa detected in the Organic Lake water column	215

List of Figures

1.1	Map of the Vestfold Hills	4
2.1	Physico-chemical and biological structure of Ace Lake from (Lauro <i>et al.</i> , 2011)	15
2.2	Epifluorescence microscopy of Ace Lake microbiota	23
2.3	Counts of microbial cells and VLPs in Ace Lake	24
2.4	Lack of VLP in 5 m and 12.7 m Ace Lake samples	25
2.5	General shotgun proteomics workflow	26
2.6	Statistical analysis of Ace Lake metaproteome	29
3.1	Plot of percent GC content <i>vs</i> coverage for Organic Lake scaffolds	40
3.2	Transmission electron micrographs of Organic Lake VLPs	41
3.3	Phylogeny of OLPV B family DNA polymerase sequences	42
3.4	Phylogeny of the 18S rRNA genes from Organic Lake	43
3.5	Maps of OLPV genomic scaffolds	44
3.6	Phylogeny of OLPV major capsid protein sequences	45
3.7	Genomic map of Organic Lake virophage	47
3.8	Genomic comparison of OLV and OLPVs	52
3.9	Lotka-Volterra models of host–OLPV–OLV population dynamics	53
3.10	Virophage capsid proteins in environmental samples	54
3.11	Phylogeny of virophage capsid proteins	56
4.1	Vertical profiles of <i>in situ</i> Organic Lake abiotic parameters	68
4.2	Bathymetry of Organic Lake	69
4.3	Vertical structure of Organic Lake	69
4.4	Epifluorescence microscopy images of Organic Lake microbiota	71
4.5	PCA of physico-chemical parameters	72
4.6	Diversity of <i>Bacteria</i> in Organic Lake	73
4.7	Diversity of <i>Eucarya</i> in Organic Lake	74
4.8	Heatmap of Organic Lake SSU composition	76
4.9	Vertical profiles of potential for carbon cycling in Organic Lake	79
4.10	Phylogeny of rhodopsin homologues	83
4.11	Maps of OL-R1 rhodopsin-containing scaffolds	84
4.12	Vertical profiles of potential for nitrogen cycling in Organic Lake	86
4.13	Vertical profiles of potential for sulphur cycling in Organic Lake	89

4.14 Phylogeny of DddD DMSP lyase homologues	92
4.15 Maps of OL-dddD-containing scaffolds	93
4.16 Phylogeny of DddL DMSP lyase homologues	94
4.17 Phylogeny of DddP DMSP lyase homologues	95
4.18 Phylogeny of DmdA DMSP demethylase homologues	96

List of Tables

2.1	Summary of metagenomic data for Ace Lake profile	17
2.2	Comparison of peptides/proteins identified with NR <i>vs.</i> matched metagenomes	28
3.1	List of primers used to close the OLV genome.	37
3.2	Summary of metagenomic data for Organic Lake 0.1 µm samples	40
3.3	OLPV and OLV proteins identified in the metaproteome	46
3.4	Annotation of Organic Lake virophage genome	48
3.5	OLV MCP in Organic Lake and Ace Lake and Community Cyberinfrastructure for Advanced Microbial Ecology Research and Analysis (CAMERA)	55
4.1	Summary of metagenomic data for Organic Lake profile	62
4.2	List of KO groups searched for in the Organic lake metagenome	65
4.3	List of query functional marker gene sequences	67
4.4	Physico-chemical properties of Organic Lake profile	70
4.5	Taxonomic origin of genes involved carbon cycling	80
4.6	Counts of genes involved in dimethylsulphopropionate (DMSP) catabolism and photoheterotrophy in aquatic metagenomes	84
4.7	Taxonomic origin of genes involved in nitrogen conversions	88
4.8	Taxonomic origin of genes involved in sulphur conversions	91
5.1	Comparison of next generation DNA sequencing platforms	108
A.1	PCR-based studies of Antarctic Lakes	138
B.1	Proteins identitfied in the Ace Lake 5 m sample 0.1 µm size-fraction metaproteome	148
B.2	Proteins identitfied in the Ace Lake 11.5 m sample 0.1 µm size-fraction metaproteome	165
B.3	Proteins identitfied in the Ace Lake 12.7 m sample 0.1 µm size-fraction metaproteome	173
B.4	Proteins identitfied in the Ace Lake 14 m sample 0.1 µm size-fraction metaproteome	191
B.5	Proteins identitfied in the Ace Lake 18 m sample 0.1 µm size-fraction metaproteome	204
B.6	Proteins identitfied in the Ace Lake 23 m sample 0.1 µm size-fraction metaproteome	208

C.1 Peptide data for Organic Lake metaproteomics analysis	214
D.1 Microbial taxa detected in the Organic Lake profile	215

List of Abbreviations

1D-SDS PAGE one dimensional-sodium dodecyl sulphate polyacrylamide gel electrophoresis

AAnP aerobic anoxygenic photosynthesis

ABC ATP-binding cassette

ACT Artemis comparison tool

ALV Ace Lake virophage

EC2 Elastic Compute Cloud

ANOSIM analysis of similarity

ApMV *Acanthamoeba polyphaga* mimivirus

BchlA bacteriochlorophyll A

BLAST basic local alignment search tool

CAMERA Community Cyberinfrastructure for Advanced Microbial Ecology Research and Analysis

CAS CRISPR-associated proteins

COG clusters of orthologous groups

CPU central processing unit

CRISPR clustered regularly interspaced short palindromic repeat

CroV *Cafeteria roenbergensis* virus

DGGE denaturing gradient gel electrophoresis

DMS dimethylsulphide

DMSO dimethylsulphoxide

DMSP dimethylsulphopropionate

DPOB DNA polymerase B

DO dissolved oxygen

DOC dissolved organic carbon

DRP dissolved reactive phosphorus

FDR false discovery rate

GOS global ocean sampling

GPU graphical processing unit

GSB green sulphur bacteria

HMMER biosequence analysis using profile hidden Markov models

HPLC high performance liquid chromatography

IMG/M Integrated Microbial Genomes and Metagenomes

JCVI J. Craig Venter Institute

KEGG Kyoto Encyclopedia of Genes and Genomes

KO KEGG Orthology

KOBAS KEGG Orthology Based Annotation System

LC liquid chromatography

MCP major capsid protein

MEGA Molecular Evolutionary Genetic Analysis

MG-RAST Metagenome Rapid Annotation using Subsystems Technology

MS mass spectrometry

MS-MS two dimensional mass spectrometry

NCBI National Center for Biotechnology Information

NCLDV nucleo-cytoplasmic large DNA virus

NGS next generation sequencing

NR non-redundant database

NSA normalised spectral abundance

OLPV Organic Lake phycodnavirus

OLV Organic Lake virophage

ORF open-reading frame

OTU operational taxonomic unit

PCA principal component analysis

PCR polymerase chain reaction

PCTE polycarbonate Track Etch

PR proteorhodopsin

PV phycodnavirus

QIIME Quanitative Insights Into Microbial Ecology

RDP Ribosomal Database Project

RE restriction endonuclease

RM restriction modification

rRNA ribosomal RNA

rTCA reverse tricarboxylic acid

RuBisCO ribulose-bisphosphate carboxylase oxygenase

SAG single-cell amplified genome

SIP stable isotope probing

SO Southern Ocean

SRB sulphate-reducing bacteria

SSU small subunit ribosomal RNA

STAMP Statistical Analysis of Metagenomic Profiles

SVG single virus genome

TEM transmission electron microscopy

TDN total dissolved nitrogen

TDP total dissolved phosphorus

TDS total dissolved sulphur

TIGRFAM the Institute of Genomic Research curated protein database

TN total nitrogen

TOC total organic carbon

TP total phosphorus

TS total sulphur

VLP virus-like particle

VIROME Viral Informatics Resource for Metagenome Exploration

WGS whole genome shotgun

WL Wood-Ljungdahl; or reductive acetyl-CoA

Chapter 1

General introduction

Co-authorship statement

Sections of this chapter have been published as:

David Wilkins, **Sheree Yau**, Timothy Williams, Michelle Allen, Mark V. Brown, Matthew Z. DeMaere, Federico M. Lauro and Ricardo Cavicchioli. Key Microbial Drivers in Antarctic Aquatic Environments. *FEMS Microbiology Reviews* (doi: 10.1111/1574-6976.12007), 2012.

I contributed the section of the publication entitled *Antarctic lakes* excluding the subsection, *Microbial mats as microcosms of Antarctic life*. This material appears in sections of this introduction.

Antarctica is a “frozen desert” of constant low temperature, little precipitation and is subject to the polar light cycle where only specially adapted organisms can survive. The continent is covered by ice up to 4 km thick that spans 13.8 million km². A tiny 0.32% of the land area is ice-free, most of which consists of exposed rocky peaks or nunataks such as in the Ellsworth, the Transantarctic and the North Victoria Land Mountains. Only 1–2% of that ice-free land is found in coastal oases; however, it is these regions where Antarctic life is concentrated (Hodgson, 2012). They are breeding sites for large animals such as seals, penguins and sea birds and some of the only locations where plants and lichens are found. Coastal oases are also distinguished by the presence of hundreds of lakes and ponds. Life in these lakes is microbially dominated with few, if any, metazoan inhabitants (Laybourn-Parry, 1997) making them ideal locations to study Antarctic microbiota. The lakes span a continuum of environmental factors such as salinity and are “natural laboratories” to examine adaptations to a property of interest. The reduced biodiversity of Antarctic lakes makes them ideal model systems to examine microbial influence on geochemistry as it is possible to encompass a large proportion of the diversity present using molecular methods and relate taxa to particular processes (Laybourn-Parry and Pearce, 2007).

This introduction will review molecular-based microbiological research on Antarctic lakes. As this thesis focused on planktonic communities from two lakes in the Vestfold Hills, emphasis will be given to describing research from these study sites and to microbial ecology of the water column.

1.1 Antarctic lakes

In Antarctica, perenially available liquid water is found predominantly in lakes. These range from subglacial lakes that are sealed beneath kilometres of ice to completely exposed rock-bound lakes. The majority of lakes are found in the coastal oases. In East Antarctica these include the Vestfold Hills, Bungar Hills, Larsemann Hills, Syowa Oasis, Schirmacher Oasis, Grearson Hills and McMurdo Dry Valleys. In West Antarctic, the Antarctic Peninsula, the sub-Antarctic islands and maritime islands house multiple lakes. Of these locations, the best studied lake systems are those of the McMurdo Dry Valleys, The Vestfold Hills and the sub-Antarctic islands.

These lakes span a wide range of physical and chemical properties from freshwater to hypersaline and constantly ice-covered to melted. Some are permanently stratified and termed meromictic if they thaw seasonally, or amictic if they are always ice-covered. Stratified lakes provide a unique opportunity to describe aquatic microbial populations along steep chemical gradients and taxa can be related to the properties of that layer. They are also of particular interest because the anoxic bottom waters help preserve a paleogeological record in the sediments of geological and climatic changes. Most lakes are ice-covered for the majority of the year making them effectively isolated, and some may be truly closed systems if ice-cover is permanent. The age of water varies considerably; for example, outflow of subglacial water at Blood Falls is estimated to be 1.5 million years old (Mikucki *et al.*, 2009) while water from Lake Miers is less than

300 years old (Green *et al.*, 1988).

Most of these lakes were formed when the retreat of the continental ice-shelf lead to isostatic uplift of the land (Burton, 1981). As a result, the majority of lakes in the coastal oases are composed of relic seawater and are predominantly saline or hypersaline (Burke and Burton, 1988). In the latter, salinity is high due to concentrated by ablation (evaporation and sublimination). Lakes close to the coastline, such as Lake Rookery in the Vestfold Hills, may still occasionally experience marine inputs (Burton, 1981).

Freshwater lakes near the continental ice shelf were likely already above sea-level as the ice receded and are not of marine origin (Bronge, 2004). Other freshwater lakes were originally marine-derived but have been flushed fresh by glacial meltwater (Pickard *et al.*, 1986). The chemistry of the exposed lakes is very much influenced by the water balance from local geographic and climatic conditions. Input sources include precipitation from the ice-shelf and glacial melt streams (Burton, 1981).

1.2 The Vestfold Hills

The Vestfold Hills (Figure 1.1) is a ice-free region of approximately 400 km² on the eastern shore of the Prydz Bay, East Antarctica in the Australian Antarctic Territory (Gibson, 1999). The region was first sighted and named in 1935 (Law, 1959). Only intermittent expeditions occurred in the area until the establishment of Davis Station (68°33'S, 78°15'E) in 1957 (Law, 1959). The Vestfold Hills are made up of three large peninsulae, Broad, Mule and Long Peninsula, separated by fjords connected to the sea. Some of these fjords are large, such as Ellis Fjord, which is 10 km long, up to 100 m deep and has become a stratified system due to its restricted opening to the ocean (Burke and Burton, 1988). The region was formed approximately 10,000 years ago in the early Holocene as the continental ice receded and the rocky peninsulae rose above sea-level (Zwartz *et al.*, 1998).

When first discovered, the Vestfold Hills was immediately noted for its extensive ice-free land and the numerous lakes (Johnstone *et al.*, 1973). The Australian Antarctic Data Centre lists more than 3,000 water bodies mapped in the Vestfold Hills, ranging in area from 1 to 8,757,944 m². More than 300 lakes and ponds have been described, including approximately 20% of the world's meromictic lakes (Gibson, 1999).

1.3 Insights from molecular studies of Antarctic lakes

The majority of molecular-based studies of Antarctic lake microbial communities have made use of polymerase chain reaction (PCR) amplification of small subunit ribosomal RNA (SSU) sequences to survey the diversity of *Bacteria* and in some cases *Archaea* and *Eucarya*. A comprehensive list of PCR-based studies of Antarctic lakes and their major findings are provided in Appendix A. Microbial composition has been determined by cloning and sequencing of ribosomal RNA (rRNA) gene amplicons (Bowman *et al.*, 2000b,a; Gordon *et al.*, 2000; Christner *et al.*, 2001; Purdy *et al.*, 2003; Karr *et al.*, 2006; Matsuzaki *et al.*, 2006; Kurosawa *et al.*, 2010; Bielewicz *et al.*, 2011), although

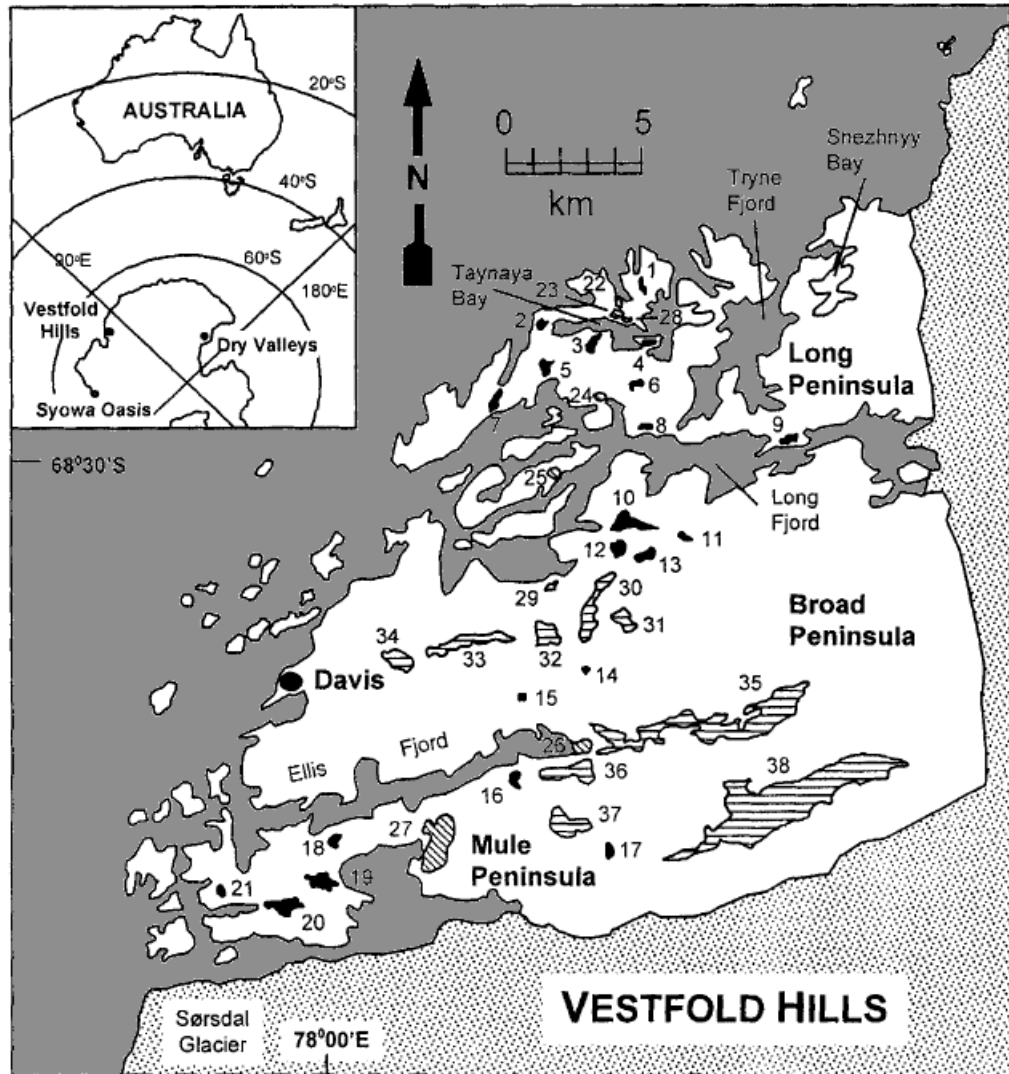


Figure 1.1: A map of the Vestfold Hills showing fjords, bays and lakes (numbered). The Southern Ocean is shown in grey, meromictic lakes coloured in black, seasonally isolated lakes and basins are striped and the continental ice-shelf is stippled. Inset is the position of the Vestfold Hills relative to Australia and to the Antarctic coastal oases. The lakes are: (1) unnamed lake 2, (2) Organic Lake, (3) Pendant Lake, (4) Glider Lake, (5) Ace Lake, (6) unnamed lake 1, (7) Williams Lake, (8) Abraxas Lake, (9) Johnstone Lake, (10) Ekho Lake, (11) Lake Farrell, (12) Shield Lake, (13) Oval Lake, (14) Ephyra Lake, (15) Scale Lake, (16) Lake Anderson, (17) Oblong Lake, (18) Lake McCallum, (19) Clear Lake, (20) Laternula Lake and (21) South Angle Lake. Map image is from Gibson (1999) with some minor modifications.

many studies have also made use of denaturing gradient gel electrophoresis (DGGE) to provide a molecular “fingerprint” of the community (Pearce, 2003; Pearce *et al.*, 2003; Karr *et al.*, 2005; Pearce, 2005; Pearce *et al.*, 2005; Unrein *et al.*, 2005; Glatz *et al.*, 2006; Mikucki and Priscu, 2007; Mosier *et al.*, 2007; Schiaffino *et al.*, 2009; Villaescusa *et al.*, 2010). Functional genes have also been targeted using PCR amplification to assess the potential of biochemical processes occurring, such as nitrogen fixation (Olson *et al.*, 1998), ammonia oxidation (Voytek *et al.*, 1999), anoxygenic photosynthesis (Karr *et al.*, 2003), and dissimilatory sulfite reduction (Karr *et al.*, 2005; Mikucki *et al.*, 2009). These PCR-based analyses of Antarctic lake communities have shed light on microbial diversity, temporal and spatial distributions and started to delve into the key drivers in whole ecosystem function.

Relatively few metagenomic studies, which entail random high-throughput sequencing of environmental DNA, have been published on Antarctic lakes (López-Bueno *et al.*, 2009; Ng *et al.*, 2010; Lauro *et al.*, 2011; Yau *et al.*, 2011). However, these few studies have been able to assess both the taxonomic composition and genetic potential of lake communities, and in many cases have linked function to specific members of the community. When coupled with functional “-omic” techniques (to date metaproteomics has been applied, but not metatranscriptomics or stable isotope probing), information has also been gained about the genetic complement expressed by the resident populations (Ng *et al.*, 2010; Lauro *et al.*, 2011; Yau *et al.*, 2011). These studies are described in section 1.4 of this introduction and in the body of this thesis.

1.3.1 Bacterial diversity: adaptation to unique physical and chemical conditions

Most molecular studies conducted on Antarctic lakes have focused on *Bacteria*. Consistent with the wide range of physical and chemical properties of Antarctic lakes, a large variation in species assemblages have been found. While exchange of microorganisms must be able to occur between lakes that are in close vicinity to each other, the data to date indicates that microbial populations are relatively unique to each type of isolated system. Nonetheless, certain trends in composition driven by physico-chemical factors and potentially biogeography, are also apparent.

Salinity

Hypersaline lakes from the Vestfold Hills (Bowman *et al.*, 2000a) and McMurdo Dry Valleys (Glatz *et al.*, 2006; Mosier *et al.*, 2007) were all dominated by *Gammaproteobacteria* and members of the *Bacteroidetes* as well as harboring lower abundance populations of *Alphaproteobacteria*, *Actinobacteria*, and *Firmicutes*. The surface waters of lakes close to marine salinity resemble marine communities dominated by *Bacteroidetes*, *Alphaproteobacteria* and *Gammaproteobacteria*, but divisions such as *Actinobacteria* and specific clades of *Cyanobacteria* have been found to be overrepresented compared to the ocean (Lauro *et al.*, 2011). Sediments from saline lakes in the Vestfold Hills (Bowman *et al.*, 2000b) and Nuramake-Ike in the Syowa Oasis (Kurosawa *et al.*, 2010)

were very similar, containing in addition to the surface clades, *Deltaproteobacteria*, *Planctomycetes*, *Spirochaetes*, *Chloroflexi* (green non-sulphur bacteria), *Verrucomicrobia* and representatives of related candidate divisions. Plankton from freshwater lakes were characterized by an abundance of *Betaproteobacteria*, although *Actinobacteria*, *Bacteroidetes*, *Alphaproteobacteria* and *Cyanobacteria* were also prominent (Pearce, 2003, 2005; Pearce *et al.*, 2005; Schiaffino *et al.*, 2009).

Trophic status

Differences in bacterial community structure are also influenced by nutrient availability. In studies of freshwater lakes in the Antarctic Peninsula and the South Shetland Islands, cluster analysis of DGGE profiles grouped together lakes of similar trophic status (Schiaffino *et al.*, 2009; Villaescusa *et al.*, 2010). Most of the variance in community structure could be explained by related chemical parameters such as phosphate and dissolved inorganic nitrogen. Similarly, three freshwater lakes, Moss, Sombre and Heywood on Signy Island are alike except that Heywood Lake is enriched by organic inputs from seals. Bacterial composition in each lake changed from winter to summer and this was again correlated to variation in physico-chemical properties (Pearce, 2005). The bacterial population of Heywood Lake had shifted from a dominance of *Cyanobacteria* towards a greater abundance of *Actinobacteria* and marine *Alphaproteobacteria* (Pearce *et al.*, 2005). This hints at a link between a copiotrophic lifestyle in the Heywood Lake *Actinobacteria* and inhibition of Antarctic freshwater *Cyanobacteria* by eutrophication. This type of study exemplifies how inferences can be made about taxa and function by examining population changes over time and over gradients of environmental parameters.

Biogeography

The relative isolation and diverse chemistries of the lakes facilitates biogeographical and biogeochemical studies. The anoxic and sulphidic bottom waters of some meromictic lakes form due to a density gradient that precludes mixing. Although sedimentation from the upper aerobic waters may occur, there is little opportunity for interchange of species with the bottom water of lakes allowing for greater divergence in community composition as nutrients can become depleted and products of metabolism can accumulate. As a result, distinct distributions of bacterial groups can inhabit these strata, and different types of microorganisms can be found in equivalent strata in different lakes.

A good example of this is the presence of common types of purple sulphur bacteria (*Chromatiales*) and green sulphur bacteria (GSB) (*Chlorobi*) in some meromictic lakes and stratified fjords in the Vestfold Hills (Burke and Burton, 1988), compared to diverse purple non-sulphur bacteria in Lake Fryxell, McMurdo Dry Valleys (Karr *et al.*, 2003). In Lake Bonney, the east and west lobes harbor overlapping but distinct communities in the suboxic waters (Glatz *et al.*, 2006). The east lobe was dominated by *Gammaproteobacteria* and the west lobe by *Bacteroidetes*, illustrating how divergent communities

can form from the same seed population. In contrast, ice communities are more readily dispersed by wind, aerosols and melt-water. 16S rRNA gene probes designed from bacteria trapped in the permanent ice-cover of Lake Bonney hybridized to microbial mat libraries sourced up to 15 km away (Gordon *et al.*, 2000). This demonstrates how a single lake may encompass microorganisms that are geographically dispersed, while also harboring others that have restricted niches and are under stronger selection pressure.

Bacterial diversity of Lake Vostok

Subglacial systems have been isolated from the open environment for hundreds of thousands to millions of years (Siegert *et al.*, 2001). The biggest of these, Lake Vostok is approximately 4 km below the continental ice-sheet. As a result they provide a reservoir of microorganisms that may have undergone significant evolutionary divergence from the same seed populations that were not isolated by the Antarctic ice cover. To date, molecular microbial studies have concentrated on the accretion ice above the ice-water interface (Priscu, 1999; Christner *et al.*, 2001). Accretion ice has been found to contain a low density of bacterial cells from *Alphaproteobacteria*, *Betaproteobacteria*, *Actinobacteria* and *Bacteroidetes* divisions closely allied to other cold environments. Molecular signatures of a thermophilic *Hydrogenophilus* species were also identified in accretion ice raising the possibility that chemoaerotrophic thermophiles were delivered to the accretion ice from hydrothermal areas in the lakes bedrock (Bulat *et al.*, 2004; Lavire *et al.*, 2006).

However, interpretation of results from samples sourced from the Lake Vostok bore hole are very challenging as it is difficult to differentiate contaminants from native Vostok microorganisms. From a study that assessed possible contaminants present in hydrocarbon-based drilling fluid retrieved from the Vostok ice core bore hole, six phylotypes were designated as new contaminants (Alekhnina *et al.*, 2007). Two of these were *Sphingomonas* phylotypes essentially identical to those found in the accretion ice-core (Christner *et al.*, 2001), which raises question about whether bacteria identified from the ice-cores are representative of Lake Vostok water, and is an example of how contamination may occur.

1.3.2 *Archaea*: methanogens and haloarchaea

Archaea have been detected mainly in anoxic sediments and bottom waters from lakes that range in salinity from fresh to hypersaline. Those with known isolates are affiliated with methanogens or haloarchaea (Bowman *et al.*, 2000b,a; Purdy *et al.*, 2003; Kurosawa *et al.*, 2010; Lauro *et al.*, 2011). Anoxia allows for the growth of methanogenic *Archaea* that mineralize fermentation products such as acetate, H₂ and CO₂ into methane, thereby performing an important step in carbon cycling. The acetoclastic methanogens thrive in environments where alternative terminal electron acceptors such as sulphate and nitrate have been depleted. One example of this is Lake Heywood where methanogenic *Archaea* were found to comprise 34% of the total microbial population in the freshwater sediment, the majority of which were *Methanosarcinales*,

which include acetate and C1-compound utilizing methanogens (Purdy *et al.*, 2003).

In general, archaeal populations appear to be adapted to their specific lake environment. Sediments from saline lakes of the Vestfold Hills were inhabited by members of the *Euryarchaeota* typically found in sediment and marine environments with the phylotypes differing between the lakes examined (Bowman *et al.*, 2000b). While a phylotype similar to *Methanosarcina* was identified, the majority were highly divergent. Similarly, *Methanosarcina* and *Methanoculleus* were detected in Lake Fryxell but other members of the *Euryarchaeota* and *Crenarchaeota* (a single sequence) were divergent, clustering only with marine clones (Karr *et al.*, 2006). Based on the lake chemical gradients and the location of these novel phylotypes in the water column the authors speculated these *Archaea* may have alternative metabolisms such as anoxic methanotrophy or sulphur-utilization.

In sediments from Lake Nurume-Ike in the Langhovde region, 205 archaeal clones grouped into three phylotypes, with the predominant archaeal clone being related to a clone from Burton Lake in the Vestfold Hills, while the other two did not match to any cultivated species (Kurosawa *et al.*, 2010). In hypersaline lakes where bottom waters do not become completely anoxic, methanogens are not present and *Archaea* have extremely low abundance. For example, only two archaeal clones of the same phylotype were recovered from deep water samples from Lake Bonney (Glatz *et al.*, 2006), and Organic Lake in the Vestfold Hills had an extremely low abundance of archaeal clones related to *Halobacteriales* (Bowman *et al.*, 2000a). In contrast to these stratified hypersaline lakes, the microbial community in the extremely hypersaline Deep Lake is dominated by haloarchaea (Bowman *et al.*, 2000a). Many of the clones identified from Deep Lake are similar to *Halorubrum* (formerly *Halobacterium*) *lacusprofundi* which was isolated from the lake (Franzmann *et al.*, 1988).

1.3.3 *Eucarya* perform multiple ecosystem roles

Single-celled *Eucarya* are important members of Antarctic aquatic microbial communities. In many Antarctic systems, eucaryal algae are the main photosynthetic organisms and in others, only heterotrophic protists occupy the top trophic level. As eucaryal cells are generally large with characteristic morphologies, microscopic identifications have been used. However, microscopy is unable to classify smaller cells such as nanoflagellates with high resolution, although these may constitute a high proportion of algal biomass. For example, five morphotypes of *Chrysophyceae*, evident in Antarctic lakes were unidentifiable by light microscopy but were able to be classified using DGGE and DNA sequencing (Unrein *et al.*, 2005). Consistent with this, molecular studies specifically targeting eucaryal diversity (Unrein *et al.*, 2005; Mosier *et al.*, 2007; Bielewicz *et al.*, 2011) have identified a much higher level of diversity than previously suspected, and the studies have discovered lineages not previously known to be present such as silicoflagellates of the family *Dictyochophyceae* (Unrein *et al.*, 2005) and fungi (Mosier *et al.*, 2007; Bielewicz *et al.*, 2011).

Most *Eucarya* in Antarctic lakes are photosynthetic microalgae that are present

in marine environments with a wide distribution including chlorophytes, haptophytes, cryptophytes and bacillariophytes. Molecular methods have afforded deeper insight into the phylogenetic diversity within these broader divisions and have revealed some patterns in their distribution. Using 18S rRNA gene amplification and DGGE, the same chrysophyte phylotypes were identified in lakes from the Antarctic Peninsula and King George Island despite being 220 km apart (Unrein *et al.*, 2005) indicating these species may be well-adapted to Antarctica or highly dispersed. Similarly, an unknown stramenopile sequence was detected throughout the 18S rRNA clone libraries of Lake Bonney demonstrating a previously unrecognized taxon occupied the entire photic zone in the lake (Bielewicz *et al.*, 2011). In contrast, other groups showed distinct vertical and temporal distributions with cryptophytes dominating the surface, haptophytes the midwaters and chlorophytes the deeper layers during the summer while stramenopiles increased in the winter (Bielewicz *et al.*, 2011).

The influence of flagellates on ecosystem function is not necessarily clear-cut as they can simultaneously inhabit several trophic levels. For instance, in Ace Lake the mixotrophic phytoflagellate *Pyramimonas gelidocola* derives a proportion of its carbon intake through bacterivory (Bell and Laybourn-Parry, 2003) but in the nearby Highway Lake, it uptakes dissolved organic carbon (Laybourn-Parry *et al.*, 2005). This illustrates potential limitations for deriving ecosystem level functions from taxonomic studies alone, even with taxa that appear physiologically straightforward. Further studies are necessary to determine the basis for apparent specific adaptations of some species to particular lakes or lake strata, and for the cosmopolitan distribution of others. Here, molecular based research of the kind that has been applied to bacteria such as functional gene surveys will undoubtedly help answer these questions.

1.4 Integrative studies to derive whole ecosystem function

The relatively low diversity of Antarctic microbial food-webs existing within effectively closed systems allows for an integrative understanding of the microbial community and biogeochemical cycling to be obtained. This can be achieved by combining molecular information of the taxonomic or functional genes with abiotic parameters or reaction rates.

1.4.1 A single gene approach

One such study was conducted on Blood Falls, an outflow of anoxic ferrous brine from the Taylor Glacier in the McMurdo Dry Valleys, where an unusual iron–sulphur cycle was inferred to exist. The water is sulphate-rich, exists in permanent darkness and is estimated to have been isolated from external inputs for 1.5 million years (Mikucki *et al.*, 2009). PCR-screening for SSU and functional gene markers for dissimilatory sulphur conversions was conducted to piece together the ecosystem function. 16S rRNA gene analysis showed the community was dominated by a close relative of *Thiomicrospira arctica*, an autotrophic sulphur-oxidizing member of the *Gammaproteobacte-*

ria (*Thiotrichales*), as well as sequences related to *Delta-* and *Gammaproteobacteria* capable of iron and/or sulphur compound reduction, and *Bacteroidetes* capable of heterotrophic growth on organic compounds (Mikucki and Priscu, 2007). A large proportion of adenosine 5'-phosphosulphate reductase genes related to those involved in dissimilatory sulphate metabolism were detected. However, dissimilatory sulphite reductase (*dsrA*) was not present and radioisotope data indicated sulphide is not produced. The implication of this is that sulphate reduction does not proceed to sulphide as typically occurs in other aquatic systems, and instead sulphate is expected to be regenerated via an alternative cycle with Fe(III) acting as the terminal electron acceptor (Mikucki *et al.*, 2009). This is a fascinating example of how a closed system has adapted to sustain life in the absence of light energy through the use of atypical chemical cycling; a pathway that was speculated to have possibly occurred in the ancient Neoproterozoic ocean (1,000 to 500 mya) (Mikucki *et al.*, 2009).

1.4.2 ‘-omics’ approaches

Motivation for adopting metagenomic and other ‘-omics’ approaches has stemmed from the inability to obtain physiological data from PCR-based taxonomic surveys and limited scope offered by screening of single functional gene markers. Although metabolic capacity can often be inferred from diversity of a single gene if there are cultured representatives with the detected genes, close relatives with defined physiologies are often not available. Inferring function can be problematic due to the existence of species and even strain level differences. For example, the majority of *Gammaproteobacteria* that have been detected in hypersaline lakes are relatives of *Marinobacter* suggesting that this genus is particularly adapted to hypersaline systems (Bowman *et al.*, 2000a; Glatz *et al.*, 2006; Matsuzaki *et al.*, 2006; Mosier *et al.*, 2007). Nonetheless, *Marinobacter* species from different lakes appear biochemically distinct as isolates from hypersaline lake Suribati-Ike were all able to respire dimethylsulphoxide (DMSO) but not nitrate (Matsuzaki *et al.*, 2006). In contrast, those from the west lobe of Lake Bonney were all able to respire nitrate (Ward and Priscu, 1997). Interestingly, in the east lobe of the same lake, nitrate respiration was inhibited although a near-identical *Marinobacter* phylotype was present; it was speculated that the inhibition may have been caused by an as yet unidentified chemical factor (Ward *et al.*, 2005; Glatz *et al.*, 2006). Metagenomics presents itself as a powerful tool to explore microbial communities because it can provide extensive information on the genetic content of uncultured taxa that is embedded within a whole community genomic context.

The first large scale metagenomic study of an Antarctic lake specifically targeted viruses (López-Bueno *et al.*, 2009). As obligate parasites, viruses cannot be isolated without first having a susceptible host in culture, which curtails the possibility of surveying anything but defined viral populations through culture-based techniques. Viruses do not have a universal gene that may be used as a taxonomic marker, or even universal genetic material, so metagenomic sequencing is an ideal approach for surveying viral diversity. Analysis of the viral component of the freshwater Lake Limnopolar,

Livingston Island uncovered the greatest depth of viral diversity of any aquatic system to date (López-Bueno *et al.*, 2009). Representatives from 12 viral families were detected, but unlike the two previous viromes that had been published at that time using comparable techniques, ssDNA viruses and large dsDNA viruses that putatively infect *Eucarya* were the dominant viral types. The ssDNA viruses were related to circoviruses, geminiviruses, nanoviruses and satellites; viruses previously only known to infect plants and animals indicating they are much more diverse than previously suspected and may constitute new viral families. Samples taken in summer showed a shift in the viral community composition towards phycodnaviruses similar to *Ostreococcus tauri* virus, OtV5. This shift potentially reflects an increase in the host algae that are stimulated to bloom by the increased light availability. Subsequent analysis has indicated multiple displacement amplification of low quantities of starting DNA used in virome study leads to a stochastic amplification bias rendering the metagenomes non-quantitative (Yilmaz *et al.*, 2010). Nonetheless, clear is that viruses perform a crucial role in shaping community structure, driving host evolution and contributing to the dissolved nutrient pool (Danovaro *et al.*, 2011) and this pioneering study has shed light on their diversity in the Antarctic environment.

A combined metagenomic and metaproteomic approach has been applied to the study of Ace Lake in the Vestfold Hills (Ng *et al.*, 2010; Ng, 2010; Lauro *et al.*, 2011). From this study, the main carbon, nitrogen and sulphur cycles within the stratified water column of Ace Lake were able to be described (Lauro *et al.*, 2011). A strictly interdependent sulphur cycle was found to exist between GSB at the oxycline and sulphate-reducing bacteria (SRB) in the anaerobic zone. The GSB were able to convert sulphide to sulphate but lacked assimilatory sulfate reduction capability (Ng *et al.*, 2010; Ng, 2010; Lauro *et al.*, 2011). Enzymes involved in dissimilatory sulphate reduction (adenylylsulphate reductase and dissimilatory sulphite reductase) were detected in the metaproteome of the anaerobic zone thereby completing the dissimilatory sulphur cycle (Ng *et al.*, 2010; Ng, 2010). It was also apparent that short circuiting of the nitrogen cycle was occurring. Nitrogen fixation proteins were not found in the metaproteome, likely due to preferential assimilation of ammonia (Ng *et al.*, 2010; Ng, 2010; Lauro *et al.*, 2011). Genes involved in nitrification and denitrification were underrepresented indicating the system had shifted away from nitrogen mineralization consistent with a mechanism to conserve bioavailable nitrogen (Lauro *et al.*, 2011). It is noteworthy that these findings are in contrast to lakes in the Dry Valleys where ammonia monooxygenase genes were present in the aerobic zone of six lakes of various salinities and extents of stratification (Voytek *et al.*, 1999). Overall, strong depth partitioning, loss of biochemical pathways common in other aquatic systems and the selection of key species were identified as important steps in transiting the microbial population from marine to a meromictic lake ecosystem.

Further results from the study of Ace Lake are presented in Chapter 2 and metagenomic and metaproteomic analyses of Organic Lake is described in Chapters 3 and 4.

1.5 Objectives

The overall aim of this thesis was to explore the microbial communities of Antarctic lakes from an ecosystem level perspective by combining metagenomics, metaproteomics and physico-chemical data. Ace Lake and Organic Lake, two lakes in the Vestfold Hills, were chosen as the study sites as there are extensive historic environmental records available for these lakes. As meromictic lakes, differences in the microbial population were able to be examined along the vertical gradients within the lakes. Finally, as they are marine-derived systems, comparison between the lake system and the marine environment was used to identify specific lake adaptations.

The specific objectives of the research were:

1. Develop epifluorescence microscopy and metaproteomic methods to complement to metagenomic sequencing.
2. Determine the microbial and viral composition of Antarctic lake communities, their functional potential and infer the ecological roles of populations in the community.
3. Integrate environmental and biological data to model the lake microbial interactions and biogeochemical processes.

Chapter 2

Development of methods to complement metagenomic sequencing for an integrative study of Ace Lake

Co-authorship statement

Sections from this chapter have been published as:

Federico M. Lauro, Matthew Z. DeMaere, **Sheree Yau**, Mark V. Brown, Charmaine Ng, David Wilkins, Mark J. Raftery, John A.E. Gibson, Cynthia Andrews-Pfannkoch, Matthew Lewis, Jeffrey M. Hoffman, Torsten Thomas, and Ricardo Cavicchioli. An integrative study of a meromictic lake ecosystem in Antarctica. *The ISME Journal* 5:879–895, 2011.

I performed the epifluorescence microscopy, metaproteomic mass spectral analysis and drafted the corresponding sections of the publication.

Contributions by others that support the work presented in this chapter are as follows. Research was designed by Federico Lauro, Mark Brown, Torsten Thomas, John Gibson and Ricardo Cavicchioli. Sample collection was performed by Federico Lauro, Mark Brown, Torsten Thomas, Jeffrey Hoffman and Ricardo Cavicchioli. DNA extraction and clone library preparation was performed by Cynthia Andrews-Pfannkoch and Jeffery Hoffman. DNA sequencing quality control was performed by Matthew Lewis. Metagenomic sequence filtering, mosaic assembly and annotation was performed by Matthew DeMaere. Protein extraction, one-dimensional sodium dodecyl sulphate-polyacrylamide gel electrophoresis and liquid chromatography mass spectrometry and preliminary analysis performed by Charmaine Ng. Assistance in mass spectrometry was provided by Mark Raftery.

2.1 Abstract

Ace Lake is a saline meromictic lake and the most studied lake in the Vestfold Hills, Antarctica. As a system of moderate biological complexity with extensive historic physical and chemical data, it was chosen as a site to implement an integrative study of the lake ecosystem. Metagenomic analysis of Ace Lake revealed microbial taxa and metabolic genes were stratified according to the lake's water column structure and also was able to infer potential for nutrient cycling (Lauro *et al.*, 2011). This study aimed to generate independent datasets complementary to metagenome data as part of the integrative analysis of the lake. A method for visualising and enumerating cells and virus-like particles (VLPs) using epifluorescence microscopy was developed that does not require use of the relatively expensive Anodisc filters. Microscopic examination confirmed the efficacy of the sequential filtration procedure used to size fractionate the lake microbiota and determined the densities of cells and VLPs. Furthermore, it independently verified the lack of VLPs associated with the lake's green sulphur bacteria (GSB). Previous metaproteomic analysis of the Ace Lake depth profile using cross-species matching of mass spectra yielded few protein identifications (Ng, 2010). However, metaproteomic analysis of the GSB layer using matching GSB metagenomic sequences as the search database gave a 3-fold increase in protein identifications (Ng *et al.*, 2010; Ng, 2010). A metaproteomic analysis workflow was developed that achieved substantial improvements in protein identification rates by similarly using metagenomic databases matched to the metaproteomic samples. This involved application of the software package SCAFFOLD 2.0 to mass spectral analysis, which additionally allowed for protein abundance estimates by spectral counting. Functional protein groups were identified that were overrepresented in each zone of the lake. These data proved crucial to support a comprehensive description of the entire Ace Lake ecosystem.

2.2 Introduction

Ace Lake is a meromictic saline lake in the Vestfold Hills that separated from the sea ~5,000 BP (Bird *et al.*, 1991). Extensive physical, chemical and biological data has been collected from Ace Lake since 1974 (see <https://data.aad.gov.au/aadc/lakes/>). The system is microbially-dominated and has reduced species diversity (Bowman *et al.*, 2000b) with the only metazoan life present being callanoid copepods. Ace Lake is a highly stratified lake system that is 25 m at its deepest point (Figure 2.1). It is ice-covered for ~11 months of the year and generally thaws in January (Rankin *et al.*, 1999). Water is marine-derived and a largely neutral water balance has ensured salinity is close to that of seawater. The lake is physically separated into an aerobic mixolimnion, a steep chemo/oxycline at 12.7 m and an anoxic monimolimnion. The monimolimnion is sulfidic and methanogenic; both compounds have presumably accumulated through the activity of sulphate-reducing bacteria (SRB) and methanogenic archaea respectively (Rankin *et al.*, 1999; Lauro *et al.*, 2011) (Figure 2.1). As a physically and chemically well-characterised system of moderate diversity, Ace Lake was chosen as a model ecosys-

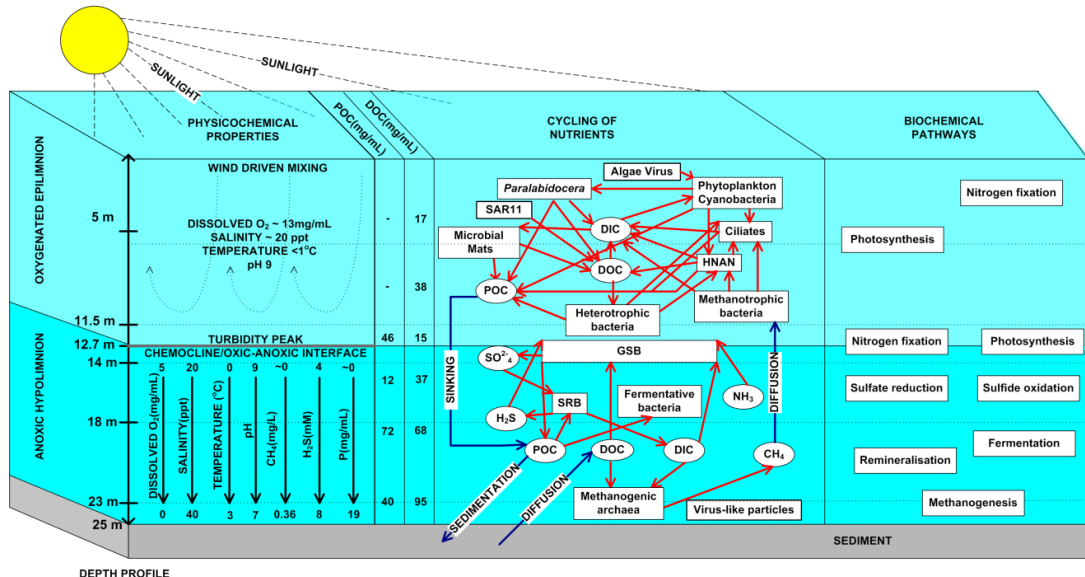


Figure 2.1: Physico-chemical and biological structure of Ace Lake. In the panel describing nutrient cycling biotic (red arrows) and abiotic (blue arrows) are shown. The panel describing biochemical pathways shows the labels of the pathways at the depths where they are most significant. The figure is from Lauro *et al.* (2011) with some modifications.

tem to implement a whole systems level analysis to piece together ecosystem functioning. Samples were obtained from the mixolimnion (5 and 11.5 m), the chemo/oxycline (12.7 m) and the monimolimnion (14, 18 and 23 m). Sampling was conducted according the design of the global ocean sampling (GOS) expedition (Rusch *et al.*, 2007) by using size fractionation of microbial biomass onto 3.0, 0.8 and 0.1 μm membrane filters.

From the metagenomic analysis conducted on the Ace Lake samples, significant differences were found in taxonomic composition between each size fraction and between the three zones of Ace Lake (Lauro *et al.*, 2011). The mixolimnion community is similar to a marine surface water assemblage consisting of a high abundance of the SAR11 clade of *Alphaproteobacteria* related to “*Candidatus Pelagibacter ubique*” and green algae of the order *Mamiellales*. However, diversity is reduced by one order of magnitude (Lauro *et al.*, 2011). Unlike Southern Ocean surface water, the mixolimnion is over-represented in *Cyanobacteria* related to *Synechococcus* and *Actinobacteria*, which may represent taxa that mark the transition from a marine to lake community. A dense, near-clonal population of green sulphur bacteria (GSB) related to *Chlorobium* termed C-ace reside at the chemo/oxycline at 12.7 m (Ng *et al.*, 2010; Lauro *et al.*, 2011). Below, in the monimolimnion is a highly diverse community that includes SRB and methanogenic Archaea. The viral community comprises *Phycodnaviridae*, *Myoviridae*, *Siphoviridae*, *Podoviridae* and unidentified viral families (Lauro *et al.*, 2011). Bacteriophage sequences were abundant in the bottom waters, whereas the surface community, was dominated by phycodnaviruses (Lauro *et al.*, 2011).

Metagenomics is an extremely powerful tool for interrogating microbial communities. However, a systems-level understanding ultimately requires the integration of data

which metagenomic sequencing alone does not provide such as abiotic parameters and functional activity (Handelsman, 2008; Warnecke and Hugenholtz, 2007). The focus of this study was to provide datasets to complement metagenome data.

A modified epifluorescence microscopy procedure was developed to determine cellular and viral densities and validate the efficacy of size-fractionation. Development of a revised method was necessary due to inability to source 25 mm diameter 0.02 µm pore-size Anodisc filters (Whatman) that have long been used with fluorescent nucleic acid dyes for this purpose (Hennes and Suttle, 1995; Noble and Fuhrman, 1998; Patel *et al.*, 2007). They were marked for discontinuation in December 2008 after the take-over of Whatman by GE Healthcare, and was the cause of a global shortage that was strongly opposed by the viral ecology community (Torrice, 2009). Since conducting this research, supply of 25 mm Anodisc filters has resumed, albeit at much greater cost per filter. The need for alternative methodologies has been great enough that protocols were developed independently by other research groups (Budinoff *et al.*, 2011; Diemer *et al.*, 2012) stressing the utility of alternatives.

Identification of proteins from a microbial community (metaproteomics) indicates which populations or processes are active in the environment and is thus a powerful tool for understanding ecosystems. Preliminary metaproteomic analysis along the vertical profile of Ace Lake has been performed using a cross-species genomic database comprising the National Center for Biotechnology Information (NCBI) non-redundant database (NR) (Ng, 2010). A focussed metaproteogenomic analysis conducted on the dense GSB layer using the matched GSB metagenome as the database resulted in 3-fold increase in protein identifications compared to using the NR database (Ng, 2010). This indicates large gains in metaproteome coverage are possible using a matched metagenomic database (Ng, 2010). However, protein identification by the ‘shotgun’ proteomics approach favoured in metaproteomics (Ram *et al.*, 2005) is computationally challenging when dealing with samples of higher species diversity. In this study, a bioinformatic analysis workflow was devised tailored to Ace Lake metaproteomic data to identify proteins as well as estimate their abundance.

2.3 Materials and methods

2.3.1 Ace Lake samples

Water samples were collected from Ace Lake ($68^{\circ}28'23.2''S$, $78^{\circ}11'20.8''E$), Vestfold Hills, Antarctica on 21 and 22 December 2006 as described previously (Ng *et al.*, 2010; Ng, 2010; Lauro *et al.*, 2011). Briefly, a hole positioned above the deepest point (25 m depth) of the lake was drilled through the 2 m ice cover of Ace Lake to reach the lake surface. Microbial biomass was collected by sequential size fractionation through a 20 µm pre-filter directly onto 3.0, 0.8 and 0.1 µm pore-size 293 mm polyethersulfone membrane filters (Rusch *et al.*, 2007), along the depth profile. Two independent sets of filters were obtained, one set for metagenomics and one for metaproteomics.

A sonde probe (YSI model 6600, YSI Inc., Yellow Springs, OH, USA) was used

Table 2.1: Summary of metagenomic data for Ace Lake December 2006 profile. S, Sanger sequencing data; *Scaffolds from 0.1 μ m fraction were assembled from a hybrid of Sanger and 454 sequences.

ID	Depth (m)	Size (μ m) reads	Trimmed reads	ORFs (reads)	Annotated COG/KEGG ORFs	>10 kbp scaffolds (reads)	Annotated scaffold ORFs
GS232 5	0.1	S: 281,490 454: 539,536	421,252 638,757	112,490/96,771 109,551/103,201	*	*	
	0.8	454: 468,122	485,021	150,660/135,451	2,809 (349,015) 269 (66,743)	45,281 3,215	
	3.0	454: 160,835	138,191	24,920/22,240	33 (2,980)	353	
GS231 11.5	0.1	S: 283,663	427,889	124,332/107,523	*	*	
	0.8	454: 523,650	608,671	99,175/95,266	2,814 (390,490)	47,987	
	3.0	454: 474,419	511,909	218,126/176,332	174 (161,891)	2,321	
GS230 12.7	0.1	S: 54,446	75,576	42,790/41,391	*	*	
	0.8	454: 442,389	492,995	201,203/227,726	88 (282,232)	3,039	
	3.0	454: 529,711	555,328	209,078/234,682	86 (313,550)	2,187	
GS229 14	0.1	S: 10,042	14,326	5,261/4,469	*	*	
	0.8	454: 413,992	458,942	100,045/88,300	228 (22,556)	2,443	
	3.0	454: 453,205	435,534	142,743/129,403	139 (45,083)	2,118	
GS228 18	0.1	S: 9,672	15,077	3,667/3,008	*	*	
	0.8	454: 362,490	389,077	51,312/44,290	29 (1,815)	260	
	3.0	454: 544,302	556,243	186,455/163,878	154 (14,806)	1,334	
GS227 23	0.1	S: 100,085	160,302	33,462/27,302	*	*	
	0.8	454: 482,527	547,170	84,257/73,074	1,136 (51,163)	12,339	
	3.0	454: 553,234	611,717	161,973/137,632	105 (7,904)	825	
TOTAL	-	8,103,379	8,926,759	2,487,574/2,283,749	8,269 (1,771,149)	126,585	

to record depth, dissolved oxygen content, pH, salinity, temperature and turbidity throughout the water column of the lake. Total organic carbon was determined using a total organic carbon analyzer, TOC-5000A (Shimadzu, Kyoto, Japan) equipped with a ASI-5000A auto sampler (Shimadzu), and particulate organic carbon by standard protocols (<http://www.epa.gov/glnpo/lmmmb/methods/about.html>) at the Centre for Water and Waste Technology, UNSW.

2.3.2 DNA extraction, sequencing and data cleanup

DNA extraction and Sanger sequencing was performed on 3730xl capillary sequencers (Applied Biosystems, Carlsbad, CA, USA) and pyrosequencing on GS20 FLX Titanium (Roche, Branford, CT, USA) at the J. Craig Venter Institute in Rockville, MD, USA (Rusch *et al.*, 2007). The scaffolds and annotations will be available via Community Cyberinfrastructure for Advanced Microbial Ecology Research and Analysis (CAMERA) and public sequence repositories such as the NCBI and the reads will be available via the NCBI Trace Archive.

Sanger reads and pyrosequencing reads were trimmed and filtered as described in Lauro *et al.* (2011). See Table 2.1 for a summary of the metagenomic data and sample IDs.

2.3.3 Metagenomic DNA assembly and annotation

Mosaic assemblies were generated for each sample fraction using Celera whole genome shotgun (WGS) Assembler v5.3 (Myers *et al.*, 2000) as described previously (Ng *et al.*, 2010; Lauro *et al.*, 2011). Each 0.1 µm fraction assembly was a hybrid of Sanger and 454 read data. See Table 2.1 for a summary of metagenomic assemblies. Annotation of each sample fraction assembly was carried out using an in-house pipeline described in DeMaere *et al.* (2011), wherein the pipeline stages consisted of genomic feature detection and subsequent annotation by basic local alignment search tool (BLAST) comparison to NR, Swissprot and Kyoto Encyclopedia of Genes and Genomes (KEGG)-peptide sequence databases and by biosequence analysis using profile hidden Markov models (HMMER) comparison against the Institute of Genomic Research curated protein database (TIGRFAM) (Haft *et al.*, 2001), clusters of orthologous groups (COG) (Tatusov *et al.*, 1997, 2003) and known marker genes (von Mering *et al.*, 2007).

2.3.4 Epifluorescence microscopy

Samples of unfiltered lake water and the flow-through from 3.0 and 0.8 µm filters from all depths were collected on November 2008 and fixed on site in formalin 1% (v/v). The samples were stored at –80°C for subsequent direct counts of cells and virus-like particles (VLPs). Enumeration was performed according to the method of Patel *et al.* (2007) with modifications. Lake water samples were filtered onto 0.01 µm pore-size polycarbonate filters (25 mm Poretics, GE Osmonics, Minnetonka, MN, USA). Filters were air dried, then placed with the back of the filter on top of a 30 ml aliquot of 0.1% (w/v) molten low-gelling-point agarose and allowed to dry at 30°C. Samples were stained by the addition of 2 µl working solution (1 in 400 dilution in 0.02 µm filtered sterile Milli-Q) of SYBR Gold (Molecular Probes, Eugene, OR, USA) to 20 µl of mounting medium (VECTASHIELD HardSet, Vector Laboratories, Burlingame, CA, USA). Stained samples were counted immediately. Samples were visualised under wide-blue filter set (excitation 460–495 nm, emission 510–550 nm) with an epifluorescence microscope (Olympus BX61, Hamburg, Germany).

2.3.5 Protein extraction

Proteins were extracted 0.1 µm pore-size membrane filters from the six depths (5, 11.5, 12.7, 14, 18 and 23 m) as described previously (Ng *et al.*, 2010; Ng, 2010; Lauro *et al.*, 2011). Briefly, separate extractions were performed on quarters of the 0.1 µm filters which served as technical replicates. Cells were lysed by three freeze-thaw cycles in liquid nitrogen and sonication in lysis buffer containing 10 mM Tris-EDTA (pH 8), 20 µl of protease inhibitor cocktail VI (Calbiochem), 0.1% sodium dodecyl sulphate, and 1 mM dithiothreitol. Buffer exchange into 10 mM Tris-EDTA (pH 8) and concentration of soluble extracted proteins was performed in a 5 kDa cut-off Amicon Ultra-15 filter unit (Millipore).

2.3.6 1D-SDS PAGE and LC-MS-MS

Extracted proteins were separated by one dimensional-sodium dodecyl sulphate polyacrylamide gel electrophoresis (1D-SDS PAGE) containing 12% SDS using a Mini-PROTEAN system (Bio-Rad, Sydney, NSW, Australia) as described previously (Saunders *et al.*, 2006). Trypsin digestion, liquid chromatography (LC) and mass spectrometry was conducted as described previously (Ng *et al.*, 2010; Ng, 2010; Lauro *et al.*, 2011). Briefly, gel slices were subject to a series of reduction, alkylation and dehydration reactions before digestion of proteins with trypsin. Peptides were separated by high performance liquid chromatography (HPLC) and positive ions generated by electrospray for mass spectra acquisition by the LTQ-FT Ultra mass spectrometer. Peak lists were generated using EXTRACT_MSM from MASCOT DAEMON (Matrix Science, Thermo, London, UK) using the default parameters.

2.3.7 Metaproteomic mass spectra analysis

The spectra generated from mass spectrometry (MS) were searched against the protein sequence database corresponding to that depth constructed from the 0.1 µm mosaic assemblies using MASCOT version 2.1 (Matrix Science). MASCOT DISTILLER (Applied Biosystems) was used as the data import filter with the following criteria applied to the two dimensional mass spectrometry (MS-MS) ion search: a maximum of one missed cleavage for trypsin, peptide mass tolerance of \pm 4 ppm, a fragment mass tolerance of \pm 0.6 Da and variable modifications of acrylamide, carbamidomethyl and oxidation. The number of protein sequences in each database were as follows: 5 m, 138,208; 11.5 m, 133,948; 12.7 m, 27,142; 14 m, 62,436; 18 m, 71,512; and 23 m, 128,878. SCAFFOLD 2.0 (version Scaffold_2.05.01, Proteome Software Inc., Portland, OR, USA) was used to validate MS-MS-based peptide and protein identifications. Peptide and protein identifications were accepted if they could be established at >95% and 99% probability, respectively, as specified by the PEPTIDE PROPHET algorithm (Keller *et al.*, 2002). Protein identifications required the identification of at least two peptides.

Proteins that contained similar peptides and could not be differentiated based on MS-MS analysis alone were grouped to satisfy the principles of parsimony and are referred to as a protein group. Spectral counting was used to semi-quantitatively estimate protein abundance. The total assigned spectra that matched to each identified protein were exported from SCAFFOLD 2.0. For similar proteins that have shared peptides (a protein ambiguity group), spectra were assigned to the protein with the most unique spectra. To normalise for variation in total spectra acquired between sample replicates, the number of spectra of each protein was multiplied by the average total spectra divided by the total spectra of the individual replicate. The spectral count of each protein was averaged across the replicates. As longer proteins are more likely to be detected, the average spectral counts were divided by the length of the protein. This value is equivalent to the normalised spectral abundance factor (Florens *et al.*, 2006; Zybailev *et al.*, 2006). In order to compare the relative abundance of proteins between depths, the normalised spectral abundance factor was divided by the average read depth

of the contig (scaffold or degenerate) to which the protein mapped.

If >90% of a scaffolds length consisted of surrogate (highly degenerate unitig) sequence, the average read depth of the surrogate was used. For identified proteins that were part of a protein group the longest protein length and largest read depth value in the group was used. Pairwise comparisons of each zone were conducted on COG assigned proteins. The normalised spectral counts from each protein was aggregated based on their COG annotation. All proteins that were part of an ambiguity group were confirmed to share the same COG annotation to ensure counts were not biased because of the common spectra.

The summed spectral counts from 5 and 11.5 m (mixolimnion), and 14, 18 and 23 m (monimolimnion) were pooled. Statistical significance of differences between each zone was assessed using Fisher's exact test, with confidence intervals at 99% significance calculated by the NewcombeWilson method and Holm-Bonferroni correction (p-value cutoff of 1e-5) in Statistical Analysis of Metagenomic Profiles (STAMP) (Parks and Beiko, 2010). All proteins identified, including their gene identifier, normalised spectral abundance, COG and KEGG Orthology identifiers, KEGG locus tag and matching COG or KEGG description are provided in Appendix B.

2.4 Results and discussion

2.4.1 Development of an epifluorescence microscopy method

An epifluorescence microscopy method was developed to allow examination of cellular morphology and enumeration of cells and VLPs in Ace Lake. The standard method for cell and VLP counts uses 25 mm diameter 0.02 μm pore-size Anodisc filters (Patel *et al.*, 2007). As mentioned above, the supply of these filters were discontinued in December 2008 (Torrice, 2009), which necessitated development of an alternative protocol.

Clear polycarbonate Track Etch (PCTE) membrane filters were selected for use as a viable alternative product as they have a defined pore-size of sufficiently small diameter (0.01 μm) to capture VLPs. Furthermore, they have been used in earlier studies for VLPs enumeration (Hara *et al.*, 1991; Proctor and Fuhrman, 1992), have a long history of use with the enumeration of cells (Hobbie *et al.*, 1977) and therefore require no new materials to be easily adopted for use. Finally, use of PCTE membranes is approximately 10 times cheaper than the use of Anodiscs and are not subject to drops in availability. However, PCTE membranes have several reported shortcoming that have precluded their standard use for viral enumeration. The 0.01 μm 25 mm PCTE filters are difficult to handle compared to 25 mm Anodisc filters that have a plastic support ring around the edge. Also, PCTE filters appear to have higher background fluorescence, have a slow flow-rate taking ~1–1.5 hours to filter 2 ml (Hara *et al.*, 1991) and have been reported to give VLP counts an order of magnitude lower than that of Anodiscs (Budinoff *et al.*, 2011).

The protocol used is detailed in section 2.3 *Materials and methods* where the main challenges of using PCTE were overcome for the purposes required for this study. 0.01

μm pore-size PCTE filters can form creases or wrinkles when mounted in the vacuum filter holder. Good placement of the PCTE filter was achieved by touching the edge of the PCTE filter against the damp backing filter, making sure it was aligned and then gently and evenly releasing it in a single direction. $0.01\ \mu\text{m}$ pore-size PCTE filters also easily become statically charged and will become attracted to surfaces so careful handling is required during manipulation. The greatest drawback in the use of PCTE filters of such small pore-size is they similarly have a tendency to crinkle when mounted on the glass slide that can make visualisation of cells and VLPs on a single focal plane difficult. Agarose was used to embed the filters to help flatten the membrane and aid in mounting. However, this was not strictly necessary if filters are dried well and pressed flat against the glass slide with a minimal volume of mountant. Even though careful handling is possible, this method likely requires more technical replicates than Anodisc filters because any localised regions with VLPs outside the focal plane will not be counted leading to greater deviation in counts. Furthermore, as similarly reported by Diemer *et al.* (2012) for $0.03\ \mu\text{m}$ PCTE membranes, distribution of VLPs on the membrane appears more variable than for Anodiscs with local regions devoid of VLPs and others with pooling of VLPs. The patchier VLPs distribution was attributed to greater irregularity in pore distribution compared to that of Anodisc filters and was considered to be the main contributing factor to variability in VLP counts (Diemer *et al.*, 2012)

Background fluorescence was at an acceptable level when the SYBR Gold stain is only incorporated into the mountant after filtration rather than staining in the column. This is one key difference between this protocol and others that use PCTE membranes (Hara *et al.*, 1991; Proctor and Fuhrman, 1992; Diemer *et al.*, 2012). Other protocols have used $0.08\ \mu\text{m}$ membranes pre-stained with Irgalan Black (Proctor and Fuhrman, 1992) or $0.03\ \mu\text{m}$ pre-stained with Sudan Black B (Diemer *et al.*, 2012) to minimise background fluorescence. Pre-staining of $0.01\ \mu\text{m}$ membranes would be an option for future optimisation of this protocol.

Only one prior report of filtration of natural water onto the PCTE membranes with $0.01\ \mu\text{m}$ pore-size was found (Hara *et al.*, 1991). Such a small pore-size necessitates a very strong seal of the filter column against the glass base with no air leaks. Leakage was eliminated by sealing the fritted base to the column with laboratory film. However, the slow flow-rate was not a property of these PCTE filters that could be overcome. As the filtration and visualisation was performed on fixed samples in the laboratory rather than in the field, the time taken for filtration of 2–3 hours for each sample was not deemed problematic for the purposes of this study. Counts of VLPs have been shown to decrease dramatically with time even when preserved with aldehyde-based fixatives (Wen *et al.*, 2004). Collecting larger sample volumes and flash freezing in liquid nitrogen and storing at -80°C helps to slow this effect (Patel *et al.*, 2007). Due to logistic constraints of working in the Antarctic, counts in the field were not possible so VLP counts are expected to be underestimated. However, all samples were processed within a similar time frame so the relative VLP abundances down the depth profile and

between size fractions are expected to be accurate as all samples would have undergone comparable amounts of VLP loss.

Overall, a viable alternative method was successfully developed for visualisation and enumeration of cells and VLPs using PCTE membrane filters for use in this study (Figure 2.2). To be a competitive alternative to Anodisc filters in terms of enumeration accuracy, further work is required that compares counts using this method and the current standard Anodisc-based protocol (Patel *et al.*, 2007) with viral samples of known densities.

2.4.2 Size and depth stratification of the community supported by cell and VLP densities

Epifluorescence microscopy images of Ace Lake microbiota showed a clear decrease in larger and particularly filamentous cells between filter size fractions (Figure 2.2). The sequential filtration of suspended microbial biomass from aquatic environments has been utilised as part of the landmark Sargasso Sea metagenomic study (Venter *et al.*, 2004) and GOS expedition (Rusch *et al.*, 2007). The Ace Lake samples were collected using the same sampling strategy as the GOS dataset but has sequence information from all three filter sizes and was able determine if size fractionation is effective at separating the microbial community and if functional differences are associated with size. Both taxonomic and functional gene composition were shown in the metagenomic analysis to differ significantly with size fraction and is indicative of resource partitioning in the community (Lauro *et al.*, 2011). The clear difference between the size fractions indicated the sequential filtration process is an effective means to separate the community and that different sized populations in the community have different ecological roles. For example, *Flavobacteria* were only detected in the 3.0 μm size fraction mixolimnion metagenomes and were inferred to be involved in mineralisation of particulate matter (Lauro *et al.*, 2011). This correlates with the absence of long rod shaped cells in the >0.8 μm microscopic image (Figure 2.2) indicating these larger cells are likely to be copiotrophic *Flavobacteria* involved in degradative processes. Depth was another variable which strongly drove differences in the Ace Lake community (Lauro *et al.*, 2011). This was again evident in the microscopy images that show the appearance of long filamentous cells only in the 12.7 m and monimolimnion samples (Figure 2.2).

Cell and VLP densities are not obtainable from metagenomic sequence data and necessitates an independent method of determination. The first studies to determine viral densities in natural systems found that viruses are the most numerous biological entities on the planet and likely play a large role in plankton mortality in the ocean (Bergh *et al.*, 1989; Proctor and Fuhrman, 1990). VLP counts from marine environments vary with depth and trophic status ranging from 10^6 to 10^8 VLP ml^{-1} (Suttle, 2005). Both cellular and VLP counts are linked with environmental factors such as trophic status (Lauro *et al.*, 2009). Enumeration of cells and VLPs in Ace Lake showed cell densities were lowest in the relatively oligotrophic mixolimnion ($0.8\text{--}1.3 \times 10^6$ cell ml^{-1}) and were by an order of magnitude higher in the copiotrophic monimolimnion

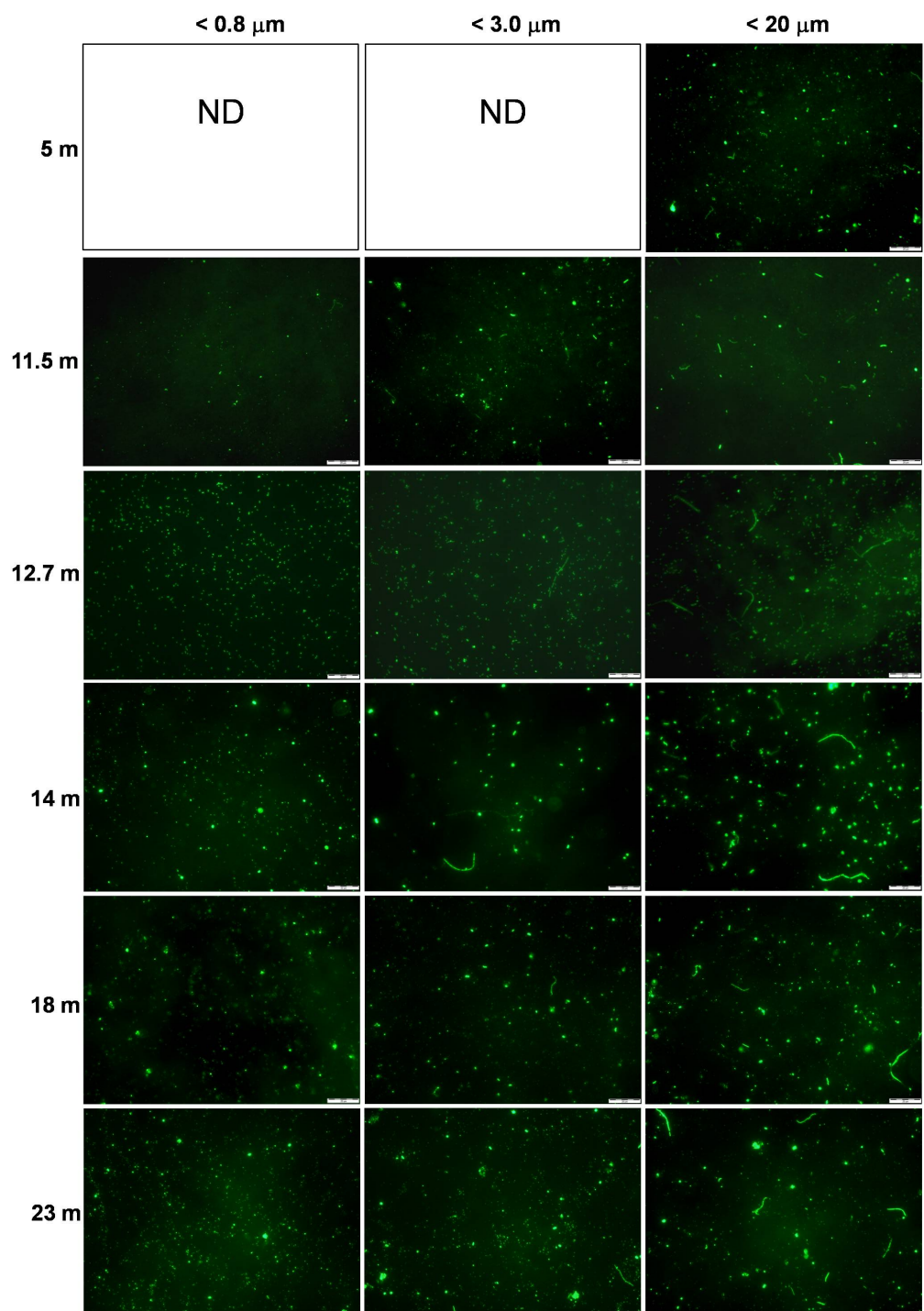


Figure 2.2: Epifluorescence microscopy images of Ace Lake microbiota. Scale bar = 20 μm . ND, not determined.

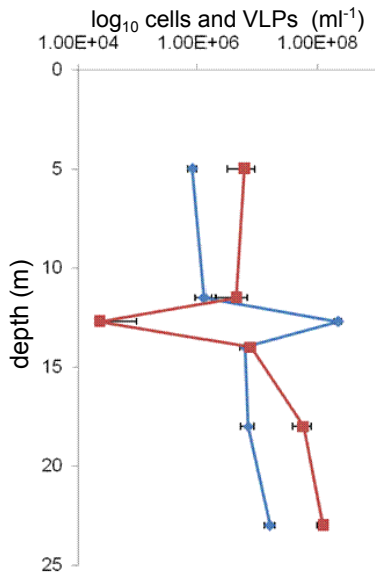


Figure 2.3: Counts of microbial cells (blue) and VLPs (red) by epifluorescence microscopy along a depth profile of Ace Lake. Error bars represent one standard deviation. No VLPs were detected at 12.7 m depth and the value reported represent the detection limit of the counting procedure (*i.e.* one VLP detected in one field of view).

(1.6×10^7 cell ml⁻¹ in the 23 m sample) (Figure 2.3). Cell densities were highest at 12.7 m (2.2×10^8 cells ml⁻¹) corresponding to the GSB layer.

VLP abundance was consistently higher than the cellular counts but the ratio of VLP to cells ranged throughout the water column from ~ 1 –8.5. The exception to this was the 12.7 m where there was an unusual lack of VLPs (Figure 2.3). These data corresponded with the metagenomic data from 12.7 m that found no viral signatures associated with the GSB at the chemo/oxycline (Lauro *et al.*, 2011). From metagenomic data alone the absence of viral signatures in the metagenome does not preclude the presence of viruses with ssDNA or RNA genomes that would not be detected by DNA sequencing method used. Epifluorescence microscopy using SYBR Gold nucleic acid stain would in principle detect VLPs containing non-dsDNA genomes (Patel *et al.*, 2007) that would otherwise be missed in the metagenome. Figure 2.4 contrasts the epifluorescence images of water from 5 m sample with the 12.7 m sample confirming the lack of visible VLPs in the latter. This provided independent support that the GSB population in Ace Lake represents an exception to viral–bacterial population dynamics that describes high rates of genotype cycling in aquatic systems (Rodriguez-Brito *et al.*, 2010).

2.4.3 Development of a metaproteomic mass spectra analysis workflow

The general shotgun proteomics workflow in Figure 2.5 shows that apart from successful sample preparation to simplify the complex protein mixture, protein identification depends greatly upon the post-MS bioinformatic analysis. This is due to how the MS-MS data are used to identify proteins (see Marcotte (2007) for a primer on shotgun

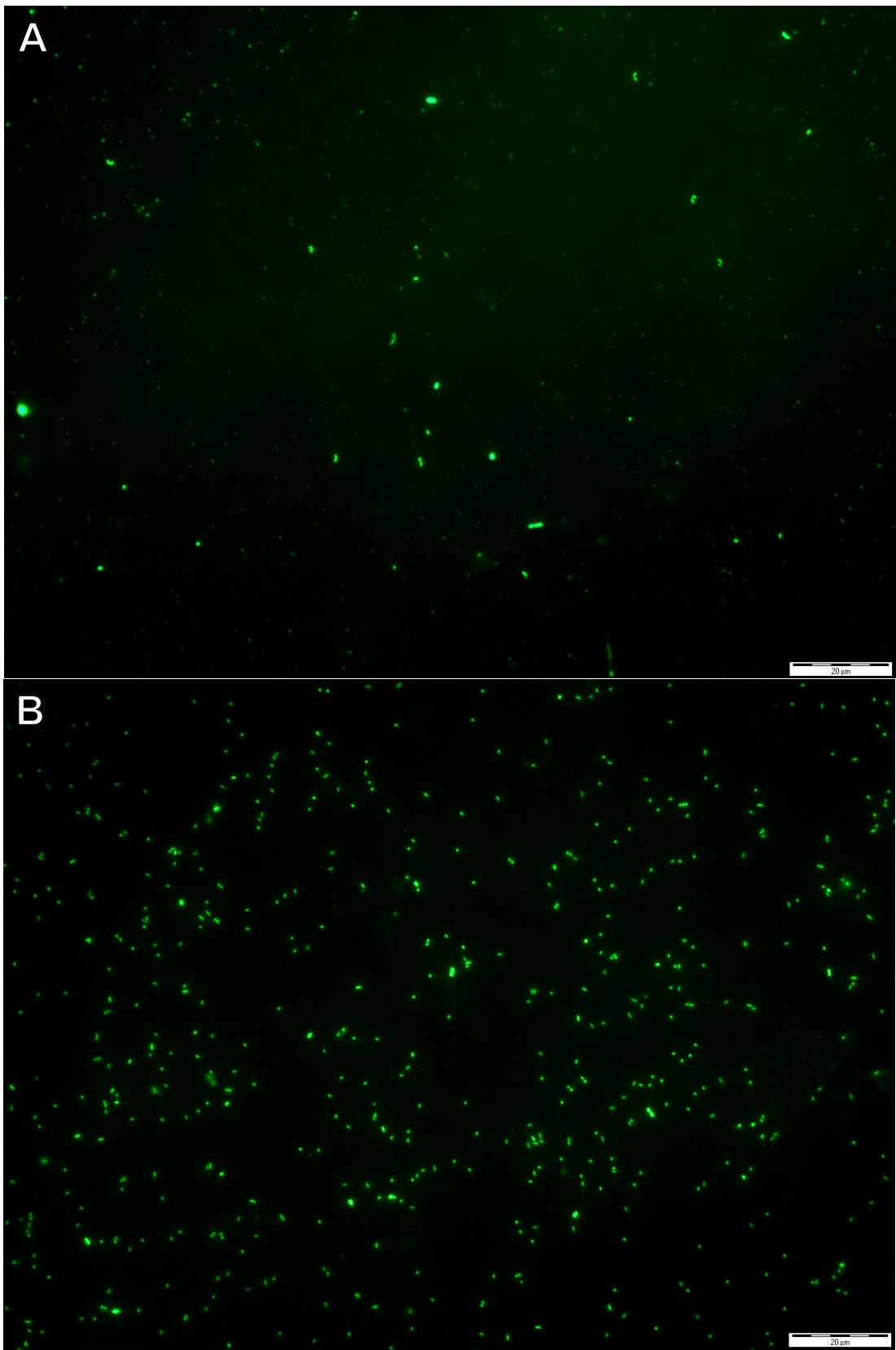


Figure 2.4: Epifluorescence microscopy images contrasting Ace Lake water samples from (A) 5 m and (B) 12.7 m. Numerous VLPs are evident in the 5 m sample, but not in the 12.7 m sample. Scale bar = 20 μ m.

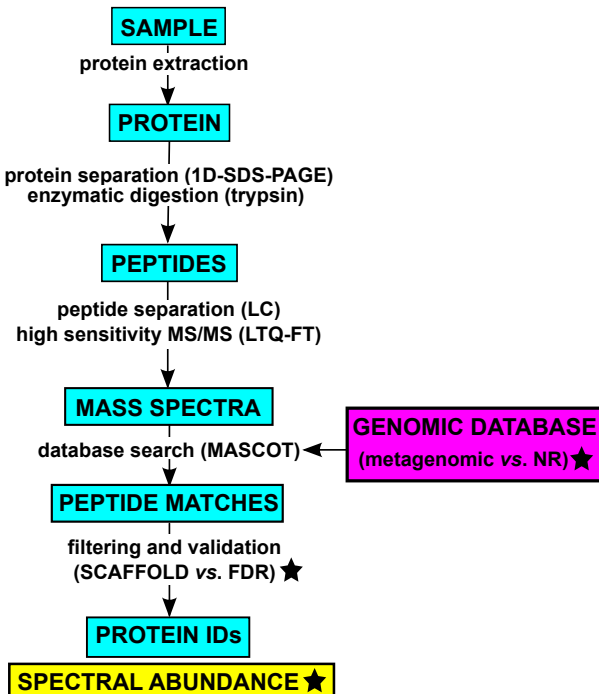


Figure 2.5: A general shotgun proteomics workflow showing how proteins are identified. The procedures or materials used in this study are specified in parentheses. The steps in the workflow that were developed in this study are marked with a star.

proteomic identification).

Briefly, the peptides from digested proteins are separated by LC and subject to a round of mass spectra acquisition where the mass of the peptides (precursor ions) are detected. Selected peptides undergo collision-induced dissociation where they fragment preferentially at the peptide bond. A second round of mass spectra is acquired of the peptide fragments (fragment ion spectra) that represents the amino acid sequence of the peptide. An *in silico* enzymatic digestion is performed on a genomic database to predict the precursor ion masses and their corresponding fragment ion spectra. The fragment ion spectrum and precursor ion mass is used to determine the most likely amino acid sequence of the peptide by comparison to the genomic database and thereby identify the protein(s) of origin. Since spectral matching depends on extremely high mass sensitivity, the ideal genomic database contains complete coverage of sequences from the organism(s) from which the proteins originated. A single amino acid change is sufficient for a peptide match to fail although matching is tolerant to synonymous changes.

Previous metaproteomic analysis was conducted on the 0.1 μm fraction samples along the depth profile of Ace Lake using NR as the search database (Ng, 2010) as metagenomic data were not yet available. The use of a cross-species database requires the genomes to be sufficiently related to identify proteins and application of stringent statistical cut-off to avoid false-positive matches. Across all six samples, a total of 10,443 peptides were identified corresponding to 308 proteins from \sim 400,000 MS-MS spectra (Ng, 2010). Rates of protein identification were low compared to a similar

metaproteomic analysis of the Sargasso Sea, which achieved a total of 5,501 peptide identifications corresponding to 1,042 proteins from ~30,000 MS-MS spectra (Sowell *et al.*, 2009). This indicated that most peptide sequences from Ace Lake were too different from the NR database for protein identification by spectral matching. A key difference in the Sargasso Sea study was the inclusion of metagenomic sequence in the search database from their target populations of SAR11, *Synechococcus*, and *Prochlorococcus* (Sowell *et al.*, 2009). The low identification rate was to be expected as it has been shown that only half the number of proteins are identifiable when using a genomic database that shares 90% amino acid identity with the matching genome (Denef *et al.*, 2007).

Once the metagenomic sequence for the GSB layer became available, re-analysis of the mass spectra to the matched GSB metagenome was performed as this sample had the lowest genomic complexity and was expected to obtain high identification rates (Ng *et al.*, 2010; Ng, 2010). In the re-analysis, 3,970 peptides were identified, mapping to 504 proteins from ~100,000 spectra, which was a near 3-fold increase in the number of protein identifications (Ng *et al.*, 2010; Ng, 2010). This indicated a similar increase in protein identifications could be achieved with the other Ace Lake samples. However, metagenomic sequence from more diverse communities adds additional bioinformatic considerations for protein matching due to their inherently greater heterogeneity. For a protein to be identified according to standard stringency cut-offs it requires at least two peptides to be mapped to it with at least one of those being unique. The converse of this is that it allows for the fact there are potentially non-unique peptides shared by other proteins. Although shared peptides occur between proteins in single genomes, a typical metagenome will contain related species or strains and therefore many more copies of closely related proteins. Protein identification scores in the focussed GSB study was also set to only accept identifications above a determined false discovery rate (FDR). This is the score given by a peptide match to a randomised version of the genomic database (Ng *et al.*, 2010; Ng, 2010).

To address the additional challenges posed by higher diversity metagenomic data, the program SCAFFOLD 2.0 was adopted for the filtering and validation of peptide and protein matches (Figure 2.5). Instead of determining a FDR, SCAFFOLD 2.0 employs the PEPTIDE PROPHET algorithm (Keller *et al.*, 2002) for protein validation. This algorithm fits a distribution of scores from correct and in-correct peptide matches and from this calculates the probability that each result is a genuine match (Keller *et al.*, 2002). More importantly, it identifies groups of proteins that cannot be distinguished based on unique peptides and so accepts all of those proteins in the group may be present in the sample. Two classes of these groups were defined: (1) protein groups, which are proteins with shared peptides that were indistinguishable from the mass spectral analysis and (2) protein ambiguity groups, which are proteins that have some shared peptides. SCAFFOLD 2.0 also facilitates the estimation of protein abundances from spectral counts based on the assumption that proteins that are more abundant will produce more mass spectra. Spectral counting is only semi-quantitative as differences

Table 2.2: Comparison of the number of peptides/proteins identified in the Ace Lake 0.1 μm size fraction metaproteomes using NR vs. matched metagenomic databases. Peptide and protein identifications using NR recorded from Ng (2010). metag, metagenomic database; *a*Proteins identified using SCAFFOLD 2.0; *b*Proteins identified using a FDR.

Depth (m)	Spectra	Spectra matched (%) (metag)	Peptide IDs (metg)	Protein IDs (metag)	Peptide IDs (NR)	Protein IDs (NR)
5	71,201	10,843 (15)	5,728	501	862	15
11.5	53,078	6,076 (11)	3,213	224	327	10
12.7	127,697	29,578 (23)	12,718	505a/504b	4,611	169
14	100,650	9,008 (9)	3,427	369	2,124	102
18	131,800	1,520 (1)	725	101	935	11
23	232,797	3,648 (2)	1,602	124	1,584	1
TOTAL	717,223	60,673 (8)	27,413	1,824	10,443	308

between low abundance proteins becomes difficult to gauge. Also, peptides likely have some intrinsic biases in their ionisation and fragmentation efficiencies. For this purpose, defining the protein groups, particularly the ambiguity groups, becomes relevant as it provides a framework to decide how to allocate spectral counts in protein ambiguity groups where spectra are shared. To find statistically significant differences in protein abundances by spectral counting, several normalisation steps had to be incorporated into the metaproteomic analysis workflow and were implemented using in-house scripts developed specifically for this analysis. Differences in the normalised protein abundances from each zone of Ace Lake were then tested using the statistical program STAMP. The steps in the final workflow is detailed in section 2.3 *Materials and methods*.

The final analysis workflow was applied to all the Ace Lake metaproteomic mass spectra datasets. Appendix B lists all proteins identified in Ace Lake using the modified workflow. Identification rates were significantly higher using the matched metagenomic database compared to NR with a 6-fold increase in total proteins identified (Table 2.2). Mass spectra re-analysed from the 12.7 m GSB layer using the modified metaproteomic workflow showed only one additional protein identification (Table 2.2). This indicates that the SCAFFOLD 2.0 protein validation algorithm is as stringent as FDR cut-offs when dealing with lower diversity samples. In addition, 125 of the 505 protein identifications were identified by SCAFFOLD 2.0 to be protein groups (Table B.3). In other words, those mass spectra mapped to two or more proteins making it impossible to distinguish which of those possible proteins were expressed. 11 proteins were also found to be part of an ambiguity group and thus shared peptides with other proteins in the sample (Table B.3). By tracking protein groups, SCAFFOLD 2.0 flags proteins that require an additional validation step, which is to verify if all members of the group have the same functional annotation. All protein groups in the 12.7 m sample that were annotated had identical designations indicating they likely had the same function. The outcomes of the inclusion of spectral counting in the metaproteomic workflow is detailed below.

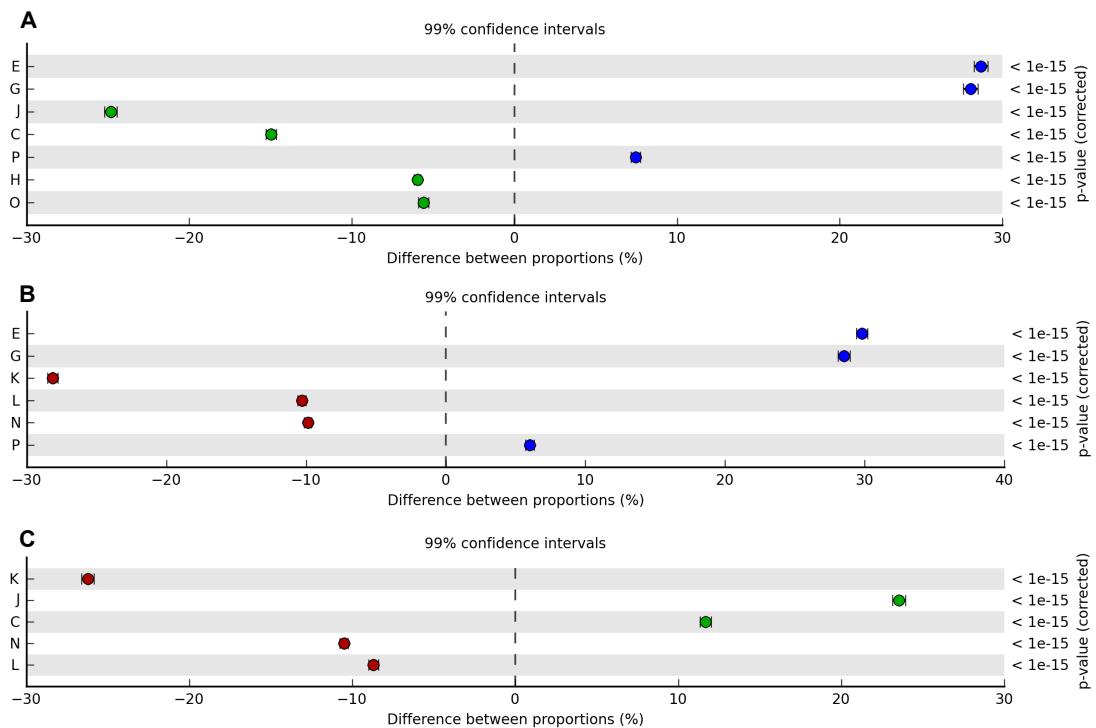


Figure 2.6: Statistical analysis of normalised mass spectra from COG annotated protein between each zone in Ace Lake. Proteins are shown grouped into COG categories. Only categories with corrected p-values <0.05 and effect size >5 are displayed. (A) Mixolimnion compared to chemo/oxycline. (B) Mixolimnion compared to monimolimnion. (C) Chemo/oxycline compared to monimolimnion. Blue, mixolimnion; green, interface; red, monimolimnion. COG category descriptions are: E, amino acid transport and metabolism; G, carbohydrate transport and metabolism; J, translation, ribosomal structure and biogenesis; C, energy production and conservation; P, inorganic ion transport and metabolism; H, co-enzyme transport and metabolism; O, post-translational modification, protein turnover and chaperones; K, transcription; L, replication, recombination and repair; N, cell motility.

2.4.4 Insights from the metaproteomic analysis of Ace Lake

Metaproteomic identifications were able to support biological inferences about each zone in the Ace Lake community. Functions defining each zone was indicated at a broad level by overrepresentation of proteins groups assigned to COG categories (Figure 2.6). This gave an indication of how functional processes were separated with depth. Large numbers of functionally annotated proteins could also be clearly linked to taxonomic groups allowing their contribution to lake ecosystem function and their evolution within the Ace Lake community to be inferred.

Mixolimnion

The most abundant proteins in the mixolimnion were assigned to transport functions from COG categories (E) amino acid transport and metabolism, (G) carbohydrate transport and metabolism and (P) inorganic ion transport and metabolism (Figure 2.6). Most of the protein identifications could be related to taxonomic groups as well as pro-

tein families. The transporters were predominately ATP-binding cassette (ABC) type, with a high COG representation of transporters for carbohydrates (~34% of normalised spectra), amino acids (~32%) and inorganic ions (~9%) (Figure 2.6, Table B.1, Table B.2). The prevalence of amino acid and simple sugar transporters and the low dissolved organic carbon (DOC) concentration in the Ace Lake mixolimnion (Figure 2.1) is likely to reflect efficient utilisation of these substrates from the DOC pool. Thus, examination of the expressed transport proteins may better indicate substrate preferences and nutritional requirements than measurements of nutrient availability.

All transporters in the metaproteome were of bacterial origin and conservative phylogenetic level assignments of the normalised spectral abundance showed the majority to originate from *Proteobacteria* (69%) (of which SAR11 comprised 46%) and *Actinobacteria* 19% (Table B.1, Table B.2). A high proportion of expressed genes with transport functions have also been reported for SAR11 from coastal (Poretsky *et al.*, 2010) and open ocean waters (Sowell *et al.*, 2009; Morris *et al.*, 2010). Oligotrophs, such as SAR11 not only possess a low-diversity of high-affinity transporters (Lauro *et al.*, 2009), but regulate the relative abundance of transporters expressed in response to DOC availability (Poretsky *et al.*, 2010). The transporter expression profile of the Ace Lake SAR11 was very similar to that of the SAR11 in the Sargasso Sea (Sowell *et al.*, 2009). Two SAR11 transport proteins that were detected in Ace Lake (Table B.1, Table B.2) were not detected in the Sargasso Sea (Sowell *et al.*, 2009): an ectoine/hydroxyectoine (167807477 and 167892279) and a zinc ABC transporter (167933120). Ectoine is a compatible solute and presence of the ectoine transporter indicates it is more available in Ace Lake than in the ocean, potentially in response to higher variability in salinity or low temperature. The zinc ABC transporter is likely to support zinc efflux in response to zinc concentrations which are ~70-fold higher in the mixolimnion of Ace Lake compared to seawater (Rankin *et al.*, 1999). Conversely, phosphate transporters were a major class detected from the Sargasso Sea (Sowell *et al.*, 2009) but were absent from the Ace Lake metaproteome consistent with lower phosphate levels in the Sargasso Sea (<5 nM) compared to Ace Lake (1–12 µM). The differences in transporter expression between Ace Lake and oceanic SAR11 are likely to signify adaptive growth strategies that have evolved in the Ace Lake SAR11 community.

Actinobacteria sequences were associated with a diverse phylogenetic cluster (Luna cluster) mainly represented by freshwater ultramicrobacteria (Hahn *et al.*, 2003). Several Luna cluster isolates contain rhodopsin genes, termed actinorhodopsins (Sharma *et al.*, 2009) and similar gene sequences were present in the Ace Lake oxic zone data and found to be expressed (167820670 and 163154474; Table B.1, Table B.2). This was the first report of expression of these actinorhodopsin sequences. The abundance of *Actinobacteria* transporters along with their small cell size and distribution in the water column indicates they occupy a similar ecological niche as SAR11. SAR11 contains proteorhodopsin, which is a related to actinorhodopsin (Sharma *et al.*, 2009). Although the physiological role of proteorhodopsin in SAR11 is yet to be fully elucidated (Fuhrman *et al.*, 2008), this provides some indication actinorhodopsins in Antarctic Luna cluster

Actinobacteria have a related functional role.

Chemo/oxycline

Proteins from the chemo/oxycline were almost all of GSB origin (Table B.3). An in-depth metaproteogenomic analysis of the GSB metabolism has been described (Ng *et al.*, 2010; Ng, 2010). Comparative analysis of proteins between the lake strata showed this depth was more similar to the monimolimnion than the mixolimnion (Figure 2.6). Compared with the mixolimnion, COG categories (J) translation, ribosomal structure and biogenesis; (C) energy production and conservation; (H) co-enzyme transport and metabolism and (O) post-translational modification, protein turnover and chaperones were overrepresented, whereas in comparison with the monimolimnion, only categories J and C were significantly overrepresented. This difference was likely due to the presence of sedimenting GSB cells in the monimolimnion. Nonetheless, overrepresentation of J and C categories indicates it is the GSB population at the chemo/oxycline that is the most metabolically active and productive in the whole lake community. The overrepresentation of category C is similarly evident in the metagenomic comparison of functional genes whereas category J is not (Lauro *et al.*, 2011). This indicates differences in the regulation of energy metabolism compared to protein translation in GSB.

Both metagenomic and microscopic analysis of the GSB layer has indicated the population lacks viruses. Mathematical modeling predicted that the absence of virus predation in the GSB could be an adaptation to longer cycles of growth and inactivity in response to the polar light regime (Lauro *et al.*, 2011). A mechanism for how virus resistance may be conferred in the population was suggested in the metaproteome. Abundant clustered regularly interspaced short palindromic repeat (CRISPR) associated CRISPR-associated proteins (CAS) proteins Cse2, Cse3 and Cse4 (165526330, 165526332 and 165526334, respectively) were detected in the 12.7 m metaproteome (Table B.3). The CAS gene locus (cas3, cse1, cse2, cse3, cse4, cas5, cas1b), to which the proteins map, shares its organisation with CAS loci of sequenced GSB, and groups with the *E. coli* subtype/variant 2. The CRISPR/CAS system has been shown in other organisms to mediate virus resistance (Karginov and Hannon, 2010; Horvath and Barrangou, 2010) and is likely to have a similar function in the Ace Lake GSB.

Monimolimnion

In parallel with taxonomic diversity increasing with depth, with the exception of the GSB layer, the rate of metaproteomic identification of proteins decreased with depth (Table 2.2). Coverage of genomic information and degree of sequence assembly from the more diverse monimolimnion was not as high as for the mixolimnion or the chemo/oxycline. This means that more peptides in the monimolimnion than in the other depths mapped to fragmentary or absent metagenomic data and failed to be identified. Annotated proteins in the monimolimnion were overrepresented in COG categories (K) transcription; (L) replication, recombination and repair and (N) motility

(Figure 2.6). Categories L and N were similarly overrepresented in the monimolimnion metagenomic samples (Lauro *et al.*, 2011) demonstrating the genomic expansion of these functions correlated with higher abundance of these proteins. However, differential abundance was greatest in the category K proteins, which showed little difference in relative abundance in the metagenomes (Lauro *et al.*, 2011) suggesting transcription proteins in the monimolimnion were up-regulated (Figure 2.6). The majority of the proteins that were detected in the monimolimnion (e.g. 67% at 23 m) (Table B.6) were for hypothetical proteins that tended to lack orthologues in well-characterized organisms. This demonstrates the extremely high level of functional novelty in the anaerobic zone of the lake. These hypothetical proteins represent potential targets for protein expression studies to determine their functional properties.

2.5 Conclusions

In this study an epifluorescence microscopy and a metaproteomic analysis workflow were developed that were able to address two key areas that metagenomics sequencing alone does not. The first of these was determining the density of cells and VLPs and assessment of gross morphology. The counts and microscopy images validated the size fractionation procedure, showed the stratification of the lake populations with depth and suggested the unusual absence of VLPs in association with the GSB layer. As a lack of viral signatures was observed by both microscopy and metagenomic analysis in the GSB layer, this provided independent lines of support that viruses were indeed absent or rare. The second was identifying which proteins were expressed by the microbial community. The bioinformatic analysis workflow specifically tailored to analyse metaproteomic mass spectral data afforded an increase in protein identifications, identified proteins with shared peptides and enabled estimation of protein abundances by spectral counting. This identified differences in the functional complement between the three strata of the lake. The mixolimnion was shown to be dominated by transporter proteins; the chemo/oxycline by energy production and biosynthetic functions; and the monimolimnion by proteins involved in transcription, replication, recombination and motility. In the lower complexity mixolimnion and chemo/oxycline samples better designations of protein functions and clear links to their taxonomic origins were possible. These provided insights into substrate usage of the dominant aerobic bacterial populations and specific adaptations to the Antarctic lake environment compared to the ocean and suggested mechanism for virus resistance in the GSB. Both the microscopic and metaproteomic analyses have added crucial information to the metagenomic datasets allowing for an integrative understanding of the whole lake ecosystem. Furthermore, these have been applied to subsequent studies of Organic Lake described in chapters 3 and 4.

Chapter 3

Virophage control of Antarctic algal host–virus dynamics

Co-authorship statement

A version of this chapter has been published as:

Sheree Yau, Federico M. Lauro, Matthew Z. DeMaere, Mark V. Brown, Torsten Thomas, Mark J. Raftery, Cynthia Andrews-Pfannkoch, Matthew Lewis, Jeffrey M. Hoffman, John A. Gibson, and Ricardo Cavicchioli. Virophage control of antarctic algal host–virus dynamics.

Proceedings of the National Academy of Sciences USA 108:6163–6168, 2011.

Contributions to this publication by other researchers is as follows. Research was designed and the manuscript edited by Federico Lauro, Mark Brown, Torsten Thomas, John Gibson and Ricardo Cavicchioli. Sample collection was performed by Federico Lauro, Mark Brown, Torsten Thomas, Jeffrey Hoffman and Ricardo Cavicchioli. DNA extraction and clone library preparation of 2006 samples was performed by Cynthia Andrews-Pfannkoch and Jeffery Hoffman. DNA sequencing quality control was performed by Matthew Lewis. Metagenomic sequence filtering, global assembly and annotation was performed by Matthew DeMaere. Assistance in mass spectrometry was provided by Mark Raftery. Assistance in analysis of eucaryal taxonomy was provided by Mark Brown. Analysis of virophage abundance over time was performed by Federico Lauro.

Apart from these contributions, I performed all other data analyses, interpretations and drafted the manuscript.

3.1 Abstract

Viruses are abundant ubiquitous members of microbial communities, and in the marine environment affect population structure and nutrient cycling by infecting and lysing primary producers. Antarctic lakes are microbially dominated ecosystems supporting truncated food webs where viruses exert a major influence on the microbial loop. Here we report the discovery of a new virophage (relative of the recently described Sputnik virophage) that preys on phycodnaviruses that infect prasinophytes (phototrophic algae). By performing metaproteogenomic analysis on samples from Organic Lake, a hypersaline meromictic lake in Antarctica, complete virophage and near-complete phycodnavirus genomes were obtained. By introducing the virophage as an additional predator of a predator-prey dynamic model we determine that the virophage stimulates secondary production through the microbial loop by reducing overall mortality of the host and increasing the frequency of blooms during polar summer light periods. Virophages remained abundant in the lake two years later, and were represented by populations with a high level of major capsid protein sequence variation (25–100% identity). Virophage signatures were also found in neighbouring Ace Lake (in abundance), and in two tropical lakes (hypersaline and fresh), an estuary, and an ocean upwelling site. These findings indicate that virophages regulate host–virus interactions and influence overall carbon flux in Organic Lake, and play previously unrecognised roles in diverse aquatic ecosystems.

3.2 Introduction

It has been known for at least 20 years that viruses frequently infect and lyse marine primary producers causing up to 70% of cyanobacterial mortality (Proctor and Fuhrman, 1990; Suttle *et al.*, 1990). Eucaryotic phytoplankton are preyed upon by large dsDNA phycodnaviruses (PVs) causing bloom termination in globally distributed species (Nagasaki *et al.*, 1994; Jacobsen *et al.*, 1996; Wilson *et al.*, 2002; Martínez-Martínez *et al.*, 2007). Elevated levels of dissolved organic carbon (DOC) (Eberlein *et al.*, 1985) and numbers of heterotrophic bacteria (Davidson and Marchant, 1992; Bratbak *et al.*, 1998; Castberg *et al.*, 2001) occur during algal blooms indicating that viral lysis of eucaryotic algae stimulates secondary production. Viruses also suppress host populations at concentrations below bloom-forming levels, with abundance being controlled by the efficiency and production rates of the infecting viruses (Larsen *et al.*, 2001; Bouvier and del Giorgio, 2007). Antarctic lakes are microbially dominated ecosystems supporting few, if any metazoans in the water column (Laybourn-Parry, 1997). In these truncated food webs, viruses are expected to play an increased role in the microbial loop (Madan *et al.*, 2005). Low complexity Antarctic lake systems are amenable to whole community based molecular analyses where the role that viruses play in microbial dynamics can be unravelled (Lauro *et al.*, 2011). Attesting to this, a metagenomic study of Lake Limnopolar, West Antarctica uncovered a dominance of eucaryotic viruses and ssDNA viruses previously unknown in aquatic systems (López-Bueno *et al.*, 2009).

Organic Lake is a shallow (~7 m) hypersaline (~230 g L⁻¹ maximum salinity) meromictic lake in the Vestfold Hills with a high concentration of dimethylsulphide (DMS) (~120 µg L⁻¹) in its bottom waters (Gibson *et al.*, 1991; Roberts *et al.*, 1993). Water temperature at the surface of the lake can vary from -14 to +15°C while remaining sub-zero at depth (Franzmann *et al.*, 1987b; Gibson, 1999). The lake is eutrophic, with organic material sourced both from autochthonous production and potential input from penguins and terrestrial algae. The high concentrations of organic material reflect slow breakdown in the highly saline lake water. The salt in the lake was trapped along with the marine biota when the lake was formed due to falling sea level ~3,000 BP (Bird *et al.*, 1991; Zwart *et al.*, 1998). Low species diversity (Shannon-Weaver diversity: 1.01) and richness (Chao non-parametric index: 32 ± 12) has been reported for the sediment community (Bowman *et al.*, 2000a). Unlike high latitude lakes, viral abundance has been reported to increase with trophic status (Madan *et al.*, 2005) and with salinity in Antarctic lakes (Laybourn-Parry *et al.*, 2001).

In order to functionally characterise its microbial community, a metaproteogenomic program for Organic Lake was established. This study reports the analysis of the surface water of Organic Lake, highlighting the presence of a relative of the recently described Sputnik virophage, a small eucaryotic virus that requires a helper *Acanthamoeba polyphaga* mimivirus (ApMV) to replicate (La Scola *et al.*, 2008). From metagenomic DNA, a complete Organic Lake virophage (OLV) genome was constructed (the second virophage genome to be described), and near-complete genomes of its probable helper Organic Lake phycodnavirus (OLPV).

3.3 Materials and methods

3.3.1 Samples and DNA sequencing

Water samples collected from Organic Lake were: 1) Surface water from the eastern side of the ice-free lake ($68^{\circ}27'25.48''S$, $78^{\circ}11'28.06''E$) December 24, 2006. 2) A depth profile collected through a 30 cm hole drilled through the surface ice above the deepest point in the lake ($68^{\circ}27'22.15''S$, $78^{\circ}11'23.95''E$), November 10, 2008. 3) Surface water from the north-east side of the partially ice-covered lake ($68^{\circ}27'21.02''S$, $78^{\circ}11'42.42''E$), December 12, 2008. Samples were sequentially filtered through a 20 μm pre-filter and biomass captured onto 3.0, 0.8 and 0.1 μm membrane filters as described previously (Ng *et al.*, 2010; Lauro *et al.*, 2011). The samples from 2008 also included 50% (v/v) RNAlater. DNA extraction, sequencing and quality validation was performed as previously described (Ng *et al.*, 2010; Lauro *et al.*, 2011). DNA sequencing was performed at the J. Craig Venter Institute in Rockville, MD, USA.

3.3.2 Transmission electron microscopy

Unfiltered Organic Lake surface water from December 24, 2006 (fixed on-site in 1% (v/v) formalin) was concentrated and a solvent exchange performed with sterile filtered ammonium acetate solution 1% (w/v) using a 50 kDa cut-off Microcon centrifugal filter device (Millipore) according to the manufacturers instructions. Formvar coated 200 mesh copper grids were floated on a droplet of sample for 30 min, excess liquid wicked off and the grid negatively stained for 30 s with uranyl acetate 2% (w/v). The sample was visualised using a JEOL1400 transmission electron microscope at 100 kV at 150,000 to 250,000 \times magnification.

3.3.3 Metagenomic assembly and annotation

Mosaic metagenomic assemblies were generated as previously described (Ng *et al.*, 2010; Lauro *et al.*, 2011). For the 0.1 μm Organic Lake 2006 sample, assembly was a hybrid of Sanger and 454 read data (Table 3.2). For all other sample size fractions, runtime parameters used were standard for 454 sequencing data. Low GC ($\geq 51\%$) scaffolds >10 kbp from the 0.1 μm 2006 assembly had high coverage ($>45\times$) indicating these were from the dominant taxa. One of these scaffolds was binned as virophage and the rest as PV.

To further separate the OLPV types and assess the completeness of their genomic content, highly conserved single copy PV orthologues were identified as follows. An all against all basic local alignment search tool (BLAST) search was conducted with protein sequences from the ten available PV genomes (*Acanthocystis turfacea* chlorella virus 1, PbCV-1, PbCV AR158, PbCV FR483, PbCV NY2A, *Emiliania huxleyi* virus 86, *Ectocarpus siliculosus* virus 1, *Feldmannia* sp. virus, *Ostreococcus* virus 5, *Ostreococcus tauri* virus 1 and ApMV (which was included as a close PV relative). BLASTp results were parsed and clustered using ORTHOMCL V1.4 (Li *et al.*, 2003; Chen *et al.*, 2006).

Table 3.1: List of primers used to close the OLV genome. Dir, direction.

Primer function	ID	Dir.	Sequence (5'-3')	Length (bp)
Outer gap spanning	SY11	forward	TTG TCT TAT GTA TTA CAA ATC ATT GAA	3,843
Outer gap spanning	SY12	reverse	CGA CAT TAA TCG GTT GTT TT	
Nested gap spanning	SY13	forward	GCA TTA CGA ATG TGT TCC AG	3,403
Nested gap spanning	SY14	reverse	TTC TCC GTG ATT GAT ATC GT	
Sequencing	SY23	forward	TCC CTA TTG ATG TCA AAA CC	-
Sequencing	SY24	forward	GAT TCT GGT TGG AGC ATA TAT TT	

Pairs of each orthologue were located on eight of the PV scaffolds. The location of each orthologue pair had a complementary distribution so the eight scaffolds were able to be sorted unambiguously into two strains (OLPV-1 and OLPV-2). OLPV-1 ribonucleotide reductase α -subunit appeared as duplicated on different scaffold ends, likely as an artefact of its proximity to an assembly break point. The remaining high coverage scaffolds were searched for predicted proteins present in one OLPV strain but not in the other and assigned to the strain in which it was absent. Comparison of OLPV-1 and OLPV-2 scaffolds was performed using tBLASTN of concatenated scaffolds from each strain and visualised using the Artemis comparison tool (ACT) (Carver *et al.*, 2005). DNA sequence data is available in Genbank and Community Cyberinfrastructure for Advanced Microbial Ecology Research and Analysis (CAMERA) (<http://web.camera.calit2.net>).

3.3.4 Organic Lake virophage genome completion and annotation

The high coverage ($77\times$), large number of Sputnik homologues that encode essential functions and length of the putative OLV scaffold from the $0.1\text{ }\mu\text{m}$ 2006 hybrid assembly indicated it was a near-complete genome. Reads from this scaffold were reassembled at high stringency and visualised using PHRED/PHRAP/CONSED (Gordon, 2004) to complete the sequence. Mate-pair data indicated a circular molecule and primers were designed to span the ends of the scaffold and sequence across the gap (Table 3.1).

Touch-down polymerase chain reaction (PCR) was performed with DNA from $0.1\text{ }\mu\text{m}$ 2006 sample, the product used for nested PCR and the final product was cloned and sequenced. The complete genome was manually annotated and visualised using ARTEMIS (Rutherford *et al.*, 2000). Translated open-reading frames (ORFs) (minimal size 120 amino acids) were compared (BLASTP) to GenBank, to the all metagenomic ORF peptide database on CAMERA (<http://web.camera.calit2.net>) and to predicted proteins from OLPV-1 and OLPV-2 scaffolds. Comparisons between the OLV genome and OLPV-1/OLPV-2 were performed with tBLASTN and visualised using ACT (Carver *et al.*, 2005).

3.3.5 Phylogenetic analysis

Translated amino acid sequences from viral marker genes of interest were retrieved from the 0.1 μm 2006 metagenomic assemblies from this study, GenBank and CAMERA all metagenomic reads ORF peptide database. Homologous sequences were aligned using MUSCLE v3.6 (Edgar, 2004). Neighbour-joining analysis, test for clade support (bootstrap analysis 2000 replicates) and tree drawing was performed with Molecular Evolutionary Genetic Analysis (MEGA) software v4 (Kumar *et al.*, 2008). Maximum likelihood analysis (JTT substitution model) and test for clade support (aLRT analysis) was performed with PHYML (10) and the tree visualised using MEGA. 18S ribosomal RNA (rRNA) gene sequences were retrieved from reads of all filter sizes, compared (BLASTN, e-value $<1.0\text{e}{-}5$) to the SILVA100 SSURef database, aligned and phylogeny performed using ARB as previously described (Ng *et al.*, 2010; Lauro *et al.*, 2011). The abundance and similarity of virophages in all lake samples and filter sizes was estimated using BLASTP (evalue $<1.0\text{e}{-}5$) to search using the OLV major capsid protein (MCP) sequence against a database of proteins predicted from sequencing reads. The database was generated as previously described (Proctor and Fuhrman, 1990) and the percent identity of the BLAST hit was used as a proxy for species similarity.

3.3.6 Metaproteomic analysis

Extraction of proteins from the 0.1 μm filter from 2006, one dimensional-sodium dodecyl sulphate polyacrylamide gel electrophoresis (1D-SDS PAGE), liquid chromatography (LC) and two dimensional mass spectrometry (MS-MS) was performed as previously described (Ng *et al.*, 2010; Lauro *et al.*, 2011). Spectral matching of MS-MS data was performed as described in chapter 2, *Materials and methods* 2.3 using metagenomic sequences from Organic Lake as the search database. The protein sequence database was generated by combining ORFs from the 3.0, 0.8 and 0.1 μm mosaic assemblies, which comprised 130,581 sequences. SCAFFOLD 3.0 (Proteome Software Inc.) was used to validate MS/MS based peptide and protein identifications using the same stringency parameters as described in chapter 2, *Materials and methods* 2.3). The peptide sequences by which the proteins were identified shown in Appendix Table C.1.

3.3.7 Model of algal host–virus and virophage dynamics

To model the effect a virophage would have on algal *Pyramimonas* algal host populations in Organic Lake, modified Lotka-Volterra equations were used describing the OLV as a predator of predator OLPV. The original equations are given by:

$$\frac{dA}{dt} = \alpha A - \varepsilon PA \quad (3.1)$$

$$\frac{dP}{dt} = \theta PA - \mu P \quad (3.2)$$

Where:

A is the number of *Pyramimonas* (prey).

P is the number of OLPV (predator).

α is the specific growth rate of the prey.

θ is the specific production rate of the predator.

ε is the rate of predator mediated death of prey.

μ is the specific decay rate of the predator.

Equation 3.1 describes the change in *Pyramimonas* abundance and equation 3.2 the change in OLPV abundance in the absence of OLV. In the presence of OLV, *Pyramimonas*, OLPV and OLV dynamics are described by the following equations:

$$\frac{dP}{dt} = \theta PA - \mu P - \omega PV \quad (3.3)$$

$$\frac{dV}{dt} = \beta PV - \gamma V \quad (3.4)$$

Where:

V is the number of the OLV (predator of predator).

ω is the rate of OLV mediated reduction in OLPV infective particles.

β is the production rate of OLV.

γ is the decay rate of OLV.

Equation 3.3 is a modified version of equation 3.2 which includes the effect of OLV on the change in abundance of OLPV. Equation 3.4 describes the growth properties of OLV as a predator of OLPV. Values for the variables for the solution shown (Figure 3.9) were as follows: initial prey (10), predator (1) and predator of predator (10) numbers, $\alpha = 0.1$, $\theta = 0.0015$, $\varepsilon = 0.01$, $\mu = 0.01$, $\omega = 0.01$, $\beta = 0.015$ and $\gamma = 0.15$. COMplex Pathway Simulator (COPASI) software (Hoops *et al.*, 2006) was used to simulate prey, predator and predator of predator dynamics using the deterministic (LSODA) method.

3.4 Results and discussion

3.4.1 Dominance of phycodnaviruses in Organic Lake

Water samples from Organic Lake were collected December 2006 and November and December 2008, and microbial biomass collected onto 3.0, 0.8 and 0.1 μm membrane filters as described previously (Lauro *et al.*, 2011). A large proportion of shotgun sequencing reads (96.2%) from the 0.1 μm size fraction of the 2006 Organic Lake metagenome (Table 3.2) had no significant hits to sequences in the RefSeq database (TBLASTx with

Table 3.2: Summary of metagenomic data for Organic Lake 0.1 μm fraction samples used in this study. SCF, scaffolds.

ID	Date	Trimmed reads	SCFs >10 kbp (reads in SCFs)	Annotated ORFs in SCFs (total ORFs)
GS233	December 2006	418,265 (Sanger: 28,481) (454: 389,784)	45 (221,573)	7,318 (21,961)
GS374	November 2008	454: 494,573	5 (771)	33,262 (83,684)
GS379	December 2008	454: 446,200	2 (40,314)	23,012 (64,779)

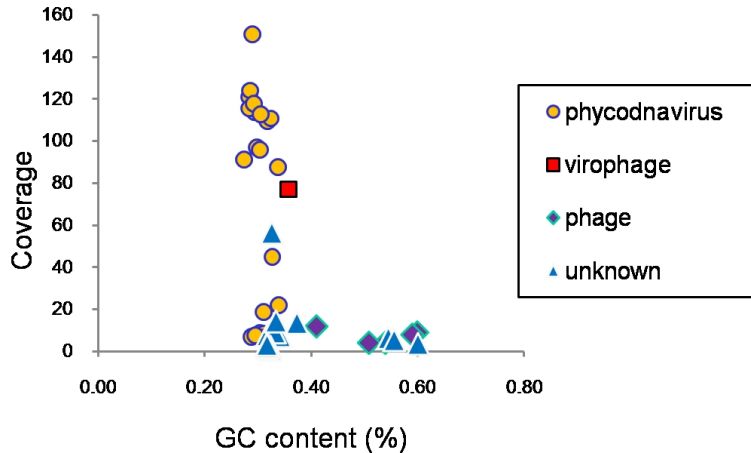


Figure 3.1: Plot of percent GC content *vs* coverage for the 2006 Organic Lake 0.1 μm hybrid assembly scaffolds >10 kb.

e-value <1.0e–3, minimum alignment length: 60 bp, minimum identity: 60%). The degree of assembly was high, with 77% of reads forming part of a scaffold, indicating the sample contained a few abundant taxa of minimal diversity. Forty-five scaffolds were longer than 10 kbp; the five longest ranged from 70 to 171 kbp. GC content and coverage were used to separate scaffolds into taxonomic groups (Figure 3.1). A broad division was evident between low ($\leq 41\%$) and high ($\geq 51\%$) GC scaffolds suggesting they constituted two taxonomic groups. All scaffolds in the high GC group that could be assigned contained phage homologues, as did the one exceptional low GC scaffold. The low coverage in the high GC group showed bacteriophages were not abundant in the 0.1 μm fraction. These scaffolds were not analysed further. The low GC scaffolds with confident assignments contained sequences matching conserved phycodnavirus (PV) or *Acanthamoeba polyphaga* mimivirus (ApMV) proteins. These PV-related scaffolds comprised 60% of assembled reads demonstrating that Organic Lake phycodnaviruses (OLPVs) were numerically dominant in the 0.1 μm fraction. transmission electron microscopy (TEM) revealed the presence of virus-like particles with the dimensions and structure typical of PVs (Figure 3.2A).

Within the low GC group, scaffolds separated into a high coverage ($>45\times$) group, including the five longest scaffolds, and a low coverage ($<22\times$) group. Two of the scaffolds in the high coverage group and one in the low coverage group contained the PV marker DNA polymerase B (DPOB). The two high coverage DPOB share 76%

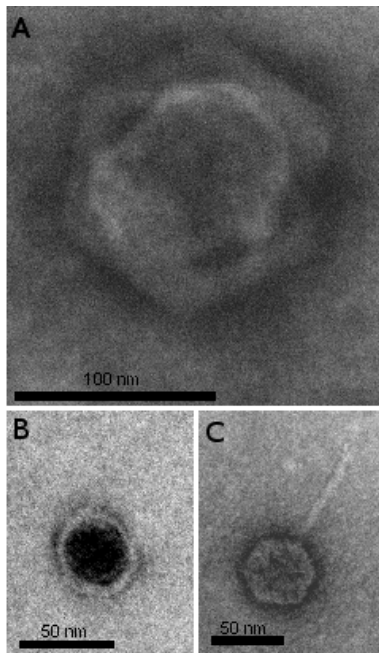


Figure 3.2: Transmission electron micrographs of negatively stained VLPs from Organic Lake. (A) VLP resembling the size and morphology of PVs, (B) Sputnik virophage and (C) bacteriophages.

amino acid identity and both share ~57% identity to the low coverage DPOB. DPOB is single-copy throughout the nucleo-cytoplasmic large DNA virus (NCLDV) family to which PVs belong (Iyer *et al.*, 2001, 2006), demonstrating that the Organic Lake surface waters contained two closely related abundant PV types (DPOB1) and (DPOB2), and a more distantly related lower abundance type (DPOB3).

Phylogenetic analysis clustered Organic Lake DPOB with unclassified lytic marine PV isolates that infect the prymnesiophytes *Chrysochromulina ericina* (CeV1) and *Phaeocystis pouchetii* (PpV), the prasinophyte *Pyramimonas orientalis* (PoV) (Jacobsen *et al.*, 1996; Sandaa *et al.*, 2001), and uncultured marine PVs related to ApMV (Monier *et al.*, 2008b,a) (Figure 3.3). As the host range of PVs broadly correlates with DPOB phylogeny (Nagasaki *et al.*, 2005; Larsen *et al.*, 2008), OLPVs would infect prasinophytes or prymnesiophytes. The most probable host is the prasinophyte, *Pyramimonas* as no prymnesiophyte 18S ribosomal RNA (rRNA) gene sequences were present in any size fraction of the Organic Lake metagenome (Figure 3.4). Neither were prymnesiophytes found in subsequent analysis of the Organic Lake profile in November 2008 (see chapter 4) suggesting they are rare or absent in the Organic Lake community.

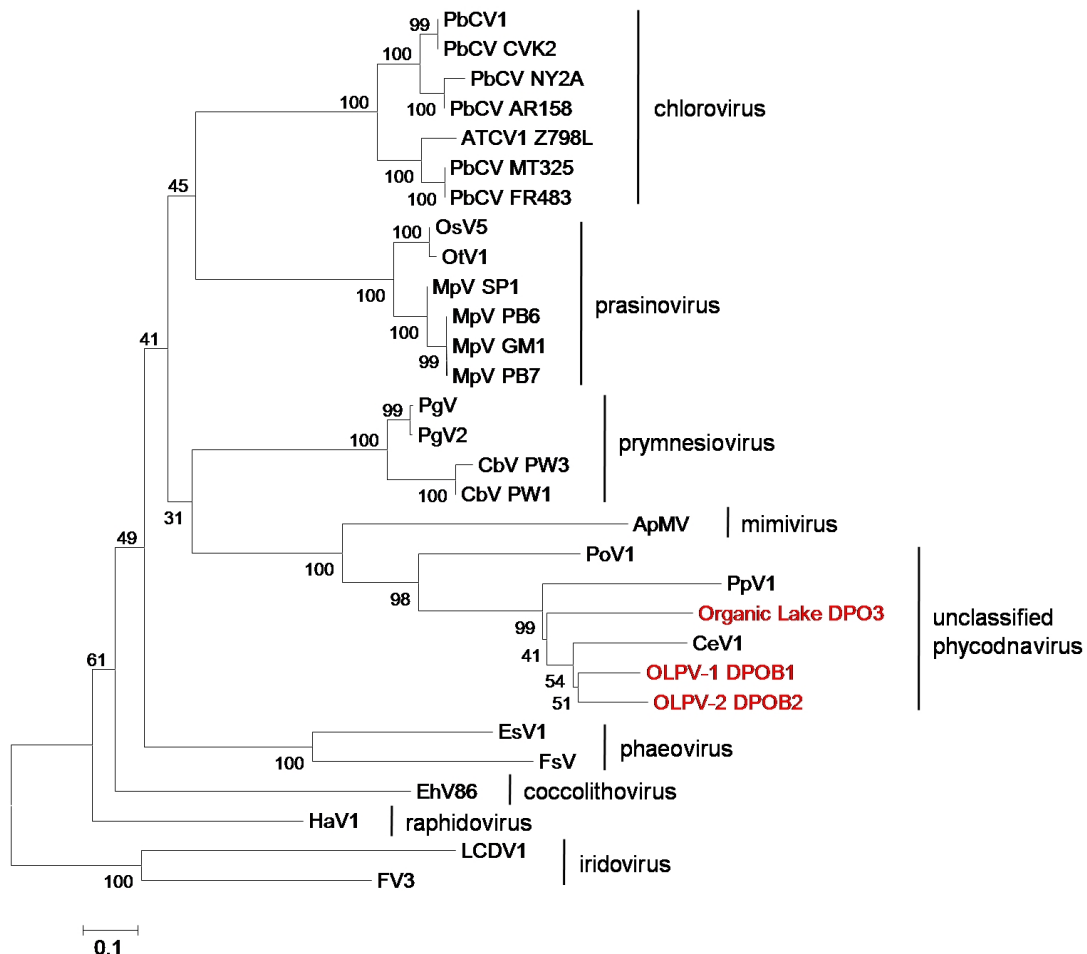


Figure 3.3: Neighbour-joining tree of B family DNA polymerase amino acid sequences from OLPV and NCLDV sequences from GenBank. Organic Lake sequences are shown in red. Abbreviations and accession numbers from bottom to top: PbCV1, *Paramecium bursaria* chlorella virus 1 (AAC00532.1); PbCV CVK2, *P. bursaria* chlorella virus CVK2 (BAA35142.1); PbCV NY2A, *P. bursaria* chlorella virus NY2A (ABT14648.1); PbCV AR158, *P. bursaria* chlorella virus AR158 (ABU43776.1); AtCV1, *Acathocystis turfacea* chlorella virus (ABT16932.1); PbCV MT325, *P. bursaria* chlorella virus MT325(ABT13573.1); PbCV FR483, *P. bursaria* chlorella virus FR483 (ABT15308.1); OsV5, *Ostreococcus* virus 5 (ABY28020.1); OtV1, *O. tauri* virus 1(YP_003495047.1); MpV SP1, *Micromonas pusilla* virus SP1(AAB66713.1); MpV PB6, *M. pusilla* virus PB6 (AAB49743.1); MpV GM1, *M. pusilla* virus GM1 (AAB49742.1); MpV PB7, *M. pusilla* virus PB7 (AAB49744.1); CbV PW1, *Chrysochromulina brevifilum* virus PW1 (AAB49739.1); CbV PW3, *C. brevifilum* virus PW3 (AAB49740.1); ApMV, *Acathamoeba polyphaga* mimivirus (AAV50591.1); PoV, *Pyramimonas orientalis* virus (ABU23717.1); PpV, *Phaeocystis pouchetii* virus (ABU23718.1); CeV1, *C. ericinia* virus 1 (ABU23716.1); EsV1, *Ectocarpus siliculosus* virus (AAK14511.1); FsV, *Feldmannia* sp. virus (AAB67116.1); EhV86, *Emiliania huxleyi* virus 86 (CAI65453.1); HaV1, *Heterosigma akashiwo* virus 1 (BAE06251.1); FV3, Frog virus 3(AAT09720.1) and LCDV1, Lymphocystis disease virus 1(NP_078724.1).

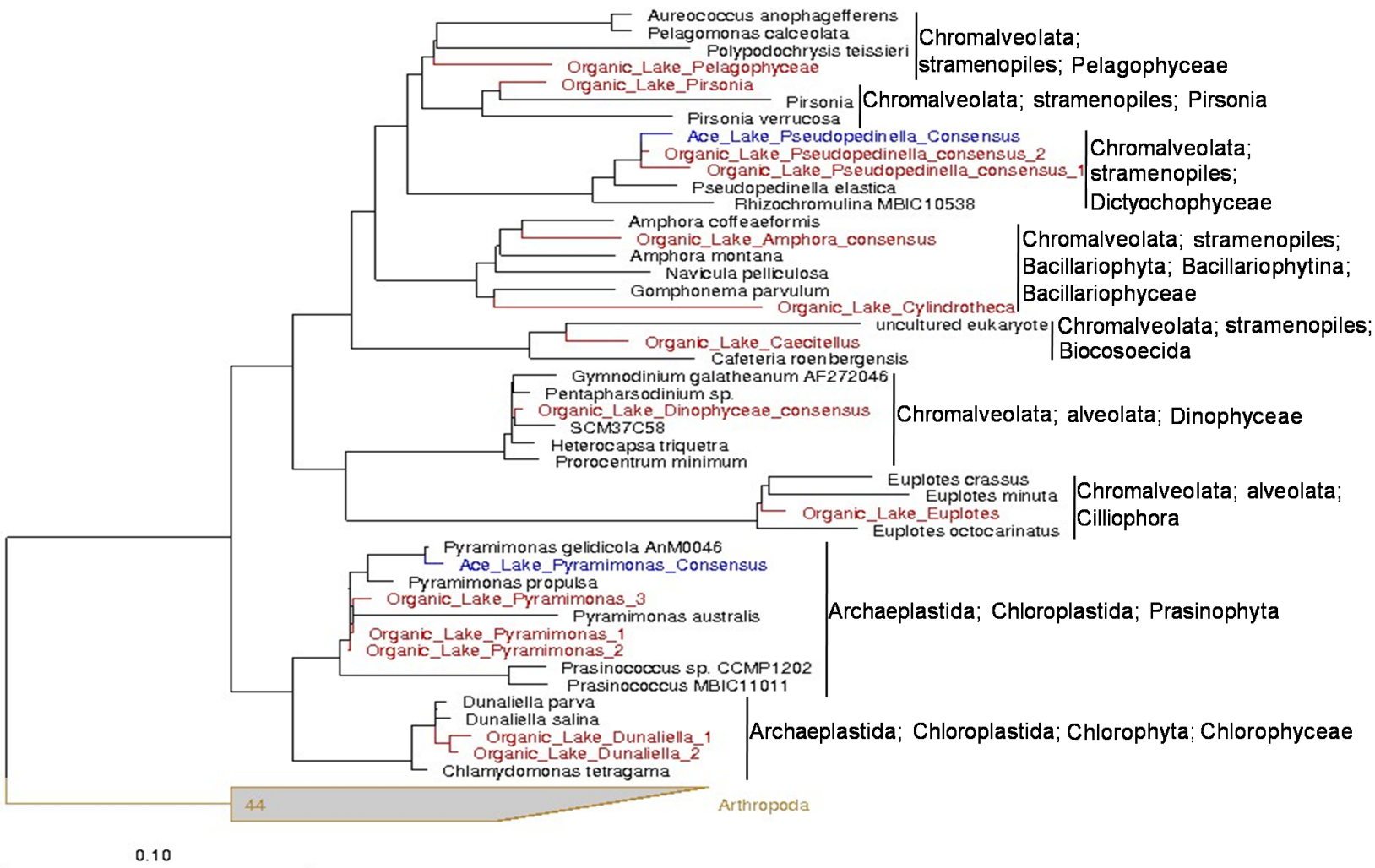


Figure 3.4: Phylogeny of the 18S rRNA genes from the 2006 Organic Lake metagenome. Organic Lake sequences are shown in red. Ace Lake sequences are shown in blue.

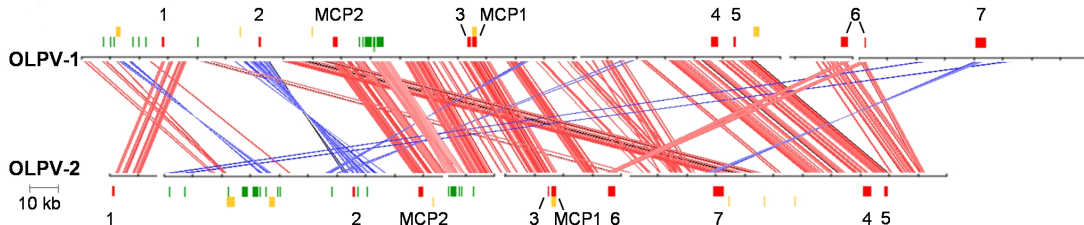


Figure 3.5: Maps of OLPV-1 and OLPV-2 scaffolds and comparison of the location of genes. Genes are marked as follows: single-copy conserved orthologues and MCP (red), regions with identity to OLV (green), proteins identified in the metaproteome (yellow), ribosomal nucleotide reductase β (1), VV A32 packaging ATPase (2), VV VLTF3 transcription factor (3), VV D5 replicative helicase (4), PbCV-1 A482R-like putative transcription factor (5), ribonucleotide reductase α (6), and DNA polymerase B (7). Lines connect homologous regions between the OLPV-1 and OLPV-2 scaffolds in the same orientation (red) and reverse orientation (blue).

Supporting the presence of more than one PV, pairs of single-copy PV orthologues (ribonucleotide reductase α and β subunits, VV A32R virion packaging helicase, PBCV1 A482R-like putative transcription factor, VV D5 ATPase and VLTF2 family transcription factor) were identified in the high coverage scaffolds that shared an average of 81% percent amino acid identity. Based on the positions of single copy genes on the scaffolds and the percent identity between them, the high coverage scaffolds were grouped into two strains designated OLPV-1 and OLPV-2 according to their DPOB phylogeny (Figure 3.3). The remaining high coverage scaffolds were assigned to either strain, resulting in two near-complete genomes of \sim 300 kbp each (Figure 3.5), that are within the range of other sequenced PV genomes (155–407 kbp). In addition, several OLPV genomic fragments contained PV homologues in high coverage scaffolds that could not be confidently assigned to either strain.

Both OLPV strains contain a PpV-like major capsid protein (MCP) designated MCP1 and another unique MCP designated MCP2 (Figure 3.6). Both OLPV MCP1s were identified in the metaproteome (Figure 3.5 and Table 3.3) but MCP2 was not. In addition to MCPs, the metaproteome contained a range of abundant structural proteins and others more likely to be packaged in the virion (e.g. chaperone), that were expressed by OLPV-1, OLPV-2 and/or an OLPV genomic fragment Table 3.3. These data suggest that MCP1 is the major structural protein, and that both OLPV-1 and OLPV-2 were in a productive cycle in the lake at the time of sampling.

3.4.2 Complete genome of an Organic Lake virophage

Sputnik is a small (50 nm) icosahedral satellite virus of mamavirus (a new strain of ApMV). It was termed a virophage because co-infection with Sputnik is deleterious to the mamavirus, resulting in abnormal virions and a decrease in mamavirus infectivity (La Scola *et al.*, 2008). One 28 kbp scaffold in the low GC high coverage group had six out of 38 predicted proteins homologous to Sputnik virophage proteins (Figure 3.7 and Table 3.4), and one PV homologue. The scaffold had a low GC content (\sim 30%), similar

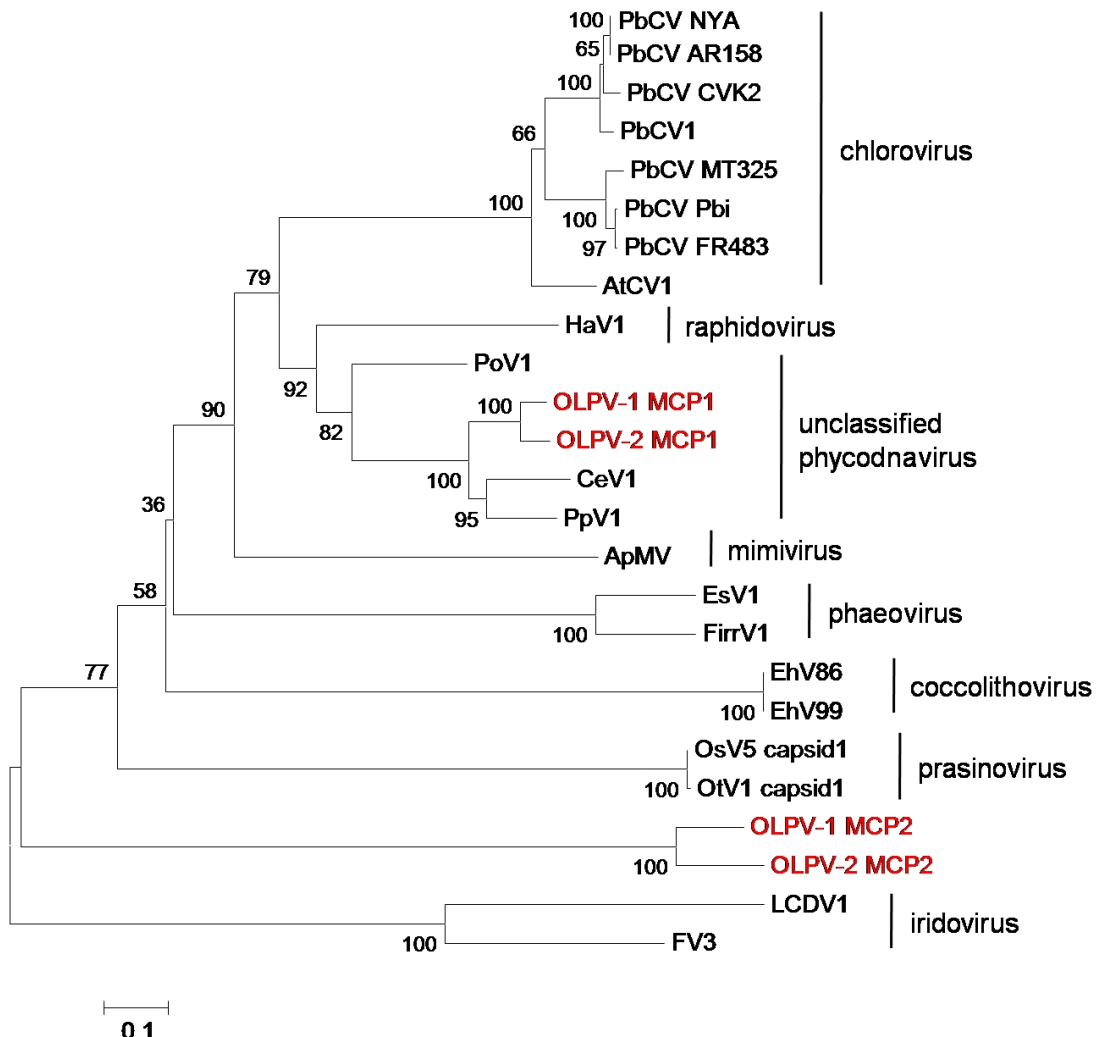


Figure 3.6: Neighbour-joining tree of major capsid protein amino acid sequences from OLPV and other NCLDV sequences from GenBank. Abbreviations and accession numbers from top to bottom: PbCV NYA, *Paramecium bursaria* chlorella virus NY2A (ABT14984.1); PbCV AR158, *P. bursaria* chlorella virus AR158 (ABU44077.1); PbCV CVK2, *P. bursaria* chlorella virus CVK2 (BAA35143.1); PbCV1, *P. bursaria* chlorella virus 1(AAA88828.1); PbCV MT325, *P. bursaria* chlorella virus MT325 (ABT14017.1); PbCV Pbi, *P. bursaria* chlorella virus Pbi (AAC27492.1); PbCV FR483, *P. bursaria* chlorella virus FR483 (ABT15755.1); AtCV1, *Acathocystis turfacea* chlorella virus 1 (ABT16414.1); HaV1, *Heterosigma akashiwo* virus 1 (BAE06835.1); PoV, *Pyramimonas orientalis* virus (ABU23714.1); CeV1, *Chrysochromulina ericinia* virus 1 (ABU23712.1); PpV1, *Phaeocystis pouchetii* virus (ABU23715.1); ApMV, *Acathamoeba polyphaga* virus (Q5UQL7.2); EsV1, *Ectocarpus siliculosus* virus (AAK14534.1); FirrV1, *Feldmannia irregularis* virus 1 (AAR26925.1); EhV86, *Emiliania huxleyi* virus 86 (CAI65508.2); EhV99, *E. huxleyi* virus 99 (ABU23713.1); OsV5, *Ostreococcus* virus 5 (ABY27849.1); OtV1, *O. tauri* virus 1 (CAY39653.1); LCDV1, Lymphocystis diseases virus 1(AAC24486.2); FV3, Frog virus 3 (AAT09750.1).

Table 3.3: OLPV and OLV proteins identified in the December 2006 0.1 µm size fraction metaproteome. Peptide sequences by which the proteins were identified are shown in Appendix Table C.1. NSA, normalised spectral abundance; Cov., coverage. *a*Proteins that have some shared peptides; *b*162322406 and 162276024 are protein homologues; *c*A group of proteins containing similar peptides that could not be differentiated by the mass spectral analysis. Only one gene number of that groups is displayed.

Gene ID	Source	NSA	Accession	Description	Cov. (%)	Peptides (unique)
162322530a	OLPV-1	0.000661	A7U6F0	Major capsid protein [<i>Phaeocystis pouchetii</i> virus]	33	15 (4)
162322348	OLPV-1	0.000120	-	-	11.3	2 (2)
162322406b	OLPV-1	0.000177	-	-	29.4	4 (4)
162313481	OLPV-1	0.000010	YP_002714448	Leucine rich repeat-containing Miro-like protein [<i>Synechococcus</i> sp. PCC7335]	3.96	2 (2)
162276060	OLPV-2	0.000897	-	-	28.9	2 (2)
162300260	OLPV-2	0.000226	-	-	34.6	2 (2)
162276024b	OLPV-2	0.000127	-	-	16	3 (3)
162275992	OLPV-2	0.000098	NP_048709	Hypothetical protein PBCV1_A352L [<i>Paramecium bursaria</i> chlorella virus 1]	16.6	2 (2)
162300108	OLPV-2	0.000046	ZP_01471812	BNR containing hypothetical protein RS9916_28494 [<i>Synechococcus</i> sp. RS9916]	7.66	5 (5)
162319393a	OLPV-2	0.000016	A7U6F0	Major capsid protein [<i>Phaeocystis pouchetii</i> virus]	26.3	13 (2)
162300134c	OLPV-1/2	0.00010	AAR21578	Heat shock protein 70 [<i>Phytophthora nicotianae</i>]	6.97	3 (3)
162286324c	OLPV	0.000176	NP_048575	Hypothetical protein PBCV1_A227L [<i>Paramecium bursaria</i> chlorella virus 1]	14.7	2 (2)
OLV9	OLV	0.001681	YP_002122381	Capsid protein V20 [Sputnik virophage]	31.1	15 (15)
OLV8	OLV	0.000334	YP_002122379	N-term: hypothetical protein V18 [Sputnik virophage]	19.1	8 (8)
			YP_002122380	C-term: minor capsid protein V19 [Sputnik virophage]		

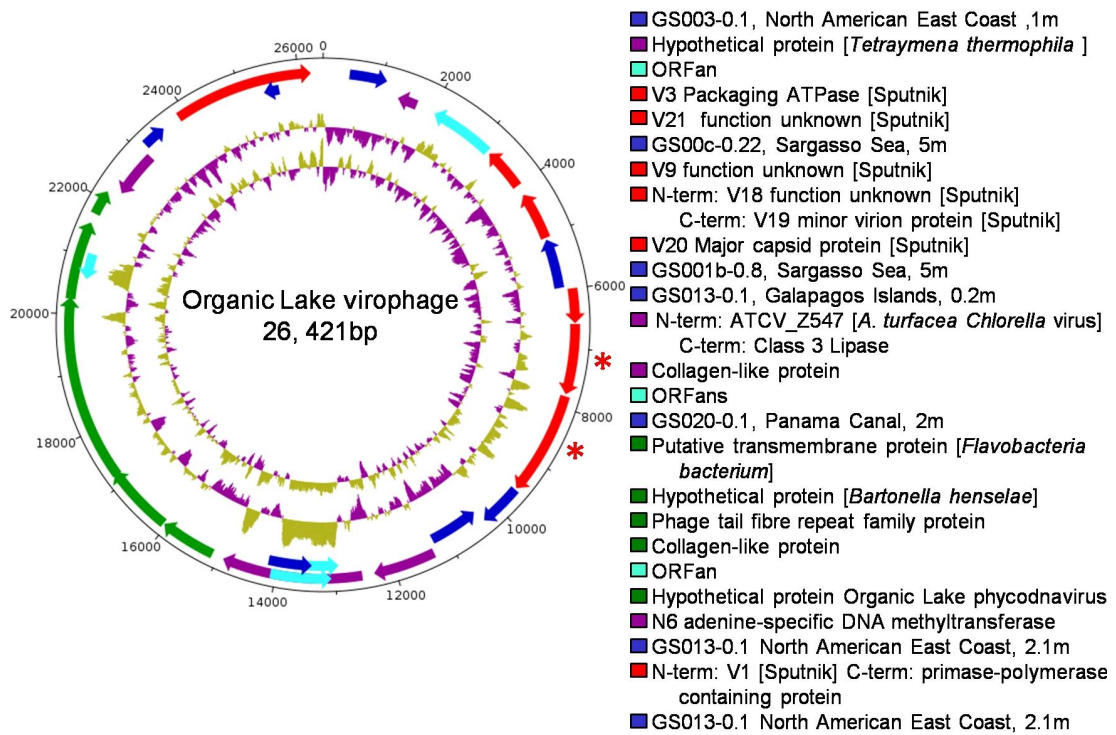


Figure 3.7: Genomic map of Organic Lake virophage. From the outside-in, circles represent, 1) predicted coding sequences on the forward strand, 2) predicted coding sequences on the reverse strand, 3) GC skew, and 4) GC plot. Predicted coding sequences are coloured: Sputnik homologues (red), OLPV homologues (green), non-Sputnik NR homologues (purple), GOS peptide database homologues (blue), and ORFan (cyan). Sequences identified in the metaproteome are marked with an asterisk. Descriptions of the predicted coding sequences from both strands are shown clockwise from position zero.

to the Sputnik genome, and was larger in size (28 kbp vs 18 kbp for Sputnik). Using polymerase chain reaction (PCR) and sequencing, the scaffold was found to represent a complete circular virophage genome. This shows the Organic Lake genome has the same circular topology as the Sputnik genome (La Scola *et al.*, 2008). Virus-like particles resembling Sputnik in size and morphology were identified by TEM (Figure 3.2B).

Table 3.4: Annotation of Organic Lake virophage genome. Top BLASTP matches of predicted coding sequences from the OLV genome compared to OLPV, NR protein database, and CAMERA metagenomic reads ORF peptide database.

	Gene ID	Start	End	NR (acc, %ID, e-value)	OLPV (geneID, %ID, e-value)	CAMERA (acc, %ID, e-value)
†	OLV1	460	1,077	-	-	GS003, 0.1, North America East Coast, 1 m (JCVI_PEP_1105157870626/41%/1e-29)
	OLV2	1,701	1,333	Hypothetical protein [<i>Tetrahymena thermophila</i> SB210] (XP_001029204.1/38% /3e-04)	-	GS012, 0.1, North American East Coast, 13.2 m (JCVI_PEP_1105080106223/42%/1.7e-11)
	OLV3	3,187	2,030	-	-	-
	OLV4	3,991	3,224	-	-	-
	OLV5	5,029	4,160	V3 [Sputnik virophage] (YP_002122364.1/ 39%/4e-24)	-	GS001b, 0.8, Sargasso Sea, 5 m (JCVI_PEP_1105131296011/43%/5e-38)
	OLV6	5,940	5,044	-	-	GS000c, 0.22, Sargasso Sea, 5m (JCVI_PEP_1105136847382/24%/6e-3)
	OLV7	5,978	6,547	V9 [Sputnik virophage] (YP_002122370.1/35%/3e-14)	-	GS020, 0.1, Panama Canal, 2 m (JCVI_PEP_1105140820785/26%/1e-12)
	OLV8	6,574	7,740	N-term: V18 [Sputnik virophage] (YP_002122379.1/27%/9e-05) C-term: V19 [Sputnik virophage] (YP_002122380.1/26%/0.16)	-	GS008, 0.1, North American East Coast, 1 m (JCVI_PEP_1105124194533/32%/6e-8)
	OLV9	7,791	9,518	V20 [Sputnik virophage] (YP_002122381.1/28%/9e-10)	-	GS033, 0.1, Galapagos Islands, 0.2 m (JCVI_PEP_1105120114513/28%/2e-14)
	OLV10	9,563	10,273	-	-	GS001b, 0.8, Sargasso Sea, 5 m (JCVI_PEP_1105163928413/61%/5e-4)
	OLV11	11,210	10,317	-	-	GS013, 0.1, North America East Coast, 2.1 m (JCVI_PEP_1105123792445/39%/9e-37)
	OLV12	11,284	12,324	N-term: Hypothetical protein ATCV_Z547R [<i>Acanthocystis turfacea</i> chlorella virus 1]	-	GS018, Caribbean Sea, 1.7 m (JCVI_PEP_1105087988121/34%/5.6e-23)

Continued on next page

Table 3.4 – *Continued from previous page*

Gene ID	Start	End	NR (acc, %ID, e-value)	OLPV (geneID, %ID, e-value)	CAMERA (acc, %ID, e-value)
			(YP_001427028.1/36%/7e-09) C-term: Lipase class 3 [<i>Bacillus thuringiensis</i> IBL200] (EEM96541.1/27%/1.7e-02)	-	-
OLV13	12,539	14,884	Collagen-like protein [<i>Bacillus megaterium</i>] (YP_001569009.1/66.67%/4e-03)	-	GS027, 0.1, Galapagos Islands, 2.2m (JCVI_PEP_1105075498120/43%/6.7e-11)
OLV14	14,023	12,905	-	-	-
OLV15	13,041	14,078	-	-	-
OLV16	15,094	13,372	-	-	GS020, 0.1, Panama Canal, 2 m (JCVI_PEP_1105127133835/36%/8.5e-11)
6†	OLV17	15,094	16,023 Putative transmembrane protein [<i>Flavobacteria</i> bacterium BAL38] (ZP_01734433.1/51%/8e-34)	Lipoprotein Q-like protein (162322444/40%/1e-24)	GS009, 0.1, North American East Coast, 1 m (JCVI_PEP_1105137954859/50%/4e-37)
	OLV18	16,054	17,211 Hypothetical protein BH13620 [<i>Bartonella henselae</i> str. Houston-1] (YP_034083.1/15%/4e-04)	<i>Cyanothece</i> sp. cce_0037-like protein (162322244/65%/2e-33)	GS000c, 0.1, Caribbean Sea, 2 m (JCVI_PEP_1105149563549/39%/2e-26)
	OLV19	17,168	20,278 Phage tail fiber repeat family protein [<i>Trichomonas vaginalis</i> G3] (XP_001296018.1/42%/4e-11)	Lipoprotein Q-like protein (162322444/65%/9e-33)	GS016, 0.1, Caribbean Sea, 2 m (JCVI_PEP_1105149563549/29%/1e-27)
	OLV20	20,266	21,570 Collagen triple helix containing protein A1Q_3499 [<i>Vibrio harveyi</i> HY01] (ZP_01986098.1/69%/6e-04)	Hypothetical protein (162322252/32%/1e-07)	GS033, 0.1, Galapagos Islands, 0.2 m (JCVI_PEP_1105153074955/69%/1e-5)
	OLV21	21,089	20,622 -	-	-
	OLV22	21,747	22,157 -	Hypothetical protein (162322266/56%/5e-31)	GS017, 0.1, Caribbean Sea, 2 m (JCVI_PEP_1105100448171/43%/4e-24)
	OLV23	23,089	22,256 D12 class N6 adenine-specific DNA methyltransferase [" <i>Candidatus Koribacter versatlis</i> " Ellin345]	-	GS002, 0.1, North America East Coast, 1 m (JCVI_PEP_1105085453201/33%/8e-18)

Continued on next page

Table 3.4 – *Continued from previous page*

Gene ID	Start	End	NR (acc, %ID, e-value)	OLPV (geneID, %ID, e-value)	CAMERA (acc, %ID, e-value)
OLV24	23,174	23,560	- (YP_592471.1/28%/1e-24)	-	GS013, 0.1, North American East Coast 2.1 m (JCVI_PEP_1105132174179/32%/1e-03)
OLV25	23,889	26,219	N-term: V13 [Sputnik virophage] (YP_002122374.1/34%/5e-31) C-term: Primase-polymerase domain containing hypothetical protein [<i>Ostreococcus lucimarinus</i> CCE9901] (XP_001421479.1/29%/9e-32)	-	GS030, 0.1, Galapagos Islands, 19 m (JCVI_PEP_1105105378071/40%/8e-38) GS013, 0.1, North America East Coast, 2.1 m (JCVI_PEP_1105129419397/51%/8e-71)
OLV26	25,666	25,376	-	-	GS013, 0.1, North American East Coast, 2.1 m (JCVI_PEP_1105129419399/54%/8e-6)

Sputnik homologues present in the Organic Lake scaffold included the V20 MCP, V3 DNA packaging ATPase, V13 putative DNA polymerase/primase and others of unknown function (V9, V18, V21 and V32) (Figure 3.7 and (Table 3.3)). The OLV is distinct to Sputnik as proteins share 27–42% amino acid identity (28% MCP identity). OLV proteins include OLV9, the homologue of Sputnik V20 MCP, and OLV8, a fusion of the uncharacterised V18 and minor virion protein V19 from Sputnik (Figure 3.7 and Table 3.4). The large number of homologues, including genes that fulfill essential functions in Sputnik (V20, V3 and V13), indicate that OLV and Sputnik have physiological similarities.

3.4.3 Gene exchange between virophage and phycodnaviruses

As PVs are related to ApMV (Iyer *et al.*, 2006) and are abundant in Organic Lake, it stands to reason that OLPV is the helper of OLV. In the OLV genome, OLV12 is a chlorella virus-derived gene, indicating that gene exchange has occurred between OLV and PVs (the function of OLV12 is discussed below). Similar observations were made for Sputnik, which carries four genes (V6, V7, V12 and V13) in common with the mamavirus, indicative of gene exchange between the viruses and possible co-evolution (La Scola *et al.*, 2008). As the V6, V7, V12 and V13 proteins have been associated with virophage-helper specificity, functional analogues in OLV would have highest identity to proteins from its helper virus, rather than Sputnik.

By comparing OLV and OLPV, a 7,408 bp region was identified in OLV encoding five proteins (OLV17–22) with identity (32–65%) to sequences in both OLPV-1 and OLPV-2 (Figure 3.5, Figure 3.8 and Table 3.4). OLV20 and OLV13 are collagen triple-helix-repeat-containing proteins, analogous to Sputnik collagen-like proteins (V6 and V7) involved in protein–protein interactions in the ApMV virus factory. Sputnik can replicate with either mamavirus or ApMV as a helper, although coinfection rates are higher with the mamavirus. V6 is the only protein with higher identity (69%) to mamavirus than ApMV (42%) (La Scola *et al.*, 2008). Since OLV20 has equivalent identity (63%) with OLPV-1 and OLPV-2, it appears that OLV may be capable of interacting with both OLPV strains. Also within the conserved region, OLV22, is a 141 aa protein of unknown function that only matches sequences from OLPV and the GOS expedition (Table 3.4). Similar to OLV22, Sputnik V12 is a small protein (152 aa) of unknown function with high identity to ApMV, and both may mediate a specific helper–virophage interaction. Other genes in this region of OLV can be mapped to OLPV, including a putative transmembrane protein (OLV17) and paralogous phage tail fibre repeat containing proteins, OLV18 and OLV19. Analogous to the collagen-like proteins, OLV19 and OLV20 probably facilitate interactions between helper and virophage.

OLV12, which is unique to OLV, consists of a C-terminal domain present in conserved hypothetical chlorella virus proteins and an N-terminal domain most closely related to class 3 lipases that may confer OLV selectivity to a PV. OLV12 may function similarly to the Sputnik V15 membrane protein in modifying the ApMV membrane

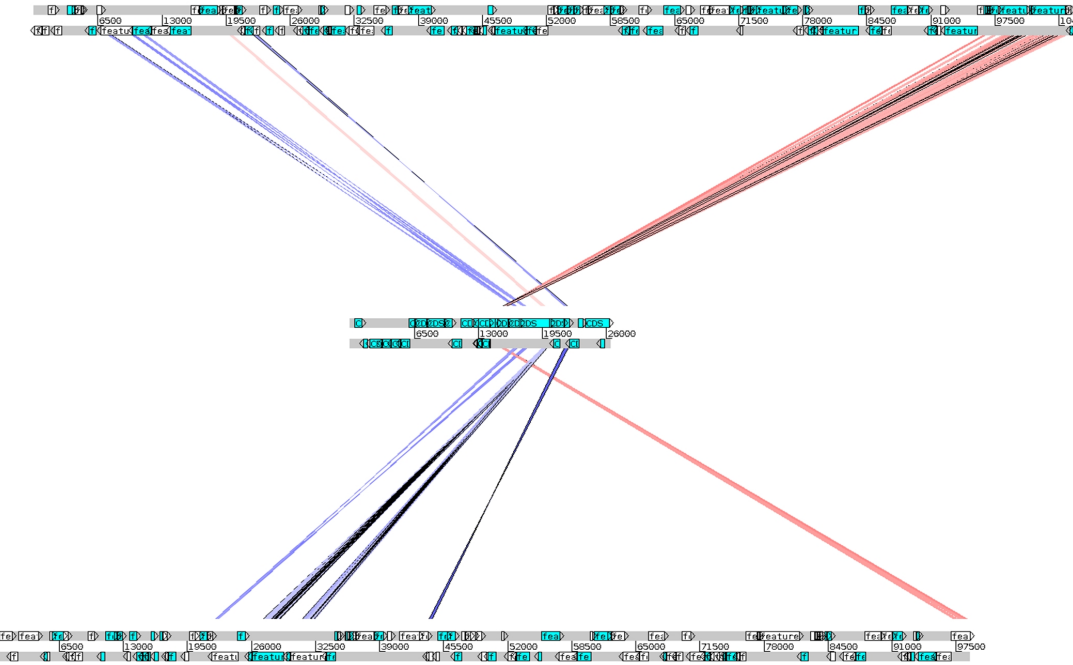


Figure 3.8: Comparison of the location of genes in OLV compared to OLPVs. OLV (centre), OLPV-1 (top), and OLPV-2 (bottom).

(La Scola *et al.*, 2008). The Sputnik V13 consists of a primase domain and SF3 helicase domain related to NCLDV homologues, involved in DNA replication. The helicase domain of OLV25 and V13 are similar, although the primase domain is more similar to a protein from *Ostreococcus lucimarinus*, implying a past association of OLV with a prasinophyte alga host.

Genes unique to OLV point to adaptations specific to its helper–host system. Most notably, OLV possesses a N6 adenine-specific DNA methyltransferase, as does OLPV. In OLPV-1, genes for a bacterial type I restriction modification (RM) system are adjacent to a gene encoding a type I methylase-S target recognition domain protein, and upstream of a DNA helicase distantly related to type III restriction endonuclease (RE) subunits. A large number of chlorella virus genomes have both 5mC and 6mA methylation (Van Etten *et al.*, 1991), and several contain functional RM systems (Nelson *et al.*, 1993). The prototype chlorella virus PbCV-1 possesses REs packaged in the virion for degrading host DNA soon after infection (Agarkova *et al.*, 2006). In contrast to OLV and OLPV, DNA methyltransferases are absent in both Sputnik and APMV, indicating that the N6 adenine-specific DNA methyltransferase has been selected in OLV to reduce endonucleolytic attack mediated by OLPV.

3.4.4 Role of virophage in algal host–phycodnavirus dynamics

The presence of the virophage adds an additional consideration to the microbial loop dynamics. In batch amoeba cultures, co-infection of amoeba with ApMV and Sputnik causes a 70% decrease in infective ApMV particles and a 3-fold decrease in lysis (La Scola *et al.*, 2008). To test how OLV affects OLPV and host population dynamics, OLV

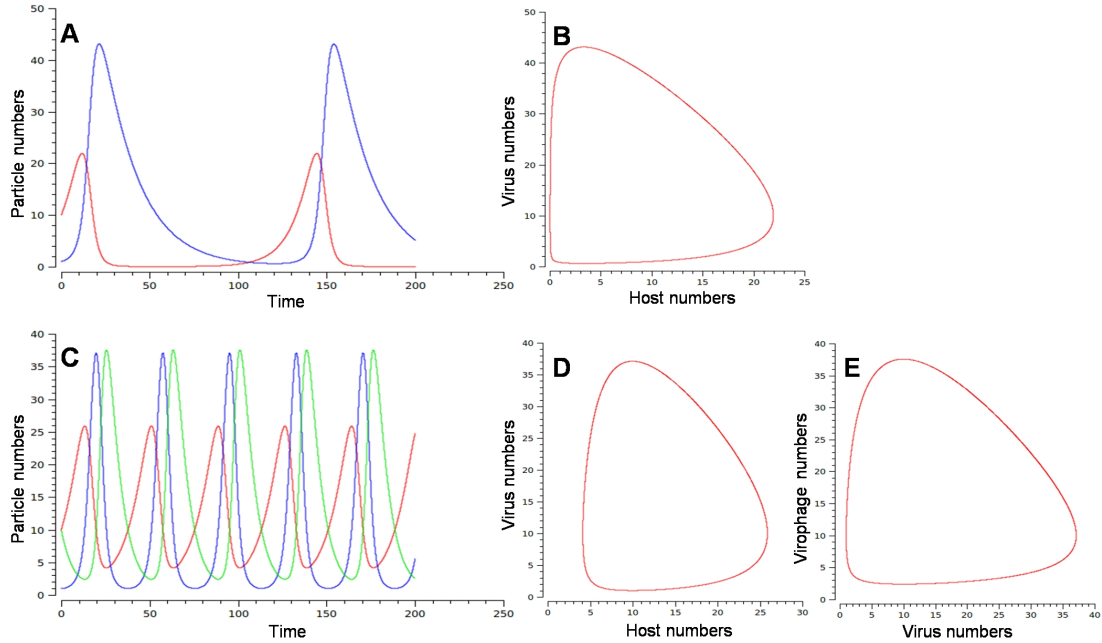


Figure 3.9: Extended Lotka-Volterra models of host-OLPV-OLV population dynamics. **(A)** Time course of host (red line) and OLPV (blue line) populations in the absence of OLV. **(B)** Orbit plot between host and OLPV populations in the absence of OLV with the host and OLPV populations approaching zero during an equilibrium cycle. **(C)** Time course describing the effect of the addition of OLV (green line) on OLPV-host population dynamics as a predator of predator resulting in increased frequency of population oscillations and a higher minimal number of hosts and OLPVs **(D)** compared to in the absence of OLV **(B)**. **(E)** The orbit plot of OLPV and OLV is also shown. Note that the time intervals are arbitrary.

was modelled as an additional predator of a predator in a Lotka-Volterra simulation (Figure 3.9).

The classic Lotka-Volterra model (Lotka, 1910) is based on a pair of first-order, non-linear, differential equations that can be used to describe the periodic oscillation of the populations of a predator and its prey (Volterra, 1926). An example of how predator (virus) populations follows that of its prey (host) populations over time is shown in Figure 3.9A where the populations are at equilibrium. The extended model shown (Figure 3.9C) is based on three equations describing the host (prey), virus (predator) and virophage (predator of predator) interactions. In this model, the effect of virophage is robust, with equilibrium solutions across a wide range of parameter values (Figure 3.9C shows one equilibrium solution). It shows the virus population following that of its host and the virophage population in turn following that of its helper virus or “host”. While the absolute number of hosts do not increase greatly as a result of OLV preying on OLPV, the frequency of host blooms increases in the presence of OLV.

This is due to OLV decreasing the number of infective OLPVs, thereby shortening the recovery time of the host population (Figure 3.9C). This is evident in the orbit plot (Figure 3.9D) as the shift of the orbit away from the axis.

The model reveals that the virophage stimulates the flux of secondary production

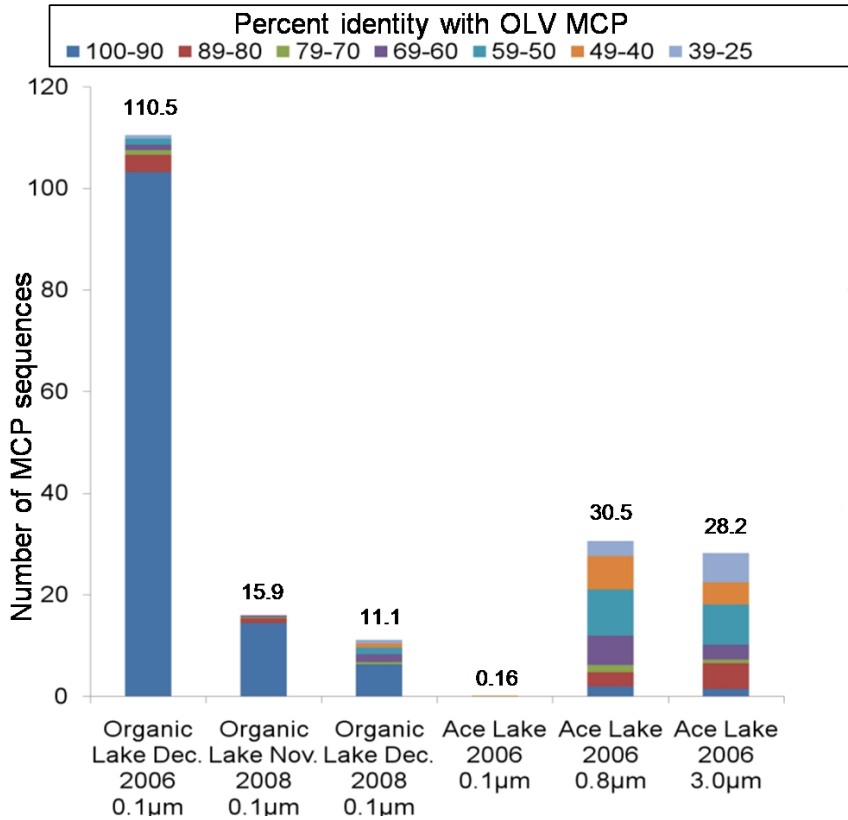


Figure 3.10: Abundance and diversity of virophage capsid proteins in environmental samples. Number of ORFs from metagenomic reads that match to OLV MCP (BLASTP e-value cut-off $1e-5$, abundance normalised to 100,000 reads per sample), and the proportion of virophage capsid types, for the Organic Lake 0.1 µm and Ace Lake 0.1, 0.8 and 3.0 µm fractions.

through the microbial loop by reducing overall mortality of the host algal cell following a bloom, and by increasing the frequency of blooms during the summer light periods. Antarctic lake systems have evolved mechanisms to cope with long light-dark cycles (Lauro *et al.*, 2011) and shortened trophic chains. In Organic Lake and similar systems, a decrease in PV virulence may be instrumental in maintaining stability of the microbial food web. For example, by increasing the frequency of algal blooms more nutrients overall would be released into the available pool for use by heterotrophic bacteria or other primary producers.

3.4.5 Ecological relevance of virophages in aquatic systems

Metagenomic analysis of Organic Lake samples taken two years later in November (when the lake was ice covered) and December 2008 (partially ice-free) revealed sequences with 99% amino acid identity to OLV MCP indicating persistence of OLV in the ecosystem (Figure 3.10 and Table 3.5). In addition, sequences with lower identity (25–90%) were detected, particularly in December, demonstrating Organic Lake virophages are highly diverse but OLV remained the dominant type.

From surface water samples of nearby Ace Lake (meromictic, surface 2% salinity), a large number of sequences were obtained that matched both the OLV MCP (Figure 3.10,

Table 3.5: BLASTP matches for OLV MCP in predicted ORFs of Organic Lake and Ace Lake contigs and CAMERA metagenomic read ORF peptide database. (E-value cut-off 1e-5, alignment length >100aa). Aln., alignment length; Cov., coverage.

Sample	Size (μm)	Gene ID	Scaffold ID	Id. (%)	Aln. (aa)	E- value	Cov. (×)
Organic Lake	0.1	OLV9	-	-	-	-	77.12
December	0.8	176157210	scf7180000034275	98.61	575	0.0	16.03
2006	3.0	181703798	deg7180000108904	98.96	575	0.0	48.65
Organic Lake	0.1	192841413	deg7180000116398	99.64	555	0.0	16.03
November	0.8	193037024	scf7180000086663	93.98	133	2e-61	2.5
2008	3.0	192638971	deg7180000028400	99.36	156	1e-76	1.86
		192955191	deg7180000024244	93.98	133	1e-61	3.10
Organic Lake	0.1	192709908	scf7180000109753	99.01	304	9e-173	4.38
December		192709920	scf7180000109753	99.59	244	1e-120	4.38
2008		192712009	deg7180000067104	54.70	117	3e-30	1.58
		192890551	deg7180000061276	36.89	122	2e-13	3.15
	0.8	193060302	deg7180000053149	53.75	160	6e-43	2.30
Ace Lake	0.1	167813925	scf7180000126822	28.86	246	3e-14	2.36
2006		167858124	scf7180000129064	21.78	381	5e-10	1.94
		167891594	scf7180000136823	24.85	326	2e-04	8.15
		167875536	deg7180000086604	22.95	244	6e-04	2.21
	0.8	176091445	deg7180000053588	91.61	143	8e-78	3.35
		175769103	deg7180000078701	88.24	153	1e-74	1.77
		176042318	deg7180000058177	81.77	181	1e-74	2.48
		176000635	deg7180000087166	53.39	221	8e-58	2.50
		176042707	deg7180000058207	50.78	193	5e-46	2.34
		175886340	deg7180000074162	58.90	146	4e-45	2.73
		176249679	deg7180000049481	61.94	155	2e-44	2.75
		175748439	deg7180000058552	76.79	112	2e-35	2.39
		175637390	deg7180000058712	50.91	165	2e-35	2.03
		176100822	deg7180000055966	53.38	133	6e-35	1.48
		176018109	deg7180000086684	59.68	124	4e-27	1.66
		176000624	deg7180000087165	53.85	104	6e-27	1.73
		175805608	deg7180000054222	48.60	107	7e-21	1.93
		175908895	deg7180000061971	51.91	131	4e-20	3.27
		175821062	deg7180000080443	46.46	127	6e-20	1.43
		176026419	deg7180000054364	52.59	116	8e-19	1.47
		176133336	scf7180000089989	38.36	146	3e-12	1.51
		176018257	deg7180000086719	31.21	173	4e-12	1.23
		176137412	deg7180000052688	29.37	126	1e-06	2.47
		175686880	scf7180000092161	24.00	125	2e-06	2.98
	3.0	175741076	deg7180000030508	85.78	232	8e-109	1.25
		175748837	deg7180000027929	55.29	170	4e-44	1.32
		175751996	deg7180000037324	51.27	158	5e-41	1.63
		175859792	scf7180000045944	30.21	288	8e-26	2.69
Punta Cormorant	0.1	JCVI_PEP_1105120114513	-	27.84	273	2e-14	-
hypersaline		JCVI_PEP_1105100621559	-	24.76	307	9e-10	-
lagoon (GS003)		JCVI_PEP_1105161421335	-	25.61	289	2e-6	-
Delaware Bay	0.1	JCVI_PEP_1105106741177	-	24.62	264	6e-14	-
(GS011)		JCVI_PEP_1105089715877	-	27.16	313	1e-17	-
Upwelling	0.1	JCVI_PEP_1105079267881	-	28.23	170	8e-11	-
(GS031)							
Lake Gatun	0.1	JCVI_PEP_1105119255775	-	26.71	149	5e-9	-
Panama (GS020)							

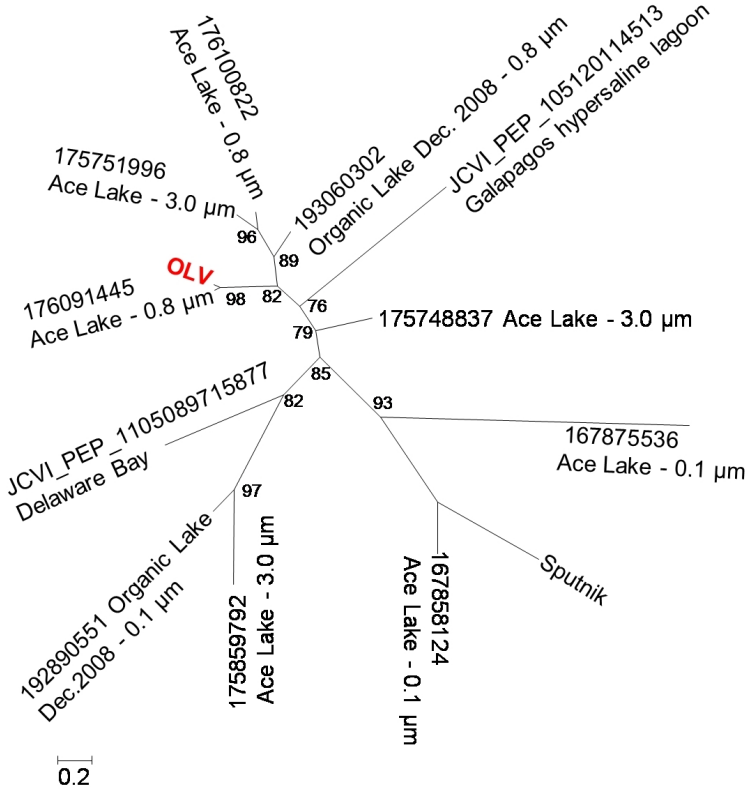


Figure 3.11: Maximum likelihood phylogenetic tree of a conserved 103 aa region of the MCP from Organic Lake, Ace Lake and GOS metagenome data and Sputnik.

Figure 3.11 and Table 3.5) and PVs (Lauro *et al.*, 2011). All Ace Lake size fractions contained matches to OLV MCP, some with high identity (80–100%) and the majority with greater variation (25–80% identity) (Figure 3.11 and Table 3.5). In contrast to Organic Lake where the largest number of matches was to the 0.1 μm size fraction, the majority of Ace Lake sequences were from the larger fractions (Figure 3.10 and Table 3.5). This indicates the Ace Lake virophages (ALVs) were associated with host cells during sampling, or possibly with helper viruses that are larger than the OLPVs.

Extending the OLV MCP search to the GOS data revealed matches (25–28% identity) to sequences from the hypersaline Punta Cormorant Lagoon (Floreana Island, Galapagos), an oceanic upwelling near Fernandina Island (Galapagos), Delaware Bay estuary (NJ, USA), and freshwater Lake Gatun (Panama) (Table 3.5). The phylogenetic analysis of a conserved 103 amino acid region of the MCPs revealed a number of clusters, with Sputnik clustering with virophage sequences from Ace Lake that had low identity (22%) to OLV MCP (Figure 3.11). To improve searches for virophages and better understand their physiology and evolution, it will be valuable to target more genomes (e.g. the ALV 167858124 relative with 40% MCP identity to Sputnik) and determine which genes are core to virophages and what relationship exists between genome complement and MCP identity.

In view of the implications of the virophage modelling (Figure 3.9), the abundance and persistence of OLV in Organic Lake and the presence of diverse virophage signatures

in a variety of lake systems (fresh to hypersaline), an estuary, an ocean upwelling site and a water cooling tower (*Sputnik*), our study indicates that numerous types of virophages exist and play a previously unrecognised role in regulating host–virus interactions and influencing ecosystem function in aquatic environments.

3.5 Acknowledgements

We thank Craig Venter, John Bowman, Louise (Cromer) Newman, Anthony Hull, John Rich and Martin Riddle for providing helpful discussion and logistical support associated with the Antarctic expedition, and Lisa Ziegler for discussion about marine viruses. We acknowledge technical support for computing infrastructure and software development from Intersect, and in particular assistance from Joachim Mai. This work was supported by the Australian Research Council and the Australian Antarctic Division. Funding for sequencing was provided by the Gordon and Betty Moore Foundation to the J. Craig Venter Institute. Mass spectrometric results were obtained at the Bioanalytical Mass Spectrometry Facility within the Analytical Centre of the University of New South Wales. This work was undertaken using infrastructure provided by NSW Government co-investment in the National Collaborative Research Infrastructure Scheme. Subsidized access to this facility is gratefully acknowledged. We thank Jenny Norman from the UNSW Electron Microscopy Unit her assistance in generating images.

Chapter 4

Strategies of carbon conservation and unusual sulphur biogeochemistry in Organic Lake

Co-authorship Statement

A version of this chapter has been submitted as:

Sheree Yau, Federico M. Lauro, Timothy J. Williams, Matthew Z. DeMaere, Mark V. Brown, John Rich, John A.E. Gibson, Ricardo Cavicchioli. Strategies of carbon conservation and unusual sulfur biogeochemistry in a hypersaline lake. (submitted), 2013.

Contributions to this manuscript by other researchers is as follows.

Research was designed and manuscript edited by Federico Lauro, Tim Williams, John Gibson and Ricardo Cavicchioli. Sample collection and bathymetry was performed by Federico Lauro, Mark Brown, John Rich and Ricardo Cavicchioli. Metagenomic sequence filtering, global assembly and annotation was performed by Matthew DeMaere. Assistance in interpretation of geochemistry provided by John Gibson. Assistance in global taxonomic and functional gene analysis provided by Federico Lauro. Assistance in analysis and interpretation of metabolic pathways provided by Timothy Williams.

Apart from these contributions, I performed all other data analyses, interpretations and drafted the manuscript.

4.1 Abstract

Organic Lake in the Vestfold Hills has the highest reported concentration of dimethylsulphide (DMS) in a natural body of water. To determine the composition and functional potential of the microbial community and learn about the unusual sulphur chemistry in Organic Lake, shotgun metagenomics was performed on size fractionated samples collected along a depth profile. Eucaryal phytoflagellates were the main photosynthetic organisms. Bacteria were dominated by the globally distributed heterotrophic taxa *Marinobacter*, *Roseovarius* and *Psychroflexus*. The dominance of heterotrophic degradation coupled with low fixation potential indicates possible net carbon loss. However, abundant marker genes for aerobic anoxygenic phototrophy, sulphur oxidation, rhodopsins and CO oxidation were also linked to the dominant heterotrophic bacteria and indicate use of photo- and lithoheterotrophy as mechanisms for conserving organic carbon. Similarly, a high genetic potential for the recycling of nitrogen compounds likely functions to retain fixed nitrogen in the lake. dimethylsulphopropionate (DMSP) lyase genes (*dddD*, *dddL* and *dddP*) were abundant indicating DMSP is a significant carbon and energy source. Unlike marine environments, DMSP demethylases (*dmdA*) were less abundant than DMSP lyases indicating that DMSP cleavage is the likely source of the high DMS concentration. DMSP cleavage, photoheterotrophy, lithoheterotrophy and nitrogen remineralisation by dominant Organic Lake bacteria are potentially important adaptations to nutrient constraints. In particular, photo- and lithoheterotrophy reduces the extent of carbon oxidation for energy production allowing more carbon to be used for biosynthetic processes. The study sheds light on how the microbial community in Organic Lake has adapted to the unique physical and chemical properties of this Antarctic lake environment.

4.2 Introduction

Due to the polar light cycle, phototrophic growth in Antarctic environments is relatively high in summer and negligible in winter (Laybourn-Parry *et al.*, 2005) and requires microbial life to survive under long periods under a scarcity of resources. To overcome this limitation, Eucaryotic phytoflagellates in Ace Lake engage in carbon mixotrophy by grazing on bacterioplankton to supplement their carbon requirements in the winter (Laybourn-Parry *et al.*, 2005). Marine heterotrophic bacteria are known to be similarly resourceful by exploiting light energy through photoheterotrophy that includes aerobic anoxygenic photosynthesis (AAnP) or via use of rhodopsins, or lithoheterotrophy such as oxidation of carbon monoxide (Moran and Miller, 2007). Heterotrophic bacteria that can harness energy sources apart from organic carbon can direct a greater proportion of carbon towards growth, which serves to conserve fixed carbon within a closed systems (Moran and Miller, 2007).

The bottom waters of Organic Lake are unusual due to the absence of hydrogen sulphide and the high concentration of the volatile gas dimethylsulphide (DMS) (Deprez *et al.*, 1986; Franzmann *et al.*, 1987b; Gibson *et al.*, 1991; Roberts and Burton, 1993; Roberts *et al.*, 1993). Concentrations of DMS as high as 5,000 nM have been recorded in Organic Lake (Gibson *et al.*, 1991), 100 times the maximum concentration recorded from seawater in the adjacent Prydz Bay and at least 1,000 times that of the open Southern Ocean (Curran *et al.*, 1998). More than forty years ago atmospheric DMS was proposed to have a regulatory effect on global cloud cover as it is a precursor of cloud condensation nuclei (Lovelock and Maggs, 1972; Charlson *et al.*, 1987). However, the first enzymes involved in DMS production were only identified in the last six years (Todd *et al.*, 2007). Rapid progress has been made in this short period and the pathways and organisms involved in DMS transformations have been extensively reviewed (Johnston *et al.*, 2008; Schäfer *et al.*, 2010; Curson *et al.*, 2011b; Reisch *et al.*, 2011; Moran *et al.*, 2012).

The main source of DMS in the marine environment is from the breakdown of dimethylsulphopropionate (DMSP). Eucaryal phytoplankton, in particular diatoms, dinoflagellates and haptophytes, produce large quantities of DMSP, an organo-sulphur compound that is thought to function principally as an osmolyte. DMSP is released due to cell lysis, grazing or leakage and follows two known fates: DMSP cleavage by DMSP lyases (DddD, -L, -P, -Q, -W and -Y) or demethylation by DMSP demethylase (DmdA). Both pathways are associated with diverse microorganisms that can utilize DMSP as a sole carbon and energy source. However, it is only the cleavage pathway that releases volatile DMS that can lead to sulphur loss through ventilation to the atmosphere. The very high levels of DMS in Organic Lake make it an ideal system for identifying the microorganisms and the processes involved in DMS accumulation.

The previous Organic Lake metaproteogenomic study examined viruses from the 0.1 μm fraction of surface water that was collected from Organic Lake in December 2006, and November and December 2008 (Yau *et al.*, 2011) (Chapter 3). In the present study we focused on the cellular population rather than viruses. Our study determined

Table 4.1: Summary of metagenomic data for Organic Lake November 2008 profile.

ID	Depth (m)	Size (μm)	Trimmed reads	Predicted ORFs (%KEGG matches)	Scaffolds (reads)	>10 kbp scaffolds (reads)	Annotated scaffold ORFs (total ORFs)
GS374	1.7	0.1	494,573	533,468 (31)	4,318 (63,194)	5 (771)	33,262 (83,684)
		0.8	472,635	470,949 (52)	4,161 (126,519)	68 (17,061)	37,857 (63,140)
		3.0	158,121	158,573 (50)	2,584 (39,591)	4 (520)	18,126 (28,425)
GS375	4.2	0.1	541,962	556,791 (30)	4,899 (80,316)	2 (232)	35,318 (87,631)
		0.8	472,570	492,130 (53)	5,104 (127,243)	80 (18,461)	42,508 (68,366)
		3.0	321,112	324,365 (56)	3,983 (98,102)	69 (14,713)	30,938 (51,452)
GS376	5.7	0.1	363,280	387,528 (25)	2,342 (39,422)	6 (1,801)	21,798 (61,595)
		0.8	484,635	448,373 (59)	6,820 (152,646)	134 (29,903)	47,846 (73, 282)
		3.0	290,428	292,358 (51)	3,571 (77,277)	58 (10,231)	28,199 (48,910)
GS377	6.5	0.1	497,363	572,892 (29)	5,029 (80,520)	14 (2,711)	36,685 (92,420)
		0.8	465,381	454,018 (51)	4,202 (129,193)	57 (17,004)	43,852 (70,382)
		3.0	187,045	211,354 (59)	2,100 (60,636)	51 (9,321)	20,713 (33,497)
GS378	6.7	0.1	516,870	586,375 (26)	3,694 (58,618)	14 (3,422)	33,243 (96,334)
		0.8	548,253	626,115 (57)	6,957 (161,202)	136 (32,889)	56,452 (88,738)
		3.0	202,310	219,992 (58)	2,304 (66,389)	57 (11,167)	22,786 (35,034)

the composition and functional potential of Organic Lake microbiota and, in conjunction with historic and contemporary physico-chemical data, generated an integrative understanding of the whole lake ecosystem.

4.3 Materials and methods

4.3.1 Characteristics of the lake and sample collection

The water level of Organic Lake was measured by surveying as +1.886 m relative to the survey mark (NMV / S / 53) located at 68°27'23.4"S, 78°11'22.6"E. Water was collected from Organic Lake on 10 November 2008 through a 30 cm hole in the 0.8 m thick ice cover above the deepest point in the lake. The sampling hole was established at 68°27'22.2"S, 78°11'23.9"E) following bathymetry measurements constructed on a metric grid. Samples were collected for metagenomics, microscopy and chemical analyses at 1.7, 4.2, 5.7, 6.5 and 6.7 m depths (maximum lake depth 6.8 m).

For metagenomics, lake water was passed through a 20 μm pore size pre-filter, and microbial biomass captured by sequential filtration onto 3.0 μm , 0.8 μm and 0.1 μm pore size 293 mm polyethersulfone membrane filters, and samples immediately preserved in buffer and cryogenically frozen in liquid nitrogen, as described previously (Ng *et al.*, 2010; Lauro *et al.*, 2011). Between 1–2 L of lake water was sufficient to saturate the holding capacity of the filters. DNA was extracted from the filters, samples sequenced using the Roche GS-FLX titanium sequencer, and reads processed to remove low quality bases, assembled and annotated, as previously described (Ng *et al.*, 2010; Lauro *et al.*, 2011). A summary of the 2.4 Gbp of metagenomic data is provided in Table 4.1.

4.3.2 Physical and chemical analyses

An *in situ* profile of pH, conductivity, turbidity, dissolved oxygen (DO) and pressure was measured using a submersible probe (YSI sonde model V6600). A temperature profile was measured using a maximum-minimum mercury thermometer as the YSI probe did not have a capacity to record temperature below -10°C . The 5.7 m sample corresponded to the turbidity maximum and the 6.5 m sample to the turbidity minimum. Conductivity at *in situ* temperature was converted to conductivity at 15°C as described previously (Gibson, 1999). The adjusted conductivity brings the temperature to within a range suitable for estimating practical salinity using the formula of Fofonoff and Millard (1983). Salinity was likely to have been underestimated as it is higher than the range (2–42) for which the conductivity–salinity relation holds. However, the relative difference in salinity between the samples would be accurate.

Density was calculated from the *in situ* conductivity and temperature using the equations described by Gibson *et al.* (1990) and expressed at temperature T as:

$$\sigma_T = (1000 - \text{density}) \text{ kg m}^{-3}$$

Ammonia, nitrate, nitrite, total nitrogen (TN), total dissolved nitrogen (TDN), dissolved reactive phosphorus (DRP), total phosphorus (TP), total dissolved phosphorus (TDP), total organic carbon (TOC), dissolved organic carbon (DOC), total sulphur (TS) and total dissolved sulphur (TDS) were determined by American Public Health Associations Standard Methods at the Analytical Services, Tasmania. Values for dissolved nutrients were measured after filtration through a $0.1 \mu\text{m}$ pore size membrane filter. All other nutrients were measured from water collected after filtration through the on-site $20 \mu\text{m}$ pore size pre-filter.

Ammonia, nitrate, nitrite, DRP, TN, TDN, TP and TDP were measured in a Flow Injection Analyser (Lachat Instruments, Colorado, USA). TOC and DOC were determined in the San++ Segmented Flow Analyser (Skalar, Breda, Netherlands). TS and TDS were analysed in the 730ES Inductively Coupled Plasma–Atomic Emission Spectrometer (Agilent Technologies, California, USA). Principal component analysis PCA was performed using the PRIMER Version 6 statistical package (Clarke and Gorley, 2006) on the normalised physical and chemical parameters.

4.3.3 Epifluorescence microscopy

Water samples collected for microscopy were preserved in formaldehyde (1% v/v). Cells and VLP were vacuum filtered onto 25 mm polycarbonate 0.015 μm pore-size membrane filters (Nuclepore Track-etched, Whatman, GE Healthcare, USA) with a 0.45 μm pore-size backing filter. The 0.015 μm filter was mounted onto a glass slide with ProLong Gold anti fade reagent (Invitrogen, Life Technologies, NY, USA) and 2 μl ($25\times$ dilution in sterile filtered milliQ water $<0.015 \mu\text{m}$) SYBR Gold nucleic acid stain (Invitrogen, Life Technologies, NY, USA). Prepared slides were visualized in an epifluorescence microscope (Olympus BX61, Hamburg, Germany) under excitation with blue light (460–495 nm, emission 510–550 nm). Cell and virus-like particle (VLP) counts were performed on the same filter over 30 random fields of view.

4.3.4 Cellular diversity analyses

Diversity of *Bacteria*, *Archaea* and *Eucarya* was assessed using small subunit ribosomal RNA (SSU) gene sequences. Metagenomic reads that matched the 16S and 18S ribosomal RNA (rRNA) genes were retrieved using METAXA (Bengtsson *et al.*, 2011). Only sequences longer than 200 bp were accepted for downstream analysis.

The Quantitative Insights Into Microbial Ecology (QIIME) pipeline (version 1.4.0) (Caporaso *et al.*, 2010) implementing UCLUST, was used to group SSU sequences into operational taxonomic units (OTUs) at 97% percent identity against the SILVA SSU reference database (release 108) (www.arb-silva.de). SSU sequences that did not cluster with sequences from SILVA were allowed to form new OTUs (no suppression). A representative sequence from each OTU was chosen and classified to the genus level using QIIME implementing the Ribosomal Database Project (RDP) classifier (Wang *et al.*, 2007) trained against SILVA. Assignments were accepted to the lowest taxonomic rank with bootstrap value $\leq 85\%$.

To allow comparison of the relative abundance of taxa, the number of SSU matches per sample filter was normalised to the average number of reads (403,577). Statistical analysis on the relative SSU abundances was performed using the PRIMER version 6 package (Clarke and Gorley, 2006). The SSU counts of each sample filter were aggregated to the genus level and square root transformed to reduce the contribution of highly abundant taxa. A resemblance matrix was computed using Bray-Curtis similarity. The upper mixed zone (1.7, 4.2 and 5.7 m) and deep zone (6.5 and 6.7 m) samples were designated as separate groups and an analysis of similarity analysis of similarity (ANOSIM) performed to test for difference between the two groups. BEST analysis was performed with the abiotic variables: conductivity, temperature, turbidity, DO, pH, TOC, TN, TP, TS, total C:N, total C:P, total N:P, cell counts and VLP counts. The Bio-Env procedure in BEST looks at all the abiotic variables in combination and finds a subset sufficient to best explain the biotic structure. A heat map with bi-clustering dendrogram was generated using R and the package ‘seriation’ (Hahsler *et al.*, 2007) on the normalised square-root transformed SSU counts.

4.3.5 Analysis of functional potential

The relative abundance and taxonomic origin of functional marker genes was used to determine the potential for carbon, nitrogen and sulphur conversions. The ORFs were predicted from trimmed metagenomic reads using METAGENE (Noguchi *et al.*, 2006) accepting those >90 bp in length. Open reading frames ORFs were translated using the standard bacterial/plastid translation table and compared to protein sequences from the KEGG Genes database (release 58) using the basic local alignment search tool (BLAST) (Altschul *et al.*, 1990).

The BLAST output was processed using KEGG Orthology Based Annotation System (KOBAS) version 2.0 (Xie *et al.*, 2011) accepting assignments to KEGG Orthology (KO) groups with e-value $<1e-05$ and rank >5 . KO groups used as functional markers are listed in Supplementary (Table 4.2). Marker enzymes were assigned to taxonomic groups based on the species of origin of the best KEGG Genes match.

Table 4.2: Full list of KEGG orthologs involved in carbon, nitrogen and sulphur conversions that were searched for in the Organic lake metagenome.

Process	Gene	KO	Notes
C fixation	ribulose-bisphosphate carboxylase large (<i>cbbL</i>)	K01601	Calvin cycle
	ribulose-bisphosphate carboxylase small (<i>cbbS</i>)	K01602	Calvin cycle
	phosphoribulokinase (<i>prkB</i>)	K00855	Calvin cycle
	ATP-citrate lyase alpha (<i>aclA</i>)	K15230	rTCA cycle
	ATP-citrate lyase beta (<i>aclB</i>)	K15231	rTCA cycle
	citryl-CoA lyase (<i>ccl</i>)	K15234	rTCA cycle
	citryl-CoA synthetase (<i>ccsB</i>)	K15233	rTCA cycle
	carbon monoxide dehydrogenase/acetyl-CoA synthase alpha (<i>cdhA</i>)	K14138	WL
	carbon monoxide dehydrogenase/acetyl-CoA synthase beta (<i>cdhB</i>)	K00190	WL
Respiration	cytochrome C oxidase subunit I (<i>coxI</i>)	K02256	Eucaryotic
	cytochrome C oxidase subunit III (<i>coxIII</i>)	K02262	Eucaryotic
	cytochrome C oxidase subunit I (<i>coxA</i>)	K02274	Bacterial
	cytochrome C oxidase subunit III (<i>coxC</i>)	K02276	Bacterial
Fermentation	L-lactate dehydrogenase (<i>ldh</i>)	K00016	
	pyruvate:ferredoxin oxidoreductase alpha (<i>porA</i>)	K00169	
CO oxidation	pyruvate:ferredoxin oxidoreductase beta (<i>porB</i>)	K00170	
	carbon-monoxide dehydrogenase large (<i>coxL</i>)	K03520	
	carbon-monoxide dehydrogenase medium (<i>coxM</i>)	K03519	
AAnP	carbon-monoxide dehydrogenase small (<i>coxS</i>)	K03518	
	photosynthetic reaction center L (<i>pufL</i>)	K08928	
	photosynthetic reaction center M (<i>pufM</i>)	K08929	
Methanogenesis	coenzyme M methyl reductase (<i>mcrB</i>)	K00401	
	methyl coenzyme M reductase system	K00400	
CH ₄ oxidation	soluble methane monooxygenase	K08684	
	nitrogenase (<i>anfG</i>)	K00531	
N fixation	nitrogenase molybdenum-iron protein alpha (<i>nifD</i>)	K02586	
	nitrogenase iron protein (<i>nifH</i>)	K02588	
	nitrogenase molybdenum-iron protein beta (<i>nifK</i>)	K02591	
	nitric oxide reductase (<i>norB</i>)	K02305	
Denitrification	nitric oxide reductase (<i>norC</i>)	K02305	
	nitrous oxide reductase (<i>nosZ</i>)	K00376	
	periplasmic cytochrome c-552 (<i>nrfA</i>)	K03385	
DNRA	hydroxylamine oxidase (<i>hao</i>)	K10535	hzo-like
	glutamate dehydrogenase (<i>gudB, rocG</i>)	K00260	
N assimilation	glutamate dehydrogenase (NAD(P)+)	K00261	
	glutamate dehydrogenase (<i>gdhA</i>)	K00262	
	assimilatory nitrate reductase	K00360	
	assimilatory nitrate reductase (<i>nasA</i>)	K00372	
	assimilatory nitrate reductase (<i>narG</i>)	K00367	
	glutamine synthetase (<i>glnA</i>)	K01915	
	glutamate synthetase (NADPH/NADH) (<i>gltB</i>)	K00265	
	glutamate synthetase (ferredoxin) (<i>gltS</i>)	K00284	
	ammonia monooxygenase subunit A (<i>amoA</i>)	K10944	
	ammonia monooxygenase subunit B (<i>amoB</i>)	K10945	

Continued on next page

Table 4.2 – *Continued from previous page*

Process	Gene	KO	Notes
DSR	ammonia monooxygenase subunit C (<i>amoC</i>)	K10946	
	adenylylsulfatereductase subunit A (<i>aprA</i>)	K00394	SRB related
	adenylylsulfatereductase subunit B (<i>aprB</i>)	K00395	SRB related
	sulfite reductase (<i>dsrA</i>)	K11180	SRB related
	sulfite reductase (<i>dsrB</i>)	K11181	SRB related
ASR	adenylyl sulfate kinase (<i>cysC</i>)	K00860	
	sulfateadenylyltransferase (<i>cysN</i>)	K00956	
	sulfateadenylyltransferase (<i>cysD</i>)	K00957	
S mineralisation	cysteine diogenase (<i>cdoI</i>)	K00456	
	thiosulfate/3-Mercaptopyruvate sulfurtransferase (<i>sseA</i>)	K01011	
DMSP reduction	anaerobic dimethyl sulfoxidereductase A (<i>dmsA</i>)	K07306	

Marker genes not represented by a KO group were assessed by BLASTP queries of marker gene sequences with experimentally confirmed function (Table 4.3) against a database of translated ORFs predicted from metagenomic reads. Matches were accepted if the e-value was $<1\text{e}-10$ and sequence identity was within the range shared by homologues of the query sequence(s) (Table 4.3). Matches to marker genes were normalised to 100 Mbp per sample and counted. Normalised frequencies of markers from the same pathway were averaged and those from different pathways were summed.

The same marker genes and BLAST procedure was used to compare the DMSP catabolism and photoheterotrophy potential of Organic Lake with nearby Ace Lake (Lauro *et al.*, 2011), Southern Ocean (SO) (Wilkins *et al.*, 2012) and global ocean sampling (GOS) metagenomes (Rusch *et al.*, 2007). Counts of single copy gene *recA* were also determined to estimate the percentage of genomes containing each marker gene (percentage of marker genes relative to *recA*). Matches to *recA* were accepted with e-value $<1\text{e}-20$ according to the cut-off established by Howard *et al.* (2008). For GOS samples, the BLAST database was generated from peptide sequences retrieved from Community Cyberinfrastructure for Advanced Microbial Ecology Research and Analysis (CAMERA) (camera.calit2.net) while the other BLAST databases were produced as for Organic Lake. The total number of trimmed base pairs for GOS samples was estimated by multiplying the number of reads from each sample by the average read length (822 bp) (Rusch *et al.*, 2007).

Marker gene sequences for phylogenetic analysis were clustered using the CD-HIT web server (Huang *et al.*, 2010) at 90% global amino acid identity. A representative sequence from the clusters that resided within a desired conserved region and homologues from cultured strains were used in phylogenetic analyses performed in Molecular Evolutionary Genetic Analysis (MEGA) 5.05 (Tamura *et al.*, 2011) implementing MUSCLE with default parameters (gap opening penalty: -2.9, gap extension penalty: 0). Neighbor-joining was used to compute the phylogenies with a Poisson substitution model, uniform rates of change and complete deletion of alignment gaps. Node support was tested with bootstrap analysis (500 replicates).

Table 4.3: Functional marker gene sequences used in this study as BLAST queries for retrieving homologues in the Organic Lake metagenomes. %ID, minimum amino acid identity for a match to be considered homologous.

Gene (%ID)	Organism	Accession	Reference
<i>dddD</i> (60)	<i>Marinomonas</i> sp.MWYL1	ABR72937.1	Todd <i>et al.</i> (2007)
	<i>Pseudomonas</i> sp.J465	ACY01992.1	Curson <i>et al.</i> (2010)
	<i>Psychrobacter</i> sp.J466	ACY02894.1	Curson <i>et al.</i> (2010)
	<i>Halomonas</i> sp. HTNK1	ACV84065.1	Todd <i>et al.</i> (2010)
<i>dddL</i> (45)	<i>Sulfitobacter</i> sp. EE36	ADK55772.1	Curson <i>et al.</i> (2008)
	<i>Rhodobacter sphaeroides</i> 2.4.1	ABA77574.1	Curson <i>et al.</i> (2008)
<i>dddP</i> (55)	<i>Roseovarius nubinhibens</i> ISM	EAP77700.1	Todd <i>et al.</i> (2009)
<i>dddQ</i>	<i>Ruegeria pomeroyi</i> DSS-3	AAV94883.1	
	<i>Roseovarius nubinhibens</i> ISM	EAP76001.1	
	marine metagenome	EAP76002.1	Todd <i>et al.</i> (2011)
		GOS_7860946	Todd <i>et al.</i> (2011)
		GOS_2632696	Todd <i>et al.</i> (2011)
		GOS_2469775	Todd <i>et al.</i> (2011)
<i>dddW</i>	<i>Ruegeria pomeroyi</i> DSS-3	AAV93771.1	Todd <i>et al.</i> (2012)
<i>dddY</i>	<i>Alcaligenes faecalis</i>	ADT64689.1	Curson <i>et al.</i> (2011a)
<i>dmdA</i> (50)	<i>Ruegeria pomeroyi</i> DSS-3	AAV95190.1	Howard <i>et al.</i> (2006)
	<i>Pelagibacter ubique</i> HTCC1062	YP_265671.1	Howard <i>et al.</i> (2006)
<i>rhodopsin</i>	<i>Dokdonia donghaensis</i> MED134	EAQ40507.1	Gómez-Consarnau <i>et al.</i> (2007)
	<i>Vibrio</i> sp. AND4	ZP_02194911.1	Gómez-Consarnau <i>et al.</i> (2010)
	<i>Salinibacter ruber</i> DSM 13855	YP_445623.1	Balashov <i>et al.</i> (2005)
<i>pufL</i> (45)	<i>Roseovarius tolerans</i>	ABK88229.1	Labrenz <i>et al.</i> (1999)
	<i>Congregibacter litoralis</i> KT71	ZP_01104363.1	Fuchs <i>et al.</i> (2007)
<i>pufM</i> (45)	<i>Roseovarius tolerans</i>	ABK88230.1	Labrenz <i>et al.</i> (1999)
	<i>Congregibacter litoralis</i> KT71	ZP_01104362.1	Fuchs <i>et al.</i> (2007)
<i>soxB</i> (45)	<i>Sulfurimonas denitrificans</i> DSM 1251	YP_392780.1	Sievert <i>et al.</i> (2008)
	<i>Thiomicrospira crunogena</i> XCL-2	ABB42141.1	Scott <i>et al.</i> (2006)
<i>soxA</i> (45)	<i>Sulfurimonas denitrificans</i> DSM 1251	YP_392780.1	Sievert <i>et al.</i> (2008)
	<i>Thiomicrospira crunogena</i> XCL-2	YP_390871.1	Scott <i>et al.</i> (2006)
<i>soxC</i> (45)	<i>Sulfurimonas denitrificans</i> DSM 1251	YP_394569.1	Sievert <i>et al.</i> (2008)
	<i>Thiomicrospira crunogena</i> XCL-2	YP_390427.1	Scott <i>et al.</i> (2006)
<i>soxD</i> (45)	<i>Sulfurimonas denitrificans</i> DSM 1251	YP_394568.1	Sievert <i>et al.</i> (2008)
	<i>Thiomicrospira crunogena</i> XCL-2	YP_390427.1	Scott <i>et al.</i> (2006)
<i>sgr</i> (60)	<i>Sulfurimonas denitrificans</i> DSM 1251	ABB43898.1	Sievert <i>et al.</i> (2008)
<i>recA</i>	<i>Escherichia coli</i> K12	P0A7G6.2	Howard <i>et al.</i> (2008)

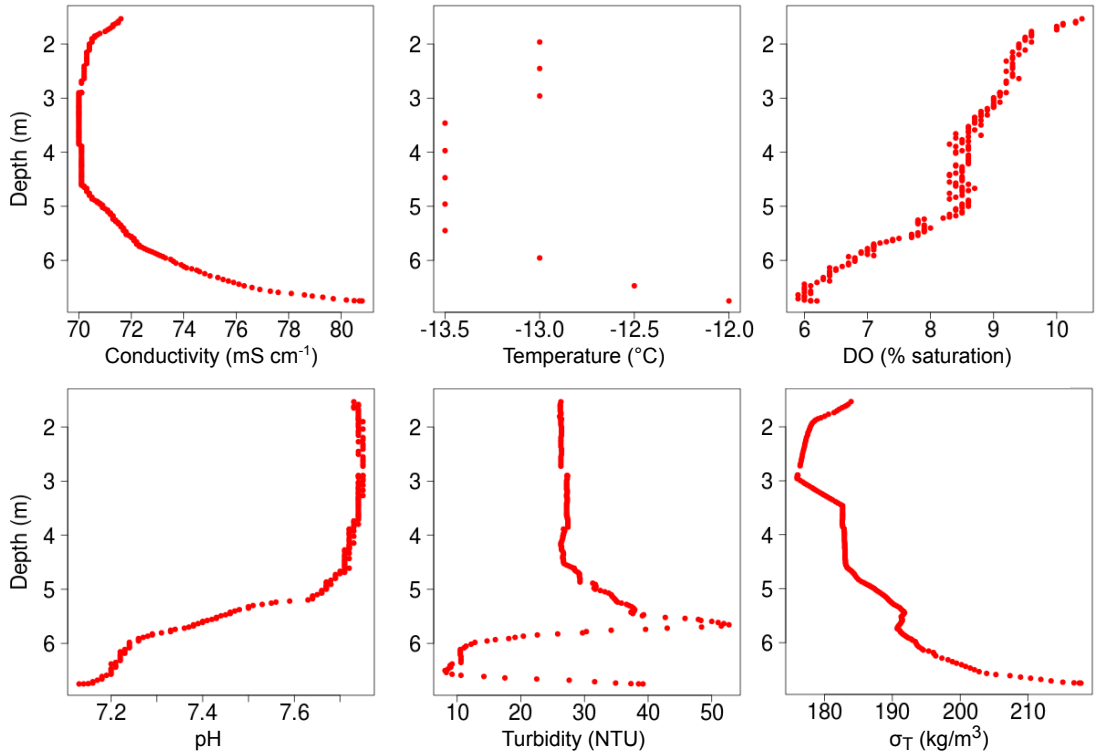


Figure 4.1: Vertical profiles of *in situ* Organic Lake abiotic parameters measured at the deepest point in the lake on 9 November 2008. $\sigma_T = (1000 - \text{density})$ was calculated from temperature and conductivity

4.4 Results and discussion

4.4.1 Abiotic properties and water column structure

In situ physico-chemical profiles (Figure 4.1) measured over the deepest point in the lake (Figure 4.2) determined the existence of two zones: an upper mixed zone above 5.7 m and a suboxic deep zone below 5.7 m (Figure 4.3). The separation of the two zones was indicated by a pycnocline and oxycline starting at 5.7 m. The pH also decreased with DO, likely due to fermentation products such as acetic, formic and lactic acids that have been reported in the bottom waters (Franzmann *et al.*, 1987b; Gibson *et al.*, 1994). The deep zone was not completely anoxic (Figure 4.1). Oxygen may be episodically introduced to bottom waters as a result of currents of cold dense water sinking during surface ice-formation (Ferris *et al.*, 1991). In comparison to meromictic lakes such as Ace Lake that have strong pycnoclines and a steep salt gradient in the anoxic zone, Organic Lake is shallow and has relatively weak stratification (Gibson, 1999).

Samples were collected from the upper mixed (1.7, 4.2 and 5.7 m) and deep (6.5 m and 6.7 m) zones. All nutrients, except for nitrate and nitrite reached maximum concentrations at 6.5 m (Table 4.4) suggestive of a layer of high biological activity above the lake bottom. Consistent with this, cell and VLP counts were highest at 6.5 m. However, turbidity was lowest at this depth demonstrating turbidity was not principally determined by cell density (Figure 4.3). Microscopy images did not show a

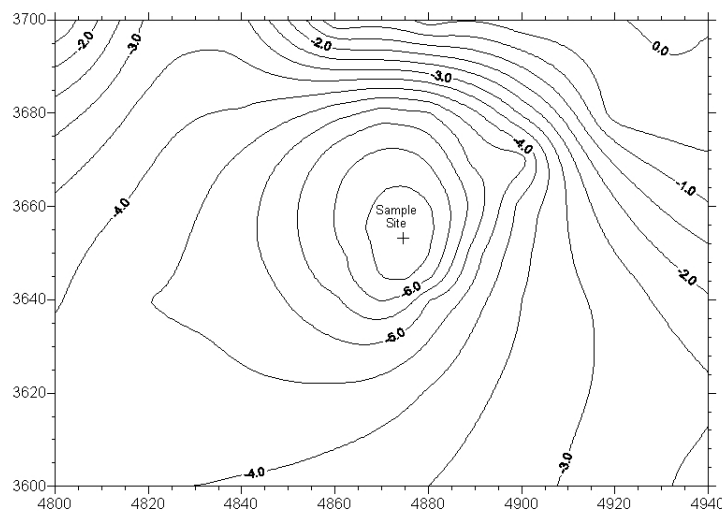


Figure 4.2: Bathymetry of Organic Lake 9 November 2008. Eastings and northings shown are abbreviated metric grid co-ordinates.

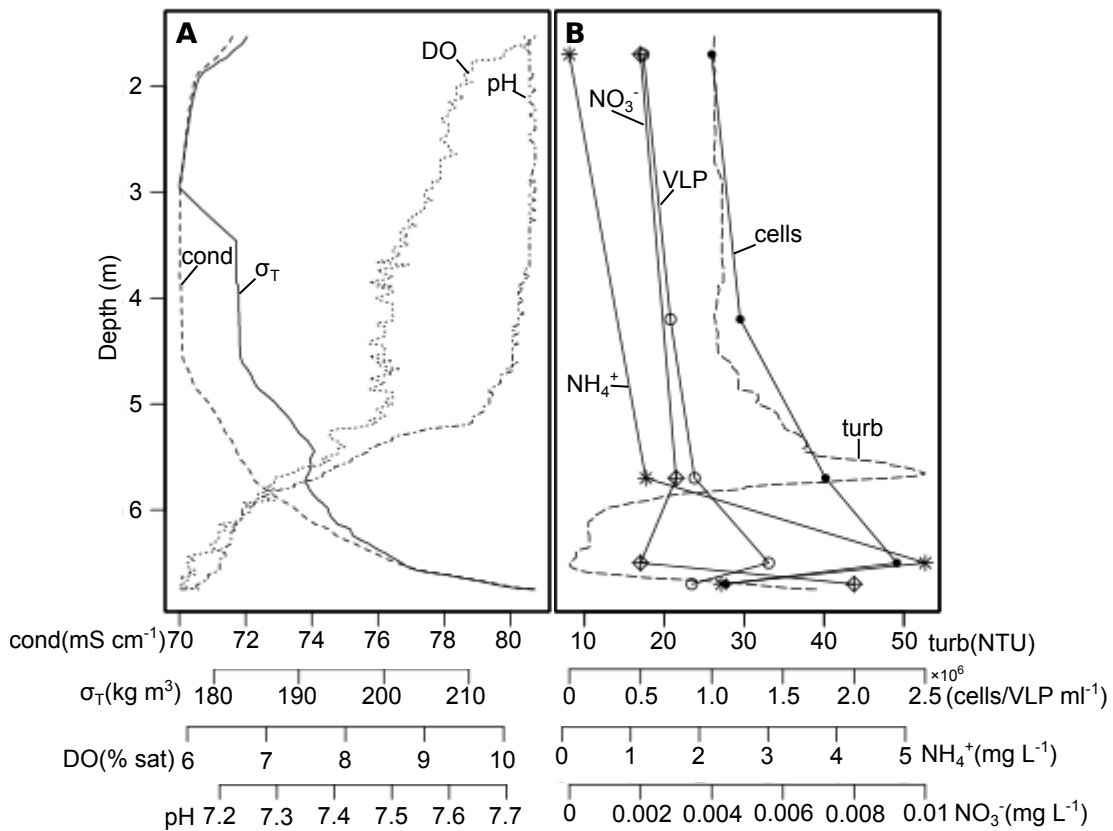


Figure 4.3: Vertical structure of Organic Lake. **(A)** Parameters that varied unimodally with depth showed two zones: an aerobic mixed zone above 5.7 m and a denser suboxic zone below. **(B)** Additional factors that revealed stratification within the deep zone. The peak in concentration at 6.5 m for ammonia was also observed for all other nutrients assayed except nitrate and nitrite, see (Table 4.4) for these values. $\sigma_T = (1000 - \text{density})$; cond, conductivity; DO, dissolved oxygen; turb, turbidity.

Table 4.4: Physico-chemical properties, cell counts and VLP counts of Organic Lake 2008 samples from a vertical profile. ND, data not determined.

	sample depths (m)				
	1.7	4.2	5.7	6.5	6.7
ammonia (mg l ⁻¹)	0.108	ND	1.22	5.29	2.32
nitrate (mg l ⁻¹)	<0.002	ND	0.003	<0.002	0.008
nitrite (mg l ⁻¹)	<0.002	ND	<0.002	0.010	0.010
DRP (mg l ⁻¹)	0.08	ND	0.10	0.20	0.18
TOC (mg l ⁻¹)	88	87	110	170	130
DOC (mg l ⁻¹)	69	ND	97	150	120
TN (mg l ⁻¹)	7.70	7.50	11	24	13
TDN (mg l ⁻¹)	0.112	ND	1.225	5.302	2.338
TP (mg l ⁻¹)	1.5	1.4	3.0	7.6	3.7
TDP (mg l ⁻¹)	0.509	ND	0.805	4.5	2
TS (mg l ⁻¹)	1010	974	1020	1410	950
TDS (mg l ⁻¹)	996	ND	1250	1290	995
particulate C:N:P (molar ratios)	49:7:1	ND	15:2:1	17:3:1	15:1:1
dissolved C:N:P (molar ratios)	350:20:1	ND	311:26:1	86:10:1	155:13:1
practical salinity	166	166	172	178	186
temperature (°C)	-13	-13.5	-13	-12.5	-12
cells ml ⁻¹	1.0±0.4×10 ⁶	1.2±0.3×10 ⁶	1.8±0.5×10 ⁶	2.3±0.8×10 ⁶	1.1±0.4×10 ⁶
VLP ml ⁻¹	5.2±2.1×10 ⁵	7.1±1.3×10 ⁵	8.8±3.4×10 ⁵	14±3.0×10 ⁵	8.6±3.3×10 ⁵

shift in cell morphology that could account for the large drop in turbidity (Figure 4.4), which suggests particulate matter primarily contributed to turbidity readings. The low turbidity and peak in cell counts and nutrients at the oxycline at 6.5 m may be caused by an active microbial community degrading particulate matter. This inference is supported by the report of high concentrations of dissolved organic acids and free amino acids in the deep zone (Gibson *et al.*, 1994) as these nutrients are indicative of the breakdown of high molecular weight carbohydrates, lipids and proteins. Furthermore, the C:N and C:P ratios throughout the lake were high compared to the Redfield ratio (Redfield *et al.*, 1963) except at 6.5 m indicating this was the only depth where dissolved nitrogen and phosphorus were not relatively limited (Table 4.4).

Principal component analysis PCA of physico-chemical parameters showed all samples, except the 6.5 m sample, separated with depth along the PC1 axis (Figure 4.5). Accordingly, turbidity, TS and cell density were the strongest explanatory variables for the separation of the 6.5 m sample from the other deep sample, indicating that increased activity at 6.5 m was related to breakdown of particulate matter and sulphur chemistry.

4.4.2 Overall microbial diversity

SSU genes (3,959 reads) that were retrieved from the metagenome data grouped into 983 OTUs. OTUs for *Bacteria* comprised 76.2%, *Eucarya* 16.3% and 7.5% of SSU sequences could not be classified. Only 2 reads, assigned to a deep sea hydrothermal clade of *Halobacteriales* (Supplementary Table S4), were assigned to *Archaea* indicating they were rare in Organic Lake.

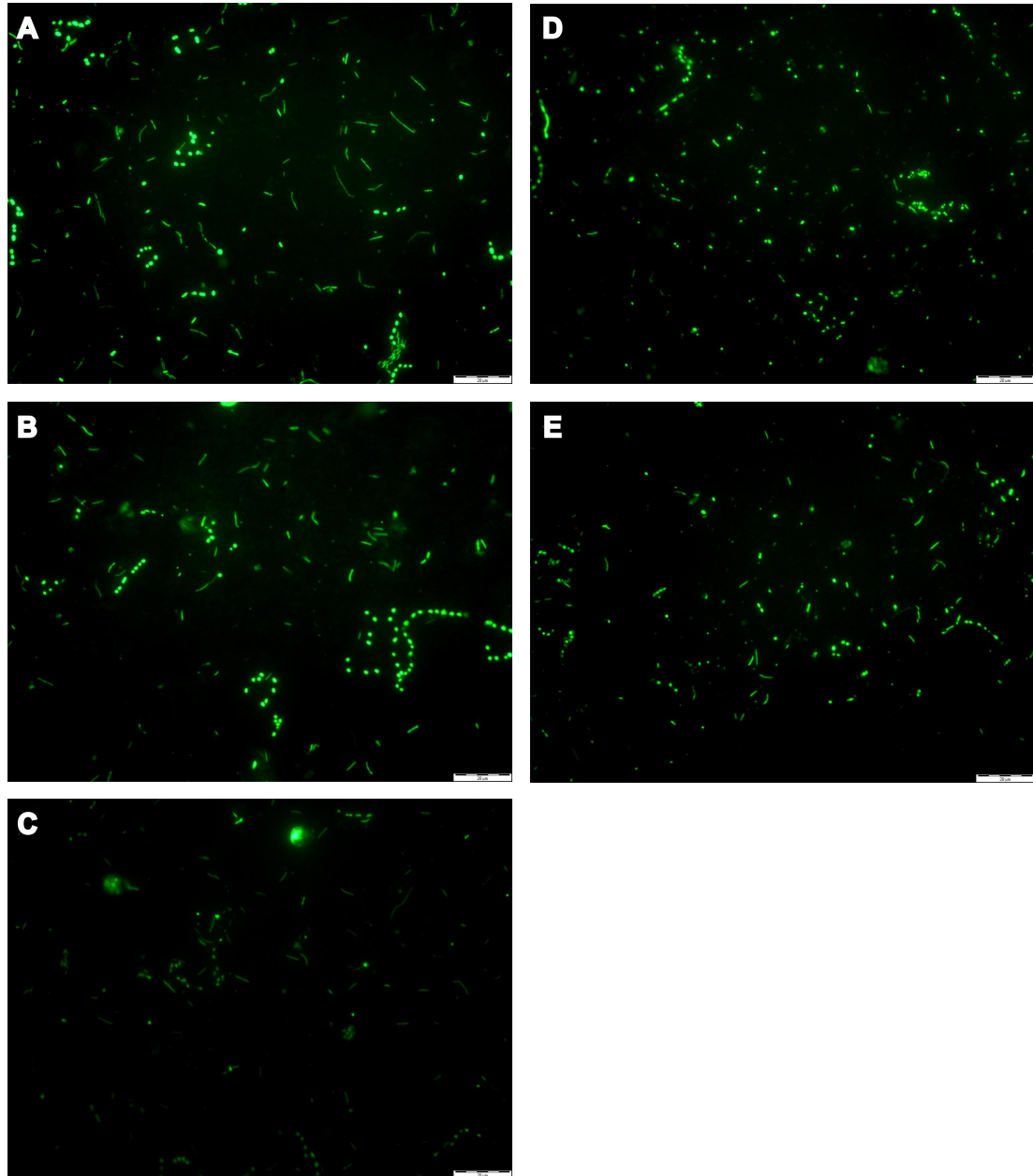


Figure 4.4: Epifluorescence microscopy images of Organic Lake microbiota ($<20\text{ }\mu\text{m}$) onto $0.015\text{ }\mu\text{m}$ polycarbonate membrane and stained with SYBR Gold. (A) 1.7 m, (B) 4.2 m, (C) 5.7 m, (D) 6.5 m, (E) 6.7 m. Scale bar = $20\text{ }\mu\text{m}$.

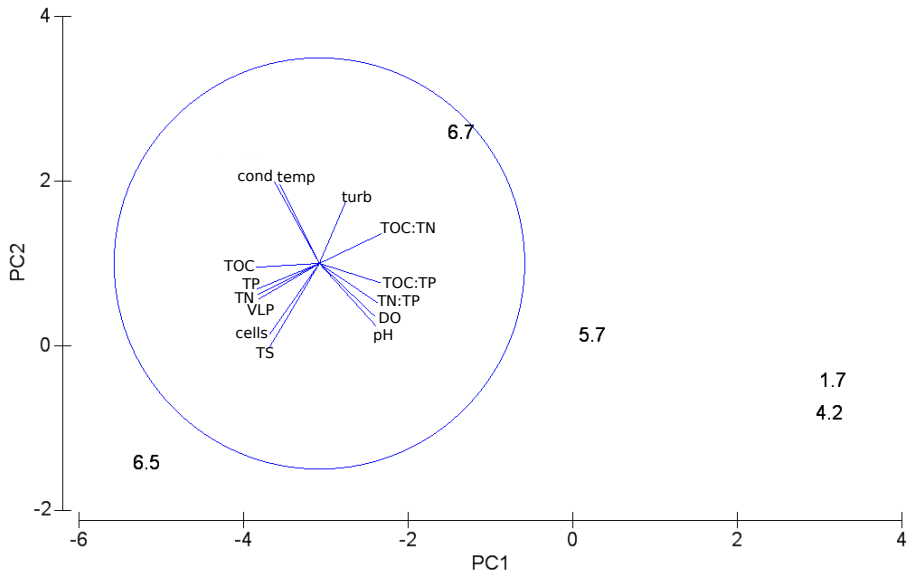


Figure 4.5: PCA of physico-chemical parameters and cell/VLP counts of the Organic Lake profile. Data points are the sampling depths 1.7, 4.2, 5.7, 6.5 and 6.7 m. The overlaid vector diagram shows the relative contributions of the variables to explaining the difference between samples. PC1 explained 74.3% and PC2 explained 14.7% of the variation between samples. cond, conductivity; temp, temperature; turb, turbidity.

The most abundant bacterial classes, *Gammaproteobacteria*, *Alphaproteobacteria* and *Flavobacteria*, were represented by OTUs on all filter sizes at all depths and each consisted of one dominant genus, *Marinobacter*, *Roseovarius* and *Psychroflexus*, respectively (Figure 4.6). Essentially all OTUs for *Cyanobacteria*/chloroplasts were classified as chloroplasts (Figure 4.6), except for three reads that could not be assigned to any lower rank (Supplementary Table S4) indicating free-living *Cyanobacteria* were rare or absent. OTUs for moderately abundant bacterial classes were *Actinobacteria*, *Deltaproteobacteria*, *Epsilonproteobacteria*, and candidate divisions OD1 and RF3. Lower abundance divisions included OTUs for *Bacilli*, *Clostridia*, *Spirochaetes*, *Lentisphaeria*, TM7, *Opitutae*, *Verrucomicrobia*, Bhi80-139, Bd1-5, SR1 and *Chlamydiae* (Figure 4.6).

The dominant eucaryal OTUs were for photosynthetic *Chlorophyta* (green algae) and *Dictyochophyceae* (silicoflagellate algae) (Figure 4.7) principally assigned to the genus *Dunaliella* and the order *Pedinellales*, respectively (Supplementary Table S4). Lower abundance eucaryal OTUs included *Bacillariophyta* (diatoms), *Dinophyceae*, *Fungi* and heterotrophic *Choanoflagellida* and *Ciliophora* (see Supplementary Table S4 for lower taxonomic rank assignments).

4.4.3 Variation of microbial composition according to size and depth

Community composition varied with size fraction and depth. This was supported by seriation analysis that showed samples clustered according to size fraction, and those clusters further separated into upper mixed and deep zone groups (Figure 4.8). A significant difference in genus-level composition between the upper mixed and deep zones was supported by ANOSIM test ($\text{Rho}: 0.53$, significance: 0.1%). Differential

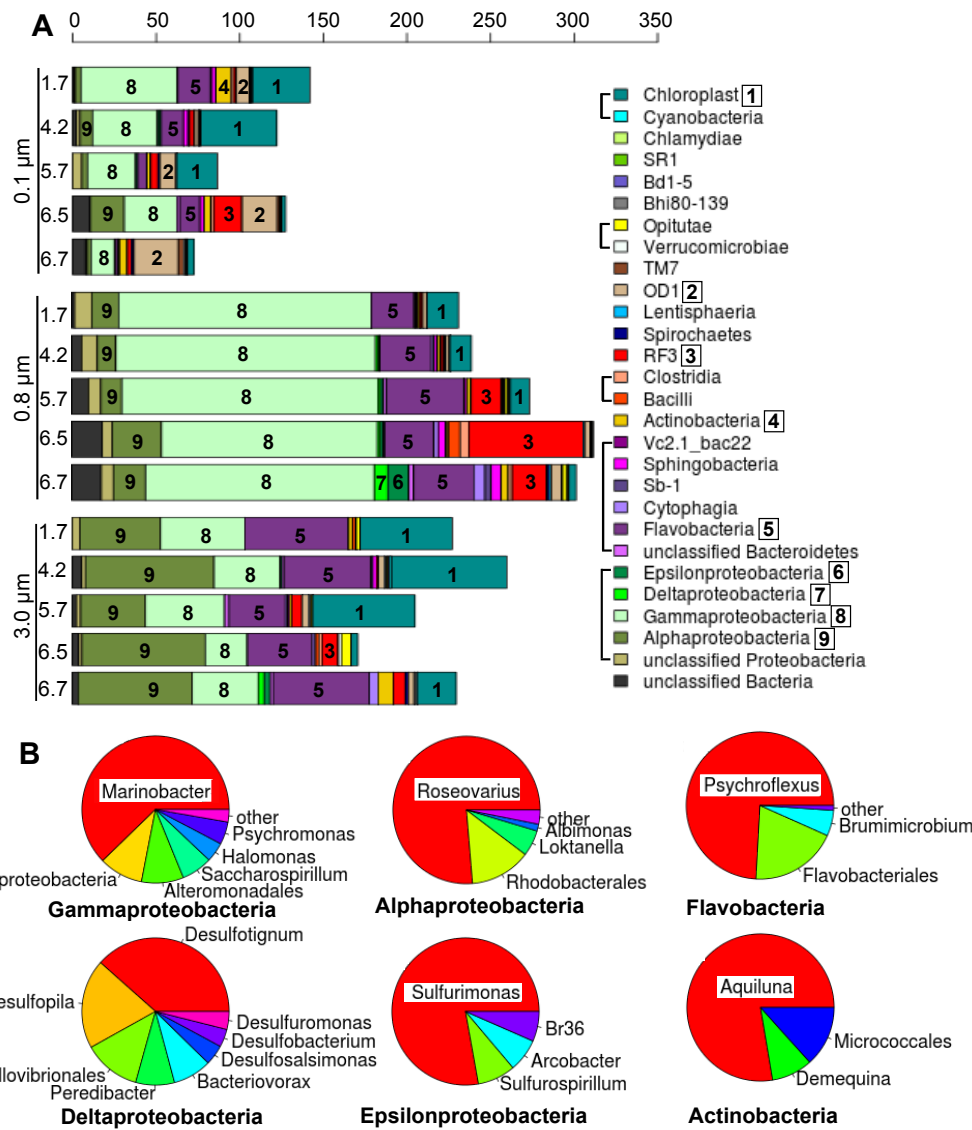


Figure 4.6: Diversity of (A) *Bacteria* from each size fraction (0.1, 0.8 and 3.0 µm) at each sample depth (1.7, 4.2, 5.7, 6.5 and 6.7 m) of Organic Lake aggregated according to class. The x-axis shows counts of SSU normalised to average reads acquired per sample filter. Taxa that belong to the same higher rank are shown grouped with a square bracket in the legend. Abundant taxa are labelled in plot with a number that corresponds to the numbered boxes in the legend. (B) Composition of abundant bacterial classes.

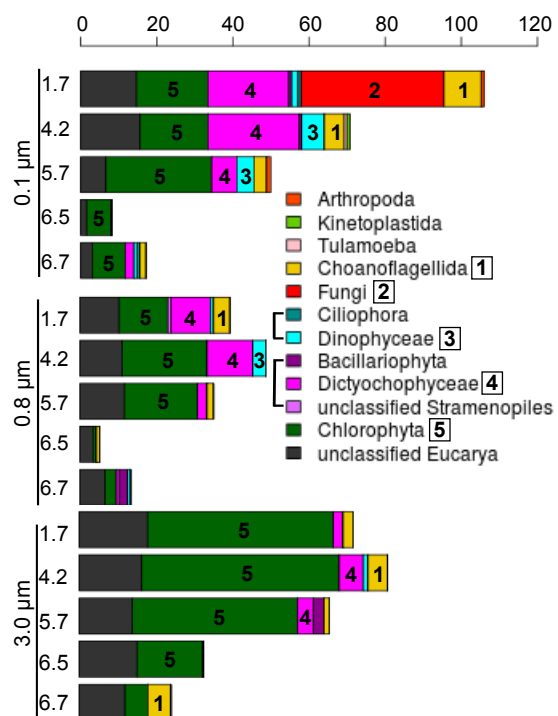


Figure 4.7: Diversity of *Eucarya* from each size fraction (0.1, 0.8 and 3.0 μm) at each sample depth (1.7, 4.2, 5.7, 6.5 and 6.7 m) of Organic Lake aggregated according to class. The x-axis shows counts of SSU normalised to average reads acquired per sample filter. Taxa that belong to the same higher rank are shown grouped with a square bracket in the legend. Abundant taxa are labelled in plot with a number that corresponds to the numbered boxes in the legend.

vertical distribution of taxa is consistent with partitioning of ecological functions in the lake and in association with the physical and chemical data, described functional roles of those taxa.

20–3.0 μm fraction community composition

The upper mixed zone samples had a relatively high OTU abundance of *Dunaliella* chloroplasts and chlorophyte algae consistent with large active photosynthetic organisms concentrating near surface light. They are likely the main source of primary production in Organic Lake and have previously been reported to be the dominant algae (Franzmann *et al.*, 1987b). The SSU sequences for these algae at the bottom of the lake are likely to be due to sedimentation of dead cells or resting cysts.

Psychroflexus OTUs were overrepresented in the surface and 6.7 m samples. Consistent with enrichment on the 3.0 μm filters, *Psychroflexus* (formerly *Flavobacterium*) *gondwanensis* (Bowman *et al.*, 1998) isolated from Organic Lake (Franzmann *et al.*, 1987b) had cells 1.5–11.5 μm in length (Dobson *et al.*, 1991). *Flavobacteria* associate with phytoplankton blooms in the Southern Ocean (Abell and Bowman, 2005a,b; Williams *et al.*, 2012), and have specialized abilities to degrade polymeric substances from algal exudates and detritus (reviewed in Kirchman (2002), (Williams *et al.*, 2012)). It is likely that Organic Lake *Psychroflexus* fills a similar ecological role. In support of this, *Psychroflexus* OTUs cluster with *Dunaliella* chloroplasts in the seriation analysis (Figure 4.8) and *P. gondwanensis* abundance in Organic Lake has been correlated with average hours of sunshine per day indicating population dynamics that is related to summer algal blooms (James *et al.*, 1994). The *Psychroflexus* OTUs in the deep zone are most likely due to sedimentation as *P. gondwanensis* non-motile and strictly aerobic (Dobson *et al.*, 1991).

Roseovarius OTUs were enriched at 4.2 m and 6.5 m suggesting different ecotypes may be present in the upper mixed zone compared to the deep zone. *Roseovarius tolerans*, an isolate from Ekho Lake in the Vestfold Hills, Antarctica has a cell size (1.1–2.2 μm ; (Labrenz *et al.*, 1999)) that would be expected to be captured on the 0.8 μm filter. The *Roseovarius* captured on the 3 μm filter may therefore be a different species, or a strain similar to *R. tolerans* from Ekho Lake that exhibits different growth characteristics (i.e. larger cell size or forms aggregates). A strain of this species from Ekho Lake is capable of microaerophilic growth (Labrenz *et al.*, 1999). Overrepresentation at 6.5 m may therefore be indicative of growth at that depth rather than sedimentation because sinking cells would be more abundant close to the lake bottom at 6.7 m. *Roseovarius* OTUs cluster with *Dunaliella* chloroplast and *Psychroflexus* OTUs in the seriation analysis (Figure 4.8), suggesting that Organic Lake *Roseovarius* may be utilising compounds released from algal-derived particulate matter, or made available by processing of complex organic matter by *Psychroflexus*. *Roseovarius* is a member of the *Roseobacter* clade, which is inferred to have an opportunistic ecology frequently associated with nutrient-replete plankton aggregates, including by-products of flavobacterial exoenzymatic attack (Moran *et al.*, 2007; Teeling *et al.*, 2012). Additionally, the diverse

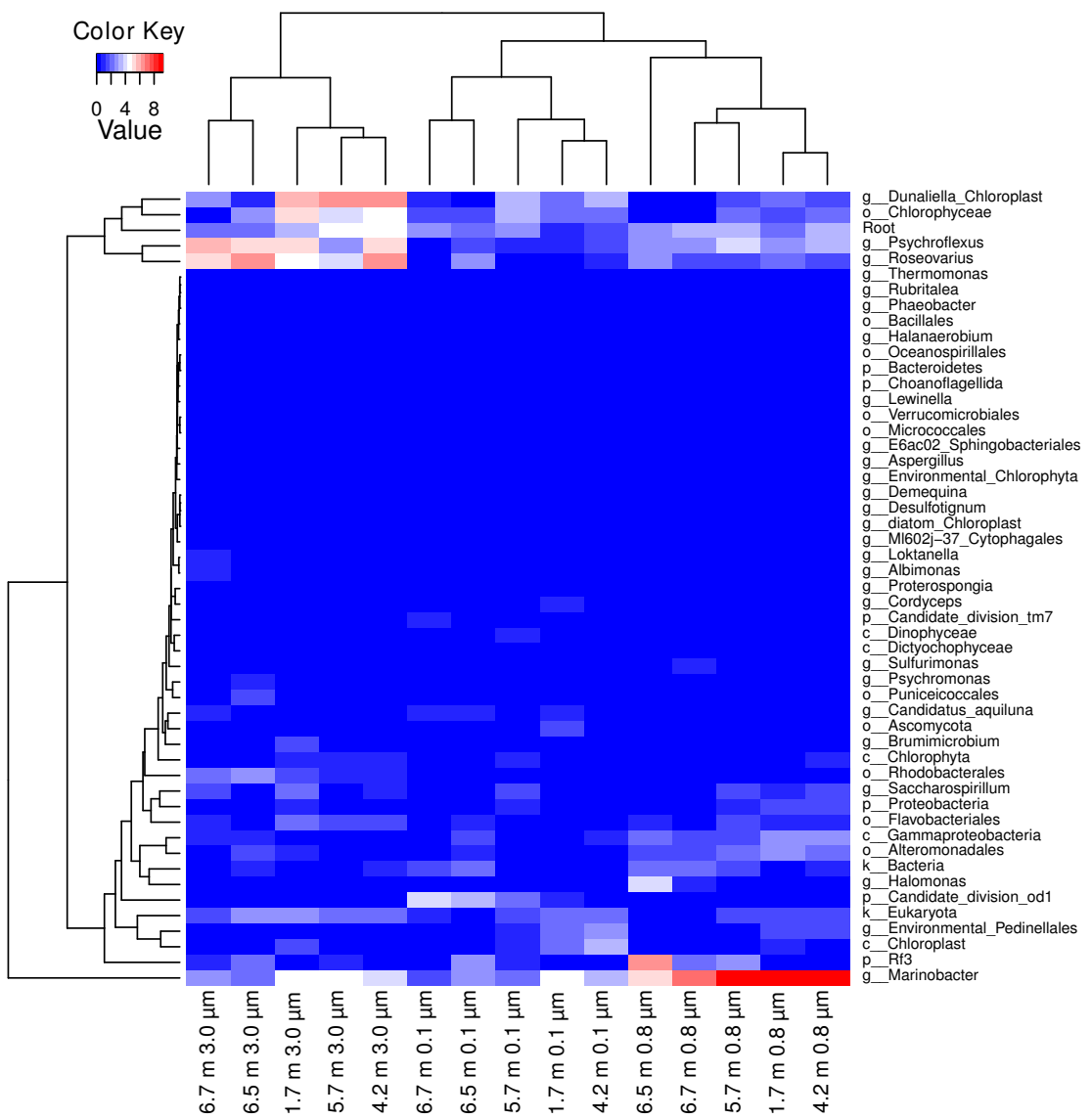


Figure 4.8: Heatmap and biclustering plot of the SSU gene composition in Organic Lake. Samples are shown according to size fraction (0.1, 0.8 and 3.0 μm) and depth (1.7, 4.2, 5.7, 6.5 and 6.7 m). SSU genes were classified to lowest taxonomic rank that gave bootstrap confidence $>85\%$ until the rank of genus. SSU gene counts were normalised and square root transformed. Taxa that comprised $<2\%$ of the sample were not included.

metabolic capabilities of the *Roseobacter* clade include DMSP degradation, AAnP and CO oxidation (reviewed in Wagner-Döbler and Biebl (2006)). All of these capabilities should facilitate growth in both the upper mixed and deep zones of Organic Lake (see 4.4.5).

3–0.8 µm size fraction community composition

On the 0.8 µm filter, OTUs for *Marinobacter* dominated at all depths except 6.5 m. Their capture on this size fraction is consistent with the cell size of isolates (1.2–3 µm) (Gauthier *et al.*, 1992). The genus is metabolically versatile, which likely permits it to occupy the entire water column. *Marinobacter* is heterotrophic and the genus includes hydrocarbon-degrading strains (e.g., Gauthier *et al.* (1992); Huu *et al.* (1996), although deep-sea metal-oxidising autotrophs have also been reported (Edwards *et al.*, 2003). Some isolates are capable of interacting with diatoms (Gärdes *et al.*, 2010) and dinoflagellates (Green *et al.*, 2006). *Marinobacter* isolates from Antarctic lakes are capable of anaerobic respiration using dimethylsulphoxide (DMSO) (Matsuzaki *et al.*, 2006) or nitrate (Ward and Priscu, 1997). Analysis of functional potential linked to *Marinobacter* revealed additional metabolic capabilities potentially related to its dominance in Organic Lake (see Carbon resourcefulness in dominant heterotrophic bacteria and Molecular basis for unusual sulphur chemistry below).

OTUs for RF3 and *Halomonas* were overrepresented at 6.5 m, and RF3 sequences were more abundant (Figure 4.8). Their relative abundance in the deep zone indicates a role in microaerophilic processes. The majority of RF3 sequences to date are from anaerobic environments including mammalian gut (Tajima *et al.*, 1999; Ley *et al.*, 2006; Samsudin *et al.*, 2011), sediment (Yanagibayashi *et al.*, 1999; Röske *et al.*, 2012), municipal waste leachate (Huang *et al.*, 2005), anaerobic sludge (Chouari *et al.*, 2005; Goberna *et al.*, 2009; Rivière *et al.*, 2009; Tang *et al.*, 2011), a subsurface oil well head (Yamane *et al.*, 2011), and the anaerobic zone of saline lakes (Humayoun *et al.*, 2003; Schmidtova *et al.*, 2009; Bowman *et al.*, 2000b). However, some members have been found in surface waters (Demergasso *et al.*, 2008; Xing *et al.*, 2009; Yilmaz *et al.*, 2012) suggesting not all members are strict anaerobes.

Several *Halomonas* isolates have been sourced from Organic Lake including two described species *Halomonas subglaciescola* and *H. meridiana*, both of which grow as rods with dimensions consistent with capture on this size fraction (Franzmann *et al.*, 1987a; James *et al.*, 1990). Despite these isolates being aerobic, *Halomonas* has been reported to be enriched at the oxycline in Organic Lake (James *et al.*, 1994) indicating *Halomonas* in the lake plays an ecological role in the suboxic zone. This capacity may be linked to the ability of free amino acids and organic acids, which are abundant in the deep zone (Gibson *et al.*, 1994), to stimulate the growth of isolates (Franzmann *et al.*, 1987a).

0.8–0.1 µm size fraction community composition

A large number of eucaryal sequences were evident in the 0.1 µm size fraction. The upper zone was overrepresented by OTUs for *Pedinellales* (silicoflagellate algae) that co-varied with chloroplasts (Figure 4.8). *Pedinellales* have only been detected in Antarctic lakes from molecular studies (Unrein *et al.*, 2005; Lauro *et al.*, 2011) including Organic Lake (Yau *et al.*, 2011) (Chapter 3), and light microscopy studies of Antarctic Peninsula freshwater lakes reported 5–8 µm diameter cells resembling *Pseudopedinella* (Unrein *et al.*, 2005). It is possible that in Organic Lake small (0.80.1 µm) free-living members or chloroplast-containing cyst forms (Thomsen, 2007) exist. However, without evidence to support this (e.g. by microscopy) it seems more likely that the lake sustains a relatively small number of active photosynthetic cells and the sequences detected arise from cysts or degraded cellular material.

OTUs for *Candidatus Aquiluna*, in the Luna-1 cluster of *Actinobacteria* (Hahn *et al.*, 2004; Hahn, 2009) were most abundant at 1.7 m. The genus has small cells (<1.2 µm; (Hahn, 2009), accounting for their concentration on this size fraction. Although originally described in freshwater lakes, the same clade was detected in abundance in Ace Lake (Lauro *et al.*, 2011) and surface Arctic seawater (Kang *et al.*, 2012) demonstrating that they play ecological roles in polar saline systems. In Ace Lake surface waters they were associated with utilisation of labile carbon and nitrogen substrates (Lauro *et al.*, 2011), and in Organic Lake surface waters they probably perform similar functions. The presence of this clade in the deep zone implies a facultative anaerobic lifestyle or sedimented cells.

The bottom of the water column was distinguished by the presence of OTUs for candidate divisions OD1 and TM7. OD1 was more abundant, and its prevalence on this size fraction is consistent with similar findings for size fractionation of ground water (Miyoshi *et al.*, 2005). OD1 is consistently associated with reduced, sulphur-rich, anoxic environments (Harris *et al.*, 2004; Elshahed *et al.*, 2005). OD1 from Zodletone Spring, Oklahoma, was reported to possess enzymes related to those from anaerobic microorganisms (Elshahed *et al.*, 2005). Genomic analyses identified OTUs for OD1 in the anoxic zone of Ace Lake (Lauro *et al.*, 2011). The distribution of OD1 in Organic Lake is consistent with an anaerobic metabolism and potential involvement in sulphur chemistry.

4.4.4 Organic Lake functional potential

To determine the potential for functional processes in Organic Lake, gene markers for carbon, nitrogen and sulphur conversions were retrieved from metagenomic reads. BEST analysis showed that variation in the population structure was significantly correlated (Rho: 0.519, significance: 0.3%) with the abiotic parameters, DO, temperature, TS and TN. The DO gradient has an obvious effect of separating aerobic from anaerobic taxa, and allows oxygen sensitive nitrogen and sulphur processes to occur in the deep zone. Functional potential, taxonomic composition and the physico-chemical data were integrated to infer the carbon, nitrogen and sulphur cycles.

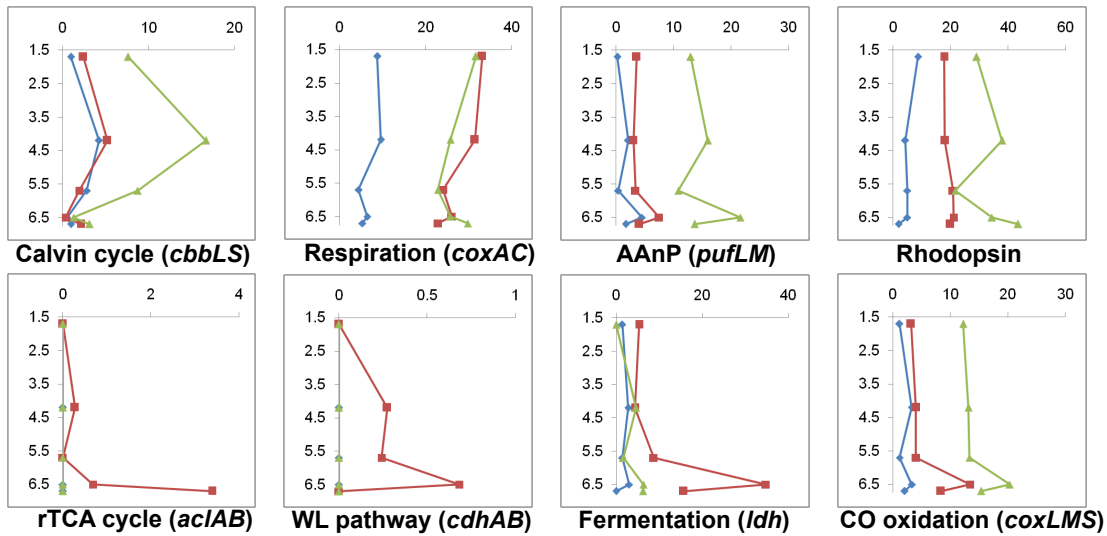


Figure 4.9: Vertical profiles of potential for carbon conversions for each size fraction in Organic Lake. The y-axis shows sample depths (m) and the x-axis shows counts of marker genes normalised to 100 Mbp of DNA sequence. The 0.1, 0.8, 3.0 μm size fractions are shown as blue, red and green, respectively. Counts for marker genes for the same pathway or enzyme complex were averaged and those from different pathways were summed. For marker gene descriptions see Table 4.2 and Table 4.3.

4.4.5 Carbon resourcefulness in dominant heterotrophic bacteria

In both the upper mixed and deep zones, potential for carbon fixation was much lower than for degradative processes, indicating potential for net carbon loss (Figure 4.9). Potential for carbon fixation via the oxygen-tolerant Calvin cycle (Figure 4.9) was originally assessed by presence of the marker genes ribulose-bisphosphate carboxylase oxygenase (RuBisCO) and phosphoribulokinase (*prkB*) (Hügler and Sievert, 2011). The majority of RuBisCO homologues were related to *Viridiplantae* (Table 4.5) supporting the ecological role of green algae as the principle photosynthetic organisms.

RuBisCO was only associated with a small proportion of *Gammaproteobacteria* (Table 4.5), principally from sulphur-oxidising *Thiomicrospira*, indicating some *Gammaproteobacteria* are autotrophs. However, the majority of *prkB* matched to *Gammaproteobacteria* (Table 4.5), predominantly *Marinobacter*. Although deep-sea, iron-oxidising autotrophic members of *Marinobacter* have been isolated (Edwards *et al.*, 2003), all genomes reported for *Marinobacter* have *prkB* but lack RuBisCO genes. Across *Marinobacter* genomes the *prkB* homologue is consistently adjacent to a gene for a putative phosphodiesterase, suggesting that the enzymes expressed by these genes may be involved in a pathway involved in pentose phosphate metabolism unrelated to carbon fixation. Albeit exceptional, this decoupling of *prkB* from RuBisCO involved in carbon fixation (forms I and II), also observed in *Ammonifex* (Hügler and Sievert, 2011), undermines the utility of *prkB* as a marker gene for the Calvin cycle within certain groups. Thus, there is no evidence for autotrophy in Organic Lake mediated by *Marinobacter*.

Evidence for carbon fixation via the reverse tricarboxylic acid (rTCA) cycle was also indicated (Figure 4.9), with genes for ATP citrate lyase (*aclAB*) linked to sulphur-

Table 4.5: Contribution of different taxonomic groups to counts of marker genes involved in carbon conversions. The taxon with the largest contribution to each process is highlighted in blue.

Taxon	Calvin cycle prkB	Respiration	Fermentation rTCA	WI	CO oxidation AAnP
<i>Acidobacteria</i>	0	0	0.02	0	0
<i>Actinobacteria</i>	0	0	0.64	0.23	0
<i>Alphaproteobacteria</i>	0.05	0	4.84	0	0
<i>Aquificae</i>	0	0	0.06	0	0
<i>Bacteroidetes</i>	0	0	3.42	0	0
<i>Betaproteobacteria</i>	0.04	0.06	0.07	0.09	0
<i>Chlorobi</i>	0	0	0	0	0
<i>Chloroflexi</i>	0	0	0.02	0	0
<i>Chrysigenetes</i>	0	0	0	0	0
<i>Cyanobacteria</i>	0.09	0	0	0	0
<i>Deferribacteres</i>	0	0	0.01	0	0
<i>Deinococcus-Thermus</i>	0.01	0	0.02	0	0
<i>Deltaproteobacteria</i>	0	0	0.09	0	0
<i>Epsilonproteobacteria</i>	0	0	0	0.28	0
<i>Firmicutes</i>	0.01	0	0.01	4.90	0
<i>Fornicata</i>	0	0	0	0	0
<i>Fusobacteria</i>	0	0	0	0	0.03
<i>Gammaproteobacteria</i>	0.05	12.1	9.86	1.03	0
<i>Nitrospirae</i>	0	0	0	0	0
<i>Planctomycetes</i>	0	0	0.02	0.08	0
<i>Spirochaetes</i>	0	0	0	0.03	0
<i>Thermobaculum</i>	0	0	0	0	0
<i>Thermotogae</i>	0.01	0	0	0	0.17
<i>Verrucomicrobia</i>	0	0	0.13	0.05	0
<i>Crenarchaeota</i>	0	0	0	0	0.01
<i>Euryarchaeota</i>	0.04	0	0	0	0
<i>Alveolata</i>	0	0	0.03	0	0
<i>Euglenozoa</i>	0	0	0	0	0
<i>Opistokonta</i>	0	0	0.16	0	0
<i>Rhodophyta</i>	0.16	0	0.03	0	0
<i>Strameopiles</i>	0.34	0	0	0	0
<i>Viridiplantae</i>	3.10	0.06	1.10	0	0

oxidising *Epsilonproteobacteria* (Table 4.5). In general, the rTCA cycle is restricted to anaerobic and microaerophilic bacteria (Hügler and Sievert, 2011), which is consistent with the detection of *Epsilonproteobacteria* in the lake bottom where oxygen is lowest, and the microaerophilic/anaerobic metabolisms characteristic of the group (Campbell *et al.*, 2006). Anaerobic carbon fixation was represented by potential for the Wood-Ljungdahl; or reductive acetyl-CoA (WL) pathway (Figure 4.9). WL-mediated carbon fixation, for which CO dehydrogenase/acetyl-CoA synthase is the key enzyme, was linked to *Firmicutes* and *Deltaproteobacteria* that are known to grow autotrophically using this pathway (Hügler and Sievert, 2011).

Potential for carbon loss by via respiration was indicated by an abundance of cytochrome C oxidase genes (*coxAC*) throughout the water column. In the deep zone, potential for fermentation was greatest at 6.5 m (Figure 4.9) and likely the main biological activity that was occurring at that depth. Fermentation was indicated by the marker gene lactate dehydrogenase (*ldh*). These genes were linked to *Firmicutes* (Table 4.5), which was only present at 6.5 m and represented by the classes *Clostridia* and *Bacilli* (Figure 4.6). As the related candidate division RF3 (Tajima *et al.*, 1999) also has relatively high abundance in this zone (Figure 4.6) (see 0.8–3.0 µm size fraction community composition above), there is circumstantial evidence that RF3 possesses fermentative metabolism and may therefore play an important ecological role in Organic Lake by degrading high molecular weight compounds to organic acids that other organisms can utilize. Assimilation of fermentation products appears to play a greater role in Organic Lake rather than complete anaerobic oxidation involving methanogens or sulphate-reducing bacteria; the former were absent and the latter were present in low abundance (Figure 4.6).

Alphaproteobacteria, predominantly *Roseovarius* (Figure 4.6), were implicated in CO oxidation (Table 4.5), which is used to generate energy for lithoheterotrophic growth (Moran and Miller, 2007), although CO oxidation may also be involved in anaplerotic C fixation (Moran and Miller, 2007). The CO oxidation capacity was at a maximum at 6.5 m (Figure 4.9), and therefore associated with the deep zone *Roseovarius* ecotype of Organic Lake. CO oxidation can function as a strategy to limit oxidation of organic carbon for energy so that a greater proportion can be directed towards biosynthesis (Moran and Miller, 2007).

Photosynthesis reaction center genes *pufLM*, involved in photoheterotrophy via AAnP, were abundant in Organic Lake (Figure 4.9, Table 4.5). These were linked to the *Roseobacter* clade of *Alphaproteobacteria* (Table 4.5), major contributors to AAnP in ocean surface waters (Béjà *et al.*, 2002; Moran and Miller, 2007). This is consistent with the known metabolic potential of bacteriochlorophyll A (BchlA) producing *Roseovarius tolerans* from Ekho Lake (Labrenz *et al.*, 1999). Photoheterotrophy can also be rhodopsin-dependent, with proteorhodopsin (PR) of marine *Flavobacteria* and *Vibrio* previously linked to light-dependent energy generation to supplement heterotrophic growth, particularly during carbon limitation (Gómez-Consarnau *et al.*, 2007, 2010). However, the function(s) of rhodopsins are diverse, and PRs are also hypothesized to

be involved in light or depth sensing (Fuhrman *et al.*, 2008).

Rhodopsin genes were abundant in Organic Lake (Figure 4.9), and were associated with all the dominant Organic Lake aerobic heterotrophic lineages (Figure 4.10). Phylogenetic analysis revealed six well-supported Organic Lake rhodopsin groups (Supplementary Figure S6). All groups had an L or M residue at position 105 (vs the SAR86 PR), denoting tuning to surface green light (Man *et al.*, 2003; Gómez-Consarnau *et al.*, 2007), and is characteristic of oceanic coastal samples (Rusch *et al.*, 2007). Four of the groups clustered with homologues of genera detected in the lake, namely *Marinobacter*, *Psychroflexus*, *Octadecabacter* and “*Ca. Aquiluna*” (Figure 4.10) (Table S4). Another group (SAL-R group) originates from the sphingobacterium *Salinibacter ruber*, which produces xanthorhodopsin (Balashov *et al.*, 2005); it is therefore likely that Organic Lake *Sphingobacteria* (Supplementary Table S4) were the origin of this rhodopsin group.

The most abundant group, OL-R1 (Figure 4.10) had no close homologues from GenBank, but it was abundant on the 3.0 μm fraction and has a distribution suggesting it originates from Organic Lake members of the *Roseobacter* clade (Figure 4.9). All ORFs adjacent to OL-R1 rhodopsin containing scaffolds were related to *Octadecabacter* further supporting their *Roseobacter* clade provenance (Figure 4.11). Genes downstream of OL-R1 were involved in carotenoid synthesis, indicating OL-R1 is a xanthorhodopsin, occurring as a retinal protein or in a carotenoid complex (Balashov *et al.*, 2005).

Photoheterotrophic potential of Organic Lake was compared with other aquatic environments including nearby Ace Lake, SO and GOS expedition samples. The Organic Lake 0.1 μm fraction had the lowest rhodopsin counts and percentage of rhodopsin containing cells of all size-matched samples surveyed (Table 4.6). Non-marine GOS samples from the 0.1 μm fraction have been noted to have lower rhodopsin abundance (Sharma *et al.*, 2008), which was similarly evident from our analysis (Table 4.6). In contrast, the 3.0 μm Organic Lake size fractions had higher rhodopsin counts than Ace Lake and comparable counts to the SO samples, although the percentage of rhodopsin containing cells was still lower than that of the SO. The paucity of rhodopsins in the Organic Lake 0.1 μm fraction is likely due to the lack of SAR11 clade, which is expected to be the main source of rhodopsin genes in Ace Lake and marine samples. This indicates that although Organic Lake has an overall lower frequency of rhodopsin genes compared to sites for which size fraction-matched metagenomes are available, the rhodopsins associated with larger or particle-associated cells are as abundant as in the marine environment.

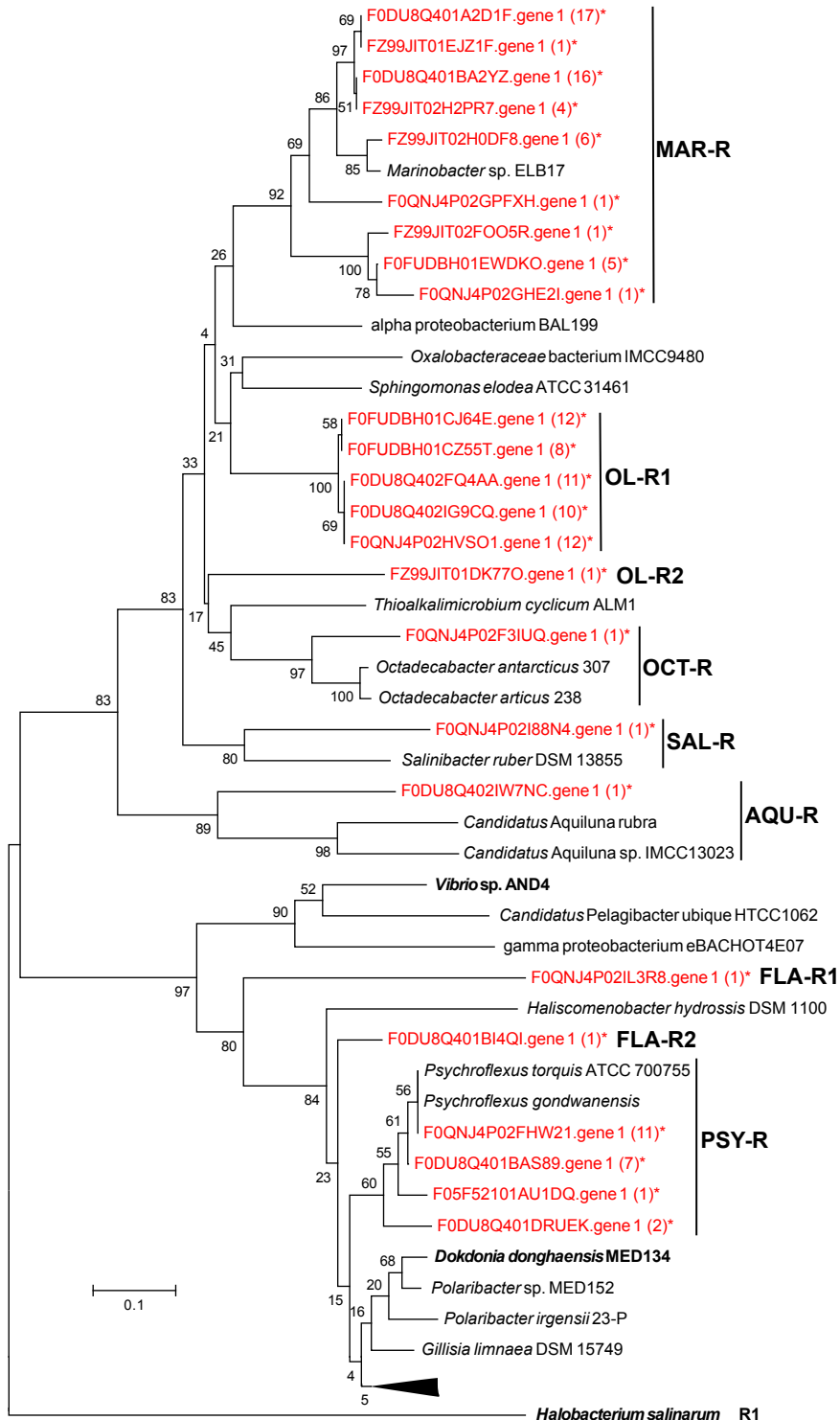


Figure 4.10: Phylogeny of rhodopsin homologs. *Halobacterium salinarum* R1 halorhodopsin was used as an outgroup. The tree was computed from a 78 amino acid region spanning the motif involved in ‘spectral tuning’ using the neighbour-joining algorithm. Organic Lake sequences from this study are shown in red and marked with an asterisk (*). Numbers in parentheses are counts of sequences that clustered with the Organic Lake homologue shown in the tree with 90% amino acid identity. Sequences with confirmed activity are shown in bold. Accession numbers from top to bottom are: EAZ99241, EDP63929, EGF32634, ZP_09955974, AEG32267, EDY76405, EDY88259, YP_445623, ACN42850, EIC91904, ZP_02194911, AAZ21446, AAT38609, AEE49633, EAST1907, sequence from John Bowman (personal correspondence), EAQ40507, EAQ40925, EAR12394, EHQ04368 and YP_001689404.

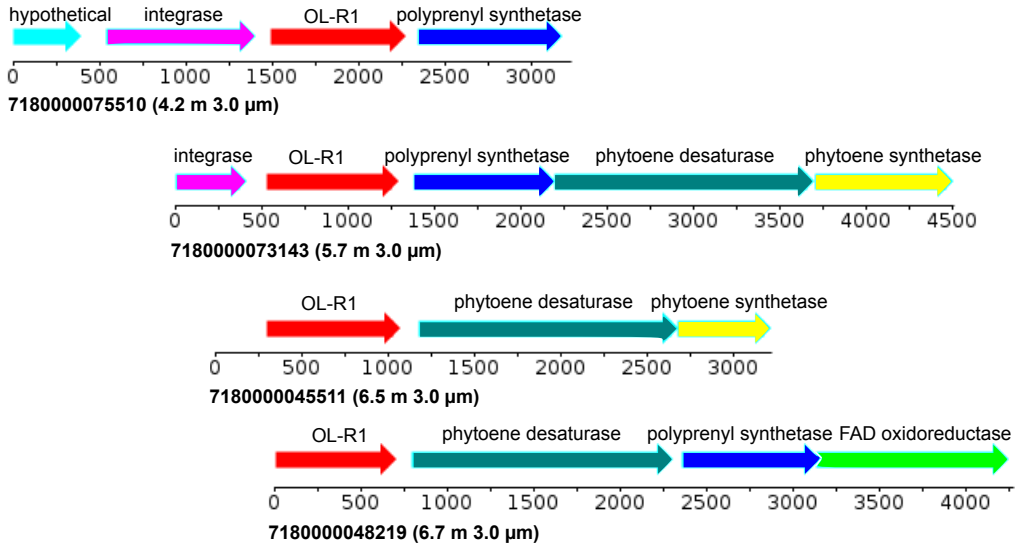


Figure 4.11: Genomic maps of Organic Lake scaffolds containing the OL-R1 rhodopsin homologue. All genes surrounding OL-R1 had best BLAST matches to *Octadecabacter* (*Alphaproteobacteria*) sequences. The scale below shows the number of base pairs. The sample depth and filter from which the scaffold was assembled is shown in parentheses beside the scaffold ID.

Table 4.6: Counts of genes involved in DMSP catabolism and photoheterotrophy in aquatic metagenomes (normalised to 100 Mbp). % = cells containing marker gene. The sample ID for each site is shown in parentheses after the site description. Values marked with an asterisk are >0 but <0.5. The sample with the highest frequency of each marker gene is highlighted in blue. The sample with the highest percentage of cells with each marker is indicated by red font colour. Counts for the following sites are averages of several samples: Ace Lake mixolimnion (GS232, GS231); Southern Ocean SZ (GS349, GS351–GS353, GS356–GS360); Southern Ocean NZ (GS363, GS346, GS364, GS366–GS368); GOS coastal (GS002–GS004, GS007–GS010, GS012–GS016, GS019, GS021, GS027–GS029, GS034–GS036); GOS open ocean (GS017, GS018, GS022, GS023, GS026, GS037, GS047); GOS estuary (GS006, GS011, GS012). Values shown in bold are the highest for that marker gene. SZ, Southern Zone; NZ, Northern Zone; GOS, Global Ocean Sampling.

Site	Size (μm)	<i>dddD</i> (%)	<i>dddL</i> (%)	<i>dddP</i> (%)	<i>dmdA</i> (%)	Rho. (%)	<i>pufLM</i> (%)	<i>recA</i>
Organic Lake 1.7 m (GS374)	0.1	2 (9)	4 (19)	0	0* (2)	1 (5)	0* (1)	21
	0.8	10 (36)	10 (39)	1 (2)	2 (7)	5 (20)	4 (14)	26
	3.0	11 (50)	5 (21)	2 (7)	9 (43)	12 (57)	13 (61)	21
Organic Lake 4.2 m (GS375)	0.1	5 (34)	5 (34)	0	1 (10)	1 (10)	2 (16)	14
	0.8	15 (54)	9 (31)	0	2 (6)	7 (23)	3 (11)	28
	3.0	23 (75)	2 (8)	1 (2.5)	20 (68)	14 (45)	16 (53)	30
Organic Lake 5.7 m (GS376)	0.1	4 (43)	1 (7)	0	1 (14)	2 (21)	0* (4)	10
	0.8	6 (20)	9 (32)	0	2 (7)	6 (22)	3 (12)	29
	3.0	19 (68)	3 (12)	0	13 (47)	6 (21)	11 (38)	28
Organic Lake 6.5 m (GS377)	0.1	10 (51)	0* (2)	0	3 (15)	1 (7)	4 (22)	20
	0.8	14 (38)	9 (23)	1 (2)	7 (20)	6 (16)	7 (20)	28
	3.0	42 (106)	5 (13)	0	20 (52)	6 (16)	22 (55)	29

Continued on next page

Table 4.6 – *Continued from previous page*

Site	Size (μm)	<i>dddD</i> (%)	<i>dddL</i> (%)	<i>dddP</i> (%)	<i>dmdA</i> (%)	Rho. (%)	<i>pufLM</i> (%)	<i>recA</i>
Organic Lake 6.7 m (GS378)	0.1	1 (7)	0* (4)	0	0	1 (7)	2 (13)	13
	0.8	12 (26)	8 (17)	0	2 (5)	8 (16)	4 (9)	47
	3.0	50 (174)	5 (17)	4 (13)	12 (43)	12 (43)	14 (48)	29
Ace Lake mixolimnion	0.1	0* (2)	0	1 (2)	15 (56)	15 (53)	0* (1)	28
	0.8	2 (3)	1 (2)	0	2 (4)	12 (27)	3 (12)	45
	3.0	0	0	0* (4)	0	5 (42)	0	11
Newcomb Bay (GS235)	0.1	6 (14)	0	3 (7)	50 (111)	89 (196)	0	45
	0.8	5 (12)	0	0	18 (41)	55 (123)	0	45
	3.0	0	0	0	2 (17)	4 (33)	0	11
Southern Ocean SZ	0.1	2 (3)	0	6 (9)	71 (101)	98 (139)	0	70
	0.8	3 (6)	0* (0*)	5 (12)	32 (81)	43 (108)	0	39
	3.0	0* (7)	0	0* (4)	4 (66)	5 (84)	0	6
Southern Ocean NZ	0.1	0* (1)	0	5 (7)	124 (159)	111 (142)	1 (1)	78
	0.8	0* (2)	0	9 (30)	28 (84)	35 (107)	2 (7)	33
	3.0	0* (3)	0	1 (9)	7 (54)	11 (89)	0* (4)	12
GOS coastal	0.1	0* (0)	0	5 (6)	44 (52)	74 (87)	5 (6)	85
GOS open ocean	0.1	0	0	7 (8)	45 (50)	66 (74)	5 (5)	90
GOS estuary	0.1	0	0	1 (1)	29 (36)	61 (77)	2 (3)	80
GOS embayment (GS005)	0.1	4 (8)	0	6 (12)	28 (54)	58 (112)	3 (6)	52
GOS Lake Gatun (GS020)	0.1	0	0	0	4 (4)	48 (53)	2 (2)	90
GOS fringing reef (GS025)	0.1	0	0	0	0	7 (39)	0	18
GOS warm seep (GS030)	0.1	0	0	7 (6)	75 (63)	83 (69)	6 (5)	120
GOS upwelling (GS031)	0.1	0	0	4 (4)	81 (77)	81 (76)	4 (4)	106
GOS mangrove (GS032)	0.1	0	0	2(3)	24(34)	25(36)	1(1)	71
GOS Punta Cormorant (GS033)	0.1	0	11 (15)	14 (21)	4 (6)	31 (43)	15 (21)	72
GOS Rangirora Atoll (GS051)	0.1	0	0	11(15)	38 (49)	73 (94)	3 (4)	77

Counts of *pufLM* genes in the Organic Lake 0.1 μm size fraction were similar to GOS sample, except for Punta Cormorant hypersaline lagoon which had the highest *pufLM* counts and percentage of AAnP cells (Table 4.6). However, the highest overall counts of *pufLM* were from the 3.0 μm size fraction of Organic Lake, likely due to the high proportion of members of the *Roseobacter* clade. Notably, *pufLM* genes were not detected in high abundance in Ace Lake or the SO samples, indicating AAnP is a unique adaptation in Organic Lake among these polar environments. The similarly high abundance of *pufLM* genes in Punta Cormorant hypersaline lagoon indicates AAnP may be advantageous in environments with salinity above marine levels.

The contribution of light-driven energy generation processes to the carbon budget is difficult to infer from genetic potential alone. For example, the relative abundance of

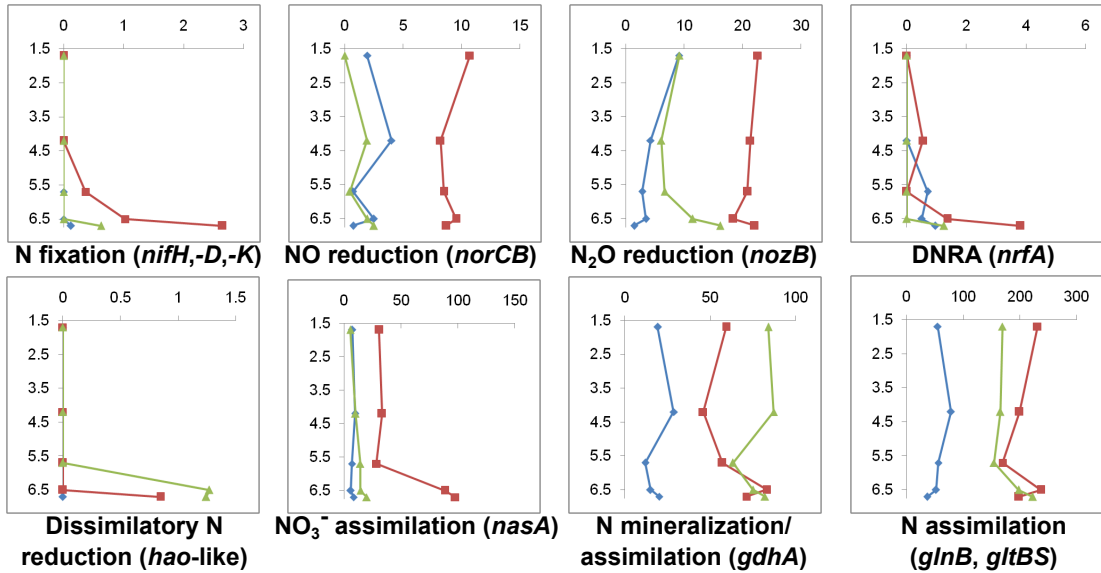


Figure 4.12: Vertical profiles of potential for nitrogen conversions for each size fraction in Organic Lake. The y-axis shows sample depths (m) and the x-axis shows counts of marker genes normalised to 100 Mbp of DNA sequence. The 0.1, 0.8, 3.0 μm size fractions are shown as blue, red and green, respectively. Counts for marker genes for the same pathway or enzyme complex were averaged and those from different pathways were summed. For marker gene descriptions see Table 4.2 and Table 4.3.

AAnP and PR genes in Arctic bacteria has been reported to be the same in winter and summer (Cottrell and Kirchman, 2009). Furthermore, regulation of pigment synthesis is complex; for example, BchlA expression in *R. tolerans* occurs in the dark but is inhibited by continuous dim light (Labrenz *et al.*, 1999). However, it is possible that the apparent negative balance in carbon conversion potential could be ameliorated by photoheterotrophy performed by bacterial groups that are abundant in Organic Lake. In particular, the Organic Lake *Psychroflexus* could play a particular role as it has a PR related to *Dokdonia*, which was shown to function under carbon-limitation (Gómez-Consarnau *et al.*, 2007). Furthermore, detection of higher AAnP potential in Organic Lake than other aquatic environments linked with taxa known to be capable of AAnP, suggests it may have a greater influence in the carbon budget of Organic Lake.

4.4.6 Regenerated nitrogen is predominant in the nitrogen cycle

Nitrogen cycling potential throughout the lake was dominated by assimilation and mineralisation/assimilation pathways (Figure 4.12). Glutamate dehydrogenase (GDH) genes (*gdhA*) were abundant (Figure 4.12), and linked predominantly to *Alpha-* and *Gammaproteobacteria* and to a lesser extent *Bacteroidetes* (Table 4.7). However, the functional significance of the readily reversible GDH depends on its origin; *Bacteroidetes* are likely to use GDH in the oxidative direction for glutamate catabolism (Williams *et al.*, 2012), whereas the use of GDH in the oxidative or reductive directions by *Proteobacteria* is likely to depend upon the source of reduced nitrogen (ammonia vs amino acids). Glutamine synthetase (*glnB*) and glutamate synthase genes (*gltBS*), were pre-

dominantly linked to *Alpha-* and *Gammaproteobacteria* (Table 4.7), indicating the potential for high-affinity ammonia assimilation by these groups in Organic Lake. The high ammonia concentration in the deep zone (Figure 4.3, Table 4.4) would result from a higher rate of mineralisation (ammonification) than assimilation. This is consistent with abundant OTUs for *Psychroflexus* (*Bacteroidetes*) in this zone, and due to either turnover of organic matter or lysis of *Bacteroidetes* cells after sedimentation in anoxic water. In addition, the gene for ammonia-generating nitrite reductase (*nrfA*) was linked to *Bacteroidetes* and *Planctomycetes* (Table 4.7), indicating ammonia may also be produced by these putative aerobic heterotrophs. Overall, the data suggest that ammonia is actively assimilated in the aerobic upper mixed zone, but is permitted to accumulate in the anaerobic deep zone.

Potential for nitrogen conversions typically found in other aquatic environments was greatly reduced in Organic Lake. There was a very low potential for nitrogen fixation that was confined to the deep zone (Figure 4.12) and principally linked to anaerobic *Epsilonproteobacteria* (Table 4.7). This diazotrophic potential may not be realized by *Epsilonproteobacteria*, given the high ammonia concentration present in the deep zone. No ammonia monooxygenase genes (*amoA*) were detected. The potential for ammonia oxidation was only represented by hydroxylamine/hydrazine oxidase-like (*hao*) genes, which were in low abundance and linked to *Deltaproteobacteria* (Table 4.7). *hao* genes are present in non-ammonia-oxidising bacteria (Bergmann *et al.*, 2005), and those from Organic Lake belong to a family of multiheme cytochrome c genes present in sulphate-reducing *Deltaproteobacteria* that have no proven role in ammonia oxidation. In the genomes of sulphate-reducing *Deltaproteobacteria* the *hao* gene is invariably situated adjacent to a gene for a NapC/NirT protein, which suggests a role in dissimilatory nitrate reduction. Collectively these data indicate an inability for nitrification to occur in the upper mixed zone and no potential for ammonia loss in the deep zone.

Denitrification genes (*norCB* and *nozB*) and genes for nitrate assimilation (*nasA*) were present throughout the water column (Figure 4.12) and were linked primarily to *Gammaproteobacteria* (Table 4.7). Low nitrate and nitrite in the deep zone (Figure 4.3, Table 4.4) indicates oxidized nitrogen has been depleted by dissimilatory or assimilatory reduction by heterotrophic *Gammaproteobacteria*. Denitrification genes are phylogenetically widespread and usually induced by low oxygen or oxidized nitrogen species (Kraft *et al.*, 2011) and thus expected to be active in the deep zone or oxycline. However, denitrification may be inhibited even if conditions appear appropriate. For example, in Lake Bonney, Antarctica, denitrification occurs in the west lobe, but not in the east lobe of the lake despite the presence of anoxia, nitrate and denitrifying *Marinobacter* species (Ward and Priscu, 1997; Ward *et al.*, 2005). Moreover, in the absence of nitrification, denitrification and nitrate assimilation would be limited by the lack of potential to re-form oxidized nitrogen. The preponderance of assimilation/mineralisation pathways geared towards reduced nitrogen appears to reflect a “short circuit” of the typical nitrogen cycle that would conserve nitrogen in a largely closed system. Hence, the predominant nitrogen source is regenerated fixed nitrogen. Similar findings were

Table 4.7: Contribution of different taxonomic groups to counts of marker genes involved in nitrogen conversions. The taxon with the largest contribution to each process is highlighted in blue.

Taxon	<i>N</i> fixation	NO reduction	<i>N</i> ₂ O reduction	DNRA	hao	<i>N</i> mineralisation	<i>NO</i> ₃ ⁻ assimilation	<i>N</i> assimilation
<i>Acidobacteria</i>	0	0	0	0	0	0.07	0	0.08
<i>Actinobacteria</i>	0	0	0	0.03	0	0.32	0	5.41
<i>Alphaproteobacteria</i>	0.01	0.12	0	0	0	6.39	5.49	49.4
<i>Aquificae</i>	0	0	0.26	0	0	0	0	0.06
<i>Bacteroidetes</i>	0	0	3.00	0.27	0	3.90	0.03	15.5
<i>Betaproteobacteria</i>	0	0.03	0	0	0	0.06	0.41	19.2
<i>Chlorobi</i>	0.03	0	0	0	0	0.2	0	0.31
<i>Chloroflexi</i>	0	0	0	0	0	0.03	0	0.03
<i>Chrysigenetes</i>	0	0	0	0	0	0.01	0	0.06
<i>Cyanobacteria</i>	0	0	0	0	0	0.29	0	0.10
<i>Deferrribacteres</i>	0	0	0	0	0	0	0	0
<i>Deinococcus-Thermus</i>	0	0	0	0	0	0.01	0	0.11
<i>Deltaproteobacteria</i>	0.04	0.01	0	0.07	0.22	0.23	0	0.58
<i>Epsilonproteobacteria</i>	0.32	0	0	0	0	0.05	0	1.49
<i>Firmicutes</i>	0.03	0	0	0.03	0	0.70	0	3.16
<i>Fornicata</i>	0	0	0	0	0	0.02	0	0
<i>Fusobacteria</i>	0	0	0	0	0	0	0	0.04
<i>Gammaproteobacteria</i>	0	3.91	8.28	0	0	4.75	14.1	50.6
<i>Nitrospirae</i>	0	0	0	0.03	0	0.01	0	0
<i>Planctomycetes</i>	0	0.01	0	0.16	0	0	0	0.26
<i>Spirochaetes</i>	0	0.01	0	0	0	0.11	0	0.15
<i>Thermobaculum</i>	0	0	0	0	0	0.10	0	0
<i>Thermotogae</i>	0	0	0	0	0	0	0	0
<i>Verrucomicrobia</i>	0	0	0.17	0.03	0	0.25	0	0.82
<i>Crenarchaeota</i>	0	0	0	0	0	0.02	0	0
<i>Euryarchaeota</i>	0	0	0	0	0	0.12	0.09	0.10
<i>Alveolata</i>	0	0	0	0	0	0.18	0	0.03
<i>Euglenozoa</i>	0	0	0	0	0	0	0	0
<i>Opistokonta</i>	0	0	0	0	0	0.15	0	0.13
<i>Rhodophyta</i>	0	0	0	0	0	0	0	0.02
<i>Strameopiles</i>	0	0	0	0	0	0.03	0	0.15
<i>Viridiplantae</i>	0	0	0	0	0	0.03	0	0.35

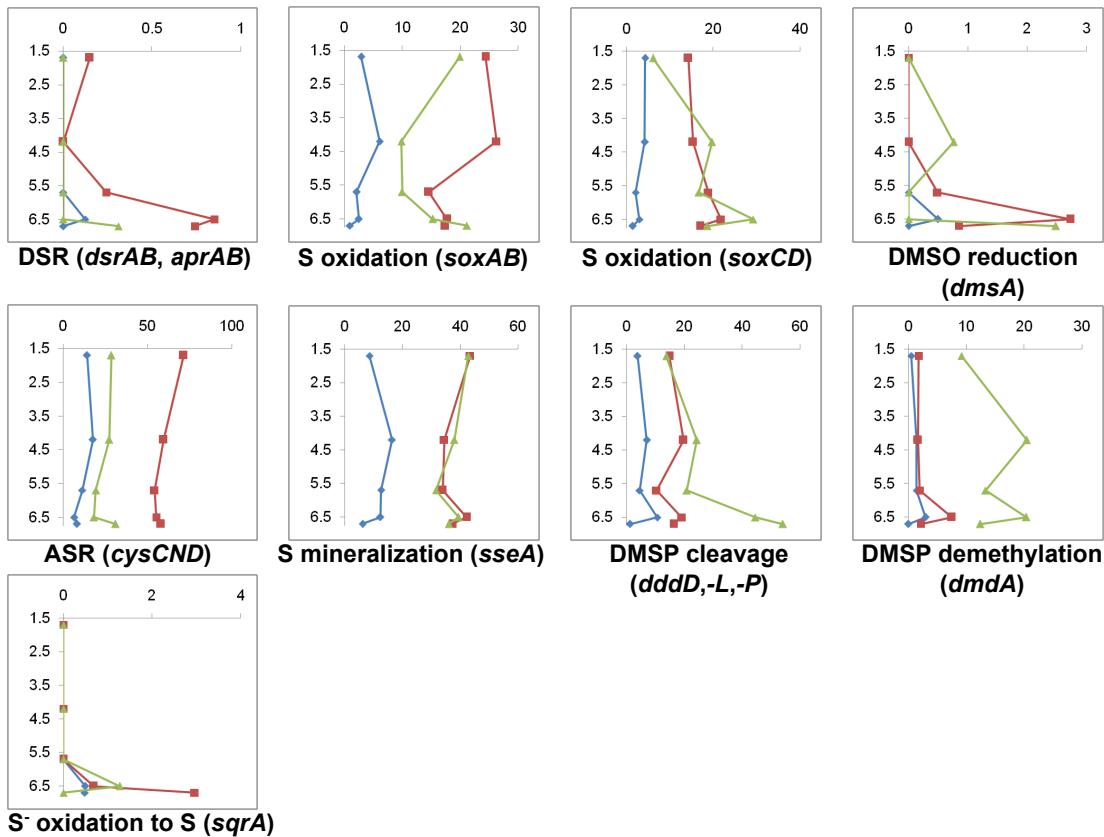


Figure 4.13: Vertical profiles of potential for sulphur conversions for each size fraction in Organic Lake. The y-axis shows sample depths (m) and the x-axis shows counts of marker genes normalised to 100 Mbp of DNA sequence. The 0.1, 0.8, 3.0 μm size fractions are shown as blue, red and green, respectively. Counts for marker genes for the same pathway or enzyme complex were averaged and those from different pathways were summed. For marker gene descriptions see Table 4.2 and Table 4.3.

also made for Ace Lake, although in this system the presence of a dense layer of green sulphur bacteria with the potential to fix nitrogen augments the nitrogen cycle (Lauro *et al.*, 2011).

4.4.7 Molecular basis for unusual sulphur chemistry

Several meromictic hypersaline lakes in the Vestfold Hills, including Organic Lake, with practical salinity >150 are characterized by an absence of hydrogen sulphide and photoautotrophic sulphur bacteria (Burke and Burton, 1988). Although sulphate is present (Franzmann *et al.*, 1987b), geochemical conditions of these lakes are not conducive to dissimilatory sulphur cycling between sulphur oxidising and sulphate reducing bacteria typical of other stratified systems such as Ace Lake (Ng *et al.*, 2010; Lauro *et al.*, 2011). Consistent with this, potential for dissimilatory sulphate reduction represented by dissimilatory sulfite reductase (*dsrAB*) and adenylylsulphate reductase (*aprAB*) linked to sulphate-reducing *Deltaproteobacteria* (Table 4.8) was low in Organic Lake. Sulphate-reduction potential was confined to the 6.7 m sample (Figure 4.13) where oxygen concentration was lowest and *Deltaproteobacteria* were present (Figure 4.6).

Capacity for oxidation of reduced sulphur compounds, represented by the sulphur oxidation multienzyme genes (*soxAB*), was present throughout the water column (Figure 4.13) and linked primarily to *Alpha-* and *Gammaproteobacteria* (Table 4.8). Sulphur-oxidising *Alpha-* and *Gammaproteobacteria* are known to oxidise sulphur compounds, such as thiosulphate, aerobically. Although a small proportion of *Gammaproteobacteria* had the capacity for autotrophy (see 4.4.5), the majority of sulphur-oxidizers were likely chemolithoheterotrophs as they were related to heterotrophic *Marinobacter* and *Roseobacter* clade. The sulphur dehydrogenase genes *soxCD* linked to *Alpha-* and *Gammaproteobacteria* were similarly present throughout the water column. *soxCD* are accessory components of the Sox enzyme system without which complete oxidation of thiosulphate cannot occur (Friedrich *et al.*, 2005). Thus the presence of *soxCD* indicates complete oxidation likely occurs, although the different distribution of *soxAB* and *soxCD* in the water column (Figure 4.13) suggests a proportion of the community may lack *soxCD* and deposit sulphur.

Sulphur-oxidising *Epsilonproteobacteria* possessing *soxAB* genes (Table 4.8) were present only in the deep zone of Organic Lake (Figure 4.6) and were related to autotrophic deep sea sulphur-oxidisers, some members of which are capable of anaerobic sulphur oxidation using nitrate (Yamamoto and Takai, 2011). It is unlikely that appreciable sulphur oxidation occurs in the deep zone as the known terminal electron acceptors, oxygen and nitrate, are depleted and the abundance of sulphur oxidising *Epsilonproteobacteria* is low (Figure 4.6). *Epsilonproteobacteria* were also linked to a capacity for oxidation of sulphide to elemental sulphur by utilising sulphide:quinone oxidoreductase (*sqrA*) (Figure 4.13, Table 4.8). In this pathway, sulphur is released as polysulphides, which is a potential biological source of the abundant polysulphides that have been detected in the lake (Roberts *et al.*, 1993).

It is likely that the limited anaerobic dissimilatory sulphur cycle contributes to the accumulation of DMS in Organic Lake in the deep zone. In the upper mixed zone, DMS could potentially be oxidized as a carbon and energy source or utilized as an electron donor by sulphur-oxidising bacteria (Schäfer *et al.*, 2010). In anoxic zones, methanogenic *Archaea* or sulphate-reducing bacteria are the main organisms known to breakdown DMS (Schäfer *et al.*, 2010). Methanogens and genes involved in methanogenesis were not detected, nor has methane been detected (Gibson *et al.*, 1994) leaving sulphate-reduction the most likely route of DMS catabolism. The low dissimilatory sulphate reduction potential in the deep zone coupled with the relatively stagnant waters would likely minimize DMS oxidation and loss by ventilation. DMS would therefore be expected to accumulate in the deep zone if production rates were higher than breakdown.

To determine the source of high DMS in the bottom waters of Organic Lake, the genes involved in DMS formation were surveyed. Genes for DMSP lyases *dddD*, *dddL* and *dddP*, were detected in Organic Lake at levels comparable to other dominant processes such as respiration and fermentation (Figure 4.13) indicating DMSP is an important carbon and energy source in Organic Lake. *dddD* was the most abundant of

Table 4.8: Contribution of different taxonomic groups to counts of marker genes involved in sulphur conversions. The taxon with the largest contribution to each process is highlighted in blue.

Taxon	DSR	<i>S</i> oxidation <i>sqrA</i>	<i>S</i> assimilation	<i>S</i> mineralisation	DMSO reduction
<i>Acidobacteria</i>	0	0	0.03	1.03	0
<i>Actinobacteria</i>	0	0	0.15	0	0
<i>Alphaproteobacteria</i>	0	2.05	0	0.85	11.7
<i>Aquificae</i>	0	0	0	0	0
<i>Bacteroidetes</i>	0	0	5.06	0.20	0
<i>Betaproteobacteria</i>	0	1.09	0	2.07	0.69
<i>Chlorobi</i>	0	0	0	0.03	0.15
<i>Chloroflexi</i>	0	0	0	0.30	0
<i>Chrysigenetes</i>	0	0	0	0.01	0
<i>Cyanobacteria</i>	0	0	0	0.13	0.05
<i>Deferribacteres</i>	0	0	0	0	0
<i>Deinococcus-Thermus</i>	0	0	0	0.09	0
<i>Delta proteobacteria</i>	0.19	0	0	0.56	0.20
<i>Epsilonproteobacteria</i>	0	0.03	0.39	0.13	0
<i>Firmicutes</i>	0	0	0	0.22	0.09
<i>Fornicata</i>	0	0	0	0	0
<i>Fusobacteria</i>	0	0	0	0.03	0.13
<i>Gammaproteobacteria</i>	0	2.64	0	22.4	14.0
<i>Nitrospirae</i>	0	0	0	0	0
<i>Planctomycetes</i>	0	0	0	0.03	0
<i>Spirochaetes</i>	0	0	0	0	0.03
<i>Thermobaculum</i>	0	0	0	0	0.08
<i>Thermotogae</i>	0	0	0	0.01	0
<i>Verrucomicrobia</i>	0	0	0	0.18	0
<i>Crenarchaeota</i>	0.02	0	0	0	0
<i>Euryarchaeota</i>	0	0	0	0.02	0.12
<i>Alveolata</i>	0	0	0	0	0
<i>Euglenozoa</i>	0	0	0	0	0.03
<i>Opistokonta</i>	0	0	0	0.11	0.03
<i>Rhodophyta</i>	0	0	0	0	0
<i>Strameopiles</i>	0	0	0	0	0
<i>Viridiplantae</i>	0	0	0	0.03	0.15

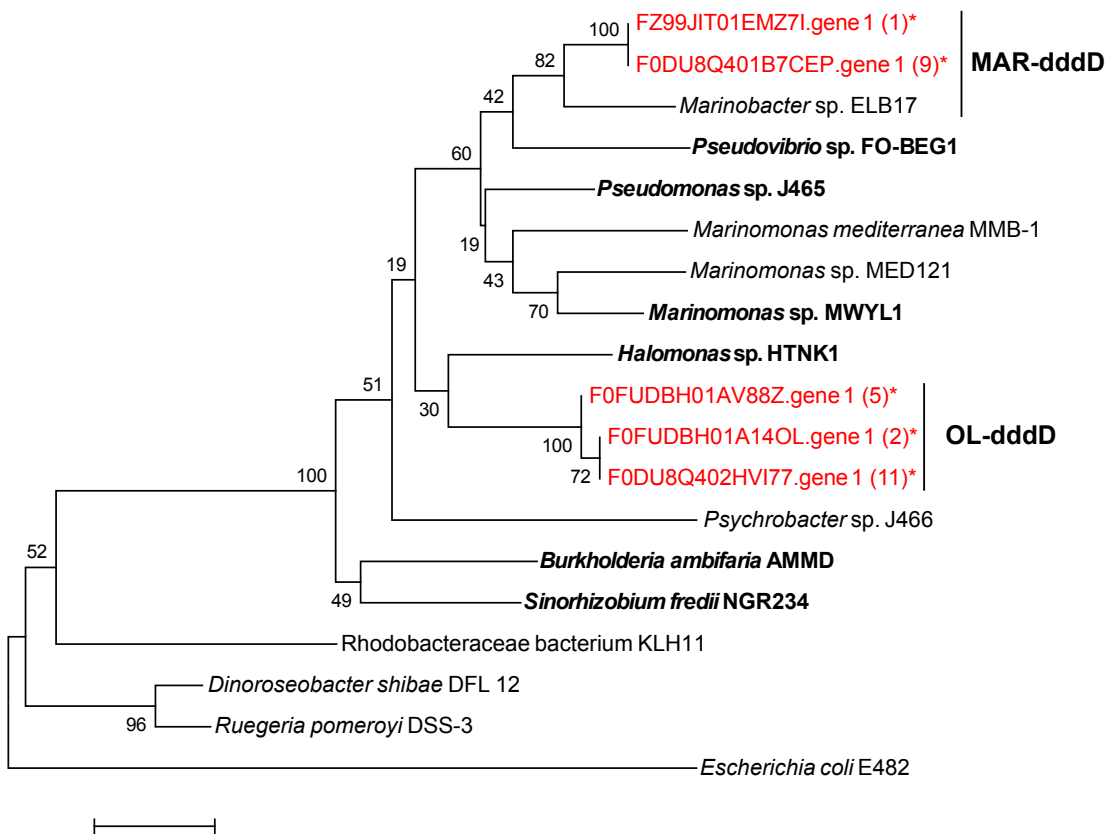


Figure 4.14: Phylogeny of DddD DMSP lyase homologues. *E. coli* carnitine coenzyme A transferase was used as an outgroup. *Dinoroseobacter shibae* DFL 12 and *Ruegeria pomeroyi* DSS-3 homologues are a non-functional outgroup (Todd *et al.*, 2011). The tree was computed from a 75 amino acid region within the conserved amino-terminal class III coenzyme A domain (CaiB) using the neighbour-joining algorithm. Organic Lake sequences from this study are shown in red and marked with an asterisk (*). Numbers in parentheses are counts of sequences that clustered with the Organic Lake homologue shown in the tree with 90% amino acid identity. Sequences with confirmed DMSP lyase activity are shown in bold. Accession numbers from top to bottom are: EBA01716, AEV37420, ACY01992, ADZ91595, EAQ63474, ABR72937, ACV84065, ACY02894, ABI89851, YP_002822700, EEE36156, ABV95365, AAV94987 and EGB36199.

the Organic Lake DMSP lyases (Table 4.6) and comprised two main types: MAR-dddD and OL-dddD (Figure 4.14). Neither of these types clustered with the non-functional *Dinoroseobacter shibae* DFL 12 and *Ruegeria pomeroyi* DSS-3 *dddD* homologues (Todd *et al.*, 2011) or carnitine coenzyme A transferase outgroups, thereby providing support for their proposed role as functional DMSP lyases. The MAR-dddD type includes the *Marinobacter* sp. ELB17 *dddD* homologue, and MAR-dddD sequences were most abundant on the 0.8 µm fraction where *Marinobacter* OTUs were also abundant, indicating MAR-dddD derives from Organic Lake *Marinobacter* (Figure 4.14). OLn-dddD did not have a close relative from cultured bacteria making its precise taxonomic origins uncertain. The abundance of OL-dddD on the 3.0 µm fraction suggests it originates from *Alphaproteobacteria*. OL-dddD containing contigs carried genes of mixed *Alpha-* and *Gammaproteobacterial* origin supporting its provenance from one of these classes and

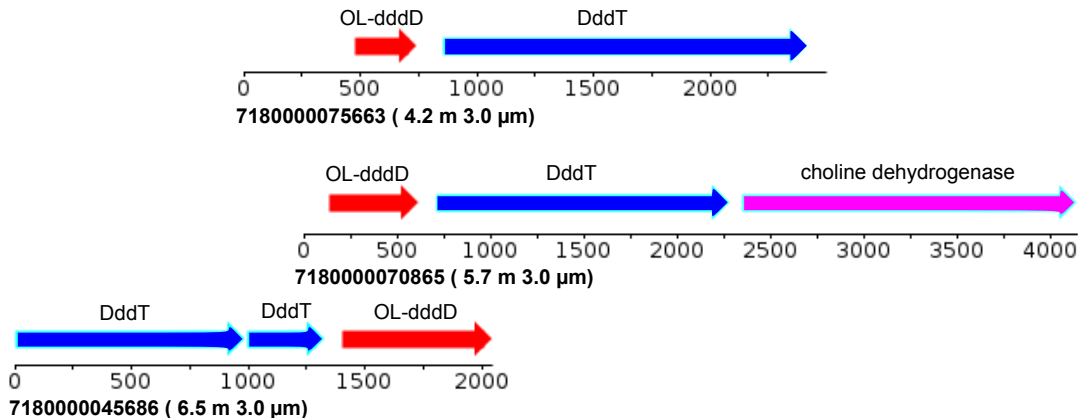


Figure 4.15: Genomic maps of Organic Lake scaffolds containing the OL-dddD homologue. DddT and choline dehydrogenase had best BLAST matches to *Halomonas* sp. HTNK1 (*Gammaproteobacteria*) and *Hoeflea phototrophica* DFL-43 (*Alphaproteobacteria*), respectively. The numbers represent base pairs. The sample depth and filter from which the scaffold was assembled is shown in parentheses beside the scaffold ID.

consistent with the “pick n’ mix” arrangement of genes found beside sequenced *dddD* regions (Johnston *et al.*, 2008) (Figure 4.15). Adjacent to OL-dddD was *dddT* (Figure 4.15), a betaine, choline, carnitine transporter (BCCT) family protein that likely functions in substrate import, demonstrating OL-dddD forms an operon-like structure, similar to *Halomonas* sp. HTNK1 (Todd *et al.*, 2010).

Two *dddL* groups were detected in Organic Lake: SUL-dddL and MAR-dddL (Figure 4.16). The former includes the *Sulfitobacter* sp. EE-36 *dddL* and the latter the *Mari nobacter manganoxydans* MnI7-9 homologue indicating they originate from *Roseobacter* clade and *Gammaproteobacteria*, respectively. *Sulfitobacter* sp. EE-36 has demonstrated DMSP lyase activity and the *dddL* gene alone is sufficient for DMS generation (Curson *et al.*, 2008). These data indicate that the Organic Lake members of the SUL-dddL group perform the same functional role. The MAR-dddL clade appears to be an uncharacterized branch of the *dddL* family. emphdddP was detected as the least abundant of the DMSP lyases (Table 4.6). Phylogenetic analyses showed Organic Lake *dddP* likely originate from *Roseovarius* (Figure 4.17). The Organic Lake sequences formed a clade with the functionally verified *Roseovarius nibinhbens* ISM *dddP* (Todd *et al.*, 2009).

A single type of DMSP demethylase, *dmdA* was identified. It clustered with *Roseobacter* clade *dmdA* (Figure 4.18), corresponding to the marine clade A (Howard *et al.*, 2006), and includes the functionally verified *R. pomeroyi* DSS-3 homologue. These data indicate that the Organic Lake sequences correspond to true DMSP demethylases and not related glycine cleavage T proteins or aminomethyltransferases (Howard *et al.*, 2006). DMSP cleavage appears to be a significant source of DMS in Organic Lake. DMSP likely originates from *Bacillariophyta* or *Dinoflagellida* as Organic Lake *Dunaliella* have been reported not to produce DMSP in culture (Franzmann *et al.*, 1987b). Based on the abundance of marker genes, DMSP cleavage is predicted to occur at highest levels in the deep zone (Figure 4.13) where the DMS concentration has been

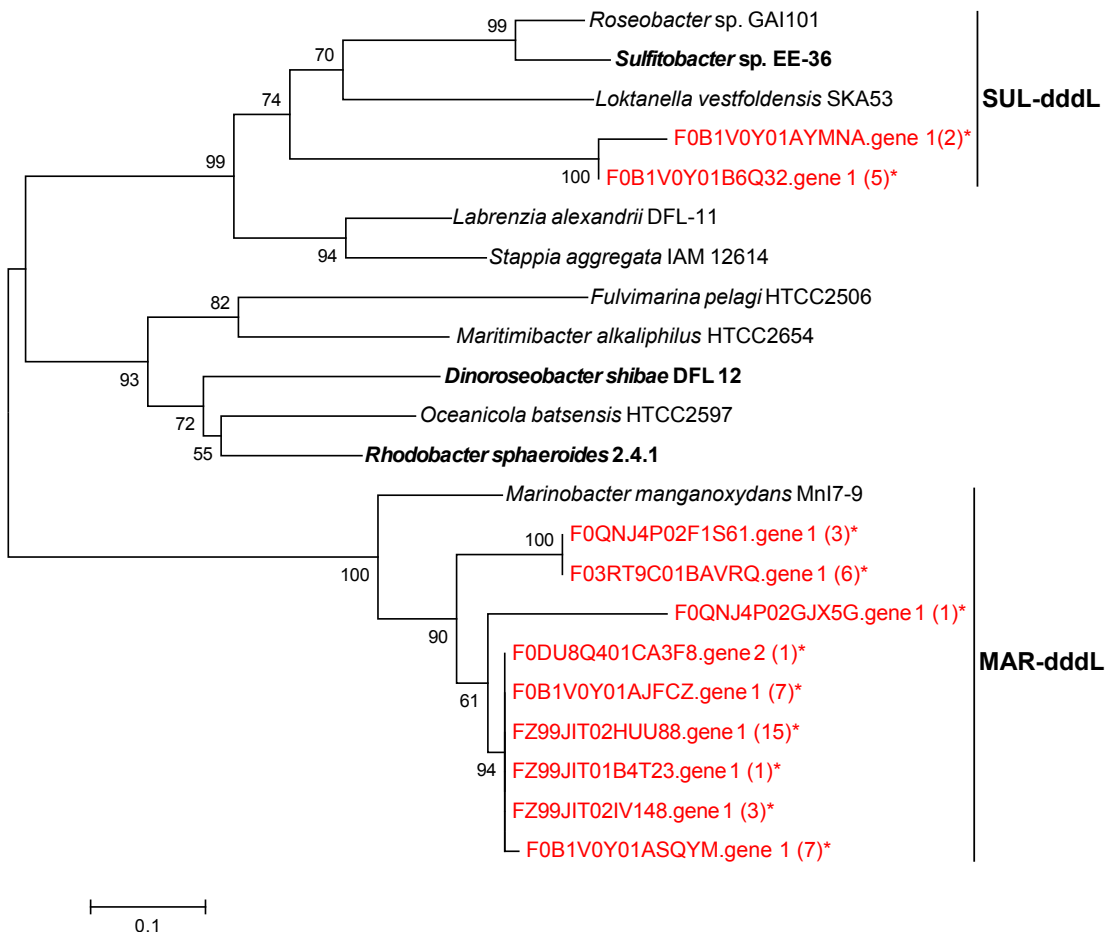


Figure 4.16: Phylogeny of DddL DMSP lyase homologues. The tree was computed from an 84 amino acid N-terminal region using the neighbour-joining algorithm. Organic Lake sequences from this study are shown in red and marked with an asterisk (*). Numbers in parentheses are counts of sequences that clustered with the Organic Lake homologue shown in the tree with 90% amino acid identity. Sequences with confirmed DMSP lyase activity are shown in bold. Accession numbers from top to bottom are: EEB86351, ADK55772, EAQ07081, EEE47811, EAV43167, EAU41122, EAQ10619, ABV95046, EAQ04071, ABA77574 and EHJ04839.

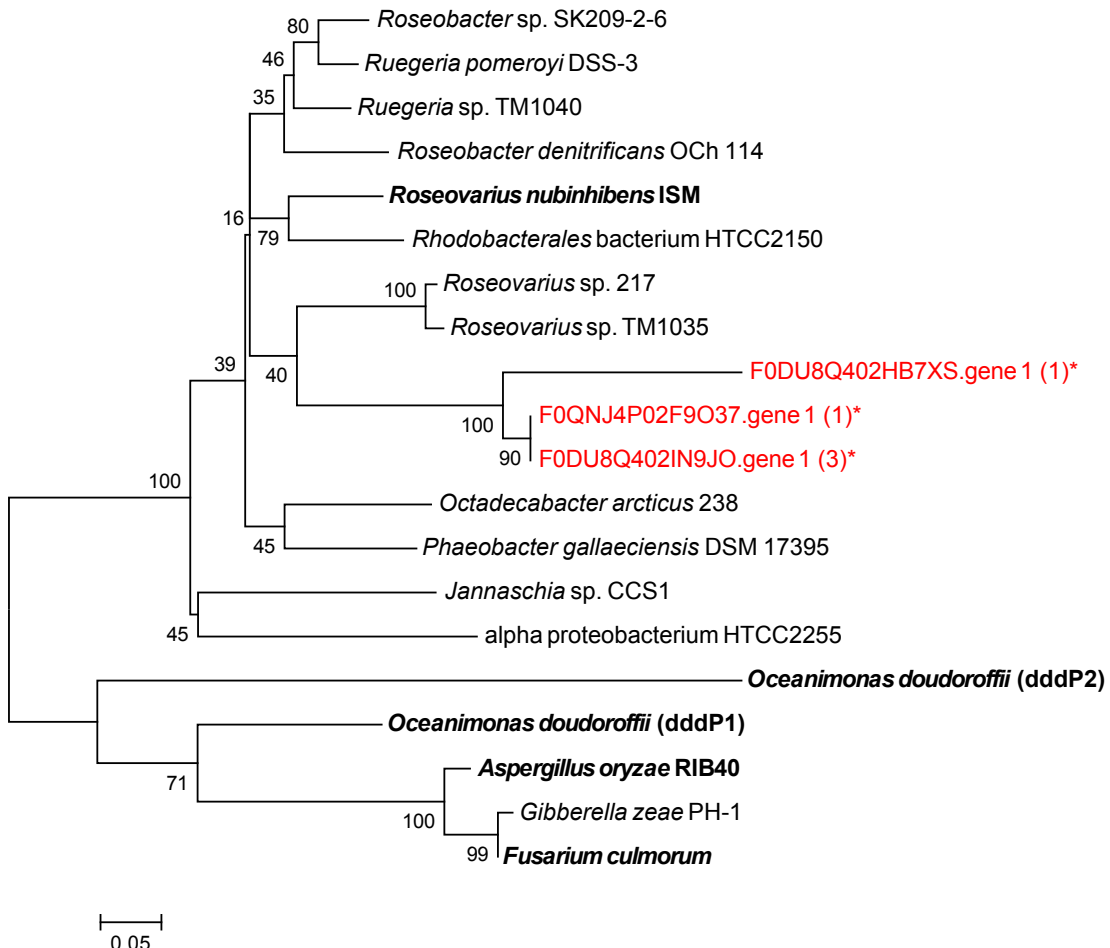


Figure 4.17: Phylogeny of DddP DMSP demethylase homologues. The tree was computed from a 129 amino acid C-terminal region using the neighbour-joining algorithm. Organic Lake sequences from this study are shown in red and marked with an asterisk (*). Numbers in parentheses are counts of sequences that clustered with the Organic Lake homologue shown in the tree with 90% amino acid identity. Sequences with confirmed DMSP lyase activity are shown in bold. Accession numbers from top to bottom are: ZP_01755203, YP_167522, YP_613011, YP_682809, EAP77700, ZP_01741265, ZP_01036399, ZP_01881042, ZP_05063825, AFO91571, YP_509721, ZP_01448542, AEQ39103, AEQ39091, XP_001823911, XP_389272 and ACF19795.

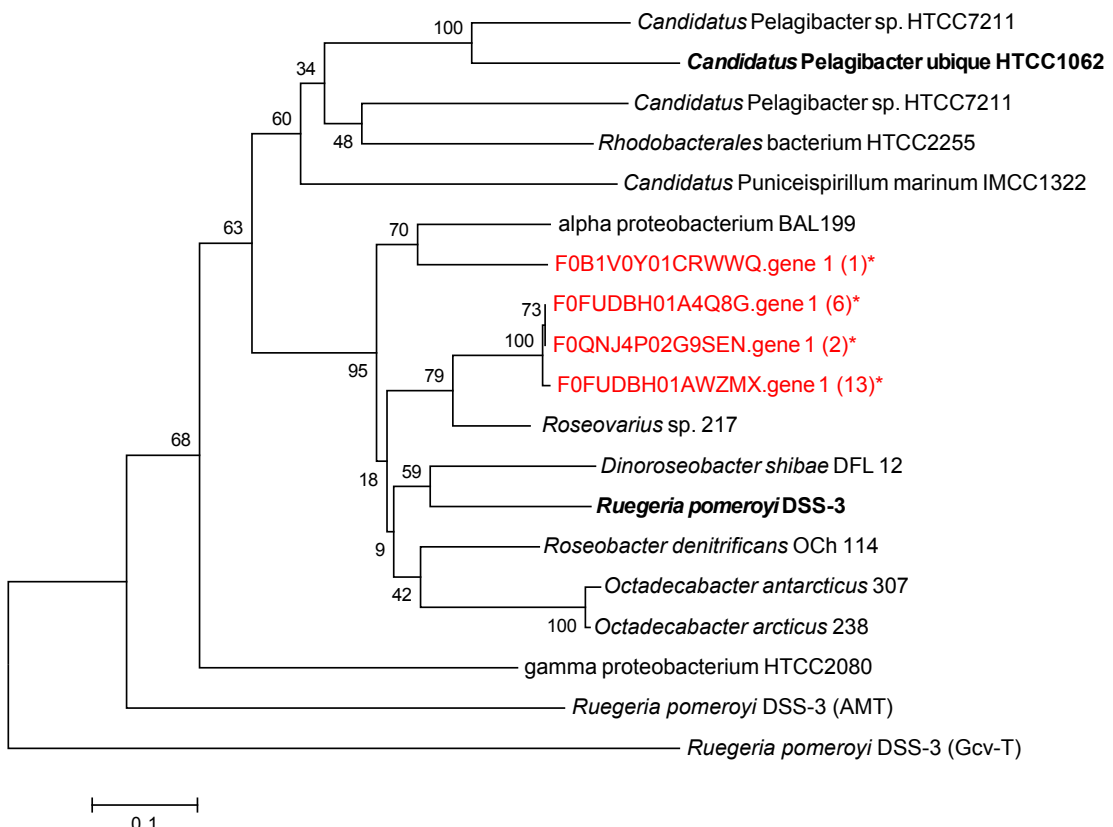


Figure 4.18: Phylogeny tree of DmdA DMSP demethylase homologues. The tree was computed from a 128 amino acid region using the neighbour-joining algorithm. Organic Lake sequences from this study are shown in red and marked with an asterisk (*). Numbers in parentheses are counts of sequences that clustered with the Organic Lake homologue shown in the tree with 90% amino acid identity. Sequences with confirmed DMSP demethylase activity are shown in bold. Accession numbers from top to bottom are: EDZ60447, YP_265671, EDZ61098, EAU51039, YP_003550401, EDP61332, EAQ26389, ABV94056, AAV94935, AAV95190, EDY79173, EDY89914, EAW42451, AAV94935 and AAV97197.

measured to be highest (Deprez *et al.*, 1986; Franzmann *et al.*, 1987b; Gibson *et al.*, 1991; Roberts and Burton, 1993; Roberts *et al.*, 1993). DMS can also be produced in anoxic environments from the reduction of DMSO, degradation of sulphur containing amino acids, and sulphide methylation (Schäfer *et al.*, 2010). Our data indicate that some DMSO reduction linked to *Firmicutes* could occur, but is not likely a major pathway (Figure 4.13), and the potential for the other DMS yielding processes could not be determined because the enzymes involved in these pathways have not been established. When cultivated, *Halomonas* isolates from Organic Lake produced DMS from cysteine (Franzmann *et al.*, 1987b) providing some evidence that DMS production from anaerobic degradation of amino acids can occur. Abiotic pathways for anaerobic production of DMS have also been proposed (Roberts *et al.*, 1993).

The potential for DMSP cleavage was more than twice that of DMSP demethylation (Figure 4.13). This is unusual compared to the marine environment or Ace Lake where DMSP demethylation potential is much higher than cleavage (Table 4.6). Previous estimates have similarly shown marine environments to have demethylation potential up to two orders of magnitude higher than cleavage (Howard *et al.*, 2008; Todd *et al.*, 2009, 2011; Reisch *et al.*, 2011). The frequency of DMSP lyase genes *dddD* and *dddL* in Organic Lake exceeded those of all other environments, except Punta Cormorant hypersaline lagoon, where *dddL* abundance was comparable (Table 4.6). This suggests selection in Organic Lake for DMSP cleavage due to functional advantage and/or selection for taxa that carry DMSP lyase genes. There is evidence that high DMSP cleavage potential is adaptive in hypersaline systems, as a high proportion of *ddd* genes were similarly detected in Punta Cormorant hypersaline lagoon and saltern ponds (Raina *et al.*, 2010). Determination of the taxonomic composition of these other hypersaline environments could indicate whether selection is occurring for functional capacity or on a taxonomic level if the taxonomic composition between these systems was significantly different but abundance of DMSP lyase genes were high.

The accumulated DMS in Organic Lake suggests conditions in Organic Lake favor the relatively inefficient lysis pathway, where both sulphur and carbon is lost to the organism performing the DMSP lysis, over the more ‘thrifty’ demethylation pathway. This is particularly pertinent to the *Roseobacter* lineages that can also perform either process. One possibility that has been proposed is that when sulphur is in excess and the organism can easily assimilate alternative sulphur sources, the lysis pathway may be competitive (Johnston *et al.*, 2008). This may be particularly the case in hypersaline systems if higher concentrations of DMSP are being produced as an osmolyte.

4.5 Conclusions

Through the use of shotgun metagenomics and size partitioning of samples, we discovered that the Organic Lake system is dominated by heterotrophic bacteria related to *Psychroflexus*, *Marinobacter* and *Roseovarius* with primary production provided largely by chlorophyte algae related to *Dunaliella*. Genetic potential for oxidation of fixed carbon by heterotrophic bacteria occurs greatly in excess of carbon fixation, suggesting

possible net carbon loss. However, by linking key metabolic processes to the dominant heterotrophic lineages we uncovered processes that were unusually abundant in Organic Lake that may serve to maximize exploitation of limited resources and minimize loss. Recalcitrant polymeric algal material and particulate matter is likely remineralized by *Psychroflexus* in the upper mixed zone and by *Firmicutes* in the deep zone to provide labile substrates for use by other heterotrophic bacteria. The generalist *Marinobacter* and *Roseovarius* lineages were associated with abundant genes involved in rhodopsin-mediated and AAnP photoheterotrophy; the latter of which was more abundant in Organic Lake than any other system surveyed. Potential for chemolithoheterotrophy, sulphur oxidation and CO oxidation was also high, and along with photoheterotropy, may provide a supplementary energy source if organic carbon becomes limiting.

In addition to being able to describe the functional capacities and potential importance of poorly understood microbial processes occurring in the lake (e.g. photoheterotrophy by *Alphaproteobacteria*), we were able to answer targeted questions about the biology of the unusual lake sulphur chemistry. The low potential for dissimilatory sulphur cycling in the deep zone and relatively stable waters, combined with the generation of DMS from DMSP, facilitate the accumulation of a high level of DMS in the lake. It appears *Marinobacter* and *Roseovarius* play a key role in DMS formation by cleaving DMSP generated by upper mixed zone eucaryal algae. The remarkable abundance of DMSP lyase genes suggests DMSP is a significant carbon source in Organic Lake and the cleavage pathway provides a selective advantage under the unique constraints of the Organic Lake environment.

In view of the minimal capacity for biological fixation of carbon and nitrogen, and yet organic richness, including high levels of DMS, in Organic Lake, we evaluated what input the lake may have received throughout its relatively brief ~3,000 year history. The volume of the lake is small ($\sim 6 \times 10^4$ m³), and exogenous input may occur from guano deposits in a small penguin rookery nearby the lake, through giant petrel or skua predation and defecation, and/or by decaying animal carcasses such as elephant seals which can weigh on the order of 1 ton and are present near the lake. It is also possible that during isolation from the ocean, the base of the water column in the marine basin that formed the lake may have acted as a sump for organic material. Phytoplankton blooms and benthic mats tend to make coastal marine basins very productive, and organic matter that sediments out of the surface waters will become trapped in the denser, more saline bottom layers (Bird *et al.*, 1991). Retention of captured organic matter in the lake may also have been facilitated by Organic Lake having become highly saline quickly (Bird *et al.*, 1991). Studies in the future that experimentally determine exogenous input and historical lake dynamics (e.g. stable isotope and biomarker analyses of lake sediment), the role of benthic communities, and metaproteogenomic analyses of interannual community composition and function, will provide improved knowledge of the unusual biogeochemistry of Organic Lake and better enable predictions to be made about how the lake may be affected by ecosystem changes.

Chapter 5

General discussion, future work and conclusions

Metagenomics has proven to be an effective way to map the diversity of Antarctic lake ecosystems and provide hints of how they work. In combination with metaproteomics and abiotic parameters, in-depth descriptions were achieved of the ecosystem functions of Ace Lake and Organic Lake. The most noteworthy contribution of these studies has been to describe taxa and microbial processes previously unknown in these lakes, and from these descriptions, generate testable hypotheses of population and ecosystem level function.

5.1 Possible future work on Organic Lake

To establish a picture of the biotic composition and function of Antarctic lake communities, an observation-driven approach was utilised that allowed for completely new discoveries about these systems to be made. Bioinformatic pipelines and theoretical models to do this have now been established. These can be applied to future, similarly observation-based studies of Ace and Organic Lakes to define how they change over time and test our existing models of how the lakes function. It is also clear that a systems level understanding of the lakes is bolstered by having well-characterised isolates related to members in the community. Guided by the studies from this thesis, isolation and characterisation of key members of the community, such as *Pyramimonas* spp., Organic Lake phycodnavirus (OLPV), Organic Lake virophage (OLV), *Marinobacter* spp. and *Roseovarius* spp. from Organic Lake, could be attempted in the future. Other complementary techniques, such as single-cell and single-virus genomics and stable isotope probing (SIP), hold promise for learning about specific populations in the community. Some experiments that could be used to test specific hypotheses generated by the study of Organic Lake are discussed below, along with their expected outcomes and implications.

5.1.1 Organic Lake community dynamics

To establish a complete understanding of Organic Lake requires descriptions of the microbial community over different time scales. Certain bacterial taxa have been observed to peak in abundance in Organic Lake during summer indicating seasonal fluctuations exist (James *et al.*, 1994). The Organic Lake community profiles from the summer of 2006 and 2008 varied substantially (chapters 3 and 4) identifying further community members that change with time. However, the rates of change and degree of variance for these populations are unknown. Currently, a baseline of the microbial community diversity over an annual cycle has not been established and is the next step towards developing an understanding of the Organic Lake community.

Metagenomic and functional data obtained over the course of a year can determine how the microbial community responds to the large seasonal changes in temperature, light and ice-cover. Winter samples in particular can determine how the community persists when the lack of light is expected to curtail photosynthetic production. At present, there are no data on the Organic Lake community composition during the winter. Paired metagenomic and metaproteomic analyses of the coastal Southern Ocean from winter and summer found winter samples were dominated by active chemolithoautotrophs including sulphur-oxidising *Gammaproteobacteria* and ammonia oxidising *Crenarchaeota* (Grzymski *et al.*, 2012; Williams *et al.*, 2012). If the Organic Lake ecosystem reflects that of the coastal Southern Ocean, the small population of chemolithoautotrophic sulphur-oxidising *Proteobacteria* found to be present (chapter 4) are expected to become dominant in the winter. Metagenomic analysis indicated recycling of reduced nitrogen compounds predominates in Organic Lake and a lack of capacity to form oxidised nitrogen compounds (chapter 4). If the model proposed for the Organic Lake nitrogen cycle holds true over the year, we can expect ammonia oxidising microorganisms will not play a part in the community as they do in other similar environments (Voytek *et al.*, 1999; Grzymski *et al.*, 2012; Williams *et al.*, 2012). Another possibility is that some bacterial populations become dormant over the winter, as seems to occur in Artic sea ice communities (Collins *et al.*, 2010).

Photosynthetic nanoflagellates detected in Organic Lake, such as *Pyramimonas*, are capable of mixotrophy (Bell and Laybourn-Parry, 2003) and likely persist over the winter by switching to heterotrophy. Strategies that might also be employed by other photosynthetic algae include utilising starch reserves or developing cyst forms. In Lake Bonney, trends between RuBisCO expression and irradiance levels differed with RuBisCO type and depth suggesting adaptations to the polar night varies between species (Kong *et al.*, 2012b). Phototrophic eucaryotes in Organic Lake likely have similarly diverse strategies to persist during prolonged darkness. Combined metagenomic and metaproteomic analysis can determine which phototrophic eucaryotes are found during the winter and indicate what metabolic processes they employ in the absence of light.

Ideally, metagenomic analyses performed over a complete annual cycle would establish a census of the community, link variations in composition to environmental

conditions and establish a benchmark of annual variability in the community. It appears some members of the Organic Lake population are persistent over long time scales. For example, *Dunaliella* (Franzmann *et al.*, 1987b), choanoflagellates (van den Hoff and Franzmann, 1986), *Marinobacter*, *Psychroflexus Roseovarius* and *Halomonas* (Bowman *et al.*, 2000a) have been recorded in Organic Lake previously and were detected again in studies from this thesis (chapters 3 and 4). How they vary throughout the year and between years is unclear. Organic Lake has been shown to be physically variable over a decadal time scale with changes in water level of ~1 m leading to large changes in the water column structure (Gibson *et al.*, 1995; Gibson and Burton, 1996). Notably, the pycnocline in Organic Lake occurred at 5.7 m in 2008; much lower than 3.5 m where it first reported in 1978 (Franzmann *et al.*, 1987b). If the lake completely mixes, this would challenge the oxygen-sensitive microbes and processes occurring in the deep zone. In West Antarctic lakes physical changes have been correlated with large and rapid ecological responses (Quayle *et al.*, 2002). Substantial differences were observed in *cbbM* gene copy number and vertical distribution between three field seasons in Lake Bonney (Kong *et al.*, 2012a) indicating sensitivity to environmental factors applies to permanently ice-covered lakes and is a general property of Antarctic lakes. However, the amount of seasonal variability needs to be established in Organic Lake for differences over longer time scales to be determined.

Sampling over the course of a summer season would be particularly valuable as these samples can be compared to the available summer datasets to give a better indication of the degree of variability between summer seasons. There was a change in the viral composition and abundance between November and December 2008 samples when the lake began to thaw (chapter 3). Similarly, there were differences in the eukaryotic community when the lake was completely thawed in 2006 and the profile in November 2008 when the lake was ice-covered. Specifically, *Dunaliella*, *Dictyochophyceae*, *Euplates*, *Dinophyceae* and *Bacillariophyta* were present in both samples, whereas *Pyramimonas*, *Pelagophyceae*, *Pirsonia* and *Caecitellus* was only detected in the December 2006 samples and fungi and *Choanoflagellida* were only in the November 2008 profile (chapter 4). It is unclear whether the variation between the summer samples, December 2006, November 2008 and December 2008 are due to differences in ice-cover/light, sampling locations (2006 and December 2008 samples were littoral, while November 2008 was over the deepest point of the lake) or other environmental factors. Metagenomic sequencing of a summer time course would provide a high resolution view of changes in the microbial community over the season that can be related to environmental conditions. This time course can be compared back to the summer 2006 and 2008 samples indicating if the differences that have been observed fall within normal range of variability over the summer season and also help interpret what factors were driving the variations.

Metagenomic sequencing of samples from a summer time course can also validate the OLV–OLPV–host model formulated in chapter 3. Genomic analysis indicated OLV is a new member of the virophage virus family, which obligately utilise a giant ‘helper’ virus

to complete their replication cycle but impair their helper's infectivity in the process. The likely helper virus of OLV is OLPV and the host was inferred to be the unicellular alga, *Pyramimonas*. The inferred interaction of the OLV, OLPV and host was used to generate a Lotka-Volterra model of their population dynamics that showed if OLV acts as a 'predator of a predator', this would lead to increased frequency of population cycles. Observations of changes in OLV, OLPV and *Pyramimonas* abundances over a summer time course can establish if a relation exists between them. An observable trend between these populations would lend further support to the claim that OLV–OLPV and *Pyramimonas* are a virophage–virus–host system. In the model, the density of each population oscillates in a phase-shifted manner in the sequence: prey, predator and predator of predator. Observed population changes can determine if the data fits the model, suggest if additional modifications to the existing model need be made or if alternative models would better fit the data. If the dynamics fit the model, observed population densities can be used to derive the parameters that govern their interaction.

5.1.2 OLV physiology and ecology

Since the discovery of the OLV, two other members of the virophage family have been reported that have afforded a new perspective on OLV. The first of these is the Mavirus (for Maverick virus) so named for its evolutionary relationship with the Maverick/Politon class of eucaryotic transposons (Fischer and Suttle, 2011). Like Sputnik, Mavirus has an absolute requirement for a helper virus, *Cafteria roenbergensis* virus (CroV), to replicate and is deleterious to its helper (Fischer and Suttle, 2011). The other virophage reported was called Sputnik 2 (its genome is almost identical to Sputnik), but unlike Sputnik, it was found both as a separate genome and integrated in its helper lentille virus (Desnues *et al.*, 2012). These two virophage systems in culture are associated with heterotrophic protists making OLV the only genomic sequence currently available for virophage affecting cosmopolitan phytoplankton species. Therefore isolating OLV, acquiring genomes of OLV relatives in Antarctic lakes and determining fundamental properties of OLV physiology and dynamics would contribute immensely to our understanding of the evolution and diversity of virophages in general and is highly relevant to other aquatic systems.

The evidence that Mavirus has the same 'virophage' phenotype as Sputnik strengthens the inference that OLV does as well. This is in part because Mavirus and CroV are quite divergent from Sputnik and mimivirus respectively, yet retain the same traits (Fischer *et al.*, 2010; Fischer and Suttle, 2011), suggesting a common feature of the whole lineage. Moreover, as both mimivirus and CroV encode much of their transcriptional machinery, they do not localise to the nucleus during infection but generate the viral factory in the cytoplasm of their host (La Scola *et al.*, 2008; Fischer *et al.*, 2010). Sputnik and Mavirus appear to replicate in the giant virus factory making use of helper virus' replication and transcription systems, not the host cell's (La Scola *et al.*, 2008; Claverie and Abergel, 2009; Fischer and Suttle, 2011). In this way, the replicative strategy of the mimivirus lineage makes them vulnerable to virophages parasitising necessary resources

during replication, which is a likely cause of reduced helper virus production (Claverie and Abergel, 2009; Fischer and Suttle, 2011; Fischer, 2011). As OLPV encodes all RNA polymerase subunits (see GenBank accession HQ704802), this is evidence that it replicates solely in the cytoplasm, thereby making it susceptible to a virophage. A larger census of virophage and helper viruses would be able to show if virophages only associate with members of the nucleo-cytoplasmic large DNA virus (NCLDV) clade that replicate in the cytoplasm. Ultimately, definitive confirmation of a detrimental effect on the helper by OLV co-infection is likely only possible by observing infection in culture.

Although Sputnik and Mavirus have similar effects on their helper viruses, their infection strategies appear different raising interesting considerations for OLV. Mavirus can be independently phagocytosed by *Cafeteria roenbergensis* in the absence of CroV – perhaps serving as a defence for the host in the case of CroV infection (Fischer and Suttle, 2011). In support of this, Mavirus possesses a retroviral-family integrase that is theorised to have been separately acquired as a way to stabilise the relationship between the ancestral Mavirus and its cellular host (Fischer and Suttle, 2011) although as yet, Mavirus has not been reported to be integrated in *Cafeteria roenbergensis*. In contrast, Sputnik seems to associate directly with the fibrils that coat the mimivirus virion, not the host *Acanthamoeba* cell (Boyer *et al.*, 2011). These two modes of infection, that is, a virophage-bearing host being infected by a giant virus *vs.* a host being infected by a virophage-bearing giant virus, produces different selection pressures that would lead to distinct effects on the population dynamics in the environment. Detection of complete OLV genomes in the 0.8–0.1 µm size fraction indicates it was captured in association with larger particles but does not distinguish how it is transmitted.

Determination of the mode of infection for OLV would improve predictive modelling of OLV driven impacts on algal blooms. This could be achieved by observation of OLV-OLPV infections in culture. However, recently developed methods for flow cytometric sorting to obtain single-cell amplified genomes (SAGs) or single virus genomes (SVGs) (Martínez Martínez *et al.*, 2011; Allen *et al.*, 2011) could be applied to Organic Lake water samples to study the mode of OLV, OLPV and host interaction. For example, a sample population of single host algal cells could be fluorescence sorted and screened for the presence of OLPV and OLV. At the same time, a sample population of single OLPV particles could be sorted and screened for the presence of OLV. This could reveal if OLV is able to associate with the host independently of OLPV or *vice versa*. Examination of the infected algal cells could also establish fundamental properties of the algae and virus populations such as proportions of infected cells and proportions of OLPV infections that include an OLV. As these methods are quite new, an experiment of this kind would require optimisation to successfully capture an adequate sample of infected cells and target giant viruses. However, just obtaining SVGs would provide invaluable information on virus diversity and genetic content making it worthwhile pursuing as a complement to metagenomic sequencing.

A final consideration for OLV and OLPV dynamics is suggested by the discovery

that Sputnik 2 can integrate into its helper lentille virus (Desnues *et al.*, 2012). Integration of Sputnik 2 is localised to a 352 bp region corresponding to the Sputnik V6 gene that encodes a collagen-like repeat-containing protein shared by Sputnik 2, lentille virus and mamavirus (Desnues *et al.*, 2012). OLV and OLPV share a homologous collagen-like repeat-containing protein that may similarly function as a site of integration. As yet, the conditions and mechanism by which Sputnik 2 integrates is unknown. Screening of metagenomic assemblies, SVGs or isolated OLPV genomes for integrated virophages can determine if this occurs in the environment. Integration of OLV and OLPV could have interesting evolutionary functions. One possibility is that integration of virophages may function analogously to lysogeny in bacteriophages if provirophages are inactive. In this scenario, virophages would integrate into their helper virus when helper virus densities are low to avoid driving their helpers to extinction. On the other hand, if integration does not entail dormancy of the virophage, it could function as a means to ensure transmission. In either case, evidence of integration can be found in future genomic studies of Organic Lake.

5.1.3 Organic lake biogeochemistry

The models of carbon, nitrogen and sulphur cycling in Organic Lake were constructed based on the presence and abundance of known marker genes along with data of the lake's chemical properties (chapter 4). As yet, metaproteomic analyses from the same samples have not been performed, but this would help corroborate the inferred pathways are active. Other inferences of Organic Lake biogeochemical function can be specifically tested on organisms in culture, tested by measuring rates of reaction *in situ* or supported with additional molecular and chemical analyses.

For the carbon cycle, it was hypothesized that aerobic anoxygenic photosynthesis (AAnP) and rhodopsin mediated photoheterotrophy can conserve carbon for use in biosynthesis reducing overall carbon loss (chapter 4). The conditions under which AAnP is active can be tested on related organisms in culture, for example *Roseovarius tolerans* from Ekho Lake in the Vestfold Hills. It is already known for *R. tolerans* constant dim light suppresses bacteriochlorophyll A (BchlA) production while darkness stimulates it (Labrenz *et al.*, 1999). *R. tolerans*, or related isolates, can be grown under a larger range of conditions to determine when AAnP becomes an active process. This might include further varying light intensity and cycle duration; varying organic carbon concentration and oxygen concentrations. To determine the contribution of light to growth, the difference in growth when AAnP is active and when it is not can be compared. Characterising AAnP in a model isolate from a similar Antarctic lake can inform an understanding of how it functions in Organic Lake. However, to gain an understanding of when AAnP is active *in situ*, levels of BchlA at different points in the year can be measured to see it correlates with seasonal changes. In the case of the influence of rhodopsin-mediated phototrophy on the Organic Lake system, the function of rhodopsins first needs to be characterised in the diverse organisms in which they are found to confirm they are indeed used in photoheterotrophic growth. In marine

Flavobacteria, there is already evidence that light stimulates growth through the action of rhodopsins (Gómez-Consarnau *et al.*, 2007). The same experimental design used to establish this can be applied to *Psychroflexus gondwanensis* isolated from Organic Lake, *Marinobacter* sp. ELB17 and *Octadecabacter antarcticus*, which are relatives of species found in Organic Lake.

In the model of the nitrogen cycle, nitrogen fixation was inferred to be negligible due to the high concentrations of ammonia while denitrification was assumed to be limited by low levels of oxidised nitrogen compounds and lack of potential for nitrification to regenerate them (chapter 4). In these cases where rates of reaction were inferred to be slow although genetic potential for them exists, the reaction rates can be directly measured. Nitrogen fixation and denitrification rates can be measured from Organic Lake water samples by incubation with ^{15}N labelled substrates or acetylene block assays. Similarly, it was inferred that carbon fixation rates from photosynthetic algae and chemolithoautotrophic bacteria were lower than respiration and fermentation based on genetic potential (chapter 4). As mentioned previously, populations of chemolithoautotrophs may increase in the winter, potentially becoming significant source of primary production. Another consideration for the carbon budget is how sustained levels of chemolithoautotrophy throughout the year compares to the short burst of photosynthetic production over the summer. Continuous rates of chemolithoautotrophy appears to occur in Lake Bonney in McMurdo Dry Valleys as their expression of RuBisCO remained constant over the polar night transition (Kong *et al.*, 2012a). Measuring rates of primary production by ^{14}C incorporation and respiration rates at different points in the season can ascertain if there truly is a shortfall in the carbon budget in Organic Lake, estimate how large it is and pinpoint if the main source of primary production is from photo- or chemoautotrophy.

Both the carbon and nitrogen cycles were also constructed with the assumption that inputs are also negligible. For instance, denitrification rates would be limited by low fixation coupled with low rates of nitrification. Nonetheless, it is possible that sufficient nitrate inputs occur that would sustain denitrification thereby by-passing the need for endogenous nitrification. Monitoring for presence of melt streams that might feed into Organic Lake and determining their chemical profiles can gauge the contribution of allochthonous carbon and nitrogen to Organic Lake.

The unusually high concentrations of dimethylsulphide (DMS) in the bottom waters of Organic Lake were inferred to originate from bacterial lysis of dimethylsulphopropionate (DMSP) (chapter 4). As DMSP lyases have only been discovered fairly recently (Todd *et al.*, 2007; Curson *et al.*, 2008), they have only been characterised from a few isolates (Todd *et al.*, 2007; Curson *et al.*, 2008, 2010; Todd *et al.*, 2010; Curson *et al.*, 2012). Confirmation that the homologues found in Organic Lake are indeed functional can be achieved by cloning into the expression vector system established by Todd *et al.* (2007) and assaying for DMSP lyase activity. This would also provide valuable insight into the DMSP lyases that are most relevant to cold and hypersaline environments.

Although it was inferred that DMSP lysis was the main source of DMS in the bottom

zone of Organic Lake, production of DMS other by anaerobic pathways are also possible. Furthermore, DMS was inferred to accumulate due to slow rates breakdown in the bottom zone. Incubating Organic Lake water samples with radio-labelled DMSP and tracking production of volatile DMS would confirm the lysis pathway is an active process and determine the rates of reaction. Performing this assay on water from different depths could determine if concentration of DMS is high in the bottom zone because it is being produced there at a higher rate. A similar assay can be performed using labelled DMS to show if DMS can be broken down and if this differs with depth. If the proposed model for sulphur cycling based on marker gene frequencies is correct, DMS breakdown in the bottom samples should be slow or not occur. While this experiment will not exclude the possibility that DMS is produced by an alternative pathway, knowing the rates of DMSP lysis and DMS breakdown and the DMS concentration in a sample can indicate the existence other sources of DMS production.

Most of the Organic lake DMSP lyase genes could be linked to a taxonomic group except the most abundant type, OL-dddD, which had indication of both *Alpha-* or *Gammaproteobacteria* origins (chapter 4). Identifying the organisms involved in DMSP lysis can be achieved with SIP. This would involve incubation of ^{13}C -labelled DMSP in Organic Lake water samples followed by sequencing of the labelled DNA. Sequencing of the small subunit ribosomal RNA (SSU) genes would determine which specific taxonomic groups were the main contributors to DMSP lysis and screening for DMSP lyase genes would identify which DMSP lyase is involved. Performing this experiment at different depths of the water column could determine if the same organisms are responsible for DMSP lysis at different depths. No marker genes yet exist for DMS oxidation although it can be readily utilised as a growth substrate by diverse microorganisms (Johnston *et al.*, 2008). The same experiment can be performed using ^{13}C -labelled DMS to determine the taxa involved in breaking it down in different depths of the lake. In conjunction with metagenomic sequencing, or flow sorting and SAGs of DMS/DMSP-degraders, the biochemical pathways involved in DMS breakdown can then be reconstructed giving a more complete understanding of Organic Lake sulphur biogeochemistry.

5.2 Perspectives on ‘-omics’ approaches

It was not so long ago that what could be called the second molecular revolution in microbial ecology began in earnest with the first shotgun metagenomic sequencing of a marine virome (Breitbart *et al.*, 2002). That metagenome, sequenced with Sanger sequencing technology, was a modest 1.28 Mbp (Breitbart *et al.*, 2002). The first shotgun sequenced metagenomes of cellular life from the Sargasso Sea (Venter *et al.*, 2004) and the Iron Mountain acid mine drainage (Tyson *et al.*, 2004) added 265 Mbp and 76 Mbp respectively to the public databanks.

5.2.1 Next generation sequencing technologies

Since the availability of high-throughput next generation sequencing (NGS) technologies, the volume of metagenomic data has increased exponentially. To put it in perspective, a single sample from the Antarctic lake datasets described in this thesis sequenced by the Roche GS-FLX titanium sequencer is 140 Mbp, while a recent study using Applied Biosystems SOLiD sequencing of a marine sample (Iverson *et al.*, 2012) analysed 55,000 Mbp – close to 400 times the amount of data. This illustrates how sequencing technology is advancing so rapidly that each new study has to develop new ways of looking into the microbial milieu captured in the particular sample.

Current NGS sequencing platforms are shown in Table 5.1 comparing sequence length, throughput and error rates. Clearly, there are trade-offs between each type with higher read depth technologies offering shorter read lengths. Application of sequencing technologies that offer greater read depths in future Antarctic lake studies can enable insight into the rare members of the community. For example, a recent study of the Western English Channel compared SSU community profiles over a six year time course with a single sample deep-sequenced with the Illumina GAIIX platform (1000 fold greater coverage) (Caporaso *et al.*, 2012). Members of the community that appeared to become seasonally absent in the shallow sequenced community profiles were actually present in low abundances in the deep-sequenced sample (Caporaso *et al.*, 2012). The ability to look into deeper into diversity of the Antarctic lake communities can discern if a similar persistent ‘seed bank’ population exists in the lakes, if succession of populations occurs or external seeding. These three different possibilities have different implications for predicting responses to change in environmental conditions in the lakes.

5.2.2 Emerging bioinformatic bottlenecks

With the higher throughput and the falling costs of sequencing, genomic projects are now experiencing ‘bioinformatic bottlenecks’ where computational analysis has become a significant challenge (reviewed by Scholz *et al.* (2012)). This is because availability of computational resources and scaling-up of algorithms to accommodate more data or computing clusters is not occurring as quickly as the accumulation of sequence data. Metagenomic sequencing projects typically entail computationally intensive BLAST-like comparisons before biological interpretations can be made. Local cluster computing, like that used in this thesis, has been a standard way to process metagenomic datasets. However, the annual cost of acquiring, running and administering a standard rack mount server has been estimated to be \$2,160–\$5,160 US per node (Wilkening *et al.*, 2009). Acquiring and maintaining the necessary computational resources to process large datasets can in some cases work out to be more expensive than the cost of sequencing itself. Moreover, the time to acquire sequence data is much shorter than the time needed to analyse it. For example, analysis of metagenomic data produced by Illumina technology using a standard pipeline was calculated to take decades on a single processor or weeks to months on 1,000 CPUs (Evanko, 2009). Without increases

Table 5.1: Comparison of next generation DNA sequencing platforms from Scholz *et al.* (2012). Indel, insertion-deletion; Sub, substitution; MP, mate pair; PE, paired end.

Platform	Run time (h)	Read length (bp)	Mbp/run	Error type	Error rate (%)
<i>Roche</i>					
454 FLX+	18–20	700	900	Indel	1
454 FLX+ Titanium	10	400	500	Indel	1
454 GS	10	400	50	Indel	1
<i>Illumina</i>					
GAIIX	14	2 × 150	96,000	Sub	>0.1
HiSeq 2000	8	2 × 100	400,000	Sub	>0.1
HiSeq 2000 V3	10	2 × 150	<600,000	Sub	>0.1
MiSeq	1	2 × 150	1,000	Sub	>0.1
<i>Life Technologies</i>					
SOLiD 4	12	50 × 35	71,000	AT bias	>0.06
SOLiD 4	12	75 × 35 PE	155,000	AT bias	>0.01
		60 × 60 MP			
<i>Ion Torrent</i>					
PGM 314 Chip	3	100	10	Indel	1
PGM 316 Chip	3	100+	100	Indel	1
PGM 318 Chip	3	200	1,000	Indel	1
<i>Pacific biosciences</i>					
RS	14/8 Smart Cells	1,500	45/smart cell	Insertions	15

in compute resources, the time taken to process massive NGS datasets will become prohibitively slow and is an important consideration for future metagenomic projects.

5.2.3 Prospects for closing the bioinformatic gap

Ultimately, for computational analysis to catch up with advances in sequencing technology requires more efficient processing, faster processors and/or faster algorithms. Ways to surpass the bioinformatic bottle neck are being developed and, if paired with careful experimental and analytical design, can make this a manageable challenge for future studies.

Webserver analyses

A shortage in computational resources can be addressed to some extent by the use of webserver pipelines specialised in metagenomic processing. These include Metagenome Rapid Annotation using Subsystems Technology (MG-RAST) (Meyer *et al.*, 2008), Community Cyberinfrastructure for Advanced Microbial Ecology Research and Analysis (CAMERA) (Sun *et al.*, 2011), Integrated Microbial Genomes and Metagenomes (IMG/M) (Markowitz *et al.*, 2008, 2012), EBI Metagenomics (Hunter *et al.*, 2012), as well as METAVIR (Roux *et al.*, 2011) and Viral Informatics Resource for Metagenome Exploration (VIROME) (Wommack *et al.*, 2012) for viral metagenomes. These web-servers take on the burden of maintaining necessary programs, storage of sequence databases and provide computational power. Each have unique features that may be more desirable for particular sample types, analyses or user preferences. One example of this is the different functional analyses offered by EBI Metagenomics and

MG-RAST, which implement InterPro and SEED subsystems respectively. One disadvantage to web servers is workflows are not readily customisable. The exception to this is WebGMA (Wu *et al.*, 2011), which hosts the most common metagenomic tools and enables them to be put together into custom pipelines, but does not contain a repository of metagenomic sequences. Current web servers have been designed towards analysis of either bacteria/archaea or viral sequences; although the metagenomes from this thesis contained significant proportions of both, as well as eucaryotic sequences. To take advantage of the range of specialist features offered by different pipelines can introduce inefficiencies such as performing similar sequence quality control steps in order to fit within their distinct analytical schemas. The different outputs then need to be combined locally and may not be directly comparable to one another due to differences in processing. Nonetheless, use of webserver pipelines is a worthwhile option in future metagenomic studies of the lakes, especially if specialist tools or specific databases are needed, and can relieve some pressure on local computing time.

Cloud computing and GPUs

Cloud computing, the use of computing infrastructure, software or platforms as a service, looks to be a promising way to make up shortfalls in computational resources by affording large amounts of readily accessible compute time (reviewed by Schatz *et al.* (2010) and Thakur *et al.* (2012)). Several major providers exist: Amazon's Elastic Compute Cloud (EC2) is the largest publicly available service and the Department of Energy's Magellen Cloud is available for academic use. Gains in efficiency for the user can occur because clouds provide access to computing power that varies 'elastically' with the demands of the task without the cost of maintaining a local cluster. These infrastructure costs are more effectively absorbed by large providers than by smaller facilities enabling clouds to provide the same resources at lower cost. Also, by having access to more computational nodes, programs like BLAST can be run in parallel increasing the throughput of analysis.

Whether it works out to be more cost efficient in practice depends of the expected volume of data and frequency of analysis (Wilkening *et al.*, 2009). The cost–benefit appears greatest if use is sporadic or if computer resources need to be augmented on an unpredictable basis (Wilkening *et al.*, 2009). To benchmark the costs and time involved in metagenomic data analysis on the EC2, Angiuoli *et al.* (2011) clustered and BLAST compared 631 Mbp of metagenomic sequence (454 GS FLX titanium) against RefSeq and COG databases. This analysis finished in a little over 6 hours using a maximum of 160 CPUs at a total cost of \$56 US (Angiuoli *et al.*, 2011), giving an indication of how clouds might be leveraged for metagenomic processing. However, additional considerations such as adequate connection speeds to upload large quantities of data, data security, data management and computing expertise must also be taken into account. Cloud resources look to be most useful in future Antarctic projects for running computationally intensive analyses, such as BLAST searches and *de novo* assembly (discussed below).

Cutting down processing times of NGS data analysis can also be achieved by hardware-driven solutions. The most promising of these is use of graphical processing units (GPUs), which enable faster processing than a conventional central processing units (CPUs). A trial comparing the use of GPUs for processing Illumina GAIIX metagenomic datasets has reported 10–15 fold increase in processing speed compared to a CPU cluster (Su *et al.*, 2012). Currently, use of GPUs seems to be limited only by availability of bioinformatics software that can run on the different architecture and access to GPU clusters. A specific metagenomic analysis pipeline called Parallel-META has been launched that can run 16S rRNA prediction from a shotgun metagenome, classify the 16S sequences by BLAST and perform comparisons of multiple samples (Su *et al.*, 2012). More pipelines such as these and increasing availability of GPU clusters will undoubtedly be useful for speeding up metagenomic analyses.

Bioinformatic tools for binning and assembly

The increased output of NGS sequencing technology is spurring development of bioinformatic programs which can solve specific metagenomic computational problems and decrease processing time. Metagenomic analyses are typically based on data from single reads, (*e.g.* chapter 4) or from assembled genomic information (*e.g.* chapter 3). These analyses entail two tasks in particular that are unique to metagenomics: classification/binning of short sequences and assembly from mixed species datasets.

Broadly, programs for classifying reads use homology-based methods, where reads are compared to known sequences, or composition-based methods, where reads are clustered according to intrinsic properties. Homology-based programs, such as MEGAN (Huson *et al.*, 2007), CARMA (Krause *et al.*, 2008), WebCARMA (Gerlach *et al.*, 2009) and TREEPHYLER, are accurate and can be used with short reads but require computationally intensive BLAST or Hidden Markov Model searches (HMMer) against known sequence databases. The latest homology-based algorithms for short reads (<100 bp) have reduced processing time by using faster search algorithms. These are METABIN (Sharma *et al.*, 2012), which claims several-fold improvement in speed by implementing BLAT search (Kent, 2002), and GENOMETA (Davenport *et al.*, 2012), which reports an order of magnitude improvement in speed by using BOWTIE. As homology-based approaches all rely on a sequence databases, their ability to discover novel taxa is limited by the database.

Compositional-based tools on the other hand are database-independent, so reads with no sequenced homologues can be categorised, and they can generally be run on a laptop computer. Some examples of popular programs are TETRA (Teeling *et al.*, 2004) (tetra nucleotide-based), PHYLOPYTHIA (machine-learning based) (McHardy *et al.*, 2006) COMPOSTBIN (PCA-based) and TACOA (kernelized nearest-neighbor) (Diaz *et al.*, 2009). These older methods can only achieve high accuracy with longer reads (300–800 bp) due to local variations in genomic composition (reviewed in Teeling and Glöckner (2012)). The latest binning algorithms, ABUNDANCEBIN that uses l-tuples (Wu and Ye, 2011) and the mixture models developed by Meinicke *et al.* (2011),

are a lot less sensitive to read lengths and can be used effectively for binning of reads produced by Illumina platforms. Finally, programs have been developed that take a combined homology- and composition-based approach including PhymmBL (Brady and Salzberg, 2009; Rosen *et al.*, 2011) and the NB-based classifier developed by Parks *et al.* (2011).

The deep sequencing capability of NGS technologies enables increased coverage of genomes in the environment and therefore a greater possibility for complete genomes to be assembled *de novo*. However, *de novo* genome assembly from a high volume of short reads is an extremely difficult computational problem requiring a great deal of computer memory to run (see Salzberg *et al.* (2012) for a review of assembly algorithms). Using sequences from a mixture of species further compounds the problem. Two recent developments that hold promise for surpassing the challenge of *de novo* assembly of metagenomes deep sequenced with NGS technologies. One study has assembled a near-complete *Rhodobacterales* genome and two variants of marine group II *Euryarchaeota* genomes from SOLiD sequenced marine metagenomes (Iverson *et al.*, 2012). Sequences assembled using VELVET only produced short contigs. Extensive post processing using in-house software, SEASTAR and TETRACALC, were necessary to further assemble these contigs into scaffolds. This involved forming scaffolds based on coverage, GC content and matepairing scores and binning those scaffolds into genomes based on nucleotide composition statistics. Software used to generate these genomes will be made available in the future at <http://armbrustlab.ocean.washington.edu/seastar>, which will allow the assembly methodology to be validated on other metagenomic samples and assessed for broad applicability. In particular, information about the computational resources and degree of manual curation necessary to achieve this sort of assembly is needed to gauge its utility.

The other recent study has developed a novel method for overcoming memory limitations encountered when using NGS data assemblers, such as VELVET, with metagenomic data (Pell *et al.*, 2012). In this approach, the *k*-mer connectivity (de Bruijn) graphs normally produced by the assembler are stored as a simplified representation based on Bloom filters, which require less memory. The representations of the de Bruijn graphs were used to partition reads into smaller connected sets that can then be separately assembled. When applied to Illumina GII sequenced soil metagenome samples, assembly was identical when using partitioned and unpartitioned data indicating this method can be used to accurately assemble metagenomic sequence with a 40-fold decrease in memory usage. Again, further testing is required to assess if this method is suitable for other metagenomic datasets.

Future Antarctic lake metagenomics projects can profit immensely from the wealth of emerging bioinformatics tools available. Complete viral genomes were able to be assembled *de novo* from the 2006 Organic Lake samples using a combination of Sanger and 454 data (chapter 3) demonstrating assembly-driven approaches are effective in Antarctic lakes. This suggests future studies utilising deep sequencing and new assembly algorithms could obtain complete genome sequences. However, no single bioinformatic

pipeline will cover all aspects of metagenomic analysis and as sequencing technologies are advancing rapidly, there is no established best practice at the moment for metagenomic analyses. Deciding on which analysis approach to take will require careful assessment of the sequence data and bioinformatic resources available.

5.2.4 'omes are only as good as our databases

Aside from the computational limitations, ‘-omics’ type analyses rely a great deal on current sequence databases and laboratory studies to make meaningful inferences. For example, detection of the OLV was contingent on the presence of a sufficiently close relative, Sputnik (*La Scola et al.*, 2008), in the non-redundant database. Similarly, the recent sequencing and characterisation of DMSP lyase genes enabled them to be detected in the Organic Lake data.

A dependency on sequence databases applies even more to metaproteomic analysis. Unlike metagenomics where fairly distantly related sequences can be matched to a metagenome to give some idea of its biological significance, spectral matching fails if protein sequences with high identity to those in the sample are not available. This makes metaproteomics much more reliant on sequence database availability and accuracy. Furthermore, identification of proteins only indicates that they are expressed, but characterisation of the same or closely related protein is still necessary to infer its function in the sample. This exemplifies how both metagenomics and metaproteomics need to be paired with basic laboratory studies for meaningful biological inferences to be made.

5.2.5 Metagenomes and metaproteomes are time capsules

Conversely, it means a great deal of metagenomics sequences and metaproteomic mass spectra data remains to be taxonomically or functionally assigned. The DNA sequence and mass spectra data that has been produced form a lasting record of the state of the microbial communities at the point in time that they were collected. It thus acts as a resource against which other datasets can be compared to gain an understanding of variability between ecosystems and as a bench mark to gauge changes overtime. The data can also be specifically mined to recover features of interest, for example sequences that encode enzymes with desired activities or bioactive compounds can be recovered by synthesis from the sequence information. As sequence databases grow and more of the microbial world is characterised, this archive of molecular data can be re-analysed to learn even more from these unique ecosystems.

Where to from here?

As mentioned above, future ‘-omic’ studies need to now encompass longer time scales, finer spatial resolutions and focussed analysis of populations and individuals that make up communities. This will allow for relationships to become apparent between molecular data and environmental parameters over space and time. Pairing ‘-omics’ tools

with complementary techniques designed to target specific individuals or populations, community functions and biogeochemical processes is a promising way to enable an even deeper understanding of ecosystems by combining their respective strengths.

The hypotheses built on environmental data can then guide laboratory research studies and thus feedback into supporting a systems-level understanding of microbial communities.

5.3 Concluding remarks

This thesis has demonstrated how metagenomics and metaproteomics can be used as a tool for characterising Antarctic lake ecosystems. The DNA sequence and mass spectra data that has been produced form a lasting record of the state of the microbial communities at the point in time that they were collected. It thus acts as a resource against which other datasets can be compared to gain an understanding of variability between ecosystems and as a bench mark to gauge changes overtime. As sequence databases grow and more of the microbial world is characterised, this archive of molecular data can be re-analysed to learn even more from these unique ecosystems.

References

- Abell G. C. J. and Bowman J. P. (2005). Ecological and biogeographic relationships of class *Flavobacteria* in the Southern Ocean. *FEMS Microbiology Ecology*, 51: 265–77.
- Abell G. C. J. and Bowman J. P. (2005). Colonization and community dynamics of class *Flavobacteria* on diatom detritus in experimental mesocosms based on Southern Ocean seawater. *FEMS Microbiology Ecology*, 53:379–391.
- Agarkova I. V., Dunigan D. D., and Van Etten J. L. (2006). Virion-associated restriction endonucleases of chloroviruses. *Journal of Virology*, 80:8114–8123.
- Alekhina I. A., Marie D., Petit J. R., Lukin V. V., Zubkov V. M., and Bulat S. A. (2007). Molecular analysis of bacterial diversity in kerosene-based drilling fluid from the deep ice borehole at Vostok, East Antarctica. *FEMS Microbiology Ecology*, 59: 289–299.
- Allen L. Z., Ishoey T., Novotny M. A., McLean J. S., Lasken R. S., and Williamson S. J. (2011). Single virus genomics: a new tool for virus discovery. *PLoS One*, 6: e17722.
- Altschul S. F., Gish W., Miller W., Myers E. W., and Lipman D. J. (1990). Basic local alignment search tool. *Journal of Molecular Biology*, 215:403–410.
- Angiuoli S. V., White J. R., Matalka M., White O., and Fricke W. F. (2011). Resources and costs for microbial sequence analysis evaluated using virtual machines and cloud computing. *PLoS One*, 6:e26624.
- Balashov S. P., Imasheva E. S., Boichenko V. A., Antón J., Wang J. M., and Lanyi J. K. (2005). Xanthorhodopsin: a proton pump with a light-harvesting carotenoid antenna. *Science*, 309:2061–2064.
- Béjà O., Suzuki M. T., Heidelberg J. F., Nelson W. C., Preston C. M., Hamada T., Eisen J. A., Fraser C. M., and Delong E. F. (2002). Unsuspected diversity among marine aerobic anoxygenic phototrophs. *Nature*, 415:5–8.
- Bell E. M. and Laybourn-Parry J. (2003). Mixotrophy in the Antarctic phytoflagellate, *Pyramimonas gelidicola* (*Chlorophyta*: *Prasinophyceae*). *Journal of Phycology*, 649:644–649.
- Bengtsson J., Eriksson K. M., Hartmann M., Wang Z., Shenoy B. D., Grelet G.-A., Abarenkov K., Petri A., Rosenblad M. A., and Nilsson R. H. (2011). Metaxa: a software tool for automated detection and discrimination among ribosomal small subunit mitochondria, and chloroplasts in metagenomes and environmental sequencing datasets. *Antonie van Leeuwenhoek*, 100:471–475.

- Bergh O., Borsheim K. Y., Bratbak G., and Heldal M. (1989). High abundance of viruses found in aquatic environments. *Nature*, 340:467–468.
- Bergmann D. J., Hooper A. B., and Klotz M. G. (2005). Structure and sequence conservation of *ji_ihao_j/i_k* cluster genes of autotrophic ammonia-oxidizing bacteria: evidence for their evolutionary history. *Applied and Environmental Microbiology*, 71: 5371–5382.
- Bielewicz S., Bell E. M., Kong W., Friedberg I., Priscu J. C., and Morgan-Kiss R. M. (2011). Protist diversity in a permanently ice-covered Antarctic lake during the polar night transition. *The ISME Journal*, 5:1559–1564.
- Bird M. I., Chivas A. R., Radnell C. J., and Burton H. R. (1991). Sedimentological and stable-isotope evolution of lakes in the Vestfold Hills, Antarctica. *Palaeogeography, Palaeoclimatology, Palaeoecology*, 84:109–130.
- Bouvier T. and Giorgio P.del (2007). Key role of selective viral-induced mortality in determining marine bacterial community composition. *Environmental Microbiology*, 9:287–297.
- Bowman J. P., Mccammon S. A., Lewis T., Skerratt J. H., Brown J. L., Nichols D. S., and Mcmeekin T. A. (1998). *ji_iPsychroflexus torquis_j/i_k* gen. nov., sp. nov., a psychrophilic species from Antarctic sea ice, and reclassification of *ji_iFlavobacterium gondwanense_j/i_k* (Dobson et al. 1993) as *ji_iPsychroflexus gondwanense_j/i_k* gen. nov., comb. nov. *Microbiology*, 144:1601–1609.
- Bowman J. P., McCammon S. A., Rea S. M., and McMeekin T. A. (2000). The microbial composition of three limnologically disparate hypersaline Antarctic lakes. *FEMS Microbiology Letters*, 183:81–88.
- Bowman J. P., Rea S. M., McCammon S. A., and McMeekin T. A. (2000). Diversity and community structure within anoxic sediment from marine salinity meromictic lakes and a coastal meromictic marine basin, Vestfold Hills, Eastern Antarctica. *Environmental Microbiology*, 2(2):227–237.
- Boyer M., Azza S., Barrassi L., Klose T., Campocasso A., Pagnier I., Fournous G., Borg A., Robert C., Zhang X., Desnues C., Henrissat B., Rossmann M. G., La Scola B., and Raoult D. (2011). Mimivirus shows dramatic genome reduction after intraamoebal culture. *Proceedings of the National Academy of Sciences USA*, 108: 10296–102301.
- Brady A. and Salzberg S. L. (2009). Phymm and PhymmBL: metagenomic phylogenetic classification with interpolated Markov models. *Nature Methods*, 6:673–676.
- Bratbak G., Jacobsen A., and Heldal M. (1998). Viral lysis of *ji_iPhaeocystis pouchetii_j/i_k* and bacterial secondary production. *Aquatic Microbial Ecology*, 16: 11–16.
- Breitbart M., Salamon P., Andresen B., Mahaffy J. M., Segall A. M., Mead D., Azam F., and Rohwer F. (2002). Genomic analysis of uncultured marine viral communities. *Proceedings of the National Academy of Sciences USA*, 99:14250–14255.
- Bronge C. (2004). Hydrographic and climatic changes influencing the proglacial Druzhby drainage system, Vestfold Hills, Antarctica. *Antarctic Science*, 8:379–388.

- Budinoff C. R., Loar S. N., LeCleir G. R., Wilhelm S. W., and Buchan A. (2011). A protocol for enumeration of aquatic viruses by epifluorescence microscopy using Anodisc 13 membranes. *BMC Microbiology*, 11:168.
- Bulat S. A., Alekhina I. A., Blot M., Petit J.-R., Angelis M.de, Wagenbach D., Lipenkov V. Y., Vasilyeva L. P., Wloch D. M., Raynaud D., and Lukin V. V. (2004). DNA signature of thermophilic bacteria from the aged accretion ice of Lake Vostok, Antarctica: implications for searching for life in extreme icy environments. *International Journal of Astrobiology*, 3:1–12.
- Burke C. and Burton H. R. (1988). Photosynthetic bacteria in meromictic lakes and stratified fjords of the Vestfold Hills, Antarctica. *Hydrobiologia*, 165:13–23.
- Burton H. R. (1981). Chemistry, physics and evolution of Antarctic saline lakes. *Hydrobiologia*, 82:339–362.
- Campbell B. J., Engel A. S., Porter M. L., and Takai K. (2006). The versatile γ -Epsilon-proteobacteria: key players in sulphidic habitats. *Nature Reviews Microbiology*, 4:458–468.
- Caporaso J. G., Kuczynski J., Stombaugh J., Bittinger K., Bushman F. D., Costello E. K., Fierer N., Peña A. G., Goodrich J. K., Gordon J. I., Huttley G. A., Kelley S. T., Knights D., Koenig J. E., Ley R. E., Lozupone C. A., McDonald D., Muegge B. D., Pirrung M., Reeder J., Sevinsky J. R., Turnbaugh P. J., Walters W. A., Widmann J., Yatsunenko T., Zaneveld J., and Knight R. (2010). QIIME allows analysis of high-throughput community sequencing data. *Nature Methods*, 7:335–336.
- Caporaso J. G., Paszkiewicz K., Field D., Knight R., and Gilbert J. A. (2012). The Western English Channel contains a persistent microbial seed bank. *The ISME journal*, 6:1089–1093.
- Carver T. J., Rutherford K. M., Berriman M., Rajandream M.-A., Barrell B. G., and Parkhill J. (2005). ACT: the Artemis Comparison Tool. *Bioinformatics*, 21:3422–3423.
- Castberg T., Larsen A., Sandaa R.-A., Brussaard C. P., Egge J., Heldal M., Thyrhaug R., Hannen E.van, and Bratbak G. (2001). Microbial population dynamics and diversity during a bloom of the marine cocolithophorid Emiliania huxleyi . *Marine Ecology Progress Series*, 221:39–46.
- Charlson R. J., Lovelock J. E., Andreae M. O., and Warren S. G. (1987). Oceanic phytoplankton, atmospheric sulphur, cloud albedo and climate. *Nature*, 326:655–661.
- Chen F., Mackey A. J., Stoeckert C. J., and Roos D. S. (2006). OrthoMCL-DB: querying a comprehensive multi-species collection of ortholog groups. *Nucleic Acids Research*, 34:D363–D368.
- Chouari R., Le Paslier D., Daegelen P., Ginestet P., Weissenbach J., and Sghir A. (2005). Novel predominant archaeal and bacterial groups revealed by molecular analysis of an anaerobic sludge digester. *Environmental Microbiology*, 7:1104–1115.
- Christner B. C., Mosley-Thompson E., Thompson L. G., and Reeve J. N. (2001). Isolation of bacteria and 16S rDNAs from Lake Vostok accretion ice. *Environmental Microbiology*, 3:570–577.

- Clarke K. and Gorley R. PRIMER V6: User Manual/Tutorial, 2006.
- Claverie J.-M. and Abergel C. (2009). Mimivirus and its virophage. *Annual review of genetics*, 43:49–66.
- Collins R. E., Rocap G., and Deming J. W. (2010). Persistence of bacterial and archaeal communities in sea ice through an Arctic winter. *Environmental Microbiology*, 12: 1828–1841.
- Cottrell M. T. and Kirchman D. L. (2009). Photoheterotrophic microbes in the Arctic Ocean in summer and winter. *Applied and Environmental Microbiology*, 75:4958–4966.
- Curran M. A., Jones G. B., and Burton H. R. (1998). Spatial distribution of dimethylsulphide and dimethylsulfoniopropionate in the Australasian sector of the Southern Ocean. *Journal of Geophysical Research*, 103:16677–16689.
- Curson A. R., Rogers R., Todd J. D., Brearley C. A., and Johnston A. W. (2008). Molecular genetic analysis of a dimethylsulfoniopropionate lyase that liberates the climate-changing gas dimethylsulfide in several marine alpha-proteobacteria and *Rhodobacter sphaeroides*. *Environmental Microbiology*, 10:757–767.
- Curson A. R., Sullivan M. J., Todd J. D., and Johnston A. W. (2010). Identification of genes for dimethyl sulfide production in bacteria in the gut of Atlantic Herring (*Clupea harengus*). *The ISME Journal*, 4:144–146.
- Curson A. R., Sullivan M. J., Todd J. D., and Johnston A. W. (2011). DddY, a periplasmic dimethylsulfoniopropionate lyase found in taxonomically diverse species of Proteobacteria. *The ISME Journal*, 5:1191–200.
- Curson A. R., Todd J. D., Sullivan M. J., and Johnston A. W. (2011). Catabolism of dimethylsulphoniopropionate: microorganisms, enzymes and genes. *Nature Reviews Microbiology*, 9:849–859.
- Curson A. R., Fowler E. K., Dickens S., Johnston A. W., and Todd J. D. (2012). Multiple DMSP lyases in the gamma-proteobacterium *Oceanimonas doudoroffii*. *Biogeochemistry*, 110:109–119.
- Danovaro R., Corinaldesi C., Dell'Anno A., Fuhrman J. A., Middelburg J. J., Noble R. T., and Suttle C. A. (2011). Marine viruses and global climate change. *FEMS Microbiology Reviews*, 35:993–1034.
- Davenport C. F., Neugebauer J., Beckmann N., Friedrich B., Kameri B., Kokott S., Paetow M., Siekmann B., Wieding-Drewes M., Wienhöfer M., Wolf S., Tümmler B., Ahlers V., and Sprengel F. (2012). Genometa - a fast and accurate classifier for short metagenomic shotgun reads. *PloS One*, 7:e41224.
- Davidson A. T. and Marchant H. J. (1992). Protist abundance and carbon concentration during a *Phaeocystis*-dominated bloom at an Antarctic coastal site. *Polar Biology*, 12:387–395.
- DeMaere M. Z., Lauro F. M., Thomas T., Yau S., and Cavicchioli R. (2011). Simple high-throughput annotation pipeline (SHAP). *Bioinformatics*, 27:2431–2432.
- Demergasso C., Escudero L., Casamayor E. O., Chong G., Balagué V., and Pedrós-Alió C. (2008). Novelty and spatio-temporal heterogeneity in the bacterial diversity of hypersaline Lake Tebenquiche (Salar de Atacama). *Extremophiles*, 12:491–504.

- Denef V. J., Shah M. B., Verberkmoes N. C., Hettich R. L., and Banfield J. F. (2007). Implications of strain- and species-level sequence divergence for community and isolate shotgun proteomic analysis. *Journal of Proteome Research*, 6:3152–3161.
- Deprez P. P., Franzmann P. D., and Burton H. R. (1986). Determination of reduced sulfur gases in Antarctic lakes and seawater by gas chromatography after solid adsorbent preconcentration. *Journal of Chromatography*, 362:9–21.
- Desnues C., La Scola B., Yutin N., Fournous G., Robert C., Azza S., Jardot P., Monteil S., Campocasso A., Koonin E. V., and Raoult D. (2012). Provirophages and transpovirons as the diverse mobilome of giant viruses. *Proceedings of the National Academy of Sciences USA*, 109:18078–18083.
- Diaz N. N., Krause L., Goesmann A., Niehaus K., and Nattkemper T. W. (2009). TACOA: taxonomic classification of environmental genomic fragments using a kernelized nearest neighbor approach. *BMC Bioinformatics*, 10:56.
- Diemer G. S., Kyle J. E., and Stedman K. M. Counting viruses using polycarbonate Track Etch membrane filters as an alternative to Anodisc membrane filters, 2012. URL http://www.web.pdx.edu/~kstedman/PCTE_virus_counting_protocol.pdf.
- Dobson S., James S., Franzmann P. D., and Mcmeekin T. A. (1991). A numerical taxonomic study of some pigmented bacteria isolated from Organic Lake, an antarctic hypersaline lake. *Archives of Microbiology*, 156:56–61.
- Eberlein K., Leal M., Hammer K., and Hickel W. (1985). Dissolved organic substances during a *Phaeocystis pouchetii* bloom in the German Bight (North Sea). *Marine Biology*, 89:311–316.
- Edgar R. C. (2004). MUSCLE: multiple sequence alignment with high accuracy and high throughput. *Nucleic acids research*, 32:1792–1797.
- Edwards K., Rogers D., Wirsen C., and McCollom T. (2003). Isolation and characterization of novel psychrophilic, neutrophilic, Fe-oxidizing, chemolithoautotrophic alpha- and gamma-*Proteobacteria* from the deep sea. *Applied and Environmental Microbiology*, 69:2906–2913.
- Elshahed M. S., Najar F. Z., Aycock M., Qu C., Roe B. A., and Krumholz L. R. (2005). Metagenomic analysis of the microbial community at Zodletone Spring (Oklahoma): insights into the genome of a member of the novel candidate division OD1. *Applied and Environmental Microbiology*, 71:7598–7602.
- Evanko D. (2009). Metagenomics versus Moores law. *Nature Methods*, 6:623.
- Ferris J. M., Gibson J. A., and Burton H. R. (1991). Evidence of density currents with the potential to promote meromixis in ice-covered saline lakes. *Palaeogeography, Palaeoclimatology, Palaeoecology*, 84:99–107.
- Fischer M. G. (2011). Sputnik and Mavirus: more than just satellite viruses. *Nature Reviews*, 10:1–2.
- Fischer M. G. and Suttle C. A. (2011). A virophage at the origin of large DNA transposons. *Science*, 332:231–234.

- Fischer M. G., Allen M. J., Wilson W. H., and Suttle C. A. (2010). Giant virus with a remarkable complement of genes infects marine zooplankton. *Proceedings of the National Academy of Sciences USA*, 107:19508–19513.
- Florens L., Carozza M. J., Swanson S. K., Fournier M., Coleman M. K., Workman J. L., and Washburn M. P. (2006). Analyzing chromatin remodeling complexes using shotgun proteomics and normalized spectral abundance factors. *Methods*, 40:303–311.
- Fofonoff N. and Millard R. J. (1983). Algorithms for computation of fundamental properties of seawater. *UNESCO Technical Papers in Marine Science*, 44.
- Franzmann P. D., Burton H. R., and Mcmeekin T. A. (1987). *Halomonas subglaciescola*, a new species of halotolerant bacteria isolated from Antarctica. *International Journal of Systematic Bacteriology*, 37:27–34.
- Franzmann P. D., Deprez P. P., Burton H. R., and Hoff J.van den (1987). Limnology of Organic Lake, Antarctica, a meromictic lake that contains high concentrations of dimethyl sulfide. *Marine and Freshwater Research*, 38:409–417.
- Franzmann P. D., Stackebrandt E., Sanderson K., Volkman J. K., Cameron D., Stevenson P., and Mcmeekin T. A. (1988). *Halorubrum lacusprofundi*, sp. nov., a halophilic bacterium isolated from Deep Lake, Antarctica. *Systematic & Applied Microbiology*, 11:20–27.
- Friedrich C. G., Bardischewsky F., Rother D., Quentmeier A., and Fischer J. (2005). Prokaryotic sulfur oxidation. *Current Opinion in Microbiology*, 8:253–259.
- Fuchs B. M., Spring S., Teeling H., Quast C., Wulf J., Schattenhofer M., Yan S., Ferriera S., Johnson J., Glöckner F. O., and Amann R. (2007). Characterization of a marine gammaproteobacterium capable of aerobic anoxygenic photosynthesis. *Proceedings of the National Academy of Sciences USA*, 104:2891–2896.
- Fuhrman J. A., Schwalbach M. S., and Stingl U. (2008). Proteorhodopsins: an array of physiological roles? *Nature Reviews Microbiology*, 6:488–494.
- Gärdes A., Kaeppele E., Shehzad A., Seebah S., Teeling H., Yarza P., Glöckner F. O., Grossart H.-P., and Ullrich M. S. (2010). Complete genome sequence of *Marinobacter adhaerens* type strain (HP15), a diatom-interacting marine microorganism. *Standards in Genomic Sciences*, 3:97–107.
- Gauthier M., Lafay B., Christen R., Fernandez L., Acquaviva M., Bonin P., and Bertrand J.-C. (1992). A new, extremely halotolerant, hydrocarbon-degrading marine bacterium. *International Journal of Systematic Bacteriology*, pages 568–576.
- Gerlach W., Jünemann S., Tille F., Goesmann A., and Stoye J. (2009). WebCARMA: a web application for the functional and taxonomic classification of unassembled metagenomic reads. *BMC Bioinformatics*, 10:430.
- Gibson J. A. (1999). The meromictic lakes and stratified marine basins of the Vestfold Hills, East Antarctica. *Antarctic Science*, 11:175–192.
- Gibson J. A. and Burton H. R. (1996). Meromictic Antarctic lakes as recorders of climate change: the structures of Ace and Organic Lakes, Vestfold Hills, Antarctica. *Papers and Proceedings of the Royal Society of Tasmania*, 130:73–78.

- Gibson J. A., Ferris J. M., and Burton H. R. (1990). Temperature density, temperature conductivity and conductivity-density relationships for marine-derived saline lake waters. *ANARE Research Notes*, 78.
- Gibson J. A., Garrick R. C., Franzmann P. D., Deprez P. P., and Burton H. R. (1991). Reduced sulfur gases in saline lakes of the Vestfold Hills, Antarctica. *Palaeogeography, Palaeoclimatology, Palaeoecology*, 84:131–140.
- Gibson J. A., Qiang X. L., Franzmann P. D., Garrick R. C., and Burton H. R. (1994). Volatile fatty and dissolved free amino acids in Organic Lake, Vestfold Hilss, East Antarctica. *Polar Biology*, 14:545–550.
- Gibson J. A., Burton H. R., and Gallagher J. (1995). Meromictic Antarctic lakes as indicators of local water balance: structural changes in Organic Lake, Vestfold Hills 1978–1994. *ANARE Research Notes*, 94:16–18.
- Glatz R., Lepp P., Ward B. B., and Francis C. (2006). Planktonic microbial community composition across steep physical/chemical gradients in permanently ice-covered Lake Bonney, Antarctica. *Geobiology*, 4:53–67.
- Goberna M., Insam H., and Franke-Whittle I. (2009). Effect of biowaste sludge maturation on the diversity of thermophilic bacteria and archaea in an anaerobic reactor. *Applied and Environmental Microbiology*, 75:2566–2572.
- Gómez-Consarnau L., González J. M., Coll-Lladó M., Gourdon P., Pascher T., Neutze R., Pedrós-Alio C., and Pinhassi J. (2007). Light stimulates growth of proteorhodopsin-containing marine *Flavobacteriia*. *Nature*, 445:210–213.
- Gómez-Consarnau L., Akram N., Lindell K., Pedersen A., Neutze R., Milton D. L., González J. M., and Pinhassi J. (2010). Proteorhodopsin phototrophy promotes survival of marine bacteria during starvation. *PLoS Biology*, 8:2–11.
- Gordon D., Priscu J. C., and Giovanonni S. J. (2000). Origin and phylogeny of microbes living in permanent Antarctic lake ice. *Microbial Ecology*, 39:197–202.
- Gordon D. Viewing and editing assembled sequences using Consed. In Baxvanis A. and Davison D., editors, *Current Protocols in Bioinformatics*, volume Chapter 11, chapter Viewing an, pages 11.2.1–11.2.43. John Wiley & Sons, New York, 2004. doi: 10.1002/0471250953.bi1102s02. URL <http://www.ncbi.nlm.nih.gov/pubmed/19664765>.
- Green D. H., Bowman J. P., Smith E. A., Gutierrez T., and Bolch C. J. (2006). *Marinobacter algicola* sp. nov., isolated from laboratory cultures of paralytic shellfish toxin-producing dinoflagellates. *International Journal of Systematic and Evolutionary Microbiology*, 56:523–527.
- Green W. J., Angle M. P., and Chave K. E. (1988). The geochemistry of Antarctic streams and their role in the evolution of four lakes of the McMurdo Dry Valleys. *Geochimica et Cosmochimica Acta*, 52:1265–1274.
- Grzymski J. J., Riesenfeld C. S., Williams T. J., Dussaq A. M., Ducklow H., Erickson M., Cavicchioli R., and Murray A. E. (2012). A metagenomic assessment of winter and summer bacterioplankton from Antarctica Peninsula coastal surface waters. *The ISME Journal*, 6:1901–1915.
- Haft D. H., Loftus B., Richardson D., Yang F., Eisen J. A., Paulsen I. T., and White O. (2001). TIGRFAMs: a protein family resource for the functional identification of proteins. *Nucleic Acids Research*, 29:41–43.

- Hahn M. W. (2009). Description of seven candidate species affiliated with the phylum *Actinobacteria*, representing planktonic freshwater bacteria. *International Journal of Systematic and Evolutionary Microbiology*, 59:112–117.
- Hahn M. W., Lünsdorf H., Wu Q., Schauer M., Höfle M. G., Boenigk J., and Stadler P. (2003). Isolation of novel ultramicrobacteria classified as *Actinobacteria* from five freshwater habitats in Europe and Asia. *Applied and Environmental Microbiology*, 69:1442–1451.
- Hahn M. W., Stadler P., Wu Q. L., and Pöckl M. (2004). The filtration-acclimatization method for isolation of an important fraction of the not readily cultivable bacteria. *Journal of Microbiological Methods*, 57:379–390.
- Hahsler M., Hornik K., and Buchta C. (2007). Getting things in order: an introduction to the R package seriation. *Journal of Statistical Software*, 25:1–34.
- Handelsman J. (2008). Metagenomics is not enough. *DNA and Cell Biology*, 27:219–221.
- Hara S., Terauchi K., and Koike I. (1991). Abundance of viruses in marine waters: assessment by epifluorescence and transmission electron microscopy. *Applied and Environmental Microbiology*, 57:2731–2734.
- Harris J. K., Kelley S. T., and Pace N. R. (2004). New perspective on uncultured bacterial phylogenetic division OP11. *Applied and Environmental Microbiology*, 70:845–849.
- Hennes K. P. and Suttle C. A. (1995). Direct counts of viruses in natural waters and laboratory cultures by epifluorescence microscopy. *Limnology and Oceanography*, 40:1050–1055.
- Hobbie J., Daley R., and Jasper S. (1977). Use of nucleopore filters for counting bacteria by fluorescence microscopy. *Applied and Environmental Microbiology*, 33:1225–1228.
- Hodgson D. A. Antarctic Lakes. In Bengtsson L., Herschy R. W., and Fairbridge R. W., editors, *Encyclopedia of Lakes and Reservoirs*, pages 26–31. Springer, Dordrecht, 2012.
- Hoops S., Sahle S., Gauges R., Lee C., Pahle J., Simus N., Singhal M., Xu L., Mendes P., and Kummer U. (2006). COPASI - a COmplex PAthway SImlator. *Bioinformatics*, 22:3067–3074.
- Horvath P. and Barrangou R. (2010). CRISPR/Cas, the immune system of bacteria and archaea. *Science*, 327:167–170.
- Howard E. C., Henriksen J. R., Buchan A., Reisch C. R., Bürgmann H., Welsh R., Ye W., González J. M., Mace K., Joye S. B., Kiene R. P., Whitman W. B., and Moran M. A. (2006). Bacterial taxa that limit sulfur flux from the ocean. *Science*, 314:649–652.
- Howard E. C., Sun S., Biers E. J., and Moran M. A. (2008). Abundant and diverse bacteria involved in DMSP degradation in marine surface waters. *Environmental Microbiology*, 10:2397–2410.
- Huang L.-N., Zhu S., Zhou H., and Qu L.-H. (2005). Molecular phylogenetic diversity of bacteria associated with the leachate of a closed municipal solid waste landfill. *FEMS Microbiology Letters*, 242:297–303.

- Huang Y., Niu B., Gao Y., Fu L., and Li W. (2010). CD-HIT Suite: a web server for clustering and comparing biological sequences. *Bioinformatics*, 26:260–262.
- Hügler M. and Sievert S. M. (2011). Beyond the Calvin cycle: autotrophic carbon fixation in the ocean. *Annual Review of Marine Science*, 3:261–289.
- Humayoun S. B., Bano N., and Hollibaugh J. T. (2003). Depth distribution of microbial diversity in Mono Lake, a meromictic soda lake in California. *Applied and Environmental Microbiology*, 69:1030–1042.
- Hunter C. I., Mitchell A., Jones P., McAnulla C., Pesseat S., Scheremetjew M., and Hunter S. (2012). Metagenomic analysis: the challenge of the data bonanza. *Briefings in Bioinformatics*, 13:743–746.
- Huson D. H., Auch A. F., Qi J., and Schuster S. C. (2007). MEGAN analysis of metagenomic data. *Genome Research*, 17:377–386.
- Huu N. B., Denner E. B., Ha D. T., Wanner G., and Stan-Lotter H. (1996). *Marinobacter aquaeolei* sp. nov., a halophilic bacterium isolated from a Vietnamese oil-producing well. *International Journal of Systematic Bacteriology*, 49: 367–375.
- Iverson V., Morris R. M., Frazer C. D., Berthiaume C. T., Morales R. L., and Armbrust E. V. (2012). Untangling genomes from metagenomes: revealing an uncultured class of marine *Euryarchaeota*. *Science*, 335:587–590.
- Iyer L. M., Aravind L., and Koonin E. V. (2001). Common origin of four diverse families of large eukaryotic DNA viruses. *Journal of Virology*, 75:11720–11734.
- Iyer L. M., Balaji S., Koonin E. V., and Aravind L. (2006). Evolutionary genomics of nucleo-cytoplasmic large DNA viruses. *Virus Research*, 117:156–184.
- Jacobsen A., Bratbak G., and Heldal M. (1996). Isolation and characterization of a new virus infecting *Phaeocystis pouchetii* (Prymnesiophyte). *Journal of Phycology*, 32:586–588.
- James S., Dobson S., Franzmann P. D., and Mcmeekin T. A. (1990). *Halomonas meridianai*, a new species of extremely halotolerant bacteria isolated from Antarctic saline lakes. *Systematic and Applied Microbiology*, 13(3):270–278.
- James S., Burton H. R., Mcmeekin T. A., and Mancuso C. (1994). Seasonal abundance of *Halomonas meridianai*, *Halomonas subglaciocola*, *Flavobacterium gondwanense* and *Flavobacterium salegens* in four Antarctic lakes. *Antarctic Science*, 6:325–332.
- Johnston A. W., Todd J. D., Sun L., Nikolaidou-Katsaraidou N., Curson A. R., and Rogers R. (2008). Molecular diversity of bacterial production of the climate-changing gas, dimethyl sulphide, a molecule that impinges on local and global symbioses. *Journal of Experimental Botany*, 59:1059–1067.
- Johnstone G., Brown D., and Lugg D. (1973). The biology of the Vestfold Hills, Antarctica. *ANARE Scientific Reports*, 123:1–60.
- Kang I., Lee K., Yang S.-J., Choi A., Kang D., Lee Y. K., and Cho J.-C. (2012). Genome sequence of "Candidatus Aquiluna" sp. strain IMCC13023, a marine member of the *Actinobacteria* isolated from an Arctic fjord. *Journal of Bacteriology*, 194:3550–3551.

- Karginov F. V. and Hannon G. J. (2010). The CRISPR system: small RNA-guided defense in bacteria and archaea. *Molecular Cell*, 37:7–19.
- Karr E. A., Sattley W. M., Jung D. O., Madigan M. T., and Achenbach L. A. (2003). Remarkable diversity of phototrophic purple bacteria in a permanently frozen Antarctic lake. *Applied and Environmental Microbiology*, 8:4910–4914.
- Karr E. A., Sattley W. M., Rice M. R., Jung D. O., Madigan M. T., and Achenbach L. A. (2005). Diversity and distribution of sulfate-reducing bacteria in permanently frozen Lake Fryxell, McMurdo Dry Valleys, Antarctica. *Applied and Environmental Microbiology*, 71:6353–6359.
- Karr E. A., Ng J. M., Belchik S. M., Matthew W. M., Madigan M. T., Achenbach L. A., and Sattley W. M. (2006). Biodiversity of methanogenic and other *ii₃Archaea*ii** in the permanently frozen Lake Fryxell, Antarctica. *Applied and Environmental Microbiology*, 72(2):1663–1666.
- Keller A., Nesvizhskii A. I., Kolker E., and Aebersold R. (2002). Empirical statistical model to estimate the accuracy of peptide identifications made by MS/MS and database search. *Analytical Chemistry*, 74:5383–5392.
- Kent W. J. (2002). BLATthe BLAST-like alignment tool. *Genome Research*, 12:656–664.
- Kirchman D. L. (2002). The ecology of *ii₃Cytophaga-Flavobacteriia*ii** in aquatic environments. *FEMS Microbiology Ecology*, 39:91–100.
- Kong W., Dolhi J. M., Chiuchiolo A., Priscu J., and Morgan-Kiss R. M. (2012). Evidence of form II RubisCO (cbbM) in a perennially ice-covered Antarctic lake. *FEMS Microbiology Ecology*, 82:1–10.
- Kong W., Ream D. C., Priscu J. C., and Morgan-Kiss R. M. (2012). Diversity and expression of RubisCO genes in a perennially ice-covered Antarctic lake during the polar night transition. *Applied and Environmental Microbiology*, 78:4358–4366.
- Kraft B., Strous M., and Tegetmeyer H. E. (2011). Microbial nitrate respiration genes, enzymes and environmental distribution. *Journal of Biotechnology*, 155:104–117.
- Krause L., Diaz N. N., Goesmann A., Kelley S., Nattkemper T. W., Rohwer F., Edwards R. A., and Stoye J. (2008). Phylogenetic classification of short environmental DNA fragments. *Nucleic Acids Research*, 36:2230–2239.
- Kumar S., Nei M., Dudley J., and Tamura K. (2008). MEGA: a biologist-centric software for evolutionary analysis of DNA and protein sequences. *Brief Bioinformatics*, 9:299–306.
- Kurosawa N., Sato S., Kawarabayashi Y., Imura S., and Naganuma T. (2010). Archaeal and bacterial community structures in the anoxic sediment of Antarctic meromictic lake Nurume-Ike. *Polar Science*, 4:421–429.
- La Scola B., Desnues C., Pagnier I., Robert C., Barrassi L., Fournous G., Merchat M., Suzan-Monti M., Forterre P., Koonin E. V., and Raoult D. (2008). The virophage as a unique parasite of the giant mimivirus. *Nature*, 455:100–104.
- Labrenz M., Collins M. D., Lawson P. A., Tindall B. J., Schumann P., and Hirsch P. (1999). *ii₃Roseovarius tolerans*ii** gen. nov., sp. nov., a budding bacterium with variable bacteriochlorophyll a production from hypersaline Ekho Lake. *International Journal of Systematic Bacteriology*, 49:137–147.

- Larsen A., Castberg T., Sandaa R.-A., Brussaard C. P., Egge J., Heldal M., Paulino A., Thyrhaug R., Hannen E. van, and Bratbak G. (2001). Population dynamics and diversity of phytoplankton, bacteria and viruses in a seawater enclosure. *Marine Ecology Progress Series*, 221:47–57.
- Larsen J. B., Larsen A., Bratbak G., and Sandaa R.-A. (2008). Phylogenetic analysis of members of the *Phycodnaviridae* virus family, using amplified fragments of the major capsid protein gene. *Applied and environmental microbiology*, 74:3048–3057.
- Lauro F. M., McDougald D., Thomas T. J., Williams T. J., Egan S., Rice S., DeMaere M. Z., Ting L., Ertan H., Johnson J., Ferriera S., Lapidus A., Anderson I. J., Kyrpides N., Munk A. C., Detter C., Han C. S., Brown M. V., Robb F. T., Kjelleberg S., and Cavicchioli R. (2009). The genomic basis of trophic strategy in marine bacteria. *Proceedings of the National Academy of Sciences USA*, 106:15527–15533.
- Lauro F. M., DeMaere M. Z., Yau S., Brown M. V., Ng C., Wilkins D., Raftery M. J., Gibson J. A., Andrews-Pfannkoch C., Lewis M., Hoffman J. M., Thomas T., and Cavicchioli R. (2011). An integrative study of a meromictic lake ecosystem in Antarctica. *The ISME Journal*, 5:879–895.
- Lavire C., Normand P., Alekhina I., Bulat S., Prieur D., Birrien J.-L., Fournier P., Hänni C., and Petit J.-R. (2006). Presence of *Hydrogenophilus thermoluteolus* DNA in accretion ice in the subglacial Lake Vostok, Antarctica, assessed using *rrs*, *cbb* and *hox*. *Environmental Microbiology*, 8:2106–2114.
- Law P. (1959). The Vestfold Hills. *ANARE Reports*, 1:1–50.
- Laybourn-Parry J. The microbial loop in Antarctic lakes. In Howard-Willsiams C., Lyons W., and Hawes I., editors, *Ecosystem Dynamics in a Antarctic Ice-Free Landscapes*, pages 231–240. Rotterdam, 1997.
- Laybourn-Parry J. and Pearce D. A. (2007). The biodiversity and ecology of Antarctic lakes: models for evolution. *Philosophical Transactions of the Royal Society of London. Series B, Biological sciences*, 362:2273–2289.
- Laybourn-Parry J., Hofer J. S., and Sommaruga R. (2001). Viruses in the plankton of freshwater and saline Antarctic lakes. *Freshwater Biology*, 46:1279–1287.
- Laybourn-Parry J., Marshall W. A., and Marchant H. J. (2005). Flagellate nutritional versatility as a key to survival in two contrasting Antarctic saline lakes. *Freshwater Biology*, 50:830–838.
- Ley R. E., Turnbaugh P. J., Klein S., and Gordon J. I. (2006). Human gut microbes associated with obesity. *Nature*, 444:1022–1023.
- Li L., Stoeckert C. J., and Roos D. S. (2003). OrthoMCL: identification of ortholog groups for eukaryotic genomes. *Genome Research*, 13:2178–2189.
- López-Bueno A., Tamares J., Velázquez D., Moya A., Quesada A., and Alcamí A. (2009). High diversity of the viral community from an Antarctic lake. *Science*, 858: 859–861.
- Lotka A. (1910). Contribution to the theory of periodic reaction. *Journal of Physical Chemistry*, 14:271–274.
- Lovelock J. E. and Maggs R. (1972). Atmospheric dimethyl sulphide and the natural sulphur cycle. *Nature*, 237:452–453.

- Madan N. J., Marshall W. A., and Laybourn-Parry J. (2005). Virus and microbial loop dynamics over an annual cycle in three contrasting Antarctic lakes. *Freshwater Biology*, 50:1291–1300.
- Man D., Wang W., Sabehi G., Aravind L., Post A. F., Massana R., Spudich E. N., Spudich J. L., and Béjà O. (2003). Diversification and spectral tuning in marine proteorhodopsins. *The EMBO Journal*, 22:1725–1731.
- Marcotte E. M. (2007). How do shotgun proteomics algorithms identify proteins? *Nature Biotechnology*, 25:755–757.
- Markowitz V. M., Ivanova N. N., Szeto E., Palaniappan K., Chu K., Dalevi D., Chen I.-M. A., Grechkin Y., Dubchak I., Anderson I. J., Lykidis A., Mavromatis K., Hugenholtz P., and Kyrpides N. C. (2008). IMG/M: a data management and analysis system for metagenomes. *Nucleic Acids Research*, 36:D534–8.
- Markowitz V. M., Chen I.-M. A., Chu K., Szeto E., Palaniappan K., Grechkin Y., Ratner A., Jacob B., Pati A., Huntemann M., Liolios K., Pagani I., Anderson I., Mavromatis K., Ivanova N. N., and Kyrpides N. C. (2012). IMG/M: the integrated metagenome data management and comparative analysis system. *Nucleic Acids Research*, 40:D123–9.
- Martínez-Martínez J., Schroeder D. C., Larsen A., Bratbak G., and Wilson W. H. (2007). Molecular dynamics of *Emiliania huxleyi* and cooccurring viruses during two separate mesocosm studies. *Applied and Environmental Microbiology*, 73:554–562.
- Martínez Martínez J., Poulton N. J., Stepanauskas R., Sieracki M. E., and Wilson W. H. (2011). Targeted sorting of single virus-infected cells of the coccolithophore *Emiliania huxleyi*. *PloS One*, 6:e22520.
- Matsuzaki M., Kubota K., Satoh T., Kunugi M., Ban S., and Imura S. (2006). Dimethyl sulfoxide-respiring bacteria in Suribati Ike, a hypersaline lake, in Antarctica and the marine environment. *Polar Bioscience*, 20:73–81.
- McHardy A. C., Martín H. G., Tsirigos A., Hugenholtz P., and Rigoutsos I. (2006). Accurate phylogenetic classification of variable-length DNA fragments. *Nature Methods*, 4:63–72.
- Meinicke P., Asshauer K. P., and Lingner T. (2011). Mixture models for analysis of the taxonomic composition of metagenomes. *Bioinformatics*, 27:1618–1624.
- Meyer F., Paarmann D., D’Souza M., Olson R., Glass E., Kubal M., Paczian T., Rodriguez A., Stevens R., Wilke A., Wilkening J., and Edwards R. A. (2008). The metagenomics RAST server - a public resource for the automatic phylogenetic and functional analysis of metagenomes. *BMC Bioinformatics*, 9:386.
- Mikucki J. A. and Priscu J. C. (2007). Bacterial diversity associated with Blood Falls, a subglacial outflow from the Taylor Glacier, Antarctica. *Applied and Environmental Microbiology*, 73:4029–4039.
- Mikucki J. A., Pearson A., Johnston D. T., Turchyn A. V., Farquhar J., Schrag D. P., Anbar A. D., Priscu J. C., and Lee P. A. (2009). A contemporary microbially maintained subglacial ferrous “ocean”. *Science*, 324:397–400.

- Miyoshi T., Iwatsuki T., and Naganuma T. (2005). Phylogenetic characterization of 16S rRNA gene clones from deep-groundwater microorganisms that pass through 0.2-micrometer-pore-size filters. *Applied and environmental microbiology*, 71:1084–1088.
- Monier A., Claverie J.-M., and Ogata H. (2008). Taxonomic distribution of large DNA viruses in the sea. *Genome biology*, 9:R106.
- Monier A., Larsen J. B., Sandaa R.-A., Bratbak G., Claverie J.-M., and Ogata H. (2008). Marine mimivirus relatives are probably large algal viruses. *Virology Journal*, 5:12.
- Moran M. A. and Miller W. L. (2007). Resourceful heterotrophs make the most of light in the coastal ocean. *Nature Reviews Microbiology*, 5:792–800.
- Moran M. A., Belas R., Schell M., González J. M., Sun F., Sun S., Binder B. J., Edmonds J., Ye W., Orcutt B., Howard E. C., Meile C., Palefsky W., Goesmann A., Ren Q., Paulsen I., Ulrich L., Thompson L., Saunders E., and Buchan A. (2007). Ecological genomics of marine Roseobacters. *Applied and Environmental Microbiology*, 73: 4559–4569.
- Moran M. A., Reisch C. R., Kiene R. P., and Whitman W. B. (2012). Genomic insights into bacterial DMSP transformations. *Annual Review of Marine Science*, 4:523–542.
- Morris R. M., Nunn B. L., Frazer C., Goodlett D. R., Ting Y. S., and Rocap G. (2010). Comparative metaproteomics reveals ocean-scale shifts in microbial nutrient utilization and energy transduction. *The ISME Journal*, 4:673–685.
- Mosier A. C., Murray A. E., and Fritsen C. H. (2007). Microbiota within the perennial ice cover of Lake Vida, Antarctica. *FEMS Microbiology Ecology*, 59:274–288.
- Myers E. W., Sutton G. G., Delcher A. L., Dew I. M., Fasulo D. P., Flanigan M. J., Kravitz S. A., Mobarry C. M., Reinert K. H., Remington K. A., Anson E. L., Bolanos R. A., Chou H.-H., Jordan C. M., Halpern A. L., Lonardi S., Beasley E. M., Brandon R. C., Chen L., Dunn P. J., Lai Z., Liang Y., Nusskern D. R., Zhan M., Zhang Q., Zheng X., Rubin G. M., Adams M. D., and Venter J. C. (2000). A whole-genome assembly of *Drosophila*. *Science*, 287:2196–2204.
- Nagasaki K., Ando M., Imai I., Itakura S., and Ishida Y. (1994). Virus-like particles in *Heterosigma akashiwo*: a possible red tide disintegration mechanism. *Marine Biology*, 119:307–312.
- Nagasaki K., Shirai Y., Tomaru Y., Nishida K., and Pietrokovski S. (2005). Algal viruses with distinct intraspecies host specificities include identical intein elements. *Applied and Environmental Microbiology*, 71:3599–3607.
- Nelson M., Zhang Y., and Van Etten J. L. DNA methyltransferases and DNA site-specific endonucleases encoded by chlorella viruses. In Jost J. and Saluz H., editors, *DNA methylation: molecular biology and biological significance*, pages 186–211. Birkhäuser, Basel, 1993.
- Ng C. *A metaproteomic analysis of microbial communities in Ace Lake, Antarctica*. PhD thesis, University of New South Wales, 2010.
- Ng C., DeMaere M. Z., Williams T. J., Lauro F. M., Raftery M., Gibson J. A., Andrews-Pfannkoch C., Lewis M., Hoffman J. M., Thomas T., and Cavicchioli R. (2010). Metaproteogenomic analysis of a dominant green sulfur bacterium from Ace Lake, Antarctica. *The ISME Journal*, 4:1002–19.

- Noble R. T. and Fuhrman J. A. (1998). Use of SYBR Green I for rapid epifluorescence counts of marine viruses and bacteria. *Aquatic Microbial Ecology*, 14:113–118.
- Noguchi H., Park J., and Takagi T. (2006). MetaGene: prokaryotic gene finding from environmental genome shotgun sequences. *Nucleic Acids Research*, 34:5623–5630.
- Olson J., Steppe T., Litaker R., and Paerl H. (1998). N₂-fixing microbial consortia associated with the ice cover of Lake Bonney, Antarctica. *Microbial Ecology*, 36:231–238.
- Parks D. H. and Beiko R. G. (2010). Identifying biologically relevant differences between metagenomic communities. *Bioinformatics*, 26:715–721.
- Parks D. H., MacDonald N. J., and Beiko R. G. (2011). Classifying short genomic fragments from novel lineages using composition and homology. *BMC Bioinformatics*, 12:328.
- Patel A., Noble R. T., Steele J. A., Schwalbach M. S., Hewson I., and Fuhrman J. A. (2007). Virus and prokaryote enumeration from planktonic aquatic environments by epifluorescence microscopy with SYBR Green I. *Nature Protocols*, 2:269–276.
- Pearce D. A. (2003). Bacterioplankton community structure in a maritime antarctic oligotrophic lake during a period of holomixis, as determined by denaturing gradient gel electrophoresis (DGGE) and fluorescence in situ hybridization (FISH). *Microbial Ecology*, 46:92–105.
- Pearce D. A. (2005). The structure and stability of the bacterioplankton community in Antarctic freshwater lakes, subject to extremely rapid environmental change. *FEMS Microbiology Ecology*, 53:61–72.
- Pearce D. A., Gast C. J., Lawley B., and Ellis-Evans J. C. (2003). Bacterioplankton community diversity in a maritime Antarctic lake, determined by culture-dependent and culture-independent techniques. *FEMS Microbiology Ecology*, 45:59–70.
- Pearce D. A., Gast C. J., van der Woodward K., and Newsham K. K. (2005). Significant changes in the bacterioplankton community structure of a maritime Antarctic freshwater lake following nutrient enrichment. *Microbiology*, 151:3237–3248.
- Pell J., Hintze A., Canino-Koning R., Howe A., Tiedje J. M., and Brown C. T. (2012). Scaling metagenome sequence assembly with probabilistic de Bruijn graphs. *Proceedings of the National Academy of Sciences USA*, 109:13272–13277.
- Pickard J., Adamson D. A., and Heath C. W. (1986). The evolution of Watts Lake, Vestfold Hills, East Antarctica, from marine inlet to freshwater lake. *Palaeogeography, Palaeoclimatology, Palaeoecology*, 53:271–288.
- Poretsky R. S., Sun S., Mou X., and Moran M. A. (2010). Transporter genes expressed by coastal bacterioplankton in response to dissolved organic carbon. *Environmental Microbiology*, 12:616–627.
- Priscu J. C. (1999). Geomicrobiology of subglacial ice above Lake Vostok, Antarctica. *Science*, 286:2141–2144.
- Proctor L. M. and Fuhrman J. A. (1990). Viral mortality of marine bacteria and cyanobacteria. *Nature*, 343:60–62.

- Proctor L. M. and Fuhrman J. A. (1992). Mortality of marine bacteria in response to enrichments of the virus size fraction from seawater. *Marine Ecology Progress Series*, 87:283–293.
- Purdy K., Nedwell D., and Embley T. (2003). Analysis of the sulfate-reducing bacterial and methanogenic archaeal populations in contrasting Antarctic sediments. *Applied and Environmental Microbiology*, 69:3181–3191.
- Quayle W. C., Peck L. S., Peat H., Ellis-Evans J., and Harrigan P. R. (2002). Extreme responses to climate change in Antarctic lakes. *Science*, 295:645.
- Raina J.-B., Dinsdale E. A., Willis B. L., and Bourne D. G. (2010). Do the organic sulfur compounds DMSP and DMS drive coral microbial associations? *Trends in Microbiology*, 18:101–108.
- Ram R. J., Verberkmoes N. C., Thelen M. P., Tyson G. W., Baker B. J., Blake II R. C., Shah M., Hettich R. L., and Banfield J. F. (2005). Community proteomics of a natural microbial biofilm. *Science*, 308:1915–1920.
- Rankin L. M., Gibson J. A., Franzmann P. D., and Burton H. R. (1999). The chemical stratification and microbial communities of Ace Lake, Antarctica: a review of the characteristics of a marine-derived meromictic lake. *Polarforschung*, 66:33–52.
- Redfield A., Ketchum B., and Richards F. The influence of organisms on the composition of sea-water. In Hill M., editor, *The Sea*, pages 26–77. 1963. URL <http://www.vliz.be/imis/imis.php?refid=28944>.
- Reisch C. R., Moran M. A., and Whitman W. B. (2011). Bacterial catabolism of dimethylsulfoniopropionate (DMSP). *Frontiers in Microbiology*, 2:1–12.
- Rivière D., Desvignes V., Pelletier E., Chaussonnerie S., Guermazi S., Weissenbach J., Li T., Camacho P., and Sghir A. (2009). Towards the definition of a core of microorganisms involved in anaerobic digestion of sludge. *The ISME Journal*, 3: 700–714.
- Roberts N. and Burton H. R. (1993). Sampling volatile organics from a meromictic Antarctic lake. *Polar Biology*, 13:359–361.
- Roberts N., Burton H. R., and Pitson G. (1993). Volatile organic compounds from Organic Lake, an Antarctic, hypersaline, meromictic lake. *Antarctic Science*, 5:361–366.
- Rodríguez-Brito B., Li L., Wegley L., Furlan M., Angly F. E., Breitbart M., Buchanan J., Desnues C., Dinsdale E. A., Edwards R. A., Felts B., Haynes M., Liu H., Lipson D., Mahaffy J., Martin-Cuadrado A. B., Mira A., Nulton J., Pašić L., Rayhawk S., Rodríguez-Mueller J., Rodríguez-Valera F., Salamon P., Srinagesh S., Thingstad T. F., Tran T., Thurber R. V., Willner D., Youle M., and Rohwer F. (2010). Viral and microbial community dynamics in four aquatic environments. *The ISME Journal*, 4: 739–751.
- Rosen G. L., Polikar R., Caseiro D. A., Essinger S. D., and Sokhansanj B. A. (2011). Discovering the unknown: improving detection of novel species and genera from short reads. *Journal of Biomedicine and Biotechnology*, page 495849.
- Röske K., Sachse R., Scheerer C., and Röske I. (2012). Microbial diversity and composition of the sediment in the drinking water reservoir Säidenbach (Saxonia, Germany). *Systematic and Applied Microbiology*, 35:35–44.

- Roux S., Faubladier M., Mahul A., Paulhe N., Bernard A., Debroas D., and Enault F. (2011). Metavir: a web server dedicated to virome analysis. *Bioinformatics*, 27: 3074–3075.
- Rusch D. B., Halpern A. L., Sutton G., Heidelberg K. B., Williamson S. J., Yooseph S., Wu D., Eisen J. A., Hoffman J. M., Remington K., Beeson K. Y., Tran B., Smith H., Baden-Tillson H., Stewart C., Thorpe J., Freeman J., Andrews-Pfannkoch C., Venter J. E., Li K., Kravitz S., Heidelberg J. F., Utterback T., Rogers Y.-H., Falcón L. I., Souza V., Bonilla-Rosso G., Eguiarte L. E., Karl D. M., Sathyendranath S., Platt T., Bermingham E., Gallardo V., Tamayo-Castillo G., Ferrari M. R., Strausberg R. L., Nealson K., Friedman R., Frazier M. E., and Venter J. C. (2007). The Sorcerer II Global Ocean Sampling expedition: northwest Atlantic through eastern tropical Pacific. *PLoS Biology*, 5:77.
- Rutherford K., Parkhill J., Crook J., Horsnell T., Rice P., Rajandream M.-A., and Barrell B. G. (2000). Artemis: sequence visualization and annotation. *Bioinformatics*, 16:944–945.
- Salzberg S. L., Phillippy A. M., Zimin A., Puiu D., Magoc T., Koren S., Treangen T. J., Schatz M. C., Delcher A. L., Roberts M., Marcais G., Pop M., and Yorke J. A. (2012). GAGE: A critical evaluation of genome assemblies and assembly algorithms. *Genome Research*, 22:557–567.
- Samsudin A. A., Evans P. N., Wright A.-D. G., and Al Jassim R. (2011). Molecular diversity of the foregut bacteria community in the dromedary camel (*Camelus dromedarius*). *Environmental Microbiology*, 13:3024–3035.
- Sandaas R.-A., Heldal M., Castberg T., Thyrhaug R., and Bratbak G. (2001). Isolation and characterization of two viruses with large genome size infecting *Chrysochromulina ericina* (*Prymnesiophyceae*) and *Pyramimonas orientalis* (*Prasinophyceae*). *Virology*, 290:272–280.
- Saunders N. F. W., Ng C., Raftery M., Guilhaus M., Goodchild A., and Cavicchioli R. (2006). Proteomic and computational analysis of secreted proteins with type I signal peptides from the Antarctic archaeon *Methanococcoides burtonii*. *Journal of Proteome Research*, 5:2457–2464.
- Schäfer H., Myronova N., and Boden R. (2010). Microbial degradation of dimethyl-sulphide and related C₁-sulphur compounds: organisms and pathways controlling fluxes of sulphur in the biosphere. *Journal of Experimental Botany*, 61: 315–334.
- Schatz M. C., Langmead B., and Salzberg S. L. (2010). Cloud computing and the DNA data race. *Nature Biotechnology*, 28:691–693.
- Schiaffino M. R., Unrein F., Gasol J. M., Farias M. E., Estevez C., Balagué V., and Izaguirre I. (2009). Comparative analysis of bacterioplankton assemblages from maritime Antarctic freshwater lakes with contrasting trophic status. *Polar Biology*, 32: 923–936.
- Schmidtova J., Hallam S. J., and Baldwin S. A. (2009). Phylogenetic diversity of transition and anoxic zone bacterial communities within a near-shore anoxic basin: Nitinat Lake. *Environmental Microbiology*, 11:3233–3251.

Scholz M. B., Lo C.-C., and Chain P. S. (2012). Next generation sequencing and bioinformatic bottlenecks: the current state of metagenomic data analysis. *Current Opinion in Biotechnology*, 23:9–15.

Scott K. M., Sievert S. M., Abril F. N., Ball L. a., Barrett C. J., Blake R. a., Boller A. J., Chain P. S. G., Clark J. a., Davis C. R., Detter C., Do K. F., Dobrinski K. P., Faza B. I., Fitzpatrick K. a., Freyermuth S. K., Harmer T. L., Hauser L. J., Hugler M., Kerfeld C. a., Klotz M. G., Kong W. W., Land M., Lapidus A., Larimer F. W., Longo D. L., Lucas S., Malfatti S. a., Massey S. E., Martin D. D., McCuddin Z., Meyer F., Moore J. L., Ocampo L. H., Paul J. H., Paulsen I. T., Reep D. K., Ren Q., Ross R. L., Sato P. Y., Thomas P., Tinkham L. E., and Zeruth G. T. (2006). The genome of deep-sea vent chemolithoautotroph *Thiomicrospira crunogena* XCL-2. *PLoS Biology*, 4:e383.

Sharma A. K., Zhaxybayeva O., Papke R. T., and Doolittle W. F. (2008). Actinorhodopsins: proteorhodopsin-like gene sequences found predominantly in non-marine environments. *Environmental Microbiology*, 10:1039–1056.

Sharma A. K., Sommerfeld K., Bullerjahn G. S., Matteson A. R., Wilhelm S. W., Jezbera J., Brandt U., Doolittle W. F., and Hahn M. W. (2009). Actinorhodopsin genes discovered in diverse freshwater habitats and among cultivated freshwater *Actinobacteria*. *The ISME Journal*, 3:726–737.

Sharma V. K., Kumar N., Prakash T., and Taylor T. D. (2012). Fast and accurate taxonomic assignments of metagenomic sequences using MetaBin. *PloS One*, 7:e34030.

Siegert M. J., Ellis-Evans J. C., Tranter M., Mayer C., Petit J.-R., Salamatian A., and Priscu J. C. (2001). Physical, chemical and biological processes in Lake Vostok and other Antarctic subglacial lakes. *Nature*, 414:603–609.

Sievert S. M., Scott K. M., Klotz M. G., Chain P. S., Hauser L. J., Hemp J., Hugler M., Land M., Lapidus A., Larimer F. W., Lucas S., Malfatti S. A., Meyer F., Paulsen I. T., Ren Q., and Simon J. (2008). Genome of the epsilonproteobacterial chemolithoautotroph *Sulfurimonas denitrificans*. *Applied and Environmental Microbiology*, 74:1145–1156.

Sowell S. M., Wilhelm L. J., Norbeck A. D., Lipton M. S., Nicora C. D., Barofsky D. F., Carlson C. A., Smith R. D., and Giovanonni S. J. (2009). Transport functions dominate the SAR11 metaproteome at low-nutrient extremes in the Sargasso Sea. *The ISME Journal*, 3:93–105.

Su X., Xu J., and Ning K. (2012). Parallel-META: efficient metagenomic data analysis based on high-performance computation. *BMC Systems Biology*, 6:S16.

Sun S., Chen J., Li W., Altintas I., Lin A., Peltier S., Stocks K., Allen E. E., Ellisman M., Grethe J., and Wooley J. (2011). Community cyberinfrastructure for Advanced Microbial Ecology Research and Analysis: the CAMERA resource. *Nucleic Acids Research*, 39:D546–551.

Suttle C. A. (2005). Viruses in the sea. *Nature*, 437:356–361.

Suttle C. A., Chan A. M., and Cottrell M. T. (1990). Infection of phytoplankton by viruses and reduction of primary productivity. *Nature*, 347:467–469.

Tajima K., Aminov R. I., Nagamine T., Ogata K., Nakamura M., Matsui H., and Benno Y. (1999). Rumen bacterial diversity as determined by sequence analysis of 16S rDNA libraries. *FEMS Microbiology Ecology*, 29:159–169.

- Tamura K., Peterson D., Peterson N., Stecher G., Nei M., and Kumar S. (2011). MEGA5: molecular evolutionary genetics analysis using maximum likelihood, evolutionary distance, and maximum parsimony methods. *Molecular Biology and Evolution*, 28:2731–2739.
- Tang Y.-Q., Ji P., Hayashi J., Koike Y., Wu X.-L., and Kida K. (2011). Characteristic microbial community of a dry thermophilic methanogenic digester: its long-term stability and change with feeding. *Applied Microbiology and Biotechnology*, 91:1447–1461.
- Tatusov R. L., Koonin E. V., and Lipman D. J. (1997). A genomic perspective on protein families. *Science*, 278:631–637.
- Tatusov R. L., Fedorova N. D., Jackson J. D., Jacobs A. R., Kiryutin B., Koonin E. V., Krylov D. M., Mazumder R., Mekhedov S. L., Nikolskaya A. N., Rao B. S., Smirnov S., Sverdlov A. V., Vasudevan S., Wolf Y. I., Yin J. J., and Natale D. A. (2003). The COG database: an updated version includes eukaryotes. *BMC Bioinformatics*, 4:41.
- Teeling H. and Glöckner F. O. (2012). Current opportunities and challenges in microbial metagenome analysis - a bioinformatic perspective. *Briefings in Bioinformatics*, 13 (6):728–742.
- Teeling H., Waldmann J., Lombardot T., Bauer M., and Glöckner F. O. (2004). TETRA: a web-service and a stand-alone program for the analysis and comparison of tetranucleotide usage patterns in DNA sequences. *BMC Bioinformatics*, 5: 163.
- Teeling H., Fuchs B. M., Becher D., Klockow C., Gardebrecht A., Bennke C. M., Kassabgy M., Huang S., Mann A. J., Waldmann J., Weber M., Klindworth A., Otto A., Lange J., Bernhardt J., Reinsch C., Hecker M., Peplies J., Bockelmann F. D., Callies U., Gerdts G., Wichels A., Wiltshire K. H., Glöckner F. O., Schweder T., and Amann R. (2012). Substrate-controlled succession of marine bacterioplankton populations induced by a phytoplankton bloom. *Science*, 336:608–611.
- Thakur R. S., Bandopadhyay R., Chaudhary B., and Chatterjee S. (2012). Now and next-generation sequencing techniques: future of sequence analysis using cloud computing. *Frontiers in Genetics*, 3:280.
- Thomsen H. A. (2007). Ultrastructural studies of the flagellate and cyst stages of *Pseudopedinella tricostata* (*Pedinellales*, *Chrysophyceae*). *British Phycological Journal*, pages 37–41.
- Todd J. D., Rogers R., Li Y. G., Wexler M., Bond P. L., Sun L., Curson A. R., Malin G., Steinke M., and Johnston A. W. (2007). Structural and regulatory genes required to make the gas dimethyl sulfide in bacteria. *Science*, 315:666–669.
- Todd J. D., Curson A. R., Dupont C. L., Nicholson P., and Johnston A. W. (2009). The *dddP* gene, encoding a novel enzyme that converts dimethylsulfoniopropionate into dimethyl sulfide, is widespread in ocean metagenomes and marine bacteria and also occurs in some Ascomycete fungi. *Environmental Microbiology*, 11:1376–1385.
- Todd J. D., Curson A. R., Nikolaidou-Katsaraidou N., Brearley C. A., Watmough N. J., Chan Y., Page P. C., Sun L., and Johnston A. W. (2010). Molecular dissection of bacterial acrylate catabolism - unexpected links with dimethylsulfoniopropionate catabolism and dimethyl sulfide production. *Environmental Microbiology*, 12:327–343.

- Todd J. D., Curson A. R., Kirkwood M., Sullivan M. J., Green R. T., and Johnston A. W. (2011). DddQ, a novel, cupin-containing, dimethylsulfoniopropionate lyase in marine roseobacters and in uncultured marine bacteria. *Environmental Microbiology*, 13:427–438.
- Todd J. D., Kirkwood M., Newton-Payne S., and Johnston A. W. (2012). DddW, a third DMSP lyase in a model *Roseobacter* marine bacterium, *Ruegeria pomeroyi* DSS-3. *The ISME Journal*, 6:223–226.
- Torrice M. Viral ecology hit by filter shortage, 2009. URL <http://news.sciencemag.org/scienceinsider/2009/10/viral-ecology-r.html>.
- Tyson G. W., Chapman J., Hugenholtz P., Allen E. E., Ram R. J., Richardson P. M., Solovyev V. V., Rubin E. M., Rokhsar D. S., and Banfield J. F. (2004). Community structure and metabolism through reconstruction of microbial genomes from the environment. *Nature*, 428:37–43.
- Unrein F., Izaguirre I., Massana R., Balagué V., and Gasol J. M. (2005). Nanoplankton assemblages in maritime Antarctic lakes: characterisation and molecular fingerprinting comparison. *Aquatic Microbial Ecology*, 40:269–282.
- Hoff J. van den and Franzmann P. D. (1986). A choanoflagellate in a hypersaline Antarctic lake. *Polar Biology*, 6:71–73.
- Van Etten J. L., Lane L. C., and Meints R. H. (1991). Viruses and viruslike particles of eukaryotic algae. *Microbiological Reviews*, 55(4):586–620.
- Venter J. C., Remington K., Heidelberg J. F., Halpern A. L., Rusch D. B., Eisen J. A., Wu D., Paulsen I., Nelson K. E., Nelson W., Fouts D. E., Levy S., Knap A. H., Lomas M. W., Nealson K., White O., Peterson J., Hoffman J. M., Parsons R., Baden-Tillson H., Pfannkoch C., Rogers Y.-H., and Smith H. O. (2004). Environmental genome shotgun sequencing of the Sargasso Sea. *Science*, 304:66–74.
- Villaescusa J. A., Casamayor E. O., Rochera C., Velázquez D., Álvaro C., Quesada A., and Camacho A. (2010). A close link between bacterial community composition and environmental heterogeneity in maritime Antarctic lakes. *International Microbiology*, 13:67–77.
- Volterra V. (1926). Variazioni e fluttuazioni del numero d'individui in specie animali conviventi. *Mem. R. Accad. Naz. dei Lincei*, 2:31–113.
- Mering C. von, Hugenholtz P., Raes J., Tringe S. G., Doerks T., Jensen L., Ward N., and Bork P. (2007). Quantitative phylogenetic assessment of microbial communities in diverse environments. *Science*, 315:1126–1130.
- Voytek M. A., Priscu J. C., and Ward B. B. (1999). The distribution and relative abundance of ammonia-oxidizing bacteria in lakes of the McMurdo Dry Valley, Antarctica. *Hydrobiologia*, 401:113–130.
- Wagner-Döbler I. and Biebl H. (2006). Environmental biology of the marine *Roseobacter* lineage. *Annual Review of Microbiology*, 60:255–280.
- Wang Q., Garrity G. M., Tiedje J. M., and Cole J. R. (2007). Naïve Bayesian classifier for rapid assignment of rRNA sequences into the new bacterial taxonomy. *Applied and Environmental Microbiology*, 73:5261–5267.

- Ward B. B. and Priscu J. C. (1997). Detection and characterization of denitrifying bacteria from a permanently ice-covered Antarctic lake. *Hydrobiologia*, pages 57–68.
- Ward B. B., Granger J., Maldonado M., Casciotti K., Harris S., and Wells M. (2005). Denitrification in the hypolimnion of permanently ice-covered Lake Bonney, Antarctica. *Aquatic Microbial Ecology*, 38:295–307.
- Warnecke F. and Hugenholtz P. (2007). Building on basic metagenomics with complementary technologies. *Genome Biology*, 8:231.
- Wen K., Ortmann A. C., and Suttle C. A. (2004). Accurate estimation of viral abundance by epifluorescence microscopy. *Applied and Environmental Microbiology*, 70: 3862–3867.
- Wilkening J., Wilke A., Desai N., and Meyer F. (2009). Using clouds for metagenomics: a case study. *IEEE International Conference*, pages 1–6.
- Wilkins D., Lauro F. M., Williams T. J., DeMaere M. Z., Brown M. V., Hoffman J. M., Andrews-Pfannkoch C., Mcquaid J. B., Riddle M. J., Rintoul S. R., and Cavicchioli R. (2012). Biogeographic partitioning of Southern Ocean microorganisms revealed by metagenomics. *Environmental Microbiology*, page (in press).
- Williams T. J., Wilkins D., Long E., Evans F., DeMaere M. Z., Raftery M. J., and Cavicchioli R. (2012). The role of planktonic Flavobacteria in processing algal organic matter in coastal East Antarctica revealed using metagenomics and metaproteomics. *Environmental Microbiology*, page (in press).
- Wilson W. H., Tarhan G. A., Schroeder D., Cox M., Oke J., and Malin G. (2002). Isolation of viruses responsible for the demise of an *Emiliania huxleyi* bloom in the English Channel. *Journal of the Marine Biological Association of the United Kingdom*, 82:369–377.
- Wommack K. E., Bhavsar J., Polson S. W., Chen J., Dumas M., Srinivasiah S., Furman M., Jamindar S., and Nasko D. J. (2012). VIROME: a standard operating procedure for analysis of viral metagenome sequences. *Standards in Genomic Sciences*, 6:427–439.
- Wu S., Zhu Z., Fu L., Niu B., and Li W. (2011). WebMGA: a customizable web server for fast metagenomic sequence analysis. *BMC Genomics*, 12:444.
- Wu Y.-W. and Ye Y. (2011). A novel abundance-based algorithm for binning metagenomic sequences using l-tuples. *Journal of Computational Biology*, 18:523–534.
- Xie C., Mao X., Huang J., Ding Y., Wu J., Dong S., Kong L., Gao G., Li C., and Wei L. (2011). KOBAS 2.0: a web server for the annotation and identification of enriched pathways and diseases. *Nucleic Acids Research*, 39:W316–322.
- Xing P., Hahn M. W., and Wu Q. L. (2009). Low taxon richness of bacterioplankton in high-altitude lakes of the Eastern Tibetan Plateau, with a predominance of *Bacteroidetes* and *Synechococcus* spp. *Applied and Environmental Microbiology*, 75:7017–7025.
- Yamamoto M. and Takai K. (2011). Sulfur metabolisms in epsilon- and gamma-*Proteobacteria* in deep-sea hydrothermal fields. *Frontiers in Microbiology*, 2: 1–8.

- Yamane K., Hattori Y., Ohtagaki H., and Fujiwara K. (2011). Microbial diversity with dominance of 16S rRNA gene sequences with high GC contents at 74 and 98 °C subsurface crude oil deposits in Japan. *FEMS Microbiology Ecology*, 76:220–235.
- Yanagibayashi M., Nogi Y., Li L., and Kato C. (1999). Changes in the microbial community in Japan Trench sediment from a depth of 6292 m during cultivation without decompression. *FEMS Microbiology Letters*, 170:271–279.
- Yau S., Lauro F. M., DeMaere M. Z., Brown M. V., Thomas T., Raftery M. J., Andrews-Pfannkoch C., Lewis M., Hoffman J. M., Gibson J. A., and Cavicchioli R. (2011). Virophage control of antarctic algal hostvirus dynamics. *Proceedings of the National Academy of Sciences USA*, 108:6163–6168.
- Yilmaz P., Iversen M. H., Hankeln W., Kottmann R., Quast C., and Glöckner F. O. (2012). Ecological structuring of bacterial and archaeal taxa in surface ocean waters. *FEMS Microbiology Ecology*, 81:373–385.
- Yilmaz S., Allgaier M., and Hugenholtz P. (2010). Multiple displacement amplification compromises quantitative analysis of metagenomes. *Nature Methods*, 7:943–944.
- Zwart D., Bird M., Stone J., and Lambeck K. (1998). Holocene sea-level change and ice-sheet history in the Vestfold Hills, East Antarctica. *Earth and Planetary Science Letters*, 155:131–145.
- Zybailov B., Mosley A. L., Sardiu M. E., Coleman M. K., Florens L., and Washburn M. P. (2006). Statistical analysis of membrane proteome expression changes in *Saccharomyces cerevisiae* research articles. *Journal of Proteome Research*, 5: 2339–2347.

Appendix A

PCR-based studies of Antarctic Lakes

Table A.1: Studies of Antarctic Lakes that have made use of PCR amplification and sequencing of marker genes. The list presented here has attempted to be comprehensive but some studies some may have been inadvertently missed. DV, McMurdo Dry Valleys; VH, Vestfold Hills; Syo, Syowa Oasis; SI, Signy Island; AP, Antarctic Peninsula; KGI, King George Island; LI, Livingston Island; CFB, *Cytophaga*, *Flavobacteria*, *Bacteroidetes* group; *Alpha-*, *Alphaproteobacteria*; *Beta-*, *Betaproteobacteria*; *Gamma-*, *Gammaproteobacteria*; *Delta-*, *Deltaproteobacteria*; *Epsilon-*, *Epsilonproteobacteria*; *Actino-*, *Actinobacteria*; *Cyano-*, *Cyanobacteria*; SRB, sulphate-reducing bacteria; FISH, fluorescence *in situ* hybridisation; FAME, fatty-acid methyl ester.

Site	Environment	Techniques	Organisms	Key processes	Notes	Reference
Lakes Bonney, Hoare, Joyce, Vanda, DV	Fresh to hypersaline, permanently ice-covered	16S, <i>amoA</i> libraries	<i>Beta-</i> , <i>Gamma-</i>	Ammonia	Nitrifying bacterial <i>amoA</i> detected in all lakes. In meromictic lakes, the population of <i>Beta</i> and <i>Gamma</i> - vertically stratified. Majority of nitrifying bacteria were <i>Beta</i> -.	(Voytek <i>et al.</i> , 1999)
Lake Bonney, DV	Hypersaline, meromictic, permanently ice-covered, separated into east and west lobes	<i>nifH</i> library of ice aggregate material and microbial mats, nitrogenase assay	<i>Cyano-</i> , <i>Gamma-</i> , <i>Alpha-</i> , <i>Delta-</i>	N ₂ fixation	Nitrogenase activity low compared to temperate environments. Heterotrophs responsible for 10–30% of nitrogenase activity. Heterotrophs likely microaerophilic.	(Olson <i>et al.</i> , 1998)
Lake Bonney, cyanobacterial mats, DV	Hypersaline, meromictic, permanently ice-covered, separated into east and west lobes	16S library of ice sediments, hybridisation of probes	<i>Cyano-</i> , <i>Acidobacterium/Holophaga</i> , green non-sulphur bacteria	Phototrophy and heterotrophy	Probes designed from 16S clone library of bacteria in the sediment in the ice matched that of the surrounding mats.	(Gordon <i>et al.</i> , 2000)
Lake Bonney, DV	Hypersaline, meromictic, permanently ice-covered, separated into east and west lobes	18S libraries of watercolumn	<i>Cryptophyta</i> , <i>Chlorophyta</i> , <i>Stramenopiles</i> , <i>Haptophyta</i> , <i>Choanoflagellida</i> , <i>Alveolata</i> , fungi, ciliates	Photosynthesis	Population vertically stratified. Cryptophytes dominant in the shallow water and haptophytes in the mid-depths and chlorophytes in the deeper waters. Stramenopiles replaced haptophytes during polar night.	(Bielewicz <i>et al.</i> , 2011)

Continued on next page

Table A.1 – *Continued from previous page*

Site	Environment	Techniques	Organisms	Key processes	Notes	Reference
Ekho, Organic, Deep Lakes, VH	Hypersaline. Ekho and Organic: meromictic and ice-covered ~9 months of the year. Deep: holomictic, never freezes.	16S libraries of sediment	Organic: <i>Cyano-/chloroplasts, CFB, Gamma-, Alpha-, Halobacteriales, Actino-.</i> Ekho: <i>Cyano-/chloroplasts, CFB, Firmicutes, Alpha-, Gamma-, Verrucomicrobiales, Spirochaetales.</i> Deep: <i>Halobacteriales, Gamma-</i>	Heterotrophy	No phylotypes common to all samples. Distribution of bacterial classes similar between Ekho and Organic with <i>Roseovarius</i> common to both. <i>Marinobacter</i> and <i>Halomonas</i> common to Organic and Deep.	(Bowman <i>et al.</i> , 2000a)
Lake Vida, DV	Hypersaline, meromictic, permanently ice-covered	16S, 18S DGGE, 16S library of ice core	16S: <i>Actino-, CFB, Gamma-, Cyano-, OD1, TM7, Firmicutes, Planctomycetales.</i> 18S: <i>Chlorophyta, fungi, Bacillariophyta, Apicomplexa, Cercozoa, Chrysophyceae, Ciliophora</i>	Phototrophy, heterotrophy	Cell density highest at the surface. Phylogeny shows <i>Marinobacter</i> related to Lake Bonney isolate and bacterial sequences are similar to marine and polar organisms.	(Mosier <i>et al.</i> , 2007)
Suribati-Ike, Syo	Hypersaline, meromictic, sulphidic anoxic bottom waters.	16S libraries of halocline	<i>Marinobacter, Halomonas, Pseudomonas, Halocella</i>	Heterotrophy	<i>Marinobacter</i> isolates capable of DMSO-respiration were relatives of those detected in lake water. Bacteria from the water column unable to respire nitrate.	(Matsuzaki <i>et al.</i> , 2006)

Continued on next page

Table A.1 – *Continued from previous page*

Site	Environment	Techniques	Organisms	Key processes	Notes	Reference
Clear, Pendant, Scale, Ace, Burton Lakes, Tay-naya Bay, VH	Saline, meromictic lakes, high levels of sulphides (120–>250 mmol kg ⁻¹)	16S libraries of anoxic sediment	Bacteria: <i>Firmicutes</i> , <i>Cyanobacteria</i> /chloroplasts, CFB, <i>Delta-</i> , <i>Alpha-</i> , <i>Planctomycetes</i> , <i>Gamma-</i> , green non-sulphur bacteria, <i>Chlamydiales</i> , <i>Verrucomicrobia</i> , <i>Actinobacteria</i> . Eucarya: 2.5% of clones. Archaea: <i>Methanosaerina barkerii</i> , unknown <i>Euryarchaeota</i> group equidistant from <i>Thermoplasma</i> , <i>Methanomicrobiales</i> , <i>Halobacteriales</i>	Sulphate reduction, methanogenesis, phototrophy, aerobic heterotrophy	Lakes with similar physico-chemical and limnological traits had more similar microbial communities.	(Bowman <i>et al.</i> , 2000b)
Lake Fryxell, DV	Brackish, meromictic, permanently ice-covered	<i>pufM</i> libraries, DGGE, RT-PCR of <i>pufM</i> transcripts	<i>Alpha-, Beta-</i> related to purple non-sulphur bacteria and aerobic anoxygenic phototrophs	Anoxygenic photosynthesis	Vertical stratification of the community down the water column. Purple and green sulphur bacteria not detected despite the high sulphide. <i>pufM</i> transcripts only found below 9 m even though <i>pufM</i> genes found throughout the water column.	(Karr <i>et al.</i> , 2003)
Lake Fryxell, DV	Brackish, meromictic, permanently ice-covered	16S DGGE of water column	<i>Methanoculleus</i> , <i>Methanosaerina</i> , unclassified <i>Euryarchaeota</i> , <i>Methanosaericinales</i> -group and marine benthic group C-like <i>Crenarchaeota</i>	Hydrogenotrophic methanogenesis, potential anoxic methanotrophy	Diverse population of methanogenic <i>Euryarchaeota</i> , unclassified <i>Euryarchaeota</i> and divergent <i>Crenarchaeota</i> detected in sediments and water column.	(Karr <i>et al.</i> , 2006)

Continued on next page

Table A.1 – *Continued from previous page*

Site	Environment	Techniques	Organisms	Key processes	Notes	Reference
Nurume-Ike, Syo	Saline, meromictic	16S library of anoxic sediment	Archaea: marine benthic group and unclassified <i>Euryarchaeota</i> . Bacteria: <i>Alpha-</i> , <i>Delta-</i> , <i>Planctomycetes</i> , <i>Cyano-</i> /chloroplast, <i>Gamma-</i> , <i>Actino-</i> , CFB, <i>Verrucomicrobia</i> and <i>Spirochaetes</i>	Heterotrophy	Distribution of bacterial classes similar to lake sediment in VH except <i>Alpha</i> -relatively overrepresented and <i>Firmicutes</i> underrepresented.	(Kurosawa <i>et al.</i> , 2010)

Continued on next page

Table A.1 – *Continued from previous page*

Site	Environment	Techniques	Organisms	Key processes	Notes	Reference
Heywood Lake, Shallow Bay, SI	Heywood: ice covered for ~9 months of the year, eutrophic due to organic inputs from seals, separated into two basins by shallow inlet. Shallow: coastal marine, ice covered during winter	Archaeal 16S, universal 16S libraries of anoxic sediment. Northern blots with methanogenic archaeal probes	Heywood blots: <i>Methanomicrobiales</i> , <i>Methanogenium</i> , <i>Methanosarcinales</i> , <i>Methanosaeta</i> . Shallow blots: <i>Methanosarcinales</i> , <i>Methanomicrobiales</i> , <i>Methanococcales</i> . Heywood Archaea: <i>Methanosaeta</i> , <i>Methanogenium</i> . Shallow Archaea: <i>Methanogenium</i> , <i>Methanolobus</i> , <i>Methanococcales</i> . Heywood SRB: <i>Desulfovibrio</i> , <i>Desulfotalea</i> / <i>Desulforhopalus</i> , <i>Desulfobulbus</i> , <i>Desulfobacteriaceae</i> . Shallow Bay SRB: <i>Desulfotalea</i> / <i>Desulforhopalus</i> , <i>Desulfobacterium</i> , <i>Desulfobulbus</i> , <i>Desulfobacteriaceae</i>	Acetoclastic and hydrogenotrophic methanogenesis, sulphur and metal oxidation, sulphate reduction	Methanogenesis and sulphate reduction detected at both sites. Diversity of methanogenic <i>Archaea</i> extremely low. Methanogenic archaea 34% and 0.2% of community in Heywood Lake and Shallow Bay respectively. SRB 0.9% and 14.7% of community in Heywood Lake and Shallow Bay respectively.	(Purdy <i>et al.</i> , 2003)

Continued on next page

Table A.1 – *Continued from previous page*

Site	Environment	Techniques	Organisms	Key processes	Notes	Reference
Sombre Lake, SI	Freshwater, ice-covered for ~9 months of the year, oligotrophic, N and P limited	16S libraries, DGGE, 16S libraries, FAME analysis of isolates, FISH of water column profile	16S of isolates: <i>Beta-, Firmicutes, Actinobacteria, Alph-, Gamma-</i> . FAME: <i>Firmicutes, Actino-, Gamma-, Beta-, Alpha-</i> . Clones: <i>Actino-, CFB, Beta-, Alpha-, Spirochaetales, Delta-, Gamma-, Verrucomicrobia.</i> FISH: <i>Beta-, CFB, Alpha-, Gamma-</i> . DGGE: <i>Actinobacteria, CFB, Beta-</i>	Heterotrophic mainly respiratory metabolism	Relative abundances shown by clone libraries and FISH the same. Few genera common to culture-dependent and independent techniques. 16S isolate library and 16S clone library were significantly different. 16S clone library covers the largest spread of phyla but is missing <i>Firmicutes</i> . Overall <i>Beta-</i> .	(Pearce, 2003)
Moss Lake, SI	Freshwater, ice-covered for ~9 months of the year, oligotrophic, N and P limited	16S DGGE and FISH of water column	<i>Beta-, CFB, Alpha-, Gamma-, Actino-, Cyano-</i> . <1% of cells hybridised with archaeal FISH probe	Heterotrophy, mainly respiratory metabolism	Very little vertical stratification of population. 16S sequences similar to temperate and cold aquatic systems.	(Pearce <i>et al.</i> , 2003)
Moss, Sombre, Heywood Lakes, SI	Freshwater, ice-covered for ~9 months of the year, oligotrophic to eutrophic status	16S DGGE of water column profile over the winter to summer transition	Not determined	Not determined	Lakes were physically and chemically stratified in winter, mixed in summer. Variation in bacterial community structure correlated with lake chemistry. Bacterial community still unstable during holomixis.	(Pearce, 2005)

Continued on next page

Table A.1 – *Continued from previous page*

Site	Environment	Techniques	Organisms	Key processes	Notes	Reference
Heywood Lake, SI	Freshwater, ice-covered for ~9 months of the year, eutrophic due to organic inputs from seals, separated into two basins by shallow inlet.	16S libraries, DGGE, 16S libraries, FAME analysis of isolates, FISH of water column profile	16S clones: <i>Beta</i> -, <i>Alpha</i> -, <i>Actino</i> -. FAME: <i>Actino</i> -, <i>Firmicutes</i> , <i>Gamma</i> -, <i>Alpha</i> -. FISH: <i>Beta</i> -, CFB, <i>Gamma</i> -, <i>Alpha</i> -. DGGE: <i>Actino</i> -, CFB, Gram-positives, <i>Beta</i> -.	Heterotrophy, mainly respiratory metabolisms, phototrophy	Clone library coverage 71.7%. Similar genera to Moss and Sombre Lakes. <i>Actino</i> - and marine <i>Alpha</i> - enriched compared to oligotrophic lakes while <i>Cyano</i> - underrepresented. Species evenness is higher than Sombre or Moss Lakes.	(Pearce <i>et al.</i> , 2005)
Lakes Boeckella, Esperanza, Flora, Encantado, Chico, Pingüi, Hope Bay, AP. Lakes L, M, W, Z, KGI	Freshwater, oligotrophic except Pingüi and Boeckella which were eutrophic and mesotrophic respectively	18S DGGE of surface water (20–3 µm)	<i>Chrysophyta</i> , <i>Chlorophyta</i> , <i>Dictyochophyceae</i> , <i>Bacillariophyceae</i> , <i>Cercozoa</i>	Photosynthesis	Molecular surveys showed a greater level of diversity exists than can be determined by light microscopy. Lake communities varied depending on trophic status. Lakes in both regions shared bands belonging to <i>Chrysophyta</i> although they were 220 km apart. <i>Dictyochophyceae</i> and <i>Cercozoa</i> restricted to oligotrophic lakes.	(Unrein <i>et al.</i> , 2005)
Lakes Boeckella, Esperanza, Flora, Encantado, Chico, Pingüi, Hope Bay, AP. Lakes W and Z, KGI.	Freshwater, oligotrophic except Pingüi and Boeckella which were eutrophic and mesotrophic respectively.	16S DGGE of surface water (20–3 µm)	CFB, <i>Actino</i> -, <i>Beta</i> -, <i>Cyano</i> -	Heterotrophy, photosynthesis	Cluster analysis showed Lake communities from the Hope Bay formed one group while Lakes Chico, Pingüi and Boeckella formed another subgroup with KGI lakes. 63.7% of variance is explained by axis 1 and 2 of Canonical Correspondence Analysis (40.4% phosphate, dissolved inorganic nitrogen and pH; 23.3% dissolved inorganic nitrogen). Temporal variation is not as pronounced as differences due to trophic status.	(Schiaffino <i>et al.</i> , 2009)

Continued on next page

Table A.1 – *Continued from previous page*

Site	Environment	Techniques	Organisms	Key processes	Notes	Reference
Lakes Limnopolar, Midge, Chester, Chica, Turbio, Somero, Refugio, LI	Fresh to saline, all oligotrophic except for Refugio, which was eutrophic	16S DGGE of from surface water	CFB, <i>Alpha-</i>	Heterotrophy, phototrophy	Cluster analysis showed deep lakes of the plateau grouped together while Somero and Refugio were separate groups. Over 90% of variance was explained by chemical parameters related to trophic status and salinity.	(Villaescusa <i>et al.</i> , 2010)
Lake Vostok	Largest subglacial lake, isolated from surface 420,000 years	16S library of accretion ice core from 3,590 m	<i>Alpha-, Beta-, Actinomycetes</i>	Potential heterotrophy	No <i>Archaea</i> were amplified with archaeal primers. No biological incorporation of selected substrates	(Priscu, 1999)
Lake Vostok	Largest subglacial lake, isolated from surface 420,000 years	16S library of accretion ice core from 3,590 and 3,603 m and isolation of bacteria	<i>Alpha-, Beta-, Firmicutes, Actino-, CFB</i>	Potential heterotrophy	Bacteria appear related to isolates from similarly cold environments. No <i>Archaea</i> were amplified using archaeal primers.	(Christner <i>et al.</i> , 2001)
Lake Vostok	Largest subglacial lake, isolated from surface 420,000 years	16S, <i>cbbL/rbcL</i> and <i>hoxV-hupL</i> library of accretion ice core from 3,561 m	<i>Hydrogenophilus thermoluteolus</i>	Potential hydrogenotrophy	Thermophilic chemolithoautotrophic <i>Hydrogenophilus thermoluteolus</i> 16S rRNA, RuBisCO and NiFe-hydrogenase genes detected.	(Lavire <i>et al.</i> , 2006)
Lake Vostok	Largest subglacial lake, isolated from surface 420,000 years	16S library of Vostok drilling fluid recovered from 4 depths of the bore hole	<i>Sphingomonas</i> , potential contaminants related to human/animal pathogens or saprophytes and environmental contaminants	Hydrocarbon degrading heterotrophs	New contaminant bacteria identified that were associated with hydrocarbon-based drilling fluid.	(Alekhanina <i>et al.</i> , 2007)

Appendix B

Proteins identified in Ace Lake metaproteomic analysis

Table B.1: Proteins identified in the Ace Lake 5 m sample 0.1 µm size-fraction metaproteome. (*) Protein group identification: proteins that contain similar peptides that could not be differentiated by the mass spectral analysis were grouped. Only one gene number of that group is displayed. (*a–z, aa–pp*) Protein ambiguity groups: proteins that have some shared peptides with one or more other proteins from the same sample depth are marked with the same letters.

Gene ID	NSA	COG/NR ID	KO	Locus	5 m – COG annotated proteins
					COG : KEGG/NR description
167852195 <i>f</i>	0.02530	COG1653	K10232	AAur_0459	sugar-binding periplasmic proteins/domains : putative alpha-glucosides-binding ABC transporter (AglE)
167782381*	0.01724	COG1879	K02058	Ping_2790	periplasmic sugar-binding proteins : bifunctional carbohydrate binding and transport protein
167813321	0.01388	COG1629		GFO_2756	outer membrane receptor proteins, mostly Fe transport : TonB-dependent outer membrane receptor
167754347	0.01044	COG1879	K02058	CMM_0792	periplasmic sugar-binding proteins : putative sugar ABC transporter, solute-binding protein
167701754 <i>a</i>	0.00967	COG0834	K09969	SAR11_0953	ABC-type amino acid transport system, periplasmic component : yhdW
167792775	0.00630	COG1879	K10552	SMc02171	periplasmic sugar-binding proteins : fructose transport system substrate-binding protein
167932252 <i>d</i>	0.00537	COG0715	K02051	SAR11_0807	ABC-type nitrate/sulfonate/taurine/bicarbonate transport systems, periplasmic components
167759671	0.00493	COG0605		NEMVE_v1g231554	superoxide dismutase
167751919 <i>h</i>	0.00468	COG3740		ROP_69760	phage head maturation protease
167907426	0.00438	COG1638		SAR11_0266	dicarboxylate-binding periplasmic protein : TRAP dicarboxylate transporter - DctP subunit (mannitol/chloroaromatic compounds)
167711086	0.00425	COG0834	K02030	TM1040_0294	ABC-type amino acid transport system, periplasmic component : lysine-arginine-ornithine-binding periplasmic protein
167819184	0.00389	COG2113	K02002	SAR11_1302	ABC-type proline/glycine betaine transport systems, periplasmic components : opuAC
167680030	0.00346	COG0683	K01999	AAur_1271	ABC-type branched-chain amino acid transport systems, periplasmic component : braC
167865828 <i>b</i>	0.00338	COG0834	K09969	HCH_05807	ABC-type amino acid transport system, periplasmic component
167684228 <i>c</i>	0.00331	COG0459	K04077	SAR11_0162	chaperonin GroEL (HSP60 family)
167868594 <i>d</i>	0.00311	COG0715	K02051	SAR11_0807	ABC-type nitrate/sulfonate/taurine/bicarbonate transport systems, periplasmic components
167785199 <i>c</i>	0.00309	COG0459	K04077	CHU_1828	chaperonin GroEL (HSP60 family)
167819050	0.00304	COG2113	K02001	Plav_1066	ABC-type proline/glycine betaine transport systems, periplasmic components
167867034	0.00284	COG0687	K02055	SAR11_1336	spermidine/putrescine-binding periplasmic protein : potD;
167700934	0.00277	COG0450		SPO3383	peroxiredoxin : thiol-specific antioxidant protein
167816084 <i>a</i>	0.00253	COG0834	K09969	SAR11_0953	ABC-type amino acid transport system, periplasmic component : yhdW
167714114	0.00179	COG0687	K02055	SAR11_1336	spermidine/putrescine-binding periplasmic protein : potD
167712994 <i>b</i>	0.00175	COG0834	K09969	HCH_05807	ABC-type amino acid transport system, periplasmic component
167824568	0.00164	COG3181		Dshi_2450	uncharacterized BCR : hypothetical protein

Continued on next page

Table B.1 – *Continued from previous page*

Gene ID	NSA	COG/NR ID	KO	Locus	COG : KEGG/NR description
167925495	0.00159	COG1653	K02027	Krad_1380	sugar-binding periplasmic proteins/domains
167695410a	0.00155	COG0834	K09969	SAR11_0953	ABC-type amino acid transport system, periplasmic component : yhdW
167695984*	0.00138	COG1879			periplasmic sugar-binding proteins
167703404	0.00134	COG1012	K00128	AAur_pTC20196	NAD-dependent aldehyde dehydrogenases
167718230	0.00125	COG0683	K01999	AAur_1271	ABC-type branched-chain amino acid transport systems, periplasmic component : braC
167735996	0.00103	COG0591		SAR11_0316	Na+/proline, Na+/panthothenate symporters and related permeases : yjcG
167739054	0.00101	COG1028	K00059	SH0230	dehydrogenases with different specificities (related to short-chain alcohol dehydrogenases) : 3-oxoacyl-[acyl-carrier protein] reductase
167701096	0.00100	COG0776		KRH_03630	bacterial nucleoid DNA-binding protein : HU_IHF family transcriptional regulator
167817334	0.00098	COG0715		FRAAL1422	ABC-type nitrate/sulfonate/taurine/bicarbonate transport systems, periplasmic components
167703266c	0.00095	COG0459	K04077	Noca_3982	chaperonin GroEL (HSP60 family)
167768609	0.00095	COG3181		RD1_2202	uncharacterized BCR
167868532	0.00093	COG3181	K07795	HCH_01639	uncharacterized BCR : putative tricarboxylic transport membrane protein
167865516	0.00088	COG0747		CMM_2185	ABC-type dipeptide/oligopeptide/nickel transport systems, periplasmic components
167911715	0.00083	COG0776	K03530	Sala_0799	bacterial nucleoid DNA-binding protein : DNA-binding protein HU-beta
167736316	0.00082	COG0174	K01915	SAR11_0747	glutamine synthase : glnA
167916441	0.00079	COG1629		BF2044	outer membrane receptor proteins, mostly Fe transport : putative TonB-dependent outer membrane receptor protein
167920571	0.00078	COG0776	K03530	SAR11_0817	bacterial nucleoid DNA-binding protein : hupA
167703332	0.00066	COG1732	K05845	Strop_1633	periplasmic glycine betaine/choline-binding (lipo)protein of an ABC-type transport system (osmoprotectant binding protein)
167662373	0.00063	COG0834		Pden_1025	ABC-type amino acid transport system, periplasmic component : extracellular solute-binding protein, family 3
167890974	0.00062	COG1878		nfa12380	uncharacterized ACR, predicted metal-dependent hydrolases
167824660	0.00061	COG0683	K01999	SAR11_1361	ABC-type branched-chain amino acid transport systems, periplasmic component : livJ2; Leu/Ile/Val-binding protein precursor
167886240	0.00061	COG0335	K02884	CHU_0120	rplS; 50S ribosomal protein L19
167921445	0.00058	COG0811		GFO_0088	biopolymer transport proteins : exbB; ExbB-like MotA/TolQ/ExbB family
167776275ee	0.00055	COG3740	K06904	BL0376	phage head maturation protease
167659892*ee	0.00055	COG3740		ROP_69760	phage head maturation protease
167786475	0.00054	COG0098	K02988	Fjoh_0380	rpsE; 30S ribosomal protein S5
167693676*	0.00054	COG0776		Arth_3916	bacterial nucleoid DNA-binding protein
167818330	0.00048	COG0683		Rxyl_0363	ABC-type branched-chain amino acid transport systems, periplasmic component : extracellular ligand-binding receptor

Continued on next page

Table B.1 – *Continued from previous page*

Gene ID	NSA	COG/NR ID	KO	Locus	COG : KEGG/NR description
167739596	0.00044	COG0545	K03772	BDI_2705	FKBP-type peptidyl-prolyl cis-trans isomerases 1
167808311c	0.00044	COG0459	K04077	SAR11_0162	chaperonin GroEL (HSP60 family)
167706214	0.00044	COG0683		Tfu_1779	ABC-type branched-chain amino acid transport systems, periplasmic component
167866918	0.00044	COG2885	K03640	SAR11_0598	outer membrane protein and related peptidoglycan-associated (lipo)proteins : ompA; OmpA family
167807477	0.00042	COG0834		MSMEG_5368	ABC-type amino acid transport system, periplasmic component : ehuB; ectoine/hydroxyectoine ABC transporter solute-binding protein
167881416e	0.00040	COG0050	K02358	CHU_3175	GTPases - translation elongation factors : tufB, tuf
167765645f	0.00034	COG1653	K10232	Sare_3967	sugar-binding periplasmic proteins/domains
167730910	0.00033	COG3181		Dshi_2450	uncharacterized BCR
167725574	0.00032	COG0450	K03386	CHU_2724	peroxiredoxin : ahpC; alkyl hydroperoxide reductase, subunit C
167768817	0.00032	COG0740	K00288	CHU_1706	protease subunit of ATP-dependent Clp proteases : methylenetetrahydrofolate dehydrogenase (NADP+)
167886236	0.00031	COG0228	K02959	CHU_0117	rpsP; 30S ribosomal protein S16
167907528	0.00031	COG0591		SAR11_0316	Na+/proline, Na+/panthothenate symporters and related permeases : yjcG
167868396	0.00029	COG2358		PBPRA0389	predicted periplasmic binding protein : putative immunogenic protein
167718328	0.00027	COG1744	K07335	AAur_1253	surface lipoprotein : basic membrane protein A and related proteins
167769503c	0.00027	COG0459		CMS_2756	chaperonin GroEL (HSP60 family)
167818958	0.00026	COG1638		TM1040_0356	dicarboxylate-binding periplasmic protein : TRAP dicarboxylate transporter - DctP subunit
167702878	0.00025	COG1879		Krad_1186	periplasmic sugar-binding proteins : periplasmic binding protein/LacI transcriptional regulator
167665756	0.00025	COG0091	K02890	GFO_2834	rplV; 50S ribosomal protein L22
167730894	0.00023	COG1638		RD1_2185	dicarboxylate-binding periplasmic protein : dctP; C4-dicarboxylate-binding periplasmic protein, putative
167680092	0.00022	COG0094	K02931	Lxx20210	rplE; 50S ribosomal protein L5
167868548	0.00020	COG0834	K10018	SAR11_1210	ABC-type amino acid transport system, periplasmic component : octopine/nopaline transport system substrate-binding protein
167892279	0.00019	COG0834	K02030	Veis_2153	ABC-type amino acid transport system, periplasmic component
167817276	0.00018	COG0347	K04751	Acel_1565	nitrogen regulatory protein PII
167862242	0.00018	COG0087	K02906	BT_2727	rplC; 50S ribosomal protein L3
167933288	0.00018	COG1638		Dshi_3326	dicarboxylate-binding periplasmic protein : TRAP dicarboxylate transporter-DctP subunit
167713980*	0.00016	COG0330	K04088	SAR11_0008	membrane protease subunits, stomatin/prohibitin homologs : hflK
167867886	0.00016	COG3181		Csal_1767	uncharacterized BCR : uncharacterized protein UPF0065
167809873	0.00016	COG0539	K02945	CHU_1951	rpsA; 30S ribosomal protein S1

Continued on next page

Table B.1 – *Continued from previous page*

Gene ID	NSA	COG/NR ID	KO	Locus	COG : KEGG/NR description
167713982	0.00015	COG0330	K04087	SAR11_0007	membrane protease subunits, stomatin/prohibitin homologs : hflC
167822210	0.00015	COG0776		SCO2950	bacterial nucleoid DNA-binding protein : hup, SCE59.09c; DNA-binding protein Hu (hs1)
167820450*	0.00015	COG1192		tlr0963	ATPases involved in chromosome partitioning : probable cell division inhibitor minD
167820614g	0.00015	COG0174	K01915	Krad_3291	glutamine synthase
167714092	0.00014	COG0683	K01999	SAR11_1346	ABC-type branched-chain amino acid transport systems, periplasmic component : livJ
167817130	0.00014	COG0711	K02109	SCO5369	F0F1-type ATP synthase b subunit
167818902	0.00014	COG1638		SAR11_0864	dicarboxylate-binding periplasmic protein
167866078	0.00013	COG0605	K00518	Arth_2086	superoxide dismutase
167865698	0.00013	COG0740	K01358	AAur_2381	protease subunit of ATP-dependent Clp proteases
167817852	0.00013	COG0683		Noca_3017	ABC-type branched-chain amino acid transport systems, periplasmic component : extracellular ligand -binding receptor
167714042	0.00012	COG0683	K01999	SAR11_1361	ABC-type branched-chain amino acid transport systems, periplasmic component : livJ2; Leu/Ile/Val-binding protein precursor
167821000	0.00012	COG1732		MSMEG_2924	periplasmic glycine betaine/choline-binding (lipo)protein of an ABC-type transport system (osmoprotectant binding protein) : permease binding-protein component
167668848g	0.00011	COG0174	K01915	CMM_1636	glutamine synthase : glnA1
167748683*	0.00010	COG0834		PFL_3548	ABC-type amino acid transport system, periplasmic component
167718146	0.00010	COG0088	K02926	Lxx20320	rplD; 50S ribosomal protein L4
167862420	0.00010	COG1629		FP0112	outer membrane receptor proteins, mostly Fe transport : probable TonB-dependent outer membrane receptor precursor
167696080*	0.00010	COG1344	K02406	Csac_1680	flagellin and related hook-associated proteins
167735512	0.00010	COG0803	K09815	Smed_1697	ABC-type Mn/Zn transport system, periplasmic Mn/Zn-binding (lipo)protein (surface adhesin A)
167719882	0.00009	COG0096	K02994	SAR11_1103	rpsH; 30S ribosomal protein S8
167660431h	0.00009	COG3740	K06904	BL0376	phage head maturation protease
167718250	0.00009	COG2213	K02799	GK1948	phosphotransferase system, mannitol-specific IIBC component
167719862*	0.00008	COG0185	K02965	SAR11_1113	rpsS; 30S ribosomal protein S19
167702806	0.00008	COG0081	K02863	KRH_05860	rplA; 50S ribosomal protein L1
167719824*e	0.00008	COG0050	K02358	SAR11_1130	GTPases - translation elongation factors : tufB, tuf
167817466	0.00008	COG0404		mll1258	glycine cleavage system T protein (aminomethyltransferase) : sarcosine dehydrogenase
167868614	0.00008	COG2113	K02002	SAR11_0797	ABC-type proline/glycine betaine transport systems, periplasmic components : proX
167933120	0.00007	COG0803	K09815	Atu1521	ABC-type Mn/Zn transport system, periplasmic Mn/Zn-binding (lipo)protein (surface adhesin A) : znuA

Table B.1 – *Continued from previous page*

Gene ID	NSA	COG/NR ID	KO	Locus	COG : KEGG/NR description
167718168	0.00007	COG0094		CMS_0295	50S ribosomal protein L5
167868724	0.00007	COG0396	K09013	SAR11_0740	iron-regulated ABC transporter ATPase subunit SufC
167718156	0.00007	COG0092	K02982	Krad_0694	ribosomal protein S3
167719956	0.00006	COG0834	K02030	SAR11_1068	ABC-type amino acid transport system, periplasmic component : pheC; cyclohexadienyl dehydratase
167730882	0.00006	COG0004		SAR11_0818	ammonia permeases : amtB; ammonium transporter
167718138e	0.00006	COG0050	K02358	Tfu_2648	GTPases - translation elongation factors: tuf
167718052	0.00006	COG1653	K02027	Krad_3469	sugar-binding periplasmic proteins/domains
167700960*	0.00006	COG3794		SMa1243	plastocyanin : Azu1 pseudoazurin (blue copper protein)
167868482	0.00005	COG0715			ABC-type nitrate/sulfonate/taurine/bicarbonate transport systems, periplasmic components
167868656	0.00005	COG0715	K02051	AZC_2351	ABC-type nitrate/sulfonate/taurine/bicarbonate transport systems, periplasmic components
167868494	0.00004	COG1638		SMa0157	dicarboxylate-binding periplasmic protein
167866460	0.00004	COG0687	K02055	SCO5667	spermidine/putrescine-binding periplasmic protein
167719840	0.00004	COG0085	K03043	SAR11_1123	DNA-directed RNA polymerase beta subunit/140 kD subunit (split gene in Mjan, Mtthe, Aful) : rpoB
167816636	0.00004	COG0459	K04077	Krad_0736	chaperonin GroEL (HSP60 family)
167701680*	0.00004	COG3740	K06904	BL0376	phage head maturation protease
167717794*	0.00003	COG0195	K02600	SAR11_0388	phage head maturation protease
167717838	0.00003	COG0443	K04043	SAR11_0368	molecular chaperone : dnaK
167834314	0.00003	COG0443		CMS_2806	molecular chaperone : dnaK
167717784	0.00003	COG1185	K00962	SAR11_0392	polyribonucleotide nucleotidyltransferase (polynucleotide phosphorylase)
167818278	0.00003	COG1022		NoCa_3113	long-chain acyl-CoA synthetases (AMP-forming) : AMP-dependent synthetase and ligase
167719850	0.00002	COG0480	K02355	SAR11_1119	translation elongation and release factors (GTPases) : fusA
167816480	0.00002	COG0086	K03046	Krad_0681	DNA-directed RNA polymerase beta' subunit/160 kD subunit (split gene in archaea and Syn)
167866408	0.00001	COG1185	K00962	Lxx09030	polyribonucleotide nucleotidyltransferase (polynucleotide phosphorylase)

5 m – KEGG and NR annotated proteins

167873078	0.03710	BAF91544		major capsid protein [uncultured Myoviridae]
167771989 <i>i</i>	0.02658		BTH_I0914	hypothetical protein
167723550 <i>j</i>	0.01559	YP_001648266		hypothetical protein [Ostreococcus virus OsV5]
167927818 <i>j</i>	0.01345	YP_001648266		hypothetical protein [Ostreococcus virus OsV5]
167933090	0.01298	YP_002590925		putative porin [Candidatus Pelagibacter sp. HTCC7211]
167711088	0.01230		K09969	putative amino acid ABC transporter, periplasmic amino acid-binding protein
167691398	0.01175		HMI_2880	phage major capsid protein, hk97 family

Continued on next page

Table B.1 – *Continued from previous page*

Gene ID	NSA	COG/NR ID	KO	Locus	COG : KEGG/NR description
167922719 <i>k</i>	0.01174			Neut_1469	phage major capsid protein, HK97 family protein
167775105 <i>l</i>	0.01103	ABC95191			GP23-major capsid protein [Stenotrophomonas phage SMB14]
167687982 <i>l</i>	0.00968	NP_944113			gp23 major head protein [Aeromonas phage Aeh1]
167748599 <i>m</i>	0.00960			M6_Spy1138	phage prohead protease
167733772	0.00952			BBta_5785	putative phage major head protein
167925660	0.00923			SRU_2178	putative outer membrane protein, probably involved in nutrient binding
167796059 <i>n</i>	0.00853			APECO1_525	hypothetical protein
167883590	0.00820			PP_1567	phage major capsid protein, HK97 family
167666520 <i>o</i>	0.00818	BAF91544			major capsid protein [uncultured Myoviridae]
167664173* <i>p</i>	0.00713			GDI3673	hypothetical protein
167667150 <i>m</i>	0.00687			LGAS_1485	predicted phage phi-C31 GP36 major capsid-like protein
167771337	0.00605	ABW90951			gp23 major capsid protein [uncultured Myoviridae]
167884290 <i>l</i>	0.00573	BAF91544			major capsid protein [uncultured Myoviridae]
167760139	0.00561			CHU_2679	probable outer membrane lipoprotein P61
167816468 <i>q</i>	0.00522			DR_A0099	hypothetical protein
167700634 <i>j</i>	0.00499	YP_001648266		OsV5_190f	hypothetical protein [Ostreococcus virus OsV5]
167687792 <i>r</i>	0.00498			Asuc_1240	phage major capsid protein, HK97 family
167842580 <i>r</i>	0.00453			BAV1464	major capsid protein
167700776	0.00447			Bpro_3745	hypothetical protein
167729766	0.00433	ZP_01224596		GB2207_03424	hypothetical protein [marine gamma proteobacterium HTCC2207]
167934698	0.00431			Swit_4452	hypothetical protein
167884738	0.00409			BBta_5785	putative phage major head protein
167669610 <i>p</i>	0.00397			GDI3673	hypothetical protein
167861688	0.00359			BDI_2874	putative outer membrane protein, probably involved in nutrient binding
167910063	0.00347			GDI3673	hypothetical protein
167893743* <i>s</i>	0.00338	YP_001648158		OsV5_081f	hypothetical protein [Ostreococcus virus OsV5]
167888926 <i>p</i>	0.00326			GDI3673	hypothetical protein
167753643*	0.00324			Daci_1946	putative phage major head protein
167742624 <i>p</i>	0.00317			GDI3673	hypothetical protein
167908539 <i>r</i>	0.00304			BAV1464	major capsid protein
167675286*	0.00284			CKO_01864	hypothetical protein
167900893 <i>n</i>	0.00278			APECO1_525	hypothetical protein
167778265 <i>p</i>	0.00275			GDI3673	hypothetical protein

Table B.1 – *Continued from previous page*

Gene ID	NSA	COG/NR ID	KO	Locus	COG : KEGG/NR description
167786471	0.00267			mlr8524	phage major capsid protein, GP36
167735768	0.00265			FRAAL2681	hypothetical protein
167773951t	0.00253			LGAS_1485	predicted phage phi-C31 GP36 major capsid-like protein
167841586j	0.00250	A7U6E7			putative major capsid protein [Chrysochromulina ericina virus]
167919545	0.00245			Pmen_3970	phage major capsid protein, HK97 family
167781901u	0.00236	YP_214367			T4-like major capsid protein [Prochlorococcus phage P-SSM2]
167923659p	0.00235			GDI3673	hypothetical protein
167852301v	0.00230			MAB_1788	bacteriophage protein
167659301	0.00224			LGAS_1485	predicted phage phi-C31 GP36 major capsid-like protein
167861686	0.00223	YP_002789013			TonB dependent/ligand-gated channel [Polaribacter sp. MED152]
167712528v	0.00215			MAB_1788	bacterial nucleoid DNA-binding protein
167678920*w	0.00209	YP_001498525		AR158_C444L	hypothetical protein [Paramecium bursaria Chlorella virus AR158]
167849540j	0.00201	YP_001648266		OsV5_190f	hypothetical protein [Ostreococcus virus OsV5]
167781903u	0.00201	YP_214367			T4-like major capsid protein [Prochlorococcus phage P-SSM2]
167863158j	0.00200	YP_001648266		OsV5_190f	hypothetical protein [Ostreococcus virus OsV5]
167663967*	0.00190			Swit_4461	hypothetical protein
167687108u	0.00182	YP_214367			T4-like major capsid protein [Prochlorococcus phage P-SSM2]
167692622i	0.00176			SG1188	hypothetical protein
167733858	0.00170	ZP_01017474			major capsid protein, HK97 family protein [Parvularcula bermudensis HTCC2503]
167852851p	0.00167			GDI3673	hypothetical protein
167864542k	0.00166			Neut_1469	phage major capsid protein, HK97 family protein
167803157	0.00165	ZP_01688540			lipoprotein, putative [Microscilla marina ATCC 23134]
167682644j	0.00153	A7U6E7			putative major capsid protein [Chrysochromulina ericina virus]
167733004*j	0.00150	A7U6F0			putative major capsid protein [Phaeocystis pouchetii virus]
167765429	0.00148			CHU_2610	gliding motility-related protein; possible GldN and/or GldO
167878228t	0.00145			LGAS_1485	predicted phage phi-C31 GP36 major capsid-like protein
167775103	0.00145	YP_214669			gp23 [Prochlorococcus phage P-SSM4]
167702908	0.00143			mma_2202	hypothetical protein
167869946	0.00135	YP_195142			major capsid protein gp23 [Synechococcus phage S-PM2]
167834518	0.00128			Haur_0657	hypothetical protein
167807747	0.00122			Saro_0657	hypothetical protein
167816420	0.00121			APECO1_525	hypothetical protein

Table B.1 – *Continued from previous page*

Gene ID	NSA	COG/NR ID	KO	Locus	COG : KEGG/NR description
167809283k	0.00119			Neut_1469	phage major capsid protein, HK97 family protein
167868514	0.00119			SAR11_1290	TRAP-type bacterial extracellular solute-binding protein
167750765	0.00118			Smed_1334	phage major capsid protein, HK97 family
167925457p	0.00115			GDI3673	hypothetical protein
167782759	0.00113			Oter_1957	band 7 protein
167871794j	0.00113	YP_001648266		OsV5_190f	hypothetical protein [Ostreococcus virus OsV5]
167756019	0.00112			CHU_0172	gldL; gliding motility-related protein
167670926x	0.00112			BBta_5785	putative phage major head protein
167821362z	0.00112			APECO1_525	hypothetical protein
167690910j	0.00111	YP_001648266		OsV5_190f	hypothetical protein [Ostreococcus virus OsV5]
167685332j	0.00110	YP_001648266		OsV5_190f	hypothetical protein [Ostreococcus virus OsV5]
167700460*	0.00110	YP_001648158		OsV5_081f	hypothetical protein [Ostreococcus virus OsV5]
167685474*aa	0.00104	YP_001648182		OsV5_105r	hypothetical protein [Ostreococcus virus OsV5]
167734326bb	0.00103			amb4267	hypothetical protein
16775653q	0.00101			Haur_0657	hypothetical protein
167733302p	0.00101			GDI3673	hypothetical protein
167663981p	0.00097			GDI3673	hypothetical protein
167763843	0.00096			Saro_0657	hypothetical protein
167768193z	0.00096			CKO_01864	hypothetical protein
167719228i	0.00095			SG1188	hypothetical protein
167844676	0.00091	ZP_03643684		BACCOPRO_02057	hypothetical protein [Bacteroides coprophilus DSM 18228]
167881504cc	0.00091			BSU26140	yqbE; hypothetical protein
167852559oo	0.00090			HSM_0907	hypothetical protein
167804465*	0.00088	ZP_03724502		ObacDRAFT_9001	hypothetical protein [Opitutaceae bacterium TAV2]
167794165p	0.00087			GDI3673	hypothetical protein
167734676	0.00085			Amet_4028	phage major capsid protein, HK97 family
167764813u	0.00084	YP_214367			T4-like major capsid protein [Prochlorococcus phage P-SSM2]
167781783p	0.00079			GDI3673	hypothetical protein
167759955	0.00077			Dgeo_0628	hypothetical protein
167733674	0.00076			Swit_4452	hypothetical protein
167878828	0.00075		K02027	SAV1394	ABC transporter solute-binding protein
167740142	0.00075	YP_002705257			gp34 [Stenotrophomonas sp. SKA14]
167834088	0.00074			Haur_0657	hypothetical protein

Continued on next page

Table B.1 – *Continued from previous page*

Gene ID	NSA	COG/NR ID	KO	Locus	COG : KEGG/NR description
167821604j	0.00072	YP_001648266		OsV5_190f	hypothetical protein [Ostreococcus virus OsV5]
167798697p	0.00070			GDI3673	hypothetical protein
167823322s	0.00070	YP_001648158		OsV5_081f	hypothetical protein [Ostreococcus virus OsV5]
167718758j	0.00070	A7U6F0			putative major capsid protein [Phaeocystis pouchetii virus]
167713806	0.00069			SG1188	hypothetical protein
167778269dd	0.00068	YP_002276820		Gdia_2460	hypothetical protein [Gluconacetobacter diazotrophicus PA1 5]
167879936s	0.00067	YP_001648158		OsV5_081f	hypothetical protein [Ostreococcus virus OsV5]
167701850	0.00064			M446_5960	hypothetical protein
167934792p	0.00064			GDI3673	hypothetical protein
167874674	0.00063			GFO_0492	conserved hypothetical protein, secreted-possibly porin
167821292	0.00062			Oant_1504	peptidase U35 phage prohead HK97
167867556	0.00062			Rru_A2587	hypothetical protein
167901481	0.00061			Cthe_1719	phage major capsid protein, HK97 family
167824444	0.00059			Smed_5134	TRAP dicarboxylate transporter-DctP subunit
167696166*	0.00059			BTH_I0915	hypothetical protein
167936648	0.00056	EEI06235		XcelDRAFT_1815	hypothetical protein [Xylanimonas cellulosilytica DSM 15894]
167910361j	0.00054	A7U6F0			putative major capsid protein [Phaeocystis pouchetii virus]
167675492*p	0.00054			GDI3673	hypothetical protein
167801933aa	0.00052	YP_001648182		OsV5_105r	hypothetical protein [Ostreococcus virus OsV5]
167725772cc	0.00051			BSU26140	yqbE; hypothetical protein
167820670	0.00050			gll0198	similar to bacteriorhodopsin
167832972t	0.00050			LGAS_1485	predicted phage phi-C31 GP36 major capsid-like protein
167867536	0.00049			TM1040_0812	hypothetical protein
167783747	0.00048			Glov_2914	cell surface receptor IPT/TIG domain protein
167893945	0.00048			Oter_3420	hypothetical protein
167740708	0.00047		K03286	Pnap_1319	OmpA/MotB domain protein; OmpA-OmpF porin, OOP family
167772783	0.00047			RCIX1696	hypothetical protein
167734614p	0.00047			GDI3673	hypothetical protein
167776587*	0.00046	YP_001648249		OsV5_172f	hypothetical protein [Ostreococcus virus OsV5]
167911245s	0.00046	YP_001648315		OsV5_239r	hypothetical protein [Ostreococcus virus OsV5]
167867748x	0.00044			Daci_1946	putative phage major head protein
167732694	0.00044			NMC0858	putative phage-related protein
167922873	0.00042			CHU_3230	hypothetical protein

Table B.1 – *Continued from previous page*

Gene ID	NSA	COG/NR ID	KO	Locus	COG : KEGG/NR description
167734178p	0.00041			GDI3673	hypothetical protein
167873260	0.00041			Sare_3763	hypothetical protein
167685638*w	0.00041	YP_001498525		AR158_C444L	hypothetical protein [Paramecium bursaria Chlorella virus AR158]
167901149	0.00040		K01358	azo1870	endopeptidase Clp; K01358 ATP-dependent Clp protease, protease subunit
167853099i	0.00040			SG1188	hypothetical protein
167761349x	0.00037			Daci_1946	putative phage major head protein
167776241	0.00037			mll0455	hypothetical protein
167824154	0.00036			SACE_4894	hydrolase, alpha/beta fold family
167843578s	0.00035	YP_001648158		OsV5_081f	hypothetical protein [Ostreococcus virus OsV5]
167682808*	0.00035	YP_001648239		OsV5_162f	hypothetical protein [Ostreococcus virus OsV5]
167703228	0.00034			Dshi_0412	beta-Ig-H3/fasciclin
167918033p	0.00034			GDI3673	hypothetical protein
167891224p	0.00033			GDI3673	hypothetical protein
167867622	0.00033			Oant_1504	peptidase U35 phage prohead HK97
167732430ff	0.00031	ZP_02092868		FAEPRf212_03171	hypothetical protein [Faecalibacterium prausnitzii M21/2]
167684500s	0.00031	YP_001648158		OsV5_081f	hypothetical protein [Ostreococcus virus OsV5]
167824164*	0.00030	YP_001648240		OsV5_163f	hypothetical protein [Ostreococcus virus OsV5]
167765431	0.00030			CHU_0173	gldM; gliding motility-related protein
167854137	0.00030	ZP_00743477		RBTH_08297	hypothetical protein [Bacillus thuringiensis serovar israelensis ATCC 35646]
167730288k	0.00028			Neut_1469	phage major capsid protein, HK97 family protein
167685472*gg	0.00027	YP_001648184		OsV5_107r	hypothetical protein [Ostreococcus virus OsV5]
167778267p	0.00027			GDI3673	hypothetical protein
167919557	0.00027			PputW619_3936	hypothetical protein
167782645	0.00026			BBta_5785	putative phage major head protein
167908551	0.00026			CC_2781	hypothetical protein
16786723p	0.00026			GDI3673	hypothetical protein
167896531	0.00026			BAV1464	major capsid protein
167821374	0.00025	YP_001919460		Mpop_5468	hypothetical protein [Methylobacterium populi BJ001]
167833472	0.00024			GDI3673	hypothetical protein
167733210	0.00024			Pmen_3970	phage major capsid protein, HK97 family
167713652*	0.00023			mlr8533	hypothetical protein
167935700p	0.00023			GDI3673	hypothetical protein
167872214hh	0.00023		K06907	Sfum_3815	phage tail sheath protein

Continued on next page

Table B.1 – *Continued from previous page*

Gene ID	NSA	COG/NR ID	KO	Locus	COG : KEGG/NR description
167881636	0.00023			RspH17025_0103	hypothetical protein
167791200p	0.00023			GDI3673	hypothetical protein
167922981p	0.00022			GDI3673	hypothetical protein
167824604	0.00022			RspH17029_3578	uncharacterized protein UPF0065
167933608ff	0.00022	ZP_02092868		FAEPRAM212_03171	hypothetical protein [Faecalibacterium prausnitzii M21/2]
167817058	0.00022		K00518	Sare_4077	superoxide dismutase
167823358*gg	0.00021	YP_001648184		OsV5_107r	hypothetical protein [Ostreococcus virus OsV5]
167892855	0.00021	YP_001648184		OsV5_107r	hypothetical protein [Ostreococcus virus OsV5]
167840790	0.00021			RspH17025_0437	hypothetical protein
167712150*s	0.00021	YP_001648158		OsV5_081f	hypothetical protein [Ostreococcus virus OsV5]
167833160bb	0.00021			amb4267	hypothetical protein
167892985j	0.00021	YP_001648266		OsV5_190f	hypothetical protein [Ostreococcus virus OsV5]
167696294oo	0.00020			HS_1377	hypothetical protein
167759041	0.00019			PP_3877	hypothetical protein
167766087s	0.00019	YP_001648153		OsV5_076f	hypothetical protein [Ostreococcus virus OsV5]
167919775	0.00019	YP_001294637		ORF044	hypothetical protein [Pseudomonas phage PA11]
167804453*	0.00017	ZP_03724505		ObacDRAFT_9004	hypothetical protein [Opitutaceae bacterium TAV2]
167833104	0.00017			Bcep1808_1173	hypothetical protein
167721370*	0.00016	YP_001648301		OsV5_225r	hypothetical protein [Ostreococcus virus OsV5]
167826943*	0.00016			Sare_3763	hypothetical protein
167865492	0.00015		K02027	Pput_3473	extracellular solute-binding protein, family 1; multiple sugar transport system substrate-binding protein
167685780*j	0.00015	YP_001648266		OsV5_190f	hypothetical protein [Ostreococcus virus OsV5]
167910713	0.00014			Bd1641	hypothetical protein
167910061p	0.00014			GDI3673	hypothetical protein
167833358s	0.00013	YP_001648158		OsV5_081f	hypothetical protein [Ostreococcus virus OsV5]
167692314*w	0.00012	YP_001498525		AR158_C444L	hypothetical protein [Paramecium bursaria Chlorella virus AR158]
167925393	0.00012			Oter_3421	hypothetical protein
167687436	0.00011		K01999	azo3443	conserved hypothetical ABC-type branched-chain amino acid transport systems, periplasmic component
167719658hh	0.00011		K06907	Dde_1889	hypothetical protein
167668360s	0.00011	YP_001648158		OsV5_081f	hypothetical protein [Ostreococcus virus OsV5]
167735772	0.00010			FRAAL2683	hypothetical protein; putative mycobacteriophage protein (GP15) similarity

Continued on next page

Table B.1 – *Continued from previous page*

Gene ID	NSA	COG/NR ID	KO	Locus	COG : KEGG/NR description
167702102	0.00010			Daci_1946	putative phage major head protein
167688622p	0.00009			GDI3673	hypothetical protein
167782867cc	0.00009			BSU26140	yqbE; hypothetical protein
167867386	0.00008			TM1040_1299	peptidase U35, phage prohead HK97
167789595	0.00008			APEC01_4044	hypothetical protein
167828425*w	0.00007	YP_001498525		AR158_C444L	hypothetical protein [Paramecium bursaria Chlorella virus AR158]
167865490	0.00007		K02027	Rmet_2229	extracellular solute-binding protein, family 1; multiple sugar transport system substrate-binding protein
167840812	0.00006	ZP_01959135		BACCAC_00731	hypothetical protein [Bacteroides caccae ATCC 43185]
167706428	0.00005	YP_001648190		OsV5_113r	hypothetical protein [Ostreococcus virus OsV5]
167867920p	0.00005			GDI3673	hypothetical protein
167842648*s	0.00005	YP_001648315		OsV5_239r	hypothetical protein [Ostreococcus virus OsV5]
167869096w	0.00005	YP_001498525		AR158_C444L	hypothetical protein [Paramecium bursaria Chlorella virus AR158]
167859444	0.00005	YP_001648151		OsV5_074f	hypothetical protein [Ostreococcus virus OsV5]
167871600	0.00005	YP_001648152		OsV5_075f	hypothetical protein [Ostreococcus virus OsV5]
167669608p	0.00004			GDI3673	hypothetical protein
167678686p	0.00004			GDI3673	hypothetical protein
167752119	0.00004	YP_001648152		OsV5_075f	hypothetical protein [Ostreococcus virus OsV5]
167825992j	0.00003	A7U6E7			putative major capsid protein [Chrysochromulina ericina virus
167818634	0.00003			PputGB1_1751	hypothetical protein
167671778*	0.00003	YP_001648124		OsV5_047f	hypothetical protein [Ostreococcus virus OsV5]
167871626s	0.00002	YP_001648158		OsV5_081f	hypothetical protein [Ostreococcus virus OsV5]
167753841	0.00002		K06907	Sfum_3815	phage tail sheath protein
167724632*	0.00002	YP_001648232		OsV5_155f	hypothetical protein [Ostreococcus virus OsV5]
167690816	0.00002	YP_001648190		OsV5_113r	hypothetical protein [Ostreococcus virus OsV5]
167742884*	0.00001			Dvul_0646	hypothetical protein
167875342j	0.00001	YP_001648145		OsV5_068f	hypothetical protein [Ostreococcus virus OsV5]

5 m – Proteins with no annotation

167699580*	0.01263
167736790ii	0.01043
167796769	0.00914
167722626jj	0.00789
167703824pp	0.00714

Continued on next page

Table B.1 – *Continued from previous page*

Gene ID	NSA	COG/NR ID	KO	Locus	COG : KEGG/NR description
167753801	0.00626				
167854251	0.00577				
167744898* <i>o</i>	0.00546				
167664175* <i>nn</i>	0.00514				
167829145 <i>pp</i>	0.00433				
167779175 <i>pp</i>	0.00423				
167881060 <i>pp</i>	0.00419				
167887022 <i>pp</i>	0.00390				
167836216 <i>jj</i>	0.00369				
167688044 <i>p</i>	0.00353				
167697984 <i>pp</i>	0.00321				
167855765 <i>jj</i>	0.00318				
167764897 <i>jj</i>	0.00297				
167718436	0.00240				
167771817	0.00226				
167699330*	0.00220				
167891152 <i>pp</i>	0.00207				
167844558 <i>pp</i>	0.00197				
167801097 <i>pp</i>	0.00197				
167891908	0.00196				
167820168 <i>ii</i>	0.00192				
167688624	0.00182				
167746546 <i>jj</i>	0.00176				
167682238 <i>p</i>	0.00175				
167722606	0.00164				
167883488 <i>pp</i>	0.00157				
167839862 <i>mm</i>	0.00139				
167820406*	0.00139				
167858104	0.00138				
167806741 <i>jj</i>	0.00138				
167678192	0.00133				
167706644	0.00133				
167787801* <i>ll</i>	0.00124				

Continued on next page

Table B.1 – *Continued from previous page*

Gene ID	NSA	COG/NR ID	KO	Locus	COG : KEGG/NR description
167781039	0.00124				
167936638	0.00116				
167733554	0.00116				
167918031	0.00112				
167790652	0.00110				
167734428	0.00102				
167925455	0.00102				
167928078	0.00100				
167682970o	0.00098				
167701282	0.00091				
167867140o	0.00087				
167809975jj	0.00087				
167750727	0.00082				
16783564ll	0.00082				
167789467pp	0.00080				
167669606	0.00078				
167733300	0.00076				
167750389jj	0.00072				
167852849	0.00072				
167827017	0.00070				
167691436	0.00068				
167816466*	0.00067				
167678688	0.00063				
167796679	0.00062				
167761163	0.00059				
167916021pp	0.00059				
167867918	0.00058				
167853885	0.00058				
167757667	0.00053				
167922983	0.00052				
167923663nn	0.00051				
167922109	0.00051				
167661777	0.00051				

Continued on next page

Table B.1 – *Continued from previous page*

Gene ID	NSA	COG/NR ID	KO	Locus	COG : KEGG/NR description
167936684	0.00050				
167867228	0.00050				
167791202	0.00049				
167819274	0.00046				
167765833*	0.00045				
167793451*	0.00045				
167732910	0.00043				
167890226	0.00043				
167718438	0.00042				
167688708	0.00041				
167699600 <i>pp</i>	0.00041				
167746630	0.00040				
167821290	0.00039				
167916161*	0.00038				
167700778	0.00037				
167701632 <i>kk</i>	0.00037				
167675494*	0.00036				
167711820	0.00034				
167663983	0.00033				
167689444*	0.00032				
167933464 <i>nn</i>	0.00032				
167891222	0.00032				
167852557	0.00031				
167843828	0.00031				
167843020	0.00031				
167677672	0.00030				
167776503*	0.00028				
167804815	0.00027				
167713808	0.00027				
167702310 <i>dd</i>	0.00026				
167913463o	0.00025				
167881302	0.00025				
167907624 <i>mm</i>	0.00025				

Table B.1 – *Continued from previous page*

Gene ID	NSA	COG/NR ID	KO	Locus	COG : KEGG/NR description
167753609*	0.00024				
167829571	0.00024				
167921665	0.00024				
167920645	0.00023				
167714058	0.00022				
167677546*	0.00021				
167913465	0.00020				
167697624*	0.00020				
167912083 <i>jj</i>	0.00019				
167766043*	0.00018				
167678558*	0.00018				
167733556	0.00017				
167663383*	0.00016				
167905220*	0.00015				
167891594	0.00015				
167883594 <i>ll</i>	0.00015				
167879460	0.00014				
167919777	0.00014				
167884588 <i>o</i>	0.00014				
167822810	0.00013				
167713494	0.00012				
167841896*	0.00010				
167804467*	0.00010				
167925043 <i>kk</i>	0.00010				
167858106	0.00009				
167788223*	0.00009				
167878206	0.00008				
167764895 <i>jj</i>	0.00008				
167767179	0.00008				
167858640	0.00008				
167683530*	0.00007				
167918035	0.00006				
167766125*	0.00006				

Continued on next page

Table B.1 – *Continued from previous page*

Gene ID	NSA	COG/NR ID	KO	Locus	COG : KEGG/NR description
167752051*	0.00005				
167890228	0.00004				
167685654*	0.00003				
167719670*	0.00002				
167879450	0.00002				

Table B.2: Proteins identified in the Ace Lake 11.5 m sample 0.1 μ m size-fraction metaproteome. (*) Protein group identification: proteins that contain similar peptides that could not be differentiated by the mass spectral analysis were grouped. Only one gene number of that group is displayed. (a-z, aa-pp) Protein ambiguity groups: proteins that have some shared peptides with one or more other proteins from the same sample depth are marked with the same letters.

Gene ID	NSA	COG/NR ID	KO	Locus	11.5 m – COG annotated proteins
					COG : KEGG/NR description
163207432	0.01734	COG0834	K09969	SAR11_0953	ABC-type amino acid transport system, periplasmic component : yhdW
163201696	0.01011	COG1879		MSMEG_1374	periplasmic sugar-binding proteins : ribose ABC transporter, periplasmic binding protein
163136433	0.00671	COG3409		Clos_2845	putative peptidoglycan-binding domain-containing protein
163539247	0.00629	COG1653		Noca_3914	sugar-binding periplasmic proteins/domains : extracellular solute-binding protein, family 1
163377029a	0.00566	COG0050	K02358	amb3148	GTPases - translation elongation factors : tuf
163451248b	0.00541	COG0715	K02051	SAR11_0807	ABC-type nitrate/sulfonate/taurine/bicarbonate transport systems, periplasmic components
163135049c	0.00533	COG1638		SAR11_0266	dicarboxylate-binding periplasmic protein : TRAP dicarboxylate transporter - DctP subunit (mannitol/chloroaromatic compounds)
163451084	0.00531	COG2113	K02002	SAR11_1302	ABC-type proline/glycine betaine transport systems, periplasmic components : opuAC
163117735	0.00526	COG2113	K02001	Plav_1066	ABC-type proline/glycine betaine transport systems, periplasmic components
163198494d	0.00415	COG0591		SAR11_0316	Na+/proline, Na+/panthothenate symporters and related permeases : yjcG
163416423*	0.00371	COG0776	K03530	SAR11_0817	bacterial nucleoid DNA-binding protein : hupA
163442042	0.00364	COG0687	K02055	SAR11_1336	spermidine/putrescine-binding periplasmic protein : potD
163208342e	0.00356	COG0834	K09969	HCH_05807	ABC-type amino acid transport system, periplasmic component
163234668*	0.00338	COG0450		SPO3383	peroxiredoxin : thiol-specific antioxidant protein
163261506	0.00336	COG1638		SAR11_0864	dicarboxylate-binding periplasmic protein
163104605	0.00336	COG2213	K02799	GK1948	phosphotransferase system, mannitol-specific IIBC component
163357996c	0.00321	COG1638		SAR11_0266	dicarboxylate-binding periplasmic protein : TRAP dicarboxylate transporter - DctP subunit (mannitol/chloroaromatic compounds)
163381848f	0.00314	COG0459	K04077	SAR11_0162	chaperonin GroEL (HSP60 family)
163145053	0.00312	COG0683	K01999	SAR11_1361	ABC-type branched-chain amino acid transport systems, periplasmic component : livJ2; Leu/Ile/Val-binding protein precursor
163388714	0.00282	COG1638		RD1_2185	dicarboxylate-binding periplasmic protein : DctP; C4-dicarboxylate-binding periplasmic protein, putative
163450920	0.00247	COG0683	K01999	SAR11_1361	ABC-type branched-chain amino acid transport systems, periplasmic component : livJ2; Leu/Ile/Val-binding protein precursor
163240441	0.00246	COG1653	K02027	PflO1_3630	sugar-binding periplasmic proteins/domains
163275955	0.00241	COG1638		TM1040_0356	dicarboxylate-binding periplasmic protein : TRAP dicarboxylate transporter - DctP subunit

Continued on next page

Table B.2 – *Continued from previous page*

Gene ID	NSA	COG/NR ID	KO	Locus	COG : KEGG/NR description
163449626	0.00229	COG1638		Dshi_3326	dicarboxylate-binding periplasmic protein : TRAP dicarboxylate transporter, DctP subunit
163450966	0.00228	COG0687	K02055	SAR11_1336	spermidine/putrescine-binding periplasmic protein : potD
163174786	0.00223	COG2358		PBPRA0389	predicted periplasmic binding protein : putative immunogenic protein
163120641	0.00219	COG1879	K02058	CMM_0792	periplasmic sugar-binding proteins : putative sugar ABC transporter, solute-binding protein
163416343	0.00204	COG3181		Csal_1767	uncharacterized BCR
163441934	0.00198	COG2885	K03640	SAR11_0598	outer membrane protein and related peptidoglycan-associated (lipo)proteins : ompA; OmpA family
163320067	0.00176	COG2165	K02650	SAR11_0054	general secretory pathway proteins G and H and related periplasmic/secreted proteins : pilA; pilin (bacterial filament)
163274197 <i>b</i>	0.00167	COG0715	K02051	SAR11_0807	ABC-type nitrate/sulfonate/taurine/bicarbonate transport systems, periplasmic components
163128105	0.00167	COG1012	K00128	AAur_pTC20196	NAD-dependent aldehyde dehydrogenases
163214443 <i>e</i>	0.00161	COG0834	K09969	HCH_05807	ABC-type amino acid transport system, periplasmic component
163174178	0.00143	COG1879		RHA1_ro08504	periplasmic sugar-binding proteins : ABC sugar transporter, periplasmic substrate binding protein
163134937 <i>d</i>	0.00138	COG0591		SAR11_0316	Na+/proline, Na+/panthothenate symporters and related permeases : yjcG
163451228	0.00132	COG2113	K02002	SAR11_0797	ABC-type proline/glycine betaine transport systems, periplasmic components : proX
163376697*	0.00129	COG0834	K10018	SAR11_1210	ABC-type amino acid transport system, periplasmic component : octopine/nopaline transport system substrate-binding protein
163104625	0.00119	COG0683	K01999	AAur_1271	ABC-type branched-chain amino acid transport systems, periplasmic component : braC
163498557	0.00116	COG3181	K07795	Mmwyl1_1799	uncharacterized BCR : putative tricarboxylic transport membrane protein
163497259	0.00107	COG0747		CMM_2185	ABC-type dipeptide/oligopeptide/nickel transport systems, periplasmic components
163296806	0.00075	COG0834	K02030	SAR11_1068	ABC-type amino acid transport system, periplasmic component: pheC; cyclohexadienyl dehydratase; polar amino acid transport system substrate-binding protein
163277703	0.00071	COG0055	K02112	Acel_0653	F0F1-type ATP synthase beta subunit
163152101* <i>f</i>	0.00066	COG0459	K04077	SAR11_0162	chaperonin GroEL (HSP60 family)
163296936 <i>a</i>	0.00055	COG0050	K02358	SAR11_1130	GTPases - translation elongation factors : tufB
163117667	0.00043	COG0174	K01915	SAR11_0747	glutamine synthase : glnA
163154554 <i>a</i>	0.00042	COG0050	K02358	Tfu_2648	GTPases - translation elongation factors : tuf
163450946	0.00036	COG0683	K01999	SAR11_1346	ABC-type branched-chain amino acid transport systems, periplasmic component : livJ
163208382	0.00035	COG0174	K01915	CMM_1636	glutamine synthase : glnA
163135037	0.00031	COG2133	K00540	RspH17025_1771	glucose/sorbose dehydrogenases
163150509	0.00028	COG0737		Haur_2906	5'-nucleotidase/2',3'-cyclic phosphodiesterase and related esterases
163195194	0.00028	COG0086	K03046	Lxx20630	DNA-directed RNA polymerase beta' subunit/160 kD subunit (split gene in archaea and Syn) : rpoC

Continued on next page

Table B.2 – *Continued from previous page*

Gene ID	NSA	COG/NR ID	KO	Locus	COG : KEGG/NR description
163169240*	0.00027	COG0330	K04088	SAR11_0008	membrane protease subunits, stomatin/prohibitin homologs : hflK
163135897	0.00014	COG1185	K00962	SAR11_0392	polyribonucleotide nucleotidyltransferase (polynucleotide phosphorylase) : pnp; polynucleotide phosphorylase/polyadenylase
11.5 m – KEGG and NR annotated proteins					
163498919g	0.04693	BAF91544			major capsid protein [uncultured Myoviridae]
163303017h	0.03153		GDI3673		hypothetical protein
163496543i	0.03095	YP_001648158			hypothetical protein [Ostreococcus virus OsV5]
163312513	0.02334	YP_002590925			putative porin [Candidatus Pelagibacter sp. HTCC7211]
163114028g	0.02078	YP_214669			gp23 [Prochlorococcus phage P-SSM4]
163447324i	0.01947	YP_001648266			hypothetical protein OsV5_190f [Ostreococcus virus OsV5]
163104039j	0.01469	YP_001498525	AR158_C444L		hypothetical protein [Paramecium bursaria Chlorella virus AR158]
163299338	0.01058		Sputw3181_2479		phage major capsid protein, HK97 family
163431599i	0.01022	YP_001648266	OsV5_190f		hypothetical protein [Ostreococcus virus OsV5]
163486997k	0.00971		SG1188		hypothetical protein
163200650	0.00948		mlr8524		phage major capsid protein, GP36
163146271*l	0.00930		BBta_5785		putative phage major head protein
163466160	0.00921		BBta_5785		putative phage major head protein
163111996h	0.00849		GDI3673		hypothetical protein
163277976	0.00767		Neut_1469		phage major capsid protein, HK97 family protein
163276037	0.00762		mma_2202		hypothetical protein
163114610i	0.00717	A7U6E7			putative major capsid protein [Chrysochromulina ericina virus]
163191828	0.00696	ZP_03701413	Flav3CDRAFT_1333		hypothetical protein [Flavobacteria bacterium MS024-3C]
163121725*	0.00678	YP_001648124	OsV5_047f		hypothetical protein [Ostreococcus virus OsV5]
163383538*	0.00611		Neut_1469		phage major capsid protein, HK97 family protein
163125121g	0.00600	YP_214669			gp23 [Prochlorococcus phage P-SSM4]
163161438	0.00539	ABW90951			gp23 major capsid protein [uncultured Myoviridae]
163404994m	0.00493		Haur_0657		hypothetical protein
163115173*n	0.00467	YP_001648182	OsV5_105r		hypothetical protein [Ostreococcus virus OsV5]
163253040	0.00435		Bpro_3745		hypothetical protein
163519031	0.00433	YP_002276820	Gdia_2460		hypothetical protein [Gluconacetobacter diazotrophicus PA1 5]
163228214o	0.00413		Daci_1946		putative phage major head protein
163291274h	0.00407		GDI3673		hypothetical protein
163206524*i	0.00403	YP_001648266	OsV5_190f		hypothetical protein [Ostreococcus virus OsV5]

Continued on next page

Table B.2 – *Continued from previous page*

Gene ID	NSA	COG/NR ID	KO	Locus	COG : KEGG/NR description
163514201	0.00400			MAB_1788	bacteriophage protein
163498539	0.00399			SAR11_1290	TRAP-type bacterial extracellular solute-binding protein
163432666	0.00396			Oter_3421	hypothetical protein
163480087	0.00392			APEC01_525	hypothetical protein
163187860	0.00390			GDI3673	hypothetical protein
163529078	0.00375			HM1_2880	phage major capsid protein, hk97 family
163526011 <i>i</i>	0.00371	A7U6E9			putative major capsid protein [Pyramimonas orientalis virus]
163180584	0.00369	BAE06835			hypothetical major capsid protein [Heterosigma akashiwo virus 01]
163459594 <i>i</i>	0.00364	BAE06835			hypothetical major capsid protein [Heterosigma akashiwo virus 01]
163503842 <i>h</i>	0.00357			GDI3673	hypothetical protein
163495193	0.00351			MAB_1788	bacteriophage protein
163385358 <i>p</i>	0.00324			GDI3673	hypothetical protein
163489449	0.00313			SG1188	hypothetical protein
163472957	0.00310			Asuc_1240	phage major capsid protein, HK97 family
163131623	0.00298	YP_195142			major capsid protein gp23 [Synechococcus phage S-PM2]
163118697 <i>i</i>	0.00289	A7U6F0			putative major capsid protein [Phaeocystis pouchetii virus]
163420549	0.00284			LGAS_1485	predicted phage phi-C31 GP36 major capsid-like protein
163142179	0.00279	ZP_03643684		BACCOPRO_02057	hypothetical protein [Bacteroides coprophilus DSM 18228]
163250350 <i>q</i>	0.00277	YP_214367			T4-like major capsid protein [Prochlorococcus phage P-SSM2]
163541257	0.00271			Swit_4452	hypothetical protein
163478791	0.00261			amb4267	hypothetical protein
163452556	0.00245			APEC01_525	hypothetical protein
163507581	0.00237			Cthe_2848	phage major capsid protein, HK97
163409546*	0.00234	YP_001648301		OsV5_225r	hypothetical protein [Ostreococcus virus OsV5]
163412911	0.00233	ZP_03724502		ObacDRAFT_9001	hypothetical protein [Opitutaceae bacterium TAV2]
163544869	0.00230			Smed_1334	phage major capsid protein, HK97 family
163323331	0.00222			LGAS_1485	predicted phage phi-C31 GP36 major capsid-like protein
163235228*	0.00221			BBta_5785	putative phage major head protein
163494515 <i>r</i>	0.00217			LGAS_1485	predicted phage phi-C31 GP36 major capsid-like protein
163372194	0.00216	ZP_01017474			major capsid protein, HK97 family protein [Parvularcula bermudensis HTCC2503]
163252031 <i>i</i>	0.00210	A7U6F0			putative major capsid protein [Phaeocystis pouchetii virus]
163390078 <i>p</i>	0.00210			GDI3673	hypothetical protein
163290252 <i>m</i>	0.00201			Haur_0657	hypothetical protein

Table B.2 – *Continued from previous page*

Gene ID	NSA	COG/NR ID	KO	Locus	COG : KEGG/NR description
163157042k	0.00196			SG1188	hypothetical protein
163199564i	0.00192	YP_001648266		OsV5_190f	hypothetical protein [Ostreococcus virus OsV5]
163490373h	0.00191			GDI3673	hypothetical protein
163445182	0.00189			Acid_4111	hypothetical protein
163229276i	0.00187	YP_001648266		OsV5_190f	hypothetical protein [Ostreococcus virus OsV5]
163485571i	0.00185	YP_001648158		OsV5_081f	hypothetical protein [Ostreococcus virus OsV5]
163499762	0.00183			BBta_5785	putative phage major head protein
163227690i	0.00181	YP_001648158		OsV5_081f	hypothetical protein [Ostreococcus virus OsV5]
163168692	0.00179			M446_5960	hypothetical protein
163109620*	0.00175	YP_001648249		OsV5_172f	hypothetical protein [Ostreococcus virus OsV5]
163105813	0.00173			APEC01_4044	hypothetical protein
163141843*i	0.00172	YP_001648266		OsV5_190f	hypothetical protein [Ostreococcus virus OsV5]
163117897h	0.00163			GDI3673	hypothetical protein
163173092	0.00163			Pmen_3970	phage major capsid protein, HK97 family
163491889	0.00161			CKO_01864	hypothetical protein
163453714h	0.00159			GDI3673	hypothetical protein
163161098q	0.00157	YP_214367			T4-like major capsid protein [Prochlorococcus phage P-SSM2]
163177212	0.00156			BBta_6597	putative peptidase S14, ClpP
163352152	0.00154			BDI_2873	putative outer membrane protein, probably involved in nutrient binding
163372026i	0.00151	YP_001648266		OsV5_190f	hypothetical protein [Ostreococcus virus OsV5]
163287382q	0.00151	YP_214367			T4-like major capsid protein [Prochlorococcus phage P-SSM2]
163379834h	0.00151			GDI3673	hypothetical protein
163124973	0.00148			BAV1464	major capsid protein
163354170	0.00145	YP_001648190		OsV5_113r	hypothetical protein [Ostreococcus virus OsV5]
163115568*s	0.00143	YP_001648153		OsV5_076f	hypothetical protein [Ostreococcus virus OsV5]
163410122s	0.00140	YP_001648315		OsV5_239r	hypothetical protein [Ostreococcus virus OsV5]
163411861r	0.00138			LGAS_1485	predicted phage phi-C31 GP36 major capsid-like protein
163220019	0.00132	ZP_00743477		RBTH_08297	hypothetical protein [Bacillus thuringiensis serovar israelensis ATCC 35646]
163134239*	0.00132	YP_001648234		OsV5_157f	hypothetical protein [Ostreococcus virus OsV5]
163174626*	0.00130		K06904	BL0376	hypothetical protein with similarity to putative maturation protease of prophage CP-9 33CE
163154474	0.00125			gll0198	similar to bacteriopsin
163467688l	0.00115			Daci_1946	putative phage major head protein
163256412	0.00111	ZP_00743477		RBTH_08297	hypothetical protein [Bacillus thuringiensis serovar israelensis ATCC 35646]

Continued on next page

Table B.2 – *Continued from previous page*

Gene ID	NSA	COG/NR ID	KO	Locus	COG : KEGG/NR description
163389410	0.00111			Oant_1504	peptidase U35 phage prohead HK97
163248889 <i>i</i>	0.00110	YP_001648266		OsV5_190f	hypothetical protein [Ostreococcus virus OsV5]
163415470 <i>i</i>	0.00104	A7U6F0			putative major capsid protein [Phaeocystis pouchetii virus]
163191410*	0.00100	YP_001648184		OsV5_107r	hypothetical protein [Ostreococcus virus OsV5]
163142589	0.00093			Pmen_3970	phage major capsid protein, HK97 family
163327003 <i>t</i>	0.00088		K06907	Dde_1889	hypothetical protein; K06907
163211634*i	0.00086	YP_001648266		OsV5_190f	hypothetical protein [Ostreococcus virus OsV5]
163393172 <i>i</i>	0.00075	YP_001648266		OsV5_190f	hypothetical protein [Ostreococcus virus OsV5]
163161074 <i>t</i>	0.00073		K06907	Dde_1889	hypothetical protein; K06907
163141653*i	0.00070	YP_001648158		OsV5_081f	hypothetical protein [Ostreococcus virus OsV5]
163110018	0.00068	YP_001294637		ORF044	hypothetical protein [Pseudomonas phage PA11]
163249021 <i>s</i>	0.00067	YP_001648315		OsV5_239r	hypothetical protein [Ostreococcus virus OsV5]
163445294*j	0.00062	YP_001498525		AR158_C444L	hypothetical protein [Paramecium bursaria Chlorella virus AR158]
163507277	0.00058			CHLREDRAFT_18622B	hypothetical protein
163298764 <i>i</i>	0.00058	YP_001648158		OsV5_081f	hypothetical protein [Ostreococcus virus OsV5]
163298596 <i>i</i>	0.00055	YP_001648266		OsV5_190f	hypothetical protein [Ostreococcus virus OsV5]
163335150	0.00053			BAV1464	major capsid protein
163327023*q	0.00046	YP_214367			T4-like major capsid protein [Prochlorococcus phage P-SSM2]
163287366 <i>t</i>	0.00038		K06907	Sfum_3815	phage tail sheath protein; K06907
163475851 <i>o</i>	0.00028			ZMO0387	major head protein
163195236*s	0.00027	YP_001648315		OsV5_239r	hypothetical protein [Ostreococcus virus OsV5]
163184761	0.00027	YP_001648134		OsV5_057f	hypothetical protein [Ostreococcus virus OsV5]
163109424*n	0.00023	YP_001648182		OsV5_105r	hypothetical protein [Ostreococcus virus OsV5]
163368976	0.00020	YP_001648211		OsV5_134r	hypothetical protein [Ostreococcus virus OsV5]
163306940	0.00018	YP_001648185		OsV5_108r	hypothetical protein [Ostreococcus virus OsV5]
163162936*	0.00017	YP_001648263		OsV5_187r	hypothetical protein [Ostreococcus virus OsV5]
163151745 <i>s</i>	0.00017	YP_001648315		OsV5_239r	hypothetical protein [Ostreococcus virus OsV5]

11.5 m – Proteins with no annotation

163171140	0.03385
163345623 <i>u</i>	0.03193
163279609	0.01466
163534693	0.00797
163109584	0.00788

Continued on next page

Table B.2 – *Continued from previous page*

Gene ID	NSA	COG/NR ID	KO	Locus	COG : KEGG/NR description
163251027	0.00668				
163250059 <i>u</i>	0.00668				
163386750 <i>u</i>	0.00650				
163254426	0.00638				
163129699	0.00610				
163113296*	0.00528				
163129983	0.00511				
163395912	0.00471				
163346783	0.00446				
163246177 <i>u</i>	0.00435				
163303354	0.00395				
163477113	0.00385				
163419181	0.00349				
163431790 <i>v</i>	0.00331				
163502200	0.00289				
163456165	0.00285				
163397872	0.00285				
163490375	0.00278				
163502202	0.00250				
163453476*	0.00247				
163503840	0.00234				
163187858	0.00225				
163224309 <i>v</i>	0.00211				
163117895	0.00204				
163285151 <i>w</i>	0.00191				
163511023 <i>u</i>	0.00182				
163156214	0.00160				
163311655	0.00157				
163286408 <i>w</i>	0.00138				
163254680	0.00138				
163439545*	0.00133				
163123675	0.00131				
163199154 <i>u</i>	0.00126				

Table B.2 – *Continued from previous page*

Gene ID	NSA	COG/NR ID	KO	Locus	COG : KEGG/NR description
163129981	0.00097				
163110772*	0.00096				
163211312	0.00094				
163207714	0.00092				
163342613	0.00074				
163217867*	0.00071				
163110016	0.00069				
163117805	0.00063				
163280533	0.00059				
163168938	0.00059				
163320197	0.00040				

Table B.3: Proteins identified in the Ace Lake 12.7 m sample 0.1 μ m size-fraction metaproteome. (*) Protein group identification: proteins that contain similar peptides that could not be differentiated by the mass spectral analysis were grouped. Only one gene number of that group is displayed. (a-z, aa-pp) Protein ambiguity groups: proteins that have some shared peptides with one or more other proteins from the same sample depth are marked with the same letters.

Gene ID	NSA	COG/NR ID	KO	Locus	12.7 m – COG annotated proteins
					COG : KEGG/NR description
165547755*	0.01035	COG0539	K02945	Cvib_1514	rpsA; 30S ribosomal protein S1
165526280	0.00768	COG0181	K01749	Cvib_1245	porphobilinogen deaminase : hydroxymethylbilane synthase
165511899	0.00756	COG0516	K00088	Cvib_1056	IMP dehydrogenase/GMP reductase
165562959	0.00530	COG1104	K04487	Cvib_0301	cysteine sulfinate desulfurinase/cysteine desulfurase and related enzymes : aminotransferase, class V
165514395*	0.00452	COG0674	K00174	Cvib_1597	pyruvate:ferredoxin oxidoreductase and related 2-oxoacid:ferredoxin oxidoreductases, alpha sub-unit
165502373	0.00380	COG0129	K01687	Cvib_1169	dihydroxy-acid dehydratase
165514465*	0.00340	COG0054	K00794	Cvib_1632	riboflavin synthase beta-chain
165525758	0.00270	COG1862	K03210	Cvib_0223	preprotein translocase subunit YajC
165514421*	0.00243	COG0250	K02601	Cvib_1610	transcription antitermination protein NusG
165526166	0.00209	COG0413	K00606	Cvib_0725	ketopantoate hydroxymethyltransferase : panB; 3-methyl-2-oxobutanoate hydroxymethyltransferase
165562961	0.00203	COG0031	K01738	Cvib_0300	cysteine synthase
165526282	0.00189	COG1587	K01719	Cvib_1246	uroporphyrinogen-III synthase
165514409*	0.00173	COG0086	K03046	Cvib_1604	DNA-directed RNA polymerase beta' subunit/160 kD subunit (split gene in archaea and Syn)
165514577*	0.00162	COG1778	K03270	Cvib_1694	uncharacterized proteins of HAD superfamily, CMP-Neu5Ac homologs : 3-deoxy-D-manno-octulosonate 8-phosphatase, YrbI family; (KDO 8-P phosphatase)
165514581*a	0.00158	COG0542		Cvib_1696	ATPases with chaperone activity, ATP-binding subunit : AAA-2 domain protein
165536856	0.00155	COG0157	K00767	Cvib_0335	nicotinate-nucleotide pyrophosphorylase [carboxylating]
165547841	0.00146	COG0493	K00266	Cvib_1478	NADPH-dependent glutamate synthase beta chain and related oxidoreductases
165514651*	0.00139	COG0797	K03642	Cvib_1727	lipoproteins : rare lipoprotein A
165525906	0.00137	COG0750	K01417	Cvib_0137	predicted membrane-associated Zn-dependent proteases 1
165501975*	0.00135	COG0740	K01358	Cvib_0441	protease subunit of ATP-dependent Clp proteases
165505943	0.00135	COG0543		Cvib_0839	2-polypropenylphenol hydroxylase and related flavodoxin oxidoreductases : oxidoreductase FAD/NAD(P)-binding domain protein
165526296	0.00133	COG0082	K01736	Cvib_1253	chorismate synthase
165547993	0.00132	COG0497	K03631	Cvib_1402	ATPases involved in DNA repair : DNA repair protein RecN

Continued on next page

Table B.3 – *Continued from previous page*

Gene ID	NSA	COG/NR ID	KO	Locus	COG : KEGG/NR description
165547777	0.00126	COG0008	K01885	Cvib_1503	glutamyl-tRNA synthetase
165553075	0.00125	COG1158	K03628	Cvib_1537	transcription termination factor : Rho
165511737	0.00121	COG1726	K03615	Cvib_0797	Na ⁺ -transporting NADH:ubiquinone oxidoreductase alpha subunit : electron transport complex, RnfABCDGE type, C subunit
165526284	0.00118	COG0483	K01092	Cvib_1247	archaeal fructose-1,6-bisphosphatase and related enzymes of inositol monophosphatase family
165525808	0.00116	COG0331	K00645	Cvib_0199	(acyl-carrier-protein) S-malonyltransferase
165550953	0.00116	COG1022	K01897	Cvib_0930	long-chain acyl-CoA synthetases (AMP-forming) : AMP-dependent synthetase and ligase
165502369	0.00105	COG0440	K01653	Cvib_1171	acetolactate synthase, small subunit
165526250	0.00104	COG1522		Cvib_1231	transcriptional regulators : AsnC family
165525708	0.00102	COG0089	K02892	Cvib_0248	rplW; 50S ribosomal protein L23
165502825*	0.00102	COG0341	K03074	Cvib_0011	secF; preprotein translocase subunit SecF
165502225	0.00101	COG0557	K01147	Cvib_0574	Exoribonucleases : RNAse R; exoribonuclease II
165514389*	0.00101	COG0446		Cvib_1594	uncharacterized NAD(FAD)-dependent dehydrogenases : FAD-dependent pyridine nucleotide-disulphide oxidoreductase
165525802	0.00100	COG0333	K02911	Cvib_0202	rpmF; 50S ribosomal protein L32
165525664	0.00098	COG0100	K02948	Cvib_0271	30S ribosomal protein S11
165511903	0.00095	COG1240	K03404	Cvib_1058	Mg-chelatase subunit ChII : protoporphyrin IX magnesium-chelatase
165514579*	0.00094	COG2877	K01627	Cvib_1695	3-Deoxy-D-manno-octulose-2-phosphate synthase
165525806	0.00094	COG0332	K00648	Cvib_0200	3-oxoacyl-(acyl carrier protein) synthase III
165519368	0.00094	COG1192	K03496	Cvib_0388	ATPases involved in chromosome partitioning
165547931	0.00093	COG0217		Cvib_1432	uncharacterized ACR : hypothetical protein
165536866	0.00091	COG0468	K03553	Cvib_0340	RecA/RadA recombinase
165514413*	0.00086	COG0222	K02935	Cvib_1606	rplL; 50S ribosomal protein L7/L12
165547847	0.00086	COG0106	K01814	Cvib_1475	phosphoribosylformimino-5-aminoimidazole carboxamide ribotide isomerase
165525912	0.00085	COG0778		Cvib_0134	nitroreductase
165547827	0.00082	COG1136	K02003	Cvib_1485	ABC-type transport systems, involved in lipoprotein release, ATPase components
165547771	0.00080	COG0776	K05788	Cvib_1506	bacterial nucleoid DNA-binding protein : histone family protein DNA-binding protein; integration host factor subunit beta
165562901	0.00080	COG0003	K01551	Cvib_0328	predicted ATPase involved in chromosome partitioning : arsenite-activated ATPase ArsA
165530868	0.00079	COG2089	K01654	fnu:FN1684	sialic acid synthase : N-acetylneuraminate synthase
165562905	0.00078	COG0629	K03111	Cvib_0326	single-strand DNA-binding protein
165502829*	0.00077	COG0446	K00540	Cvib_0009	uncharacterized NAD(FAD)-dependent dehydrogenases : sulfide dehydrogenase (flavocytochrome), flavoprotein subunit

Continued on next page

Table B.3 – *Continued from previous page*

Gene ID	NSA	COG/NR ID	KO	Locus	COG : KEGG/NR description
165511991	0.00076	COG1418	K06950	Cvib_1112	predicted HD superfamily hydrolase : hypothetical protein
165547765	0.00075	COG0503	K00759	Cvib_1509	adenine/guanine phosphoribosyltransferases and related PRPP-binding proteins
165515181	0.00075	COG0711	K02109	Cvib_1741	F0F1-type ATP synthase b subunit
165502313	0.00075	COG0209	K00525	Cvib_1199	ribonucleotide-diphosphate reductase subunit alpha
165525750a	0.00074	COG0542		Cvib_0227	ATPases with chaperone activity, ATP-binding subunit : AAA ATPase, central domain protein
165525840	0.00074	COG0360	K02990	Cvib_0181	rpsF; 30S ribosomal protein S6
165547781	0.00073	COG0723	K02636	Cvib_1501	Rieske Fe-S protein : plastoquinol–plastocyanin reductase; cytochrome b6-f complex iron-sulfur subunit
165548025	0.00073	COG0058	K00688	Cvib_1386	alpha-glucan phosphorylase
165511773	0.00072	COG0524		Cvib_0779	sugar kinases, ribokinase family : PfkB domain protein
165514433*	0.00071	COG0480	K02355	Cvib_1616	translation elongation and release factors (GTPases) : fusA; elongation factor G
165526086	0.00071	COG2089	K01654	Cvib_1025	sialic acid synthase : N-acetylneuraminate synthase
165502143	0.00070	COG3040	K03098	Cvib_0516	bacterial lipocalin
165547991	0.00070	COG0329	K01714	Cvib_1403	dihydrodipicolinate synthase/N-acetylneuraminate lyase
165536870	0.00069	COG0136	K00133	Cvib_0342	aspartate semialdehyde dehydrogenase
165502129	0.00067	COG0158	K03841	Cvib_0509	fructose-1,6-bisphosphatase
165525834	0.00067	COG0359	K02939	Cvib_0184	rplI; 50S ribosomal protein L9
165547783	0.00065	COG1290	K00412	Cvib_1500	cytochrome b subunit of the bc complex : cytochrome b/b6, N-terminal domain protein; ubiquinol-cytochrome c reductase
165553031	0.00065	COG0184	K02956	Cvib_1557	rpsO; 30S ribosomal protein S15
165502097	0.00065	COG0127	K01516	Cvib_0493	non-canonical purine NTP pyrophosphatase, RdgB/HAM1 family
165514535*	0.00064	COG0366		Cvib_1672	glycosidases : trehalose synthase
165536860	0.00064	COG0544	K03545	Cvib_0337	FKBP-type peptidyl-prolyl cis-trans isomerase (trigger factor)
165519356	0.00060	COG1410	K00548	Cvib_0382	methionine synthase I, cobalamin-binding domain : metH; 5-methyltetrahydrofolate–homocysteine methyltransferase
165525900	0.00058	COG0284	K01591	Cvib_0140	orotidine 5'-phosphate decarboxylase
165547983	0.00057	COG0674	K03737	Cvib_1407	pyruvate:ferredoxin oxidoreductase and related 2-oxoacid:ferredoxin oxidoreductases, alpha sub-unit
165547901	0.00057	COG3155		Cvib_1447	uncharacterized sigma cross-reacting protein 27A (ES1 or KNP-I alpha protein) : isoprenoid biosynthesis protein with amidotransferase-like domain
165562941	0.00057	COG2319		Cvib_0309	WD-40 repeat protein
165526078	0.00056	COG0589		Cvib_1021	universal stress protein UspA and related nucleotide-binding proteins
165516491	0.00056	COG0760		Cvib_1572	parvulin-like peptidyl-prolyl isomerase : PpiC-type peptidyl-prolyl cis-trans isomerase

Continued on next page

Table B.3 – *Continued from previous page*

Gene ID	NSA	COG/NR ID	KO	Locus	COG : KEGG/NR description
165562981	0.00053	COG1043	K00677	Cvib_0290	acyl-[acyl carrier protein]-UDP-N-acetylglucosamine O-acyltransferase
165502845*	0.00052	COG0706	K03217	Cvib_1771	preprotein translocase subunit YidC
165525718	0.00051	COG0480	K02355	Cvib_0243	translation elongation and release factors (GTPases) : fusA; elongation factor G
165526290	0.00051	COG0511		Cvib_1250	biotin carboxyl carrier protein : biotin/lipoyl attachment domain-containing protein
165557791	0.00051	COG0074		Cvib_0866	succinyl-CoA synthetase alpha subunit : ATP citrate lyase subunit 2
165547973	0.00050	COG1493	K06023	Cvib_1412	serine kinase of the HPr protein, regulates carbohydrate metabolism
165502247	0.00050	COG0234	K04078	Plut_0541	groES; co-chaperonin GroES
165514671*	0.00050	COG0636	K02110	Plut_2097	FOF1-type ATP synthase c subunit/Archaeal/vacuolar-type H+-ATPase subunit K : ATP synthase F0, C subunit
165502267	0.00050	COG1077	K03569	Cvib_0595	HSP70 class molecular chaperones involved in cell morphogenesis : cell shape determining protein, MreB/Mrl family
165525868	0.00049	COG0188	K02469	Cvib_0172	DNA gyrase subunit A
165514647*	0.00048	COG0167	K00226	Cvib_1724	dihydroorotate dehydrogenase 2
165509259*	0.00046	COG0793	K03797	Cvib_0018	periplasmic protease : carboxyl-terminal protease
165548143	0.00046	COG0261	K02888	Cvib_1329	rplU; 50S ribosomal protein L21
165514553*	0.00045	COG0001	K01845	Cvib_1681	glutamate-1-semialdehyde 2,1-aminomutase
165525814	0.00044	COG0304	K09458	Cvib_0196	3-oxoacyl-[acyl-carrier-protein] synthase II
165547833	0.00043	COG2226	K03183	Cvib_1482	methylase involved in ubiquinone/menaquinone biosynthesis : demethylmenaquinone methyl-transferase
165547919	0.00042	COG0036	K01783	Cvib_1438	ribulose-5-phosphate 3-epimerase
165525676	0.00042	COG1841	K02907	Cvib_0264	rplD; 50S ribosomal protein L30
165502421	0.00042	COG0443	K04043	Cvib_1158	chaperone protein DnaK
165525692	0.00042	COG0093	K02874	Cvib_0256	rplN; 50S ribosomal protein L14
165525970	0.00042	COG1220	K03667	Cvib_0959	ATP-dependent protease, ATPase subunit : hslU
165525828	0.00041	COG0292	K02887	Cvib_0187	rplT; 50S ribosomal protein L20
165502239	0.00040	COG0596		Cvib_0581	predicted hydrolases or acyltransferases (alpha/beta hydrolase superfamily)
165525710	0.00039	COG0088	K02926	Cvib_0247	rplD; 50S ribosomal protein L4
165502125	0.00039	COG2838	K00031	Cvib_0507	monomeric isocitrate dehydrogenase
165526072	0.00039	COG1038	K01571	Cvib_1018	pyruvate carboxylase, C-terminal domain/subunit : biotin/lipoyl attachment domain-containing protein; oxaloacetate decarboxylase, alpha subunit
165562947	0.00038	COG0040	K00765	Cvib_0307	hisG; ATP phosphoribosyltransferase
165519380	0.00038	COG0447	K01661	Cvib_0394	dihydroxynaphthoic acid synthase
165514407*	0.00038	COG0439	K01961	Cvib_1603	acetyl-CoA carboxylase, biotin carboxylase

Continued on next page

Table B.3 – *Continued from previous page*

Gene ID	NSA	COG/NR ID	KO	Locus	COG : KEGG/NR description
165547843	0.00038	COG0543	K00528	Cvib_1477	2-polyprenylphenol hydroxylase and related flavodoxin oxidoreductases : ferredoxin–NADP(+) reductase subunit alpha
165502249	0.00038	COG0459	K04077	Cvib_0586	chaperonin GroEL (HSP60 family)
165525978	0.00038	COG0190	K00288	Cvib_0963	methenyltetrahydrofolate cyclohydrolase (NADP+)
165548015	0.00037	COG0115	K00826	Cvib_1391	4-amino-4-deoxychorismate lyase : branched-chain amino acid aminotransferase
165526070	0.00037	COG1883	K01572	Cvib_1017	Na ⁺ -transporting methylmalonyl-CoA/oxaloacetate decarboxylase, beta subunit
165502323	0.00037	COG2406	K03594	Cvib_1194	uncharacterized ACR : ferritin, Dps family protein
165502157	0.00036	COG0182	K08963	Cvib_0532	translation initiation factor 2B subunit I family (IF-2BI); methylthioribose-1-phosphate isomerase
165502159	0.00036	COG0005	K03783	Cvib_0533	purine nucleoside phosphorylase
165526084	0.00035	COG0326	K04079	Cvib_1024	heat shock protein 90; molecular chaperone HtpG
165547741*	0.00034	COG1109	K01840	Cvib_1521	phosphoglucomutase
165547943	0.00033	COG0365	K01895	Cvib_1426	acyl-coenzyme A synthetases/AMP-(fatty) acid ligases : acetyl-coenzyme A synthetase
165547811	0.00033	COG1118	K02017	Cvib_1494	ABC-type sulfate/molybdate transport systems, ATPase component
165501997*	0.00032	COG0404	K00605	Cvib_0451	glycine cleavage system T protein (aminomethyltransferase)
165548139	0.00032	COG0039	K00026	Cvib_1331	malate dehydrogenase
165547815	0.00031	COG0725	K02020	Cvib_1492	ABC-type molybdate transport system, periplasmic component
165526254	0.00031	COG3349	K00514	Cvib_1233	uncharacterized ACR : zeta-carotene desaturase
165519338*	0.00031	COG1023	K00033	Cvib_0374	6-phosphogluconate dehydrogenase, family 2
165525774	0.00031	COG0315	K03637	Cvib_0215	moaC; bifunctional molybdenum cofactor biosynthesis protein C/molybdopterin-binding protein
165514597*	0.00031	COG0248		Cvib_1704	Ppx/GppA phosphatase
165505937	0.00030	COG1908		Cvib_0842	coenzyme F420-reducing hydrogenase, delta subunit : methyl-viologen-reducing hydrogenase, delta subunit
165505095	0.00030	COG1192		Cvib_0908	ATPases involved in chromosome partitioning : cobyric acid a,c-diamide synthase
165547897	0.00030	COG0178	K03701	Cvib_1449	excinuclease ABC subunit A
165553023	0.00030	COG0532	K02519	Cvib_1561	translation initiation factor 2 (GTPase) : infB
165553083	0.00029	COG3637		Cvib_1533	opacity protein and related surface antigens : porin
165562903	0.00029	COG0543	K02823	Cvib_0327	2-polyprenylphenol hydroxylase and related flavodoxin oxidoreductases : dihydroorotate oxidase B, electron transfer subunit
165547817	0.00029	COG0157	K03813	Cvib_1491	nicotinate-nucleotide pyrophosphorylase : ModD protein; molybdenum transport protein
165511803	0.00028	COG0152	K01923	Cvib_0763	phosphoribosylaminoimidazole-succinocarboxamide synthase
165502273	0.00028	COG1049	K01682	Cvib_0598	aconitase B: bifunctional aconitate hydratase 2/2-methylisocitrate dehydratase

Continued on next page

Table B.3 – *Continued from previous page*

Gene ID	NSA	COG/NR ID	KO	Locus	COG : KEGG/NR description
165525716	0.00028	COG0050	K02358	Cvib_0244	GTPases - translation elongation factors : tuf
165505137*	0.00027	COG0724		Cvib_0890	RNA-binding proteins (RRM domain)
165511799	0.00027	COG0021	K00615	Cvib_0765	transketolase subunit A
165502001*	0.00027	COG0694	K07400	Cvib_0453	thioredoxin-like proteins and domains : nitrogen-fixing NifU domain protein
165525700	0.00027	COG0092	K02982	Cvib_0252	rpsC; 30S ribosomal protein S3
165548043	0.00027	COG0848		Cvib_1377	biopolymer transport protein ExbD/TolR
165502837*	0.00027	COG0426		Cvib_0005	uncharacterized flavoproteins : beta-lactamase domain protein
165502823*	0.00027	COG0760	K03771	Cvib_0012	parvulin-like peptidyl-prolyl isomerase : PpiC-type peptidyl-prolyl cis-trans isomerase
165525682	0.00026	COG0097	K02933	Cvib_0261	rplF; 50S ribosomal protein L6
165509275*	0.00026	COG0055	K02112	Cvib_0025	F0F1 ATP synthase subunit beta
165514365a	0.00026	COG0542	K03696	Cvib_1580	ATPases with chaperone activity, ATP-binding subunit : AAA-2 domain protein; ATP-dependent Clp protease
165525766	0.00026	COG3245		Cvib_0219	cytochrome c5
165514371*	0.00026	COG0451		Cvib_1582	nucleoside-diphosphate-sugar epimerases : NAD-dependent epimerase/dehydratase
165525810	0.00026	COG1028	K00059	Cvib_0198	dehydrogenases with different specificities (related to short-chain alcohol dehydrogenases) : 3-oxoacyl-[acyl-carrier-protein] reductase
165502383	0.00025	COG0823	K03641	Cvib_1164	periplasmic component of the Tol biopolymer transport system : WD40 domain protein beta propeller; TolB protein
165557763	0.00025	COG0137	K01940	Cvib_0882	argininosuccinate synthase
165502177	0.00024	COG0591		Cvib_0542	Na+/proline, Na+/panthothenate symporters and related permeases
165525720	0.00024	COG0049	K02992	Cvib_0242	30S ribosomal protein S7
165553085	0.00024	COG0729	K07277	Cvib_1532	predicted outer membrane protein : surface antigen (D15)
165525770	0.00024	COG0345	K00286	Cvib_0217	pyrroline-5-carboxylate reductase
165514453*	0.00023	COG0527	K00928	Cvib_1626	aspartokinases
165509301*	0.00023	COG2920	K00396	Cvib_0038	sulfite reductase, gamma subunit : DsrC family protein
165514489*	0.00023	COG1538		Cvib_1644	outer membrane protein : outer membrane efflux protein
165562971	0.00022	COG0105	K00940	Cvib_0295	nucleoside diphosphate kinase
165562957	0.00022	COG0822	K04488	Cvib_0302	NifU homologs involved in Fe-S cluster formation
165501969*	0.00022	COG1752		Cvib_0421	predicted esterase of the alpha-beta hydrolase superfamily : surface antigen (D15)
165526170	0.00022	COG1832	K06929	Cvib_0723	predicted CoA-binding protein
165514455*	0.00021	COG0224	K02115	Cvib_1627	ATP synthase F1, gamma subunit
165562919	0.00021	COG1629	K02014	Plut_0256	outer membrane receptor proteins, mostly Fe transport : ferric siderophore receptor, putative, TonB receptor family

Continued on next page

Table B.3 – *Continued from previous page*

Gene ID	NSA	COG/NR ID	KO	Locus	COG : KEGG/NR description
16550965	0.00020	COG0541	K03106	Cvib_0936	signal recognition particle GTPase : subunit FFH/SRP54 (SRP54)
165502821*	0.00020	COG0187	K02470	Cvib_0013	DNA gyrase subunit B
165509279*	0.00020	COG1274	K01596	Cvib_0027	phosphoenolpyruvate carboxykinase (GTP)
165514471*	0.00020	COG0407	K01599	Cvib_1635	uroporphyrinogen-III decarboxylase
165505923	0.00020	COG0653	K03070	Cvib_0853	preprotein translocase subunit SecA (ATPase, RNA helicase)
165526076	0.00020	COG1951	K01676	Cvib_1020	tartrate dehydratase alpha subunit/Fumarate hydratase class I, N-terminal domain
165547989	0.00020	COG0403	K00282	Cvib_1404	glycine cleavage system protein P (pyridoxal-binding), N-terminal domain : glycine dehydrogenase subunit 1
165550943	0.00020	COG0399		Cvib_0925	predicted pyridoxal phosphate-dependent enzyme apparently involved in regulation of cell wall biogenesis : DegT/DnrJ/EryC1/StrS aminotransferase
165519308*	0.00019	COG1233		Cvib_0356	phytoene dehydrogenase and related proteins : FAD dependent oxidoreductase
165525704	0.00019	COG0185	K02965	Cvib_0250	rpsS; 30S ribosomal protein S19
165502209	0.00019	COG0493	K00266	Cvib_0559	NADPH-dependent glutamate synthase beta chain and related oxidoreductases : gltD
165548183	0.00019	COG0057	K00134	Cvib_1310	glyceraldehyde-3-phosphate dehydrogenase
165509303*	0.00018	COG2221	K00396	Cvib_0039	oxidoreductase related to nitrite reductase : sulfite reductase, dissimilatory-type alpha subunit
165502855*	0.00018	COG0126	K00927	Cvib_1766	pgk; phosphoglycerate kinase
165548189	0.00018	COG0399		Cvib_1298	predicted pyridoxal phosphate-dependent enzyme apparently involved in regulation of cell wall biogenesis : DegT/DnrJ/EryC1/StrS aminotransferase
165502083	0.00018	COG0723	K09879	Cvib_0486	Rieske Fe-S protein : isorenieratene synthase
165502241	0.00018	COG1959		Cvib_0582	predicted transcriptional regulator : transcriptional regulator, BadM/Rrf2 family
165505101	0.00018	COG1744	K07335	Cvib_0906	surface lipoprotein
165562997	0.00018	COG1348	K04037	Cvib_0283	nitrogenase subunit NifH (ATPase) : chlL, bchL; protochlorophyllide reductase iron-sulfur ATP-binding protein
165514479*	0.00017	COG0517		Plut_1996	CBS domains
165509257*	0.00017	COG2171	K00674	Cvib_0017	tetrahydrodipicolinate N-succinyltransferase : dapD; 2,3,4,5-tetrahydropyridine-2-carboxylate N-succinyltransferase
165525898	0.00017	COG0449	K00820	Cvib_0141	glucosamine 6-phosphate synthetase, contains amidotransferase and phosphosugar isomerase domains : glutamine-fructose-6-phosphate transaminase
165526040	0.00017	COG0226	K02040	Cvib_0998	phosphate binding protein; phosphate transport system substrate-binding protein
165526106	0.00017	COG0718	K09747	Cvib_1034	uncharacterized BCR : conserved hypothetical protein 103
165525660	0.00017	COG0202	K03040	Cvib_0273	DNA-directed RNA polymerase subunit alpha
165563007	0.00017	COG0218	K03978	Cvib_0278	yihA, ysxC, engB; GTPase EngB
165526124	0.00016	COG0589		Cvib_1041	universal stress protein UspA and related nucleotide-binding proteins

Continued on next page

Table B.3 – *Continued from previous page*

Gene ID	NSA	COG/NR ID	KO	Locus	COG : KEGG/NR description
165526138	0.00016	COG1554		Cvib_1047	trehalose and maltose hydrolases (possible phosphorylases) : beta-phosphoglucomutase family hydrolase
165525892	0.00016	COG0724		Cvib_0162	RNA-binding proteins (RRM domain)
165514417*	0.00016	COG0081	K02863	Cvib_1608	rplA; 50S ribosomal protein L1
165550985	0.00016	COG0260	K01255	Cvib_0947	leucyl aminopeptidase
165514655*	0.00016	COG1899	K00809	Cvib_1729	deoxyhypusine synthase
165525670	0.00016	COG0024	K01265	Cvib_0267	methionine aminopeptidase : type I
165526140	0.00015	COG0809	K07568	Cvib_1048	S-adenosylmethionine:tRNA-ribosyltransferase-isomerase (queuine synthetase) : queuosine biosynthesis protein
165502015	0.00015	COG0264	K02357	Cvib_0459	elongation factor Ts : tsf
165514419*	0.00015	COG0080	K02867	Plut_1966	rplK; 50S ribosomal protein L11
165553033	0.00015	COG1561		Cvib_1556	uncharacterized stress-induced protein : hypothetical protein
165519394	0.00015	COG0372	K01647	Cvib_0401	citrate synthase
165548035	0.00015	COG0112	K00600	Cvib_1381	glycine hydroxymethyltransferase
165525666	0.00014	COG0099	K02952	Cvib_0270	rpsM; 30S ribosomal protein S13
165502377	0.00014	COG0811	K03562	Cvib_1167	biopolymer transport proteins : MotA/TolQ/ExbB proton channel
165519372	0.00014	COG0289	K00215	Cvib_0390	dihydridipicolinate reductase
165526294	0.00014	COG0113	K01698	Cvib_1252	delta-aminolevulinic acid dehydratase
165553057	0.00014	COG0142	K00795	Cvib_1546	geranyltransterase
165511739	0.00014	COG1805	K03614	Cvib_0796	Na ⁺ -transporting NADH:ubiquinone oxidoreductase subunit 2 : electron transport complex, RnfABCDGE type, D subunit
165553087	0.00014	COG0020	K00806	Cvib_1531	undecaprenyl pyrophosphate synthetase
165502433	0.00013	COG0633	K08953	Cvib_1151	ferredoxin : chlorosome envelope protein J
165526246	0.00013	COG0174	K01915	Cvib_1230	glutamine synthetase, catalytic region
165502389	0.00013	COG1729		Cvib_1161	uncharacterized BCR : tetratricopeptide domain protein
165562927	0.00012	COG2265	K03428	Cvib_0317	SAM-dependent methyltransferases related to tRNA (uracil-5)-methyltransferase : Mg-protoporphyrin IX methyl transferase
165511967	0.00012	COG1538		Cvib_1100	outer membrane protein : outer membrane efflux protein
165514411*	0.00012	COG0085	K03043	Cvib_1605	rpoB; DNA-directed RNA polymerase subunit beta
165502197	0.00012	COG0045	K01903	Cvib_0553	succinyl-CoA synthetase (ADP-forming) beta subunit
165525686	0.00012	COG0199	K02954	Plut_0194	rpsN; 30S ribosomal protein S14
165548039	0.00012	COG0811	K03561	Cvib_1379	biopolymer transport proteins : MotA/TolQ/ExbB proton channel
165509331*	0.00012	COG0007	K02302	Cvib_0053	uroporphyrinogen-III C-methyltransferase

Continued on next page

Table B.3 – *Continued from previous page*

Gene ID	NSA	COG/NR ID	KO	Locus	COG : KEGG/NR description
165518169*	0.00012	COG2221	K00396	Cvib_0040	oxidoreductase related to nitrite reductase : sulfite reductase, dissimilatory-type beta subunit
165547929	0.00012	COG0077	K04518	Cvib_1433	prephenate dehydratase
165557761	0.00012	COG0165	K01755	Cvib_0883	argininosuccinate lyase
165511743	0.00012	COG1347	K03613	Cvib_0794	Na ⁺ -transporting NADH:ubiquinone oxidoreductase subunit 4 : SoxR-reducing system protein RsxE; electron transport complex protein RnfE
165511765	0.00012	COG0003	K01551	Cvib_0783	predicted ATPase involved in chromosome partitioning : arsenite-activated ATPase ArsA
165502673*	0.00011	COG1396		Plut_1890	predicted transcriptional regulators: XRE family
165505117	0.00011	COG0698	K01808	Cvib_0896	ribose 5-phosphate isomerase RpiB
165526204	0.00011	COG0019	K01586	Cvib_0705	diaminopimelate decarboxylase
165526060	0.00011	COG0526	K03671	Cvib_1012	thiol-disulfide isomerase and thioredoxins
165501979*	0.00010	COG0568	K03086	Cvib_0443	DNA-directed RNA polymerase sigma subunits (sigma70/sigma32) : RpoH
165525702	0.00010	COG0091	K02890	Cvib_0251	rplV; 50S ribosomal protein L22
165562969	0.00010	COG1225		Cvib_0296	peroxiredoxin
165548179	0.00010	COG0484	K03686	Cvib_1312	molecular chaperones (contain C-terminal Zn finger domain) : chaperone protein DnaJ
165526058	0.00010	COG0492	K00384	Cvib_1011	thioredoxin reductase
165514477*	0.00010	COG1053	K00239	Cvib_1638	succinate dehydrogenase/fumarate reductase, flavoprotein subunits
165514475*	0.00010	COG0479	K00240	Cvib_1637	succinate dehydrogenase/fumarate reductase Fe-S protein : succinate dehydrogenase subunit B
165514463*	0.00010	COG0204	K00655	Cvib_1631	1-acyl-sn-glycerol-3-phosphate acyltransferase
165512005	0.00010	COG0499	K01251	Cvib_1122	S-adenosyl-L-homocysteine hydrolase; adenosylhomocysteinase
165511973	0.00010	COG2077	K00435	Cvib_1103	peroxiredoxin : thiol peroxidase (atypical 2-Cys peroxiredoxin)
165519288*	0.00009	COG0031	K01697	Cvib_0346	cysteine synthase
165502065	0.00009	COG2177	K09811	Cvib_0478	cell division protein FtsX
165502349	0.00009	COG1610	K09117	Cvib_1181	uncharacterized ACR : GatB/YqeY domain protein
165502361	0.00009	COG0065	K01703	Cvib_1175	homoaconitate hydratase family protein; K01703 3-isopropylmalate/(R)-2-methylmalate dehydratase large subunit
165526160	0.00009	COG0047	K01952	Cvib_0728	phosphoribosylformylglycinamide synthase I
165526016	0.00009	COG3118	K05838	Cvib_0982	thioredoxin domain-containing protein
165525690	0.00009	COG0198	K02895	Plut_0192	rplX; 50S ribosomal protein L24
165519322*	0.00009	COG2606		Cvib_0364	uncharacterized ACR : YbaK/prolyl-tRNA synthetase associated region
165502387	0.00009	COG2885		Cvib_1162	outer membrane protein and related peptidoglycan-associated (lipo)proteins : OmpA/MotB domain protein
165525762	0.00009	COG0075	K00839	Cvib_0221	serine-pyruvate aminotransferase/archaeal aspartate aminotransferase : aminotransferase, class V

Continued on next page

Table B.3 – *Continued from previous page*

Gene ID	NSA	COG/NR ID	KO	Locus	COG : KEGG/NR description
165511763	0.00009	COG0722	K01626	Cvib_0784	3-Deoxy-D-arabino-heptulosonate 7-phosphate (DAHP) synthase : phospho-2-dehydro-3-heoxyheptonate aldolase; 3-deoxy-7-phosphoheptulonate synthase
165525764	0.00009	COG3245		Cvib_0220	cytochrome c5
165514427*	0.00009	COG0821	K03526	Cvib_1613	essential bacterial protein, involved in density-dependent regulation of peptidoglycan biosynthesis : 4-hydroxy-3-methylbut-2-en-1-yl diphosphate synthase
165525908	0.00009	COG0216	K02835	Cvib_0136	prfA; peptide chain release factor 1
165526270	0.00009	COG1217	K06207	Cvib_1242	predicted membrane GTPase involved in stress response : GTP-binding protein TypA
165526178	0.00008	COG0845	K02005	Cvib_0719	membrane-fusion protein : efflux transporter, RND family, MFP subunit; HlyD family secretion protein
165525656*	0.00008	COG0357	K03501	Cvib_0275	predicted S-adenosylmethionine-dependent methyltransferase involved in bacterial cell division: gidB; glucose-inhibited division protein B
165519392	0.00008	COG1432		Cvib_0400	uncharacterized ACR : hypothetical protein
165526108	0.00008	COG0021	K00615	Cvib_1035	transketolase subunit B
165502205	0.00008	COG0588	K01834	Cvib_0557	phosphoglycerate mutase 1
165548031	0.00008	COG0458	K01955	Cvib_1383	carbamoyl-phosphate synthase large subunit (split gene in MJ)
165509283*	0.00008	COG3360	K09165	Cvib_0029	uncharacterized ACR : protein of unknown function DUF1458; hypothetical protein
165514653*	0.00008	COG0176	K00616	Cvib_1728	putative translaldolase
165514561*	0.00008	COG0243	K08352	Cpha266_2562	anaerobic dehydrogenases, typically selenocysteine-containing : formate dehydrogenase; thiosulfate reductase
165525714	0.00008	COG0051	K02946	Cvib_0245	rpsJ, nusE; 30S ribosomal protein S10
165525826	0.00008	COG0290	K02520	Cvib_0189	infC; translation initiation factor IF-3
165509297*	0.00008	COG0425		Cvib_0036	predicted redox protein, regulator of disulfide bond formation : SirA family protein
165526206	0.00008	COG0267	K02913	Cvib_0704	rpmG; 50S ribosomal protein L33
165562999	0.00008	COG2710	K04039	Cvib_0282	nitrogenase molybdenum-iron protein, alpha and beta chains : light-independent protochlorophyllide reductase subunit B
165525658	0.00008	COG0203	K02879	Cvib_0274	rplQ; 50S ribosomal protein L17
165501991*	0.00008	COG1704	K03744	Cvib_0448	uncharacterized ACR : LemA family protein
165525684	0.00007	COG0096	K02994	Cvib_0260	rpsH; 30S ribosomal protein S8
165501995*	0.00007	COG3762	K08988	Cvib_0450	predicted membrane protein : protein of unknown function DUF477
165525960	0.00007	COG1979	K00001	Cvib_0955	uncharacterized oxidoreductases, Fe-dependent alcohol dehydrogenase family
165525712	0.00007	COG0087	K02906	Cvib_0246	rplC; 50S ribosomal protein L3
165519466	0.00007	COG0489	K03593	Cvib_0454	ATP-binding protein involved in chromosome partitioning : protein of unknown function DUF59

Continued on next page

Table B.3 – *Continued from previous page*

Gene ID	NSA	COG/NR ID	KO	Locus	COG : KEGG/NR description
165536850*	0.00007	COG0003	K01551	Cvib_0332	predicted ATPase involved in chromosome partitioning : arsenite-activated ATPase ArsA
165511901b	0.00007	COG1429	K03403	Cvib_1057	cobalamin biosynthesis protein CobN and related Mg-chelatases : hydrogenobyrinic acid a,c-diamide cobaltochelatase
165553047	0.00007	COG2825	K06142	Cvib_1549	outer membrane protein : outer membrane chaperone Skp (OmpH)
165547985	0.00007	COG0566	K03218	Cvib_1406	rRNA methylases : RNA methyltransferase, TrmH family, group 3
165548057	0.00007	COG0635	K02495	Cvib_1370	coproporphyrinogen III oxidase and related Fe-S oxidoreductases
165525972	0.00007	COG0638	K01419	Cvib_0960	proteasome protease subunit : ATP-dependent HslUV protease, peptidase subunit HslV
165548053	0.00007	COG1252	K03885	Cvib_1373	NADH dehydrogenase, FAD-containing subunit : FAD-dependent pyridine nucleotide-disulphide oxidoreductase
165502427	0.00007	COG1595	K03088	Cvib_1154	DNA-directed RNA polymerase specialized sigma subunits, sigma24 homologs : RpoE; RNA polymerase sigma-70 factor, ECF subfamily
165514401*	0.00006	COG0776	K03530	Plut_1957	bacterial nucleoid DNA-binding protein : histone-like DNA-binding protein; HU-beta
165502013*	0.00006	COG0052	K02967	Cvib_0458	rpsB; 30S ribosomal protein S2
165525904	0.00006	COG0743	K00099	Cvib_0138	1-deoxy-D-xylulose 5-phosphate reductoisomerase
165514571*	0.00006	COG0461	K00762	Cvib_1691	pyrE; orotate phosphoribosyltransferase
165502127	0.00006	COG1692	K09769	Cvib_0508	uncharacterized BCR : metallophosphoesterase
165502831*	0.00006	COG2863	K00540	Cvib_0008	cytochrome c553 : sulfide dehydrogenase (flavocytochrome), cytochrome c subunit
165512003	0.00006	COG0192	K00789	Cvib_1121	Sadenosylmethionine synthetase
165562939	0.00006	COG1278	K03704	Cvib_0310	cold shock proteins : cold-shock DNA-binding protein family (beta-ribbon, CspA family)
165502325	0.00006	COG1592		Cvib_1193	rubrerythrin
165514457*	0.00006	COG0056	K02111	Cvib_1628	F0F1 ATP synthase subunit alpha
165502099	0.00006	COG0854	K03474	Cvib_0494	pyridoxal phosphate biosynthetic protein PdxJ; pyridoxine 5-phosphate synthase
165562943	0.00006	COG2319		Cvib_0309	WD-40 repeat protein
165548049	0.00006	COG0160	K00818	Cvib_1374	PLP-dependent aminotransferases : acetylornithine and succinylornithine aminotransferase
165547915	0.00006	COG0458	K01955	Cvib_1440	carbamoyl-phosphate synthase large subunit (split gene in MJ)
165501985*	0.00006	COG0612		Cvib_0445	predicted Zn-dependent peptidases
165501959*	0.00006	COG1611	K06966	Cvib_0416	predicted Rossmann fold nucleotide-binding protein : conserved hypothetical protein 730
165511907	0.00006	COG1239	K03405	Cvib_1059	Mg-chelatase subunit ChII : protoporphyrin IX magnesium-chelatase
165502365	0.00006	COG0473	K00052	Cvib_1173	isocitrate/isopropylmalate dehydrogenase
165547721*	0.00005	COG0154	K02433	Cvib_1530	aspartyl/glutamyl-tRNA(Asn/Gln) amidotransferase subunit A
165512001	0.00005	COG1209	K00973	Cvib_1120	dTDP-glucose pyrophosphorylase : 3 glucose-1-phosphate thymidylyltransferase
165526008	0.00005	COG0605	K04564	Cvib_0978	superoxide dismutase, Fe-Mn family
165525688	0.00005	COG0094	K02931	Cvib_0258	rplE; 50S ribosomal protein L5

Continued on next page

Table B.3 – *Continued from previous page*

Gene ID	NSA	COG/NR ID	KO	Locus	COG : KEGG/NR description
165548233	0.00005	COG0149	K01803	Cvib_1275	triosephosphate isomerase
165525674	0.00005	COG0200	K02876	Cvib_0265	rplO; 50S ribosomal protein L15
165511945	0.00005	COG1143	K00338	Cvib_1088	formate hydrogenlyase subunit 6/NADH:ubiquinone oxidoreductase 23 kD subunit (chain I)
165511741	0.00005	COG2869		Cvib_0795	Na ⁺ -transporting NADH:ubiquinone oxidoreductase gamma subunit : electron transport complex, RnfABCDGE type, G subunit
165502243	0.00005	COG0178	K03701	Cvib_0583	excinuclease ABC subunit A
165526286	0.00005	COG0777	K01966	Cvib_1248	acetyl-CoA carboxylase beta subunit : propionyl-CoA carboxylase beta chain
165548017	0.00005	COG0205	K00850	Cvib_1390	6-phosphofructokinase
165502343	0.00005	COG2873	K01740	Cvib_1184	O-acetylhomoserine/O-acetylserine sulfhydrylase
165511795	0.00005	COG0436	K00812	Cvib_0768	PLP-dependent aminotransferases : aspartate aminotransferase
165514397*	0.00005	COG1013	K00175	Cvib_1598	pyruvate:ferredoxin oxidoreductase and related 2-oxoacid:ferredoxin oxidoreductases, beta sub-unit
165553021	0.00005	COG0195	K02600	Cvib_1562	nusA; transcription elongation factor NusA; N utilization substance protein A
165514415*	0.00005	COG0244	K02864	Cvib_1607	rplJ; 50S ribosomal protein L10
165525916	0.00005	COG0446		Cvib_0131	uncharacterized NAD(FAD)-dependent dehydrogenases : FAD-dependent pyridine nucleotide-disulphide oxidoreductase
165526186	0.00005	COG2885		Cvib_0715	outer membrane protein and related peptidoglycan-associated (lipo)proteins : OmpA/MotB domain protein
165514585*	0.00005	COG2062	K08296	Cvib_1698	phosphohistidine phosphatase SixA
165525698	0.00005	COG0197	K02878	Cvib_0253	rplP; 50S ribosomal protein L16
165501973*	0.00005	COG1351	K03465	Plut_0366	predicted alternative thymidylate synthase: thyX
165548141	0.00004	COG0211	K02899	Cvib_1330	rpmA; 50S ribosomal protein L27
165547947	0.00004	COG1185	K00962	Cvib_1424	polyribonucleotide nucleotidyltransferase (polynucleotide phosphorylase)
165502321	0.00004	COG0450	K03386	Cvib_1195	peroxiredoxin (alkyl hydroperoxide reductase subunit C)
165525706	0.00004	COG0090	K02886	Cvib_0249	rplB; 50S ribosomal protein L2
165562989	0.00004	COG0241	K05602	Cvib_0287	histidinol-phosphate phosphatase family protein
165502123	0.00004	COG0623	K00208	Cvib_0506	enoyl-[acyl-carrier-protein] reductase [NADH]
165502053	0.00004	COG1734		Cvib_0476	DnaK suppressor protein : transcriptional regulator, TraR/DksA family
165502207	0.00004	COG0069	K00284	Cvib_0558	glutamate synthase (NADH) large subunit; K00284 glutamate synthase (ferredoxin)
165514485*	0.00004	COG0841		Cvib_1642	cation/multidrug efflux pump : acriflavin resistance protein
165550957	0.00004	COG0335	K02884	Cvib_0932	rplS; 50S ribosomal protein L19
165547723*	0.00004	COG0074	K01902	Cvib_1529	succinyl-CoA synthetase (ADP-forming) alpha subunit
165502827*	0.00004	COG0342	K03072	Cvib_0010	secD; preprotein translocase subunit SecD

Continued on next page

Table B.3 – *Continued from previous page*

Gene ID	NSA	COG/NR ID	KO	Locus	COG : KEGG/NR description
165547889	0.00004	COG1151	K00378	Cvib_1455	6Fe-6S prismane cluster-containing protein : hydroxylamine reductase
165501971*	0.00004	COG0777	K01963	Cvib_0422	acetyl-CoA carboxylase beta subunit : acetyl-coenzyme A carboxylase carboxyl transferase subunit alpha
165526020	0.00004	COG0277		Cvib_0987	FAD linked oxidase domain protein
165526194	0.00004	COG1825	K02897	Cvib_0711	50S ribosomal protein L25/general stress protein Ctc
165512009	0.00004	COG0596		Cvib_1124	predicted hydrolases or acyltransferases (alpha/beta hydrolase superfamily)
165525836	0.00004	COG0238	K02963	Cvib_0183	rpsR; 30S ribosomal protein S18
165525680	0.00003	COG0256	K02881	Cvib_0262	rplR; 50S ribosomal protein L18
165547963	0.00003	COG0780	K06879	Cvib_1417	enzyme related to GTP cyclohydrolase I : 7-cyano-7-deazaguanine reductase
165514617*	0.00003	COG0550	K03168	Cvib_1714	topoisomerase IA
165525894	0.00003	COG1090	K07071	Cvib_0161	predicted nucleoside-diphosphate sugar epimerases (SulA family) : domain of unknown function DUF1731
165525944	0.00003	COG0376	K03782	cpb:Cphamn1_0152	catalase/peroxidase HPI
165553059	0.00003	COG1304	K01823	Cvib_1545	L-lactate dehydrogenase (FMN-dependent) and related alpha-hydroxy acid dehydrogenases : isopentenyl pyrophosphate isomerase
165502021	0.00003	COG3347		Cvib_0462	uncharacterized ACR : short chain dehydrogenase
165502163	0.00003	COG0652	K03767	Cvib_0535	peptidyl-prolyl cis-trans isomerase (rotamase) - cyclophilin family
165526224	0.00003	COG0451	K01795	Cvib_1219	nucleoside-diphosphate-sugar epimerases : NAD-dependent epimerase/dehydratase
165548235	0.00003	COG0422	K03147	Cvib_1273	thiamine biosynthesis protein ThiC
165553035	0.00003	COG0194	K00942	Cvib_1555	gmk; guanylate kinase
165550983	0.00003	COG1004	K00012	Cvib_0945	Predicted UDP-glucose 6-dehydrogenase
165519410	0.00003	COG0254	K02909	Plut_0349	rpmE; 50S ribosomal protein L31
165519370	0.00003	COG1475	K03497	Cvib_0389	predicted transcriptional regulators : chromosome segregation DNA-binding protein; ParB family
165505127	0.00003	COG0191	K01624	Cvib_0892	fructose-bisphosphate aldolase
165514563*	0.00003	COG0437	K04014	Cpha266_2563	Fe-S-cluster-containing hydrogenase components 1 : 4Fe-4S ferredoxin, iron-sulfur binding domain protein; formate-dependent nitrite reductase, Fe-S protein
165562929	0.00003	COG1032	K04035	Cvib_0316	Fe-S oxidoreductases family 2 : magnesium-protoporphyrin IX monomethyl ester anaerobic oxidative cyclase
165562921	0.00003	COG1629	K02014	CT1953	outer membrane receptor proteins, mostly Fe transport : ferric siderophore receptor, putative, TonB receptor family
165519408	0.00003	COG0233	K02838	Cvib_0408	ribosome recycling factor
165526146	0.00003	COG1032		Cvib_1051	Fe-S oxidoreductases family 2 : radical SAM domain protein

Table B.3 – *Continued from previous page*

Gene ID	NSA	COG/NR ID	KO	Locus	COG : KEGG/NR description
165519340*	0.00003	COG0364	K00036	Cvib_0375	glucose-6-phosphate 1-dehydrogenase
165502423	0.00003	COG0640	K03892	Cvib_1156	predicted transcriptional regulators : ArsR family
165562991	0.00003	COG0297	K00703	Cvib_0286	glycogen/starch synthase, ADP-glucose type
165501977*	0.00003	COG0525	K01873	Cvib_0442	valS; valyl-tRNA synthetase
165515179	0.00003	COG0712	K02113	Cvib_1740	FOF1-type ATP synthase delta subunit (mitochondrial oligomycin sensitivity protein)
165509255*	0.00003	COG1530	K08301	Cvib_0016	ribonucleases G and E : Rne/Rng family
165526126	0.00002	COG0330		Plut_1305	membrane protease subunits, stomatin/prohibitin homologs : band 7 protein
165563005	0.00002	COG0104	K01939	Cvib_0279	adenylosuccinate synthetase
165502333	0.00002	COG0513	K05592	Cvib_1189	superfamily II DNA and RNA helicases : DEAD/DEAH box helicase domain protein
165514511*	0.00002	COG0702		Cvib_1655	predicted nucleoside-diphosphate-sugar epimerases : NAD-dependent epimerase/dehydratase
165511735	0.00002	COG2878		Cvib_0798	predicted alternative beta subunit of Na ⁺ -transporting NADH:ubiquinone oxidoreductase : ferredoxin
165548065	0.00002	COG1509	K01843	Cvib_1367	L-lysine 2,3-aminomutase
165502839*	0.00002	COG0592	K02338	Cvib_0002	DNA polymerase sliding clamp subunit (PCNA homolog) : DNA polymerase III, beta subunit
165502087	0.00002	COG1463		Cvib_0488	permease component of an ABC-transporter : mammalian cell entry related domain protein
165525662	0.00002	COG0522	K02986	Cvib_0272	rpsD; 30S ribosomal protein S4
165519336*	0.00002	COG1028		Cvib_0372	dehydrogenases with different specificities (related to short-chain alcohol dehydrogenases)
165525742	0.00002	COG0536	K03979	Cvib_0231	predicted GTPase : obgE, yhbZ, obg, cgtA; GTPase ObgE
165557789	0.00002	COG0045		Cvib_0867	succinyl-CoA synthetase beta subunit : ATP citrate lyase subunit 1
165502295	0.00002	COG1945	K02626	Cvib_1209	uncharacterized ACR : pyruvoyl-dependent arginine decarboxylase
165562923b	0.00002	COG1429	K06050	Cvib_0320	cobalamin biosynthesis protein CobN and related Mg-chelatases : hydrogenobyrinic acid a,c-diamide cobaltochelatase
165525722	0.00002	COG0048	K02950	Cvib_0241	rpsL; 30S ribosomal protein S12
165525678	0.00002	COG0098	K02988	Cvib_0263	rpsE; 30S ribosomal protein S5
165502367	0.00002	COG0059	K00053	Cvib_1172	ketol-acid reductoisomerase
165514527*	0.00002	COG0330		Cvib_1667	membrane protease subunits, stomatin/prohibitin homologs : SPFH domain, band 7 family protein
165502009*	0.00002	COG0102	K02871	Cvib_0456	rplM; 50S ribosomal protein L13
165505071	0.00002	COG0589		Cvib_0918	universal stress protein UspA and related nucleotide-binding proteins
165525694	0.00002	COG0186	K02961	Cvib_0255	rpsQ; 30S ribosomal protein S17
165547949	0.00002	COG0414	K01918	Cvib_1423	pantothenate synthetase; pantoate-beta-alanine ligase
165548085	0.00002	COG2873	K01740	cch:Cag_1257	O-acetylhomoserine/O-acetylserine sulphhydrylase
165502203	0.00001	COG2070		Cvib_0556	dioxygenases related to 2-nitropropane dioxygenase

Continued on next page

Table B.3 – *Continued from previous page*

Gene ID	NSA	COG/NR ID	KO	Locus	COG : KEGG/NR description
16550995	0.00001	COG0563	K00939	Cvib_0952	adenylate kinase and related kinases
165525902	0.00001	COG0465	K03798	Cvib_0139	ATP-dependent Zn proteases : FtsH; cell division protease
165509287*	0.00001	COG0243		Plut_0027	anaerobic dehydrogenases, typically selenocysteine-containing : molybdenum enzyme related to thiosulfate reductase and polysulfide reductase, large subunit
165526192	0.00001	COG0462	K00948	Cvib_0712	phosphoribosylpyrophosphate synthetase : ribose-phosphate pyrophosphokinase
165502889*	0.00001	COG0206	K03531	Cvib_1749	cell division protein FtsZ
165509325*	0.00001	COG0437		Cvib_0050	Fe-S-cluster-containing hydrogenase components 1 : 4Fe-4S ferredoxin, iron-sulfur binding domain protein
165525812	0.00001	COG0236	K02078	Cvib_0197	acyl carrier protein
165502351	0.00001	COG0300	K00059	Cvib_1180	short-chain dehydrogenase/reductase SDR
165502011*	0.00001	COG0103	K02996	Cvib_0457	rpsI; 30S ribosomal protein S9
165514403*	0.00001	COG0231	K02356	Cvib_1601	translation elongation factor P (EF-P)
165553067	0.00001	COG0268	K02968	Cvib_1540	rpsT; 30S ribosomal protein S20
165519310*	0.00001	COG0668		Cvib_0357	small-conductance mechanosensitive channel
165511815	0.00001	COG3808	K01507	Cvib_0758	inorganic pyrophosphatase : hppA; membrane-bound proton-translocating pyrophosphatase
165502023	0.00001	COG1830	K08321	Cvib_0463	DhnA-type fructose-1,6-bisphosphate aldolase and related enzymes
165514567*	0.00001	COG0446	K00540	Cpha266_2569	uncharacterized NAD(FAD)-dependent dehydrogenases : sulfide-quinone reductase
165502077	0.00001	COG0138	K01492	Cvib_0483	phosphoribosylaminoimidazolecarboxamide formyltransferase / IMP cyclohydrolase
165514431*	0.00001	COG0148	K01689	Cvib_1615	enolase
165525838	0.00000	COG0629	K03111	Plut_0115	single-strand DNA-binding protein
165502007*	0.00000	COG1160	K03977	Cvib_0455	predicted GTPases: engA, yfgK, yphC; GTP-binding protein EngA
165526038	0.00000	COG0226	K02040	Cvib_0997	phosphate binding protein; phosphate transport system substrate-binding protein

12.7 m – KEGG and NR annotated proteins

165547733*	0.01965		Cvib_1525	hypothetical protein
165512927	0.01028		Cpha266_2650	hypothetical protein
165511987	0.00235	K03075	Cvib_1110	secG; preprotein translocase subunit SecG
165514495*	0.00209	K08946	Cvib_1647	chlorosome envelope protein B
165512925	0.00200	K08252	Cpha266_2649	lipopolysaccharide biosynthesis; receptor protein-tyrosine kinase
165571674	0.00148		dac:Daci_1946	putative phage major head protein
165563017	0.00148		ava:Ava_1043	methyltransferase FkbM
165502419	0.00139	K08943	Cvib_1159	photosystem P840 reaction center protein PscD
165519328*	0.00133	K08946	Cvib_0367	chlorosome envelope protein B
165547761*	0.00123		Cvib_1511	hypothetical protein

Continued on next page

Table B.3 – *Continued from previous page*

Gene ID	NSA	COG/NR ID	KO	Locus	COG : KEGG/NR description
165525930	0.00094			Cvib_0125	hypothetical protein
165525844	0.00090			Cvib_0179	hypothetical protein
165526256	0.00077		K08951	Cvib_1234	chlorosome envelope protein H
165552335*	0.00074		K08947	Cvib_0329	chlorosome envelope protein C
165526330	0.00072			cpb:Cphamn1_2160	CRISPR-associated protein, CSE2 family
165547799	0.00067			Cvib_1499	alpha amylase, catalytic region
165512931*	0.00063			cch:Cag_0645	hypothetical protein
165547879	0.00057			Cvib_1459	cytochrome c, putative
165502219	0.00057			amr:AM1_B0391	hypothetical protein
165526074	0.00052			Cvib_1019	sodium pump decarboxylase, gamma subunit
165514639*	0.00052			Cvib_1720	hypothetical protein
165562993	0.00049			Cvib_0285	hypothetical protein
165548153	0.00048		K08944	Cvib_1325	bacteriochlorophyll A protein
165531268c	0.00047			bvi:Bcep1808_1173	hypothetical protein
165526332	0.00047			cpb:Cphamn1_2161	CRISPR-associated protein, CSE3 family
165502381	0.00046			Cvib_1165	TonB-like protein
165511855	0.00037			Cvib_0746	hypothetical protein
165514665*	0.00035		K05807	Cvib_1734	putative lipoprotein
165548239	0.00034			Plut_0883	hypothetical protein
165501961	0.00034			Cvib_0417	hypothetical protein
165550963	0.00034		K02959	Plut_0966	rpsP; 30S ribosomal protein S16
165505939	0.00033			Cvib_0841	4Fe-4S ferredoxin, iron-sulfur binding domain protein
165519418d	0.00032			Cvib_0413	hypothetical protein
165547769	0.00029			Cvib_1507	hypothetical protein
165519030*	0.00027			cbf:CLI_2438	hypothetical protein
165525752	0.00027			Cvib_0226	hypothetical protein
165511809	0.00026			Cvib_0760	cytochrome c family protein
165514873*	0.00024			Cvib_1579	hypothetical protein
165550993	0.00024			Cvib_0951	hypothetical protein
165514437*	0.00024		K08941	Cvib_1618	4Fe-4S ferredoxin, iron-sulfur binding domain protein; photosystem P840 reaction center iron-sulfur protein
165547729	0.00023			Cvib_1527	hypothetical protein
165502893	0.00022			Cvib_1747	O-methyltransferase, family 2

Continued on next page

Table B.3 – *Continued from previous page*

Gene ID	NSA	COG/NR ID	KO	Locus	COG : KEGG/NR description
165547803	0.00022			Cvib_1498	hypothetical protein
165514537*	0.00020			Cvib_1673	alpha amylase, catalytic region
165525748	0.00016			Cvib_0228	hypothetical protein
165502181	0.00015			Cpha266_0714	hypothetical protein
165526208	0.00015		K07164	Cvib_0703	protein of unknown function DUF164
165502165	0.00014			Cvib_0536	TPR repeat-containing protein
165526334	0.00013			cte:CT1975	hypothetical protein
165547961	0.00013		K08942	Cvib_1418	photosystem P840 reaction center cytochrome c-551
165502029	0.00012			Cvib_0466	hypothetical protein
165505111	0.00011			Cvib_0901	hypothetical protein
165557793	0.00011			Cvib_0865	chlorosome envelope protein B
165548243	0.00011			cpb:Cphamn1_0811	hypothetical protein
165562965	0.00011			Cvib_0298	hypothetical protein
165551017	0.00010	ZP_01060966		MED217_12439	hypothetical protein
165548069	0.00010			Cvib_1365	GCN5-related N-acetyltransferase
165548181	0.00010			Cvib_1311	hypothetical protein
165514447*	0.00009			Cvib_1623	cytochrome c, class I
165513587	0.00007			Cvib_0828	hypothetical protein
165509309*	0.00007			Cvib_0042	hypothetical protein
165502185	0.00006			Cpha266_0718	hypothetical protein
165548171	0.00006			Cvib_1316	hypothetical protein
165502237	0.00006			Cvib_0580	hypothetical protein
165570114c	0.00005			bvi:Bcep1808_1173	hypothetical protein
165532404*	0.00004	K08945		Cvib_0330	bacteriochlorophyll C binding protein; chlorosome envelope protein A
165514439*	0.00004	K08940		Cvib_1619	photosystem P840 reaction center, large subunit
165505087	0.00004			Cvib_0912	hypothetical protein
165526028	0.00004			Cvib_0992	phosphate uptake regulator, PhoU
165547971	0.00004			Cvib_1413	hypothetical protein
165511805	0.00003			Cvib_0762	hypothetical protein
165525848	0.00003			Cvib_0177	hypothetical protein
165548087	0.00003			Cvib_1356	MOSC domain containing protein
165519298*	0.00003			Cvib_0351	hypothetical protein
165508719	0.00003		xft:PD0972		hypothetical protein

Continued on next page

Table B.3 – *Continued from previous page*

Gene ID	NSA	COG/NR ID	KO	Locus	COG : KEGG/NR description
165562895	0.00003			Cvib_0331	hypothetical protein
165509277*	0.00002			Cvib_0026	redoxin domain protein
165523112	0.00002			pmn:PMN2A_1227	hypothetical protein
165553037	0.00001			Plut_1772	hypothetical protein
165548159	0.00001			Cvib_1322	sporulation domain protein
165525928d	0.00001			Cvib_0126	hypothetical protein
12.7 m – Proteins with no annotation					
165502275	0.00389				
165497987	0.00265				
165499977*	0.00077				
165506645e	0.00072				
165563289e	0.00049				
165566413e	0.00035				
165563289	0.00012				
165503831	0.00006				
165525058e	0.00006				
165519980*	0.00005				
165549781e	0.00005				
165509979*	0.00002				

Table B.4: Proteins identified in the Ace Lake 14 m sample 0.1 µm size-fraction metaproteome. (*) Protein group identification: proteins that contain similar peptides that could not be differentiated by the mass spectral analysis were grouped. Only one gene number of that group is displayed. (a–z, aa–pp) Protein ambiguity groups: proteins that have some shared peptides with one or more other proteins from the same sample depth are marked with the same letters.

Gene ID	NSA	COG/NR ID	KO	Locus	14 m – COG annotated proteins
					COG : KEGG/NR description
166198186	0.06300	COG0149	K01803	Cvib_1275	triosephosphate isomerase
166137511	0.04782	COG0157	K03813	Cvib_1491	nicotinate-nucleotide pyrophosphorylase : ModD protein; molybdenum transport protein
166198448	0.04506	COG0776	K03530	Plut_1957	bacterial nucleoid DNA-binding protein : histone-like DNA-binding protein; HU-beta
166172204	0.03837	COG0329	K01714	Cvib_1403	dihydrodipicolinate synthase/N-acetylneuraminate lyase
166126920	0.03524	COG0526	K03671	Cvib_1012	thiol-disulfide isomerase and thioredoxins
166145532a	0.03313	COG0459	K04077	Cvib_0586	chaperonin GroEL (HSP60 family)
166124688	0.03285	COG1899	K00809	Cvib_1729	deoxyhypusine synthase
166179415	0.02422	COG2406	K03594	Cvib_1194	uncharacterized ACR : ferritin, Dps family protein
166074810	0.02266	COG2165			general secretory pathway proteins G and H and related periplasmic/secreted proteins
166188979	0.01945	COG0459	K04077	Cvib_0586	chaperonin GroEL (HSP60 family)
166184768	0.01314	COG1629	K02014	CT1953	outer membrane receptor proteins, mostly Fe transport : ferric siderophore receptor, putative, TonB receptor family
166090652	0.01164	COG1629	K02014	CT1953	outer membrane receptor proteins, mostly Fe transport : ferric siderophore receptor, putative, TonB receptor family
166103931	0.01162	COG2885		Cvib_0715	outer membrane protein and related peptidoglycan-associated (lipo)proteins : OmpA/MotB domain protein
166147146	0.01120	COG0522	K02986	Cvib_0272	rpsD; 30S ribosomal protein S4; K02986 small subunit ribosomal protein S4
166118837	0.01040	COG0605	K04564	Cvib_0978	superoxide dismutase : Fe-Mn family
166147056	0.01018	COG0045		Cvib_0867	succinyl-CoA synthetase beta subunit : ATP citrate lyase subunit 1
166109428	0.00951	COG1704	K03744	Cvib_0448	uncharacterized ACR : LemA family protein
166140297	0.00925	COG2165			general secretory pathway proteins G and H and related periplasmic/secreted proteins
166105505	0.00911	COG0723	K02636	Cvib_1501	rieske Fe-S protein : plastoquinol-plastocyanin reductase; cytochrome b6-f complex iron-sulfur subunit
166164770	0.00908	COG0284	K01591	Cvib_0140	orotidine 5'-phosphate decarboxylase
166118277	0.00863	COG0080	K02867	Plut_1966	rplK; 50S ribosomal protein L11
166129078	0.00843	COG0055	K02112	Cvib_0025	FOF1-type ATP synthase beta subunit
166150726	0.00842	COG0054	K00794	Cvib_1632	riboflavin synthase beta-chain : 6,7-dimethyl-8-ribityllumazine synthase

Continued on next page

Table B.4 – *Continued from previous page*

Gene ID	NSA	COG/NR ID	KO	Locus	COG : KEGG/NR description
166160341	0.00833	COG2165		MXAN_5783	general secretory pathway proteins G and H and related periplasmic/secreted proteins : pilA; pilin
166090624	0.00817	COG0446	K00540	Cvib_0009	uncharacterized NAD(FAD)-dependent dehydrogenases : sulfide dehydrogenase (flavocytochrome), flavoprotein subunit
166091252	0.00741	COG0181	K01749	Cvib_1245	porphobilinogen deaminase : hydroxymethylbilane synthase
166159279	0.00737	COG0074		Cvib_0866	succinyl-CoA synthetase alpha subunit : ATP citrate lyase subunit 2
166131402	0.00732	COG0776	K05788	Cvib_1506	bacterial nucleoid DNA-binding protein : histone family protein DNA-binding protein; integration host factor subunit beta
166196008	0.00715	COG0056	K02111	Cvib_1628	F0F1-type ATP synthase alpha subunit
166145114	0.00711	COG0050	K02358	Cvib_0244	GTPases - translation elongation factors : tuf
166114564	0.00664	COG0056	K02111	Cvib_1628	F0F1-type ATP synthase alpha subunit
166136070	0.00664	COG2838	K00031	Cvib_0507	monomeric isocitrate dehydrogenase
166175476	0.00652	COG0724		Cvib_0890	RNA-binding proteins (RRM domain) : RNP-1 like RNA-binding protein
166136072	0.00648	COG0623	K00208	Cvib_0506	enoyl-[acyl-carrier-protein] reductase (NADH)
166076054	0.00647	COG0633	K08953	Cvib_1151	ferredoxin : chlorosome envelope protein J
166097866a	0.00589	COG0459	K04077	Acid345_1097	chaperonin GroEL (HSP60 family)
166097888	0.00584	COG0191	K01624	Cvib_0892	fructose/tagatose bisphosphate aldolase
166157335	0.00575	COG0450	K03386	Cvib_1195	peroxiredoxin
166112774	0.00570	COG0191	K01624	Cvib_0892	fructose/tagatose bisphosphate aldolase
166114562	0.00568	COG0224	K02115	Cvib_1627	F0F1-type ATP synthase gamma subunit
166073786	0.00553	COG0045	K01903	Cvib_0553	succinyl-CoA synthetase beta subunit
166094904	0.00543	COG0330		Cvib_1667	membrane protease subunits, stomatin/prohibitin homologs : SPFH domain, band 7 family protein
166105507	0.00538	COG1290	K00412	Cvib_1500	cytochrome b subunit of the bc complex : ubiquinol-cytochrome c reductase cytochrome b subunit
166073832	0.00525	COG0359	K02939	Cvib_0184	rplI; 50S ribosomal protein L9
166145084	0.00522	COG0094	K02931	Cvib_0258	rplE; 50S ribosomal protein L5
166107961	0.00493	COG0674	K03737	Cvib_1407	pyruvate:ferredoxin oxidoreductase and related 2-oxoacid:ferredoxin oxidoreductases, alpha subunit
166118279	0.00485	COG0081	K02863	Cvib_1608	rplA; 50S ribosomal protein L1
166102730	0.00462	COG0776	K03530	ECA1151	bacterial nucleoid DNA-binding protein : hupB, hopD; transcriptional regulator HU subunit beta
166081105	0.00459	COG0674	K00174	Cvib_1597	pyruvate:ferredoxin oxidoreductase and related 2-oxoacid:ferredoxin oxidoreductases, alpha subunit : 2-oxoglutarate ferredoxin oxidoreductase, alpha subunit

Continued on next page

Table B.4 – *Continued from previous page*

Gene ID	NSA	COG/NR ID	KO	Locus	COG : KEGG/NR description
166176327b	0.00459	COG0050	K02358	Cvib_0244	GTPases - translation elongation factors : tuf
166154349	0.00458	COG0776	K03530	Maqu_1837	bacterial nucleoid DNA-binding protein : DNA-binding protein HU-beta
166147144	0.00453	COG0522	K02986	Cvib_0272	rpsD; 30S ribosomal protein S4
166171164	0.00439	COG1038	K01571	Cvib_1018	pyruvate carboxylase, C-terminal domain/subunit : biotin/lipoyl attachment domain-containing protein; oxaloacetate decarboxylase, alpha subunit
166161092	0.00429	COG0074	K01902	Cvib_1529	succinyl-CoA synthetase alpha subunit
166169642	0.00428	COG0003	K01551	Cvib_0783	predicted ATPase involved in chromosome partitioning : arsenite-activated ATPase ArsA
166129916	0.00422	COG1185	K00962	Cvib_1424	polyribonucleotide nucleotidyltransferase (polynucleotide phosphorylase)
166145082	0.00408	COG0094	K02931	Cvib_0258	rplE; 50S ribosomal protein L5
166129918	0.00407	COG1185	K00962	Cvib_1424	polyribonucleotide nucleotidyltransferase (polynucleotide phosphorylase)
166175528	0.00404	COG0261	K02888	Cvib_1329	rplU; 50S ribosomal protein L21
166116994	0.00393	COG1274	K01596	Cvib_0027	phosphoenolpyruvate carboxykinase (GTP)
166102162	0.00393	COG0330		Plut_1305	membrane protease subunits, stomatin/prohibitin homologs : band 7 protein
166112188	0.00388	COG1049	K01682	Cvib_0598	aconitase B : bifunctional aconitate hydratase 2/2-methylisocitrate dehydratase
166098678	0.00381	COG0443	K04043	Cvib_1158	molecular chaperone : DnaK
166168134	0.00358	COG0052	K02967	Cvib_0458	rpsB; 30S ribosomal protein S2; K02967 small subunit ribosomal protein S2
166074098	0.00356	COG0233	K02838	Cvib_0408	ribosome recycling factor
166169194	0.00350	COG0001	K01845	Cvib_1681	glutamate-1-semialdehyde 2,1-aminomutase
166125344	0.00346	COG0174	K01915	Cvib_1230	glutamine synthetase
166137459	0.00346	COG0335	K02884	Cvib_0932	rplS; 50S ribosomal protein L19
166118281	0.00345	COG0244	K02864	Cvib_1607	rplJ; 50S ribosomal protein L10
166145072	0.00342	COG0098	K02988	Cvib_0263	rpsE; 30S ribosomal protein S5
166166464c	0.00335	COG0057	K00134	Cvib_1310	glyceraldehyde-3-phosphate dehydrogenase/erythrose-4-phosphate dehydrogenase
166077950	0.00311	COG0039	K00026	Cvib_1331	malate/lactate dehydrogenases
166175692	0.00303	COG1378		NEQ098	predicted transcriptional regulators : hypothetical protein
166145074	0.00301	COG0256	K02881	Cvib_0262	rplR; 50S ribosomal protein L18
166145070	0.00294	COG0200	K02876	Cvib_0265	rplO; 50S ribosomal protein L15
166145094	0.00270	COG0197	K02878	Cvib_0253	rplP; 50S ribosomal protein L16
166188981	0.00259	COG0234	K04078	Plut_0541	Co-chaperonin GroES (HSP10)
166193190	0.00256	COG1049	K01682	Cvib_0598	aconitase B : bifunctional aconitate hydratase 2/2-methylisocitrate dehydratase
166170748	0.00252	COG0115	K00826	Cvib_1391	branched-chain amino acid aminotransferase/4-amino-4-deoxychorismate lyase
166166696	0.00245	COG0085	K03043	Cvib_1605	DNA-directed RNA polymerase beta subunit/140 kD subunit (split gene in Mjan, Mthe, Aful)
166177107	0.00243	COG0652	K03767	Cvib_0535	peptidyl-prolyl cis-trans isomerase (rotamase) - cyclophilin family

Continued on next page

Table B.4 – *Continued from previous page*

Gene ID	NSA	COG/NR ID	KO	Locus	COG : KEGG/NR description
166185496	0.00241	COG0588	K01834	Cvib_0557	phosphoglycerate mutase 1
166083171	0.00234	COG0192	K00789	Cvib_1121	Sadenosylmethionine synthetase
166086944	0.00222	COG1014	K03737	Cvib_1407	pyruvate:ferredoxin oxidoreductase and related 2-oxoacid:ferredoxin oxidoreductases, gamma subunit
166154673	0.00220	COG0629	K03111	Cvib_0326	single-strand binding protein
166176323	0.00216	COG0480	K02355	Cvib_0243	translation elongation and release factors (GTPases) : fusA; elongation factor G
166136530	0.00213	COG0711	K02109	Cvib_1741	FOF1-type ATP synthase b subunit
166176321	0.00213	COG0049	K02992	Cvib_0242	30S ribosomal protein S7
166145098	0.00203	COG0091	K02890	Cvib_0251	rplV; 50S ribosomal protein L22
166090169a	0.00200	COG0459	K04077	Oter_2054	chaperonin GroEL (HSP60 family)
166087916	0.00197	COG0462	K00948	Cvib_0712	phosphoribosylpyrophosphate synthetase
166177021	0.00192	COG0001	K01845	Cvib_1681	glutamate-1-semialdehyde 2,1-aminomutase
166152385	0.00189	COG0086	K03046	Cvib_1604	DNA-directed RNA polymerase beta' subunit/160 kD subunit (split gene in archaea and Syn)
166145088	0.00188	COG0093	K02874	Cvib_0256	rplN; 50S ribosomal protein L14
166190942	0.00188	COG0085	K03043	Cvib_1605	DNA-directed RNA polymerase beta subunit/140 kD subunit (split gene in Mjan, Mthe, Aful)
166118275	0.00187	COG0250	K02601	Cvib_1610	transcription antitermination protein NusG
166145096	0.00183	COG0092	K02982	Cvib_0252	rpsC; 30S ribosomal protein S3
166091362	0.00181	COG2319		Cvib_0309	WD-40 repeat protein
166124685	0.00181	COG0176	K00616	Cvib_1728	translaldolase
166135982	0.00177	COG0126	K00927	Cvib_1766	pgk; phosphoglycerate kinase
166164640	0.00175	COG1729		Cvib_1161	uncharacterized BCR : tetratricopeptide domain protein
166087918	0.00167	COG1825	K02897	Cvib_0711	50S ribosomal protein L25/general stress protein Ctc
166189760	0.00167	COG0148	K01689	Cvib_1615	enolase
166102164	0.00157	COG0589		Cvib_1041	universal stress protein UspA and related nucleotide-binding proteins
166154669	0.00154	COG0003	K01551	Cvib_0328	predicted ATPase involved in chromosome partitioning : arsenite-activated ATPase ArsA
166131420	0.00154	COG1611	K06966	Cvib_0416	predicted Rossmann fold nucleotide-binding protein : conserved hypothetical protein 730
166103031	0.00153	COG0724		Cag_1551	RNA-binding proteins (RRM domain) : RNP-1 (RNA recognition motif)
166145110	0.00150	COG0087	K02906	Cvib_0246	rplC; 50S ribosomal protein L3
166143572	0.00147	COG0103	K02996	Cvib_0457	rpsI; 30S ribosomal protein S9
166081107	0.00142	COG1013	K00175	Cvib_1598	pyruvate:ferredoxin oxidoreductase and related 2-oxoacid:ferredoxin oxidoreductases, beta sub-unit : 2-oxoglutarate ferredoxin oxidoreductase subunit beta
166119893	0.00140	COG0113	K01698	Cvib_1252	delta-aminolevulinic acid dehydratase : porphobilinogen synthase
166145108	0.00135	COG0088	K02926	Cvib_0247	rplD; 50S ribosomal protein L4

Continued on next page

Table B.4 – *Continued from previous page*

Gene ID	NSA	COG/NR ID	KO	Locus	COG : KEGG/NR description
166091020	0.00135	COG0112	K00600	Cvib_1381	glycine hydroxymethyltransferase
166125448	0.00133	COG1239	K03405	Cvib_1059	Mg-chelatase subunit ChII
166079276	0.00131	COG0499	K01251	Cvib_1122	S-adenosyl-L-homocysteine hydrolase
166145076	0.00128	COG0097	K02933	Cvib_0261	rplF; 50S ribosomal protein L6
166145078	0.00127	COG0096	K02994	Cvib_0260	rpsH; 30S ribosomal protein S8
166102716	0.00125	COG0446	K00540	Cpha266_2569	uncharacterized NAD(FAD)-dependent dehydrogenases : sulfide-quinone reductase
166176319	0.00124	COG0048	K02950	Cvib_0241	rpsL; 30S ribosomal protein S12
166079074	0.00122	COG1049	K01682	Cvib_0598	aconitase B : bifunctional aconitate hydratase 2/2-methylisocitrate dehydratase
166111074	0.00118	COG0539	K02945	Cvib_1514	rpsA; 30S ribosomal protein S1
166136657	0.00118	COG1360	K02557	Pcar_1973	flagellar motor protein : chemotaxis protein MotB
166124033	0.00118	COG0158	K03841	Cvib_0509	fructose-1,6-bisphosphatase
166176325	0.00117	COG0480	K02355	Plut_0177	translation elongation and release factors (GTPases) : fusA; elongation factor G
166137753	0.00115	COG1778	K03270	Cvib_1694	uncharacterized proteins of HAD superfamily, CMP-Neu5Ac homologs : 3-deoxy-D-manno-octulosonate 8-phosphate phosphatase, YrbI family
166125498	0.00112	COG0377	K00331	Cvib_1092	NADH:ubiquinone oxidoreductase 20 kD subunit and related Fe-S oxidoreductases
166144212	0.00110	COG2101	K03120	AF0373	transcription initiation factor TFIID (TATA-binding protein)
166171940	0.00110	COG0100	K02948	Cvib_0271	30S ribosomal protein S11
166195033	0.00109	COG0809	K07568	Cvib_1048	S-adenosylmethionine:tRNA-ribosyltransferase-isomerase (queuine synthetase)
166186408	0.00109	COG0365	K01895	Plut_1637	acyl-coenzyme A synthetases/AMP-(fatty) acid ligases
166177113	0.00106	COG0005	K03783	Cvib_0533	purine nucleoside phosphorylase
166154527	0.00105	COG0413	K00606	Cvib_0725	ketopantoate hydroxymethyltransferase : panB; 3-methyl-2-oxobutanoate hydroxymethyltransferase
166150004	0.00105	COG1028		Cvib_0372	dehydrogenases with different specificities (related to short-chain alcohol dehydrogenases)
166187454	0.00104	COG0059	K00053	Cvib_1172	ketol-acid reductoisomerase
166112410*	0.00100	COG0086	K03046	HM1_1371	DNA-directed RNA polymerase beta' subunit/160 kD subunit (split gene in archaea and Syn)
166118285	0.00099	COG0085	K03043	Cvib_1605	DNA-directed RNA polymerase beta subunit/140 kD subunit (split gene in Mjan, Mthe, Aful)
166147142	0.00098	COG0202	K03040	Cvib_0273	DNA-directed RNA polymerase alpha subunit/40 kD subunit
166091254	0.00097	COG1587	K01719	Cvib_1246	uroporphyrinogen-III synthase
166123058	0.00096	COG1028	K00059	Cvib_1180	dehydrogenases with different specificities (related to short-chain alcohol dehydrogenases): 3-oxoacyl-[acyl-carrier protein] reductase
166083688	0.00096	COG0330	K04088	Pcar_2262	membrane protease subunits, stomatin/prohibitin homologsh: HflK
166081389	0.00095	COG0241	K05602	Cvib_0287	histidinol phosphatase and related phosphatases
166104095	0.00094	COG1837	K06960	CAC1756	predicted RNA-binding protein (KH domain)

Continued on next page

Table B.4 – *Continued from previous page*

Gene ID	NSA	COG/NR ID	KO	Locus	COG : KEGG/NR description
166137513	0.00094	COG0725	K02020	Cvib_1492	ABC-type molybdate transport system, periplasmic component
166073556	0.00093	COG0592	K02338	Cvib_0002	DNA polymerase sliding clamp subunit (PCNA homolog)
166085896	0.00092	COG0086	K03046	Cvib_1604	DNA-directed RNA polymerase beta' subunit/160 kD subunit (split gene in archaea and Syn)
166171160	0.00092	COG0511	K01571	Cvib_1018	biotin carboxyl carrier protein : oxaloacetate decarboxylase, alpha subunit
166143662	0.00089	COG0289	K00215	Cvib_0390	dihydrodipicolinate reductase
166128308	0.00082	COG2873	K01740	Cag_1257	O-acetylhomoserine/O-acetylserine sulfhydrylase
166096460	0.00082	COG1561		Cvib_1556	uncharacterized stress-induced protein
166174470	0.00080	COG3040	K03098	Cvib_0516	bacterial lipocalin : Blc
166142836	0.00079	COG0480	K02355	Cvib_1616	translation elongation and release factors (GTPases) : fusA; elongation factor G
166198126	0.00078	COG0326	K04079	Cvib_1024	molecular chaperone, HSP90 family : HtpG
166187456	0.00077	COG0440	K01653	Cvib_1171	acetolactate synthase, small subunit
166195031	0.00076	COG1554		Cvib_1047	trehalose and maltose hydrolases (possible phosphorylases) : beta-phosphoglucomutase family hydrolase
166112772	0.00076	COG0191	K01624	Cvib_0892	fructose/tagatose bisphosphate aldolase
166167622	0.00075	COG0499	K01251	Cvib_1122	S-adenosyl-L-homocysteine hydrolase
166163472	0.00074	COG3637		Cvib_1533	opacity protein and related surface antigens : porin, opacity type
166186410	0.00070	COG0365	K01895	Cvib_1426	acyl-coenzyme A synthetases/AMP-(fatty) acid ligases
166137755	0.00069	COG2877	K01627	Cvib_1695	3-Deoxy-D-manno-octulosonic acid (KDO) 8-phosphate synthase : 2-dehydro-3-deoxyphosphooctonate aldolase
166109758	0.00069	COG2171	K00674	Cvib_0017	tetrahydrodipicolinate N-succinyltransferase : dapD; 2,3,4,5-tetrahydropyridine-2-carboxylate N-succinyltransferase
166164026	0.00068	COG3808	K01507	Cvib_0758	inorganic pyrophosphatase : hppA
166139077	0.00068	COG1837	K06960	Bcer98_2495	predicted RNA-binding protein (KH domain)
166087626c	0.00067	COG0057	K00134	Bcer98_3682	glyceraldehyde-3-phosphate dehydrogenase/erythrose-4-phosphate dehydrogenase
166134708	0.00066	COG0760		Cvib_1572	parvulin-like peptidyl-prolyl isomerase : PpiC-type peptidyl-prolyl cis-trans isomerase
166150020	0.00066	COG2606		Cvib_0364	uncharacterized ACR : YbaK/prolyl-tRNA synthetase associated region
166179493	0.00066	COG0058	K00688	Cvib_1386	alpha-glucan phosphorylase; starch phosphorylase
166164028	0.00063	COG3808	K01507	Plut_1202	inorganic pyrophosphatase : hppA
166083948	0.00063	COG0173	K01876	Cvib_1052	aspS; aspartyl-tRNA synthetase
166090630	0.00063	COG1252	K03885	Cvib_1373	NADH dehydrogenase, FAD-containing subunit : FAD-dependent pyridine nucleotide-disulphide oxidoreductase
166150732	0.00063	COG0407	K01599	Cvib_1635	uroporphyrinogen-III decarboxylase
166134876	0.00060	COG0195	K02600	Cvib_1562	transcription elongation factor NusA : N utilization substance protein A

Continued on next page

Table B.4 – *Continued from previous page*

Gene ID	NSA	COG/NR ID	KO	Locus	COG : KEGG/NR description
166151470b	0.00057	COG0050	K02358	Nwi_1362	GTPases - translation elongation factors : tuf
166180979	0.00056	COG3245		Cvib_0219	cytochrome c5
166110008	0.00055	COG1429	K03403	Cvib_1057	cobalamin biosynthesis protein CobN and related Mg-chelatases : hydrogenobyrinic acid a,c-diamide cobaltochelatase
166093481	0.00054	COG0260	K01255	Cvib_0947	leucyl aminopeptidase
166084291	0.00053	COG3360	K09165	Cvib_0029	uncharacterized ACR : protein of unknown function DUF1458
166134544	0.00053	COG2920	K00396	Cvib_0038	sulfite reductase, gamma subunit : DsrC family protein
166183160	0.00052	COG1077	K03569	Cvib_0595	HSP70 class molecular chaperones involved in cell morphogenesis: MreB/Mrl family
166079969	0.00052	COG0539	K02945	Cvib_1514	rpsA; 30S ribosomal protein S1
166074910	0.00051	COG0003	K01551	Cvib_0332	predicted ATPase involved in chromosome partitioning : arsenite-activated ATPase ArsA
166078208	0.00049	COG1032	K04035	Cvib_0316	Fe-S oxidoreductases family 2 : magnesium-protoporphyrin IX monomethyl ester anaerobic oxidative cyclase
166148744	0.00048	COG0217		Cvib_1432	uncharacterized ACR : hypothetical protein
166164642	0.00047	COG2885		Cvib_1162	outer membrane protein and related peptidoglycan-associated (lipo)proteins : OmpA/MotB domain protein
166124690	0.00046	COG1899	K00809	Cvib_1729	deoxyhypusine synthase
166074701	0.00046	COG0360	K02990	Cvib_0181	rpsF; 30S ribosomal protein S6
166078272	0.00044	COG0811	K03562	Cvib_1167	biopolymer transport proteins : MotA/TolQ/ExbB proton channel
166160978	0.00044	COG2077	K00435	Cvib_1103	Peroxiredoxin : thiol peroxidase (atypical 2-Cys peroxiredoxin)
166089421	0.00042	COG0330		SYN_00180	membrane protease subunits, stomatin/prohibitin homologs : bacterial HflC protein
166184106	0.00041	COG1351	K03465	Plut_0366	predicted alternative thymidylate synthase : thyX
166146666	0.00040	COG1538		Plut_2001	outer membrane protein : LipD protein, putative
166107875b	0.00039	COG0050	K02358	Pcar_0699	GTPases - translation elongation factors : tufA, tuf
166185036	0.00038	COG0436	K00812	Cvib_0768	PLP-dependent aminotransferases : aspartate aminotransferase
166085075	0.00038	COG0694	K07400	Cvib_0453	thioredoxin-like proteins and domains : nitrogen-fixing NifU domain protein
166166220	0.00038	COG0330	K04087	Pcar_2263	membrane protease subunits, stomatin/prohibitin homologsh: HflC protein
166156045	0.00037	COG3155		Cvib_1447	uncharacterized sigma cross-reacting protein 27A (ES1 or KNP-I alpha protein) : isoprenoid biosynthesis protein with amidotransferase-like domain
166197986	0.00034	COG0342	K03072	Cvib_0010	preprotein translocase subunit SecD
166147140	0.00034	COG0203	K02879	Cvib_0274	rplQ; 50S ribosomal protein L17
166073820	0.00033	COG0188	K02469	Cvib_0172	DNA gyrase (topoisomerase II) A subunit
166181669	0.00033	COG0082	K01736	Cvib_1253	chorismate synthase
166159821	0.00033	COG2884	K09812	Cvib_1198	predicted ATPase involved in cell division : FtsE

Continued on next page

Table B.4 – *Continued from previous page*

Gene ID	NSA	COG/NR ID	KO	Locus	COG : KEGG/NR description
166145122	0.00031	COG3347		Cvib_0462	uncharacterized ACR : short chain dehydrogenase
166081203	0.00030	COG0468	K03553	Cvib_0340	RecA/RadA recombinase
166160944	0.00029	COG0226	K02040	Cvib_0998	ABC-type phosphate transport system, periplasmic component
166171936	0.00029	COG0024	K01265	Cvib_0267	methionine aminopeptidase
166177115	0.00028	COG0182	K08963	Cvib_0532	translation initiation factor eIF-2B alpha subunit : methylthioribose-1-phosphate isomerase
166121954	0.00027	COG1239	K03404	Cvib_1058	Mg-chelatase subunit ChII
166114512	0.00027	COG0729	K07277	Cvib_1532	predicted outer membrane protein : surface antigen (D15)
166123620a	0.00026	COG0459	K04077	MXAN_4895	chaperonin GroEL (HSP60 family)
166160942	0.00025	COG0226	K02040	Cvib_0997	ABC-type phosphate transport system, periplasmic component
166080265	0.00024	COG2878		Cvib_0798	predicted alternative beta subunit of Na ⁺ -transporting NADH:ubiquinone oxidoreductase : ferredoxin
166184114	0.00023	COG0568	K03086	Cvib_0443	DNA-directed RNA polymerase sigma subunits (sigma70/sigma32)
166163480	0.00023	COG1158	K03628	Cvib_1537	transcription termination factor: Rho
166132366	0.00023	COG1233		Cvib_0356	phytoene dehydrogenase and related proteins : FAD dependent oxidoreductase
166116816	0.00021	COG0542	K03696	Cvib_1580	ATPases with chaperone activity, ATP-binding subunit : ATP-dependent Clp protease ATP-binding subunit ClpC
166128316	0.00020	COG1629		Cvib_1353	outer membrane receptor proteins, mostly Fe transport : TonB receptor family
166163448	0.00020	COG0635	K02495	Cvib_1370	coproporphyrinogen III oxidase and related Fe-S oxidoreductases
166159573	0.00019	COG1151	K00378	Cvib_1455	6Fe-6S prismane cluster-containing protein : hydroxylamine reductase
166163870	0.00017	COG0209	K00525	Cvib_1199	ribonucleotide-diphosphate reductase subunit alpha
166135202	0.00013	COG0544	K03545	Cvib_0337	FKBP-type peptidyl-prolyl cis-trans isomerase (trigger factor)
166164774	0.00012	COG0743	K00099	Cvib_0138	1-deoxy-D-xylulose 5-phosphate reductoisomerase
166180975	0.00012	COG0075	K00839	Cvib_0221	serine-pyruvate aminotransferase/archaeal aspartate aminotransferase
166078200	0.00011	COG1429	K06050	Cvib_0320	cobalamin biosynthesis protein CobN and related Mg-chelatases : hydrogenobyrinic acid a,c-diamide cobaltochelatase
166185488	0.00010	COG0069	K00284	Cvib_0558	glutamate synthase domain 2

14 m – KEGG and NR annotated proteins

166154667	0.12890		K08947	Cvib_0329	chlorosome envelope protein C
166116826	0.07870		K08944	Cvib_1325	bacteriochlorophyll A protein
166103043	0.07473			Cpha266_0714	hypothetical protein
166154665	0.04995		K08945	Cvib_0330	bacteriochlorophyll C binding protein
166084321	0.01855		K08951	Cvib_1234	chlorosome envelope protein H
166197596	0.01757			Cvib_0837	hypothetical protein

Continued on next page

Table B.4 – *Continued from previous page*

Gene ID	NSA	COG/NR ID	KO	Locus	COG : KEGG/NR description
166078646	0.01703		K06142	Cvib_1549	outer membrane chaperone Skp (OmpH)
166183346	0.01613			CKO_01864	hypothetical protein
166103041	0.01438			Cpha266_0714	hypothetical protein
166128026	0.01374		K08943	Cvib_1159	photosystem P840 reaction center protein PscD; K08943 photosystem P840 reaction center protein PscD
166178625	0.01011			Plut_1996	CBS
166169946	0.00965			Psyr_2789	hypothetical protein
166128030	0.00924	ZP_02034709	K08943	Cvib_1159	photosystem P840 reaction center protein PscD
166105997	0.00871	ZP_03762235		BACCAP_00296	hypothetical protein [Bacteroides capillosus ATCC 29799]
166112572	0.00846			Daci_1946	putative phage major head protein
166160856	0.00694	ZP_03762235		CLOSTASPAR_06273	hypothetical protein [Clostridium asparagiforme DSM 15981]
166112574d	0.00672			Daci_1946	putative phage major head protein
166114838	0.00665			Cvib_0125	hypothetical protein
166191606	0.00636		K08940	Cvib_1619	photosystem P840 reaction center, large subunit; K08940 photosystem P840 reaction center large subunit
166147050	0.00612			Plut_1061	citrate lyase, subunit 1
166145430e	0.00533			Haur_0657	hypothetical protein
166076418	0.00499			Daci_1946	putative phage major head protein
166198192e	0.00493			Haur_0657	hypothetical protein
166177839	0.00469			Bcep1808_1173	hypothetical protein
166150012	0.00390		K08946	Cvib_0367	chlorosome envelope protein B;
166199138	0.00360		K08942	Cvib_1418	photosystem P840 reaction center cytochrome c-551
166145106	0.00354		K02926	Cvib_0247	rplD; 50S ribosomal protein L4
166115656	0.00353			Cag_0645	hypothetical protein
166171962	0.00347			BC1894	phage protein
166191394	0.00334			Cvib_0413	hypothetical protein
166075542	0.00331			Cvib_1747	O-methyltransferase, family 2
166195894	0.00312			CKL_1862	hypothetical protein
166194857	0.00290		K08941	Cvib_1618	4Fe-4S ferredoxin, iron-sulfur binding domain protein; photosystem P840 reaction center iron-sulfur protein
166111558	0.00220			Cvib_1311	hypothetical protein
166177105	0.00197			Cvib_0536	TPR repeat-containing protein
166147988d	0.00160			Daci_1946	putative phage major head protein

Continued on next page

Table B.4 – *Continued from previous page*

Gene ID	NSA	COG/NR ID	KO	Locus	COG : KEGG/NR description
166143915	0.00156			GDI3673	hypothetical protein
166114744	0.00144			Cvib_0488	mammalian cell entry related domain protein
166136528	0.00134		K05807	Cvib_1734	putative lipoprotein
166189288	0.00132		K08946	Cvib_1647	chlorosome envelope protein B
166153135	0.00118			Cvib_1720	hypothetical protein
166115588	0.00099			Aave_2895	hypothetical protein
166126712	0.00099			Cphamn1_2160	CRISPR-associated protein, CSE2 family
166127542	0.00096			Cphamn1_0811	hypothetical protein
166085087	0.00091			Swit_4452	hypothetical protein
166129356	0.00081			Cvib_0992	phosphate uptake regulator, PhoU
166195535	0.00080			Cthe_1719	phage major capsid protein, HK97 family
166080497	0.00077			NEQ258	hypothetical protein
166126708	0.00075			CT1975	hypothetical protein
166148084	0.00075			Cvib_0912	hypothetical protein
166093483	0.00074		K01255	Cvib_0947	leucyl aminopeptidase
166170746	0.00073		K00850	Cvib_1390	6-phosphofructokinase
166140451	0.00071			amb4267	hypothetical protein
166097432	0.00047			GbCGDNIH1_1574	hypothetical protein
166135078	0.00039			Cvib_1499	alpha amylase, catalytic region
166091036	0.00024			Cvib_0951	hypothetical protein

14 m – Proteins with no annotation

166113938	0.28150
166170056 <i>f</i>	0.23381
166104559	0.21346
166166078	0.11573
166119911 <i>g</i>	0.10078
166141831	0.09127
166155401	0.06411
166178565 <i>f</i>	0.05428
166161827	0.05400
166123502	0.04548
166117935	0.04149
166175637	0.03938

Continued on next page

Table B.4 – *Continued from previous page*

Gene ID	NSA	COG/NR ID	KO	Locus	COG : KEGG/NR description
166162109	0.03622				
166120729	0.02777				
166089615	0.02167				
166089117 <i>h</i>	0.02020				
166122468 <i>f</i>	0.01992				
166196000	0.01976				
166181749 <i>k</i>	0.01745				
166122470 <i>g</i>	0.01725				
166177993	0.01674				
166183514 <i>i</i>	0.01619				
166106257	0.01486				
166168914	0.01399				
166098369	0.01350				
166184074	0.01201				
166118161	0.01166				
166098372	0.01130				
166152065	0.01097				
166142782	0.01080				
166094970	0.01010				
166198840	0.00950				
166086220	0.00949				
166147768	0.00898				
166083420	0.00834				
166197698	0.00829				
166128790	0.00815				
166198884	0.00771				
166185832	0.00744				
166115262 <i>j</i>	0.00733				
166178177	0.00673				
166178731	0.00648				
166198482	0.00636				
166133494	0.00557				
166115313	0.00555				

Continued on next page

Table B.4 – *Continued from previous page*

Gene ID	NSA	COG/NR ID	KO	Locus	COG : KEGG/NR description
166130570	0.00540				
166112498	0.00516				
166160740	0.00453				
166184588	0.00451				
166073347	0.00441				
166078332	0.00433				
166189276 <i>i</i>	0.00432				
166098374	0.00416				
166165646	0.00377				
166141123	0.00348				
166133904	0.00341				
166197188	0.00341				
166098366	0.00332				
166161640	0.00304				
166150071	0.00276				
166185272	0.00270				
166173254 <i>k</i>	0.00243				
166142790	0.00238				
166115308	0.00236				
166166040	0.00235				
166194855	0.00231				
166181319	0.00213				
166115336	0.00206				
166082335	0.00195				
166166084	0.00187				
166097710	0.00163				
166195563	0.00154				
166184076	0.00149				
166118309	0.00144				
166161638	0.00126				
166115340 <i>j</i>	0.00118				
166160259	0.00108				
166199068	0.00102				

Table B.4 – *Continued from previous page*

Gene ID	NSA	COG/NR ID	KO	Locus	COG : KEGG/NR description
166077062	0.00085				
166116936	0.00077				
166095512	0.00076				
166186728	0.00071				
166110378g	0.00062				
166155981h	0.00056				
166132092	0.00056				
166176653	0.00051				
166102418	0.00048				
166176585	0.00040				
166128640	0.00035				
166135852	0.00023				

Table B.5: Proteins identified in the Ace Lake 18 m sample 0.1 µm size-fraction metaproteome. (*) Protein group identification: proteins that contain similar peptides that could not be differentiated by the mass spectral analysis were grouped. Only one gene number of that group is displayed. (a-z, aa-pp) Protein ambiguity groups: proteins that have some shared peptides with one or more other proteins from the same sample depth are marked with the same letters.

Gene ID	NSA	COG/NR ID	KO	18 m – COG annotated proteins	
				Locus	COG : KEGG/NR description
186212528a	0.05178	COG1378		NEQ098	predicted transcriptional regulators : hypothetical protein
186260184a	0.01990	COG1378		NEQ098	predicted transcriptional regulators : hypothetical protein
186323634	0.00815	COG1629			outer membrane receptor proteins, mostly Fe transport
186330135	0.00354	COG2165			general secretory pathway proteins G and H and related periplasmic/secreted proteins
186203427	0.00268	COG0459	K04077	Cvib_0586	chaperonin GroEL (HSP60 family)
186325396	0.00029	COG0330	K04088	MXAN_3171	membrane protease subunits, stomatin/prohibitin homologs : HflK
186302986	0.00014	COG1629	K02014	CT1953	outer membrane receptor proteins, mostly Fe transport : ferric siderophore receptor, putative, TonB receptor family
18 m – KEGG and NR annotated proteins					
186250193	0.03535			SAK_0748	prophage LambdaSa04, major capsid protein, HK97 family
186108954	0.01496	ZP_02186589		BAL199_17233	hypothetical protein [alpha proteobacterium BAL199]
186340319	0.01172	YP_002433801		Dalk_4655	hypothetical protein [Desulfatibacillum alkenivorans AK-01]
186120387	0.01077	ZP_02034709		BACCAP_00296	hypothetical protein [Bacteroides capillosus ATCC 29799]
186267822	0.00917			amb4267	hypothetical protein
186322918	0.00767	ZP_02186589		BAL199_17233	hypothetical protein [alpha proteobacterium BAL199]
186104395	0.00674		K08944	Cvib_1325	bacteriochlorophyll A protein
186171273	0.00587	ZP_03013728		BACINT_01287	hypothetical protein [Bacteroides intestinalis DSM 17393]
186216762	0.00511	YP_001648266			hypothetical protein OsV5_190f [Ostreococcus virus OsV5]
186188521	0.00474	AAU84208		GZ37D1_55	hypothetical protein [uncultured archaeon GZfos37D1]
186193139	0.00263			Cthe_1719	phage major capsid protein, HK97 family
186096477	0.00240			Cthe_1719	phage major capsid protein, HK97 family
186213938	0.00211			Nwi_1542	phage major capsid protein, HK97
186288435	0.00189			Bcep1808_1173	hypothetical protein
186186444	0.00140	YP_002765714		RER_22670	hypothetical protein [Rhodococcus erythropolis PR4]
186201365	0.00119	ABW90952			gp23 major capsid protein [uncultured Myoviridae]
186179269	0.00109			HSM_0907	hypothetical protein
186355884	0.00077			Aave_2365	hypothetical protein

Continued on next page

Table B.5 – *Continued from previous page*

Gene ID	NSA	COG/NR ID	KO	Locus	COG : KEGG/NR description
186166939	0.00060	EEH89810			conserved hypothetical protein [Acidaminococcus sp. D21]
186255081	0.00050			BCE_0400	phage major capsid protein, HK97 family
18 m – Proteins with no annotation					
186096775	0.00241				
186097423	0.00916				
186098091	0.00174				
186111007	0.00078				
186111572	0.00059				
186115457	0.00104				
186115570*	0.00011				
186115576	0.00019				
186123594	0.00212				
186125293	0.00370				
186127924	0.00058				
186131984	0.00104				
186132934	0.00114				
186132940	0.00646				
186133174	0.02253				
186133182	0.00132				
186133258	0.00558				
186133464	0.04461				
186133598b	0.00897				
186133600c	0.02301				
186133668	0.00039				
186133988	0.00027				
186135915	0.00096				
186144849	0.00090				
186146871	0.00261				
186150520	0.03110				
186150522	0.01653				
186152236	0.00251				
186157988	0.00347				
186166888	0.00138				

Continued on next page

Table B.5 – *Continued from previous page*

Gene ID	NSA	COG/NR ID	KO	Locus	COG : KEGG/NR description
186172010	0.00060				
186174298	0.00457				
186180639 <i>b</i>	0.01514				
186180725 <i>b</i>	0.00639				
186185958	0.00054				
186187134	0.00088				
186188427	0.00024				
186188638	0.00083				
186195344	0.00123				
186196955	0.01096				
186204438	0.00232				
186211626	0.00145				
186213126 <i>d</i>	0.00737				
186218287	0.00057				
186221108 <i>c</i>	0.00454				
186221116 <i>b</i>	0.00898				
186221121	0.00041				
186225633 <i>d</i>	0.03121				
186226973	0.00110				
186234910	0.00076				
186235104	0.00646				
186239503	0.00082				
186243868 <i>c</i>	0.00678				
186243873* <i>b</i>	0.00555				
186247349	0.01576				
186251752	0.00149				
186255283	0.00020				
186263169	0.00052				
186289901	0.00120				
186296333	0.00288				
186296791	0.00187				
186303307	0.00035				
186305449	0.00032				

Table B.5 – *Continued from previous page*

Gene ID	NSA	COG/NR ID	KO	Locus	COG : KEGG/NR description
186308018	0.00041				
186308756	0.01295				
186321445	0.00459				
186321482c	0.04544				
186331727	0.00234				
186334026	0.00196				
186335225	0.00205				
186335471	0.00241				
186344860	0.00118				
186346285	0.01518				
186348107	0.00077				

Table B.6: Proteins identified in the Ace Lake 23 m sample 0.1 µm size-fraction metaproteome. (*) Protein group identification: proteins that contain similar peptides that could not be differentiated by the mass spectral analysis were grouped. Only one gene number of that group is displayed. (a-z, aa-pp) Protein ambiguity groups: proteins that have some shared peptides with one or more other proteins from the same sample depth are marked with the same letters.

Gene ID	NSA	COG/NR ID	KO	23 m – COG annotated proteins	
				Locus	COG : KEGG/NR description
184741277	0.0177260374	COG0776		SYN_02859	bacterial nucleoid DNA-binding protein : DNA-binding protein HU
184609007	0.0163322511	COG1450		Oter_2851	general secretory pathway protein D : type II and III secretion system protein
184630330	0.0120879409	COG1837	K06960	CLL_A1247	predicted RNA-binding protein (KH domain) : hypothetical protein
184814744	0.0077327225	COG3409			putative peptidoglycan-binding domain-containing protein
184723188	0.0066459022	COG1653		Noca_3914	sugar-binding periplasmic proteins/domains : extracellular solute-binding protein, family 1
184729342	0.0051513355	COG0459	K04077	Oter_2054	chaperonin GroEL (HSP60 family)
184751721	0.0020388185	COG0776	K03530	azo0315	bacterial nucleoid DNA-binding protein : hupB
184834728	0.0019935223	COG0683		SYN_00789	ABC-type branched-chain amino acid transport systems, periplasmic component
184819943	0.0019174738	COG0776	K03530	Plut_1957	bacterial nucleoid DNA-binding protein : histone-like DNA-binding protein; HU-beta
23 m – KEGG and NR annotated proteins					
184829089	0.0475406733			Smed_1892	hypothetical protein
184693861a	0.0216206417	A7U6E7			putative major capsid protein [Chryschromulina ericina virus]
184663677a	0.0212217442	A7U6E7			putative major capsid protein [Chryschromulina ericina virus]
184759346	0.0207154065	YP_001648266		OsV5_190f	hypothetical protein [Ostreococcus virus OsV5]
184796349	0.0192247663	ZP_03706494		CLOSTMETH_01228	hypothetical protein [Clostridium methylpentosum DSM 5476]
184674523a	0.0187892597	A7U6E7			putative major capsid protein [Chryschromulina ericina virus]
184727907	0.0127809571	ZP_03013728		BACINT_01287	hypothetical protein [Bacteroides intestinalis DSM 17393]
184858354	0.0124452859			Bcep1808_1173	hypothetical protein
184615458b	0.0078367298	YP_002299293		RC1_3116	hypothetical protein [Rhodospirillum centenum SW]
184717784a	0.0076061482	A7U6F0			putative major capsid protein [Phaeocystis pouchetii virus]
184783470b	0.0067095701			amb4267	hypothetical protein
184677323*	0.0063474779			plu3036	hypothetical protein
184765239*	0.0059538672	AAU84208		GZ37D1_55	hypothetical protein [uncultured archaeon GZfos37D1]
184728060*	0.0045225808			amb4267	hypothetical protein
184610116	0.0041891092			Bd3266	cell wall surface anchor family protein
184609428	0.0041019864	ZP_02421392		EUBSIR_00216	hypothetical protein [Eubacterium siraeum DSM 15702]

Continued on next page

Table B.6 – *Continued from previous page*

Gene ID	NSA	COG/NR ID	KO	Locus	COG : KEGG/NR description
184762189a	0.0033887653	A7U6E7			putative major capsid protein [Chrysochromulina ericina virus]
184616650*	0.0033268581		K08945	Cvib_0330	bacteriochlorophyll C binding protein; chlorosome envelope protein A
184654290	0.0032936278			Plut_0689	gas vesicle synthesis protein GvpA
184683542	0.0032484407			Daci_1946	putative phage major head protein
184717084	0.002738548	AAU84208			hypothetical protein [uncultured archaeon GZfos37D1]
184761703	0.0024990088			Fjoh_3203	Ig domain protein, group 2 domain protein
184619854	0.0024860025	ACO64625			predicted protein [Micromonas sp. RCC299]
184806079	0.0021551868			BTH_I0914	hypothetical protein
184598462	0.0020259568			Cthe_1719	phage major capsid protein, HK97 family
184636514	0.0015699028			PTH_2189	hypothetical protein
184699280	0.0015641493			HSM_0907	hypothetical protein
184785344	0.0015021373			nfa430	putative phage head
184622093	0.001315815		K08946	Cvib_1647	chlorosome envelope protein B
184698829	0.0012425497		K08947	Cvib_0329	chlorosome envelope protein C
184699260	0.0010486715		K08946	Cvib_0367	chlorosome envelope protein B
184602186	0.0009043858			NT01CX_0836	phage capsid family protein, putative
184619542	0.0008436094	ZP_03544057		CtesDRAFT_PD3290	hypothetical protein [Comamonas testosteroni KF-1]
184693284	0.0005379065		K06142	Cvib_1549	outer membrane chaperone Skp (OmpH)
184853817	0.0004762266			Cvib_1511	hypothetical protein

23 m – Proteins with no annotation

184639659	0.043948442
184736526c	0.0410393566
184780301	0.0345039918
184816235	0.0320951789
184703327	0.0281144943
184757685	0.022912986
184749374	0.0220139867
184768326	0.0218597042
184855542	0.0213743088
184647188	0.0212601049
184857022d	0.0195650245
184844109e	0.0194066816
184673540	0.0168790128

Continued on next page

Table B.6 – *Continued from previous page*

Gene ID	NSA	COG/NR ID	KO	Locus	COG : KEGG/NR description
184673891	0.0159922741				
184752115	0.0149669571				
184830016	0.0143696973				
184689526	0.0142884591				
184830014c	0.013541019				
184736969	0.0124982161				
184794003	0.0121750493				
184716841*h	0.0116730875				
184614058e	0.0116322781				
184843043	0.0114527624				
184606136	0.0109961608				
184701852	0.0098313448				
184689528d	0.0095741457				
184818291	0.0091862116				
184717128	0.009020845				
184634342	0.0088512597				
184632228f	0.0081738064				
184609952*	0.0081082036				
184743077h	0.0079540129				
184744668f	0.0070087865				
184693008	0.006893361				
184699860	0.0067135304				
184644432*	0.006647				
184624307	0.0066303306				
184717134h	0.0062908799				
184687320*	0.0060878247				
184609995f	0.0059803992				
184606128	0.0059392396				
184798514	0.0055080342				
184820885	0.005452628				
184774274	0.0052574756				
184634936d	0.0051381512				
184807615	0.0048919091				

Continued on next page

Table B.6 – *Continued from previous page*

Gene ID	NSA	COG/NR ID	KO	Locus	COG : KEGG/NR description
184717137 <i>f</i>	0.004760532				
184634670	0.0043741057				
184699106 <i>g</i>	0.004352547				
184694334	0.0043236572				
184701357 <i>g</i>	0.004288858				
184668292 <i>f</i>	0.0042073202				
184616142	0.0041536143				
184705566*i	0.0040360086				
184656354	0.0038949394				
184699180	0.003299837				
184792136	0.0032690762				
184803016	0.0031682001				
184676233	0.0031358313				
184634894	0.0025039289				
184655451	0.0024076365				
184694448 <i>i</i>	0.0020805881				
184616145	0.0019821169				
184693324	0.0019590879				
184708522	0.0018904341				
184651766	0.0018816493				
184654540	0.0015312301				
184705454 <i>f</i>	0.0014295277				
184705654	0.001336639				
184805593	0.0013247477				
184716621	0.0013232094				
184743075 <i>f</i>	0.0012215426				
184814882	0.0011662333				
184792312	0.0010937152				
184829092	0.0008401013				
184716837 <i>f</i>	0.0007628766				
184796632	0.0004119362				
184845751	0.0002006189				
184730970*	0.0001861843				

Table B.6 – *Continued from previous page*

Gene ID	NSA	COG/NR ID	KO	Locus	COG : KEGG/NR description
184613774*	0.0001709224				

Appendix C

Peptide sequences of OLV and OLPV proteins identified in the metaproteome

Table C.1: Peptide data for Organic Lake metaproteomic analysis. (a)Proteins that have some shared peptides; (b)162322406 and 162276024 are protein homologues; (c)A group of proteins containing similar peptides that could not be differentiated by the mass spectral analysis. Only one gene number of that groups is displayed.

Gene ID	Peptide sequences	
162322530 <i>a</i>	R.AIDECLWAVSSLSPSSSADV.K.V K.ALGAQPFNYTDAVDALPNSIK.A R.EGTYFDQVQPFQHHTR.Y R.HSNFAMESIEQTNGQADFGR.R K.HYGDWMQIWCQLTLDK.N R.IDNATLQLVLSNATVEGTNTAK.V K.INDDL.R.A	R.LNFNHPCK.E K.LQLNGQDR.F R.NGDLAYR.T R.NYNVLR.I R.QVCAPR.N R.RVNCTISR.N R.VNCTISR.N
162322348	K.GNVDVYQENK.L	K.IESDAEPSWVR.G
162322406 <i>b</i>	R.QNQSCGGVNQVNGTHVNR.T R.TAFHLDGDSR.Q	K.TNDGTLVGK.S K.YVSESSTYTR.F
162313481	K.ITTIPENIGQLVK.I	R.SNLQGVTEEQLMSNK.I
162276060	K.TPTGLEFSLTGR.A	R.VNHTDACSTGNK.E
162300260	R.VDIEGGTPFFL.K.E	K.YTFQPSELSNTYFSK.E
162276024 <i>b</i>	K.LGGGISSR.S R.SEVGFQSTMVGSDVAMQR.K K.NINLLSAGANYGINTVGSSLR.N	R.TSLHMGDVLSR.K
162275992	K.NDNITLLDTK.Q	R.NPNLQIR.S
162300108	K.NVVINSEGTHIASVNNK.G K.QDVITDQTNLNVGR.L	K.YENGSWNTLGQLIR.G R.LTVNNSIISK.E
162319393 <i>a</i>	R.AIDECLWAVNTLSPDSSSDVK.V K.ALGAQPFNYTDAIDALPNSVK.A R.EGTYFDQVQPFQHHTR.S R.IDNATLQLVLSNATVEGTNTAK.V R.IMSGMGLAYSN K.INDDL.R.A R.LNFNHPCK.E	K.LQLNGQDR.F R.NGDLAYR.T R.NYNVLR.I R.QVCAPR.N R.RVNCTISR.N R.VNCTISR.N
162300134 <i>c</i>	K.ATAGDTHLGGEDFDNR.M R.IINEPTAAAIAYGLDK.K	R.VEIIANDQGNR.T
162286324 <i>c</i>	K.DVPLVANFSAK.F	K.MKLENTVEK.M
OLV9	K.AGLLSEMDAYSLYQMSR.R K.ELVLSFSSGVK.F K.FGTQASTLFLK.D R.GSSATMSGLLTK.S K.GVASAVESAIGGAK.T K.HIQTTPSMVDK.Y R.ITSDVQVAVK.D K.IYLVVRPQYR.S	R.NGSQQTWNEFR.G K.NILPYDEFVAYK.T F.NVNVPSENTLVDR.N K.SEVLEAK.E K.VSVQSADILNVITK.Q R.YISLHPSQYAK.L K.YTSLGSIIVIDPVR.D
OLV8	K.AGTPIPGVVIYEPSYPR.W K.DIGTDMPYFIFDK.D K.GGYADYR.S K.TLLEFGQSK.D	K.TLPVFIPTIK.Y K.TNGTTPPR.F K.YSEDDTNESIR.N K.QAFIGLQK.T

Appendix D

Microbial taxa detected in the Organic Lake water column

Table D.1: Analysis of SSU gene sequences shown in phylum, class and genus ranks as defined by the SILVA taxonomy, except RF3 which is placed with the Firmicutes according to (Tajima *et al.*, 1999). SSU gene sequences were classified to the genus level or to the lowest rank with bootstrap confidence >85% (see chapter 4 *Materials and methods*). The best BLAST matches to environmental SSU clone sequences are shown for the abundant candidate divisions RF3 and OD1.

Phylum	Class	Genus
<i>Bacteroidetes</i>	<i>Flavobacteria</i>	<i>Psychroflexus</i> unclassified <i>Flavobacteriales</i> <i>Brunimicrobium</i> <i>Owenweeksia</i> <i>Stenothermobacter</i> <i>Persicivirga</i> <i>Sphingobacteria</i> <i>Lewinella</i> E6aC02 Ns11-12_marine_gp WCHB1-69 <i>Cytophagia</i> Ml602j-37 unclassified <i>Cytophagales</i> <i>Cyclobacterium</i> <i>Marivirga</i> VC2.1_bac22 SB-1
<i>Proteobacteria</i>	<i>Gammaproteobacteria</i>	VC2.1_bac22 SB-1 <i>Marinobacter</i> unclassified <i>Gammaproteobacteria</i> unclassified <i>Alteromonadales</i> <i>Saccharospirillum</i> <i>Halomonas</i> <i>Psychromonas</i> <i>Glaciecola</i> unclassified <i>Oceanospirillales</i> <i>Pseudomonas</i> <i>Thiomicrospira</i> <i>Thermomonas</i> unclassified <i>Enterobacteriales</i> Bps-ck174 <i>Modicisalibacter</i> <i>Leucothrix</i> <i>Thiorhodovibrio</i> <i>Pseudospirillum</i>

Continued on next page

Table D.1 – *Continued from previous page*

Phylum	Class	Genus
	<i>Alphaproteobacteria</i>	<i>Roseovarius</i> unclassified <i>Rhodobacterales</i> <i>Loktanella</i> <i>Albimonas</i> TK34 <i>Phaeobacter</i> unclassified <i>Alphaproteobacteria</i> <i>Sphingomonas</i> <i>Octadecabacter</i> Db1-14 <i>Oceanicaulis</i> <i>Sulfitobacter</i> unclassified <i>Rhodospirillales</i> <i>Roseibaca</i> <i>Sulfurimonas</i> <i>Sulfurospirillum</i> <i>Arcobacter</i> Br36
	<i>Epsilonproteobacteria</i>	
	<i>Deltaproteobacteria</i>	<i>Desulfotignum</i> <i>Desulfopila</i> unclassified <i>Bdellovibrionales</i> <i>Peredibacter</i> <i>Bacteriovorax</i> <i>Desulfosalsimonas</i> <i>Desulfobacterium</i> <i>Desulfuromonas</i> <i>Dunaliella chloroplast</i> unclassified chloroplast diatom chloroplast
<i>Cyanobacteria</i>	Chloroplast	
<i>Actinobacteria</i>	<i>Cyanobacteria</i> <i>Actinobacteria</i>	unclassified <i>Cyanobacteria</i> “ <i>Candidatus Aquiluna</i> ” unclassified <i>Micrococcales</i> <i>Demequina</i>
<i>Firmicutes</i>	RF3	FJ231138 Laguna Lejía FM210971 Lake Shangmatala AF142888 Ekho Lake DQ909718 hydrothermal vent HM973420 oil reservoir AB546068 oil well head GU196243 anaerobic digester
	<i>Clostridia</i>	<i>Halanaerobium</i> unclassified <i>Clostridiales</i> unclassified <i>Halanaerobiales</i> <i>Fusibacter</i> <i>Fastidiosipila</i> unclassified <i>Bacillales</i> <i>Paraliobacillus</i>
<i>Lentisphaerae</i>	<i>Lentisphaeria</i>	Wchb1-41 unclassified <i>Victivallales</i> R76-b128
<i>Spirochaetes</i>	<i>Spirochaetes</i>	<i>Spirochaeta</i> unclassified <i>Spirochaetales</i>
<i>Verrucomicrobia</i>	<i>Verrucomicrobiae</i>	unclassified <i>Verrucomicrobiales</i> <i>Rubritalea</i> unclassified <i>Puniceicoccales</i> marine <i>Puniceicoccales</i>
<i>Chlamydiae</i> Candidate divisions	<i>Chlamydiae</i> OD1	unclassified <i>Chlamydiales</i> DQ521564 Lake Vida JN454910 hypersaline mat EU050865 Artic sediment

Continued on next page

Table D.1 – *Continued from previous page*

Phylum	Class	Genus
		JF743552 marine sediments
		GU197432 endosymbionts
		JN408878 soil rhizosphere
		JN440560 hypersaline mat
		AY862782 Lake Tebenquiche
		AF419697 hydrothermal sediment
		HM481393 contaminated water
		JN441150 hypersaline mat
		JN447858 hypersaline mat
	TM7	TM7
	SR1	SR1
	Bd1-5	Bd1-5
	Bhi80-139	Bhi80-139
<i>Euryarchaeota</i>	<i>Halobacteria</i>	Deep_sea_hydrothermal_vent_gp_6 (dhveg-6)
<i>Viridiplantae</i>	<i>Chlorophyta</i>	unclassified <i>Chlorophyceae</i>
		unclassified <i>Chlorophyta</i>
		<i>Chlorophyta</i>
		<i>Dunaliella</i>
<i>Stramenopiles</i>	<i>Bacillariophyta</i>	<i>Cylindrotheca</i>
	<i>Dictyochophyceae</i>	<i>Chaetoceros</i>
	unclassified <i>Stramenopiles</i>	unclassified <i>Dictyochophyceae</i>
<i>Metazoa</i>	<i>Arthropoda</i>	unclassified <i>Pedinellales</i>
	<i>Neocallimastigomycota</i>	unclassified <i>Stramenopiles</i>
<i>Fungi</i>	<i>Dikarya</i>	unclassified <i>Hexapoda</i>
		<i>Neocallimastix</i>
		unclassified <i>Neocallimatigomycetes</i>
		unclassified <i>Ascomycota</i>
		<i>Aspergillus</i>
		<i>Aureobasidium</i>
		<i>Cordyceps</i>
		<i>Penicillium</i>
		<i>Verticillium</i>
		<i>Cryptococcus</i>
		unclassified <i>Basidiomycota</i>
<i>Alveolata</i>	<i>Dinophyceae</i>	unclassified <i>Dinophyceae</i>
		<i>Karlodinium</i>
		unclassified <i>Gymnodiniales</i>
	<i>Ciliophora</i>	<i>Euplates</i>
<i>Choanoflagellida</i>	<i>Codonosigidae</i>	<i>Tunicothrix</i>
		<i>Proterospongia</i>
		unclassified <i>Choanoflagellida</i>